ANALYSIS OF EARTH MOTION ACCELEROGRAMS

by

Victor Jenschke
Graduate Student

Ray W. Clough
Professor of Civil Engineering

Joseph Penzien
Professor of Civil Engineering

University of California
Berkeley

January 1964

TABLE OF CONTENTS

		Page
I.	Introduction	1
II.	Ground Motion Characterization	3
	A. General	3
	B. Response Spectra	5
	C. Fourier Spectra	7
	D. Power Spectral Density	8
III.	Analytical Outline and Numerical Procedure	9
IV.	Acceleration Corrections	12
	A. Dynamical Instrumental Correction	12
	B. Base Line Correction	15
V.	Computer Program Description	17
	A. General	17
	B. Flow Scheme	17
	C. Program Check	19
VI.	Results	21
VII.	Discussion of Results	27
	A. General	27
	B. Base Line Correction	28
	C. Dynamical Instrumental Correction	31
	D. Response Spectra	34
	E. Fourier Spectra	39
	F. Power Spectral Density	41
	G. Selection of a Single Representative Spectrum	42
	H. Correlation Between Geophysical and Spectral Parameters	44

Table of Contents (Cont'd.)

		Page
I.	Errors	47
	A. Tabulation Errors, base line correction error and instrumental correction error	47
	B. Interpolation Errors	49
	C. Plotter Error and Truncation Error	49
	D. Computer Time Estimate	50
	E. Advantages of Digital Method	51
VIII.	Conclusions and Recommendations	51
IX.	Acknowledgements	54
X.	Bibliography	55
XI.	Appendices	56
	1. Summary of Formulas	56
	2. Computer Program	57
	3. List of Graphs	66

NOMENCLATURE

$a(t)$ = accelerogram function

$Ra(\omega)$ = response spectra of $a(t)$

$RD(\omega)$ = relative displacement spectra

$RV(\omega)$ = relative velocity spectra

$AA(\omega)$ = absolute acceleration spectra

$PSRV(\omega)$ = pseudo relative velocity spectra

$PSAA(\omega)$ = pseudo absolute acceleration spectra

$Fa(\omega)$ = complex Fourier transform of $a(t)$

$PSDY(\omega)$ = power spectral density

$RD(t)$ = relative displacement

$RV(t)$ = relative velocity

$PSRV(t)$ = pseudo-relative velocity

$PSAA(t)$ = pseudo-absolute acceleration

$CT(\omega)$ = cosine transform

$ST(\omega)$ = sine transform

$PHS(\omega)$ = phase spectra

$PSDY_t(\omega)$ = time dependent power spectral density

$A(t)$ = reduced accelerogram function

$A(t,\omega)$ = time dependent amplitude function

$\phi(t,\omega)$ = time dependent phase function

ϵ = damping ratio of seismograph = $EXP(\pi\rho/(1-\rho^2)^{1/2})$

ρ = damping coefficient of seismograph

λ = damping coefficient of single degree system

ω = undamped natural frequency of single degree system

ω_D = damped natural frequency of single degree system

Nomenclature (Cont'd.)

T_o = time derivation of acceleration function

$v(t)$ = ground velocity

$d(t)$ = ground displacement

FOREWORD

The research described in this report, "Analysis of Earth Motion Accelerograms", was conducted under the supervision and technical responsibility of R. W. Clough and J. Penzien, Professors of Civil Engineering, Division of Structural Engineering and Structural Mechanics, University of California, Berkeley. This research was performed under the sponsorship of the Plowshare Division, Ernest O. Lawrence Radiation Laboratory, Livermore, California and is submitted in this final report in fulfillment of Purchase Order No. 1256100 for Contract No. W-7405-Eng. 48 with the Atomic Energy Commission.

I. INTRODUCTION

A great amount of information is available in the field of earthquake engineering concerning the characterization of strong motion earthquakes for purposes of estimating structural response. The complexities of ground acceleration-time histories, as recorded by seismographs, do not allow one to visualize, by simple inspection, the factors which influence structural response. Therefore, apart from a direct interpretation of measured ground accelerations, other methods have been developed for characterizing earthquakes such as the response spectra technique. This method has proved to be very useful when upper bounds or estimates of maximum structural response are desired and has also been used as a direct measure of earthquake intensity.

Due to the possible future use of underground high yield nuclear explosions for peaceful purposes, it is important that an attempt be made to characterize the surface ground accelerations produced by such explosions and that these characteristics be compared with those of strong motion earthquakes. Since structures may be located in the immediate vicinity of future underground explosions, it is very desirable that response spectra be made available based on ground accelerations of past underground explosions. These response spectra can be used as an aid in predicting damage to structures during future events as well as a direct means of predicting the intensity of ground motion expected. It was, therefore, one of the objectives of the investigation reported herein to provide such information.

While the response spectra technique mentioned above aids greatly in predicting structural behavior and in characterizing ground motion, it was felt that perhaps some additional understanding of this general

problem could be obtained by supplementing the response spectra analysis with an independent characterization of ground motion in the frequency domain. The natural characterization in this case is the Fourier spectra due to the fact it corresponds to the spectral representation of the second order linear operators describing the behavior of a linear system having constant coefficients. The Fourier spectra resolves the ground acceleration-time function into simple harmonic functions whose frequencies are distributed in a continuous manner over the wide frequency range.

A third possible way of characterizing accelerograms, namely a probabilistic approach using the power spectral density function, was considered in this investigation. The hypothesis of a stationary ergodic random process was examined.

Since the last two of the above methods of characterizing accelerograms, i.e. through the Fourier spectra and the power spectral density, have not been previously applied to earthquake accelerograms a number of past earthquakes were included in the investigation.

The major tasks of the investigation were (1) developing an efficient Fortran program for the IBM 7090 which would calculate the various spectra mentioned above, and (2) developing a program so that all numerical results could be plotted directly on a digital CALCOMP plotter.

Special attention was also given to the influence of seismometer characteristics on the recorded acceleration and a method was developed for eliminating the instrumental error associated with its frequency and damping characteristics.

Some effort was also spent on a study of accelerogram base line correction and its influence on the various spectra results.

A total of 10 earthquake and 19 blast ground motion accelerograms were analyzed, comparisons were made, and some general conclusions and recommendations have been stated.

II. GROUND MOTION CHARACTERIZATION

A. General - Acceleration-time measurements are generally accepted as the standard measurements used to characterize strong ground motion which may be produced by an earthquake or underground nuclear explosion. The total ground acceleration at a specific point not only varies in intensity with time but also varies in direction as well; therefore, a vector function would be needed to completely define the acceleration time history. However, the standard accelerogram obtained by a seismometer or accelerometer measures each of the three components of the ground motion separately. Any one of these components may be used directly in characterizing ground motion.

When interpreting ground motion accelerograms, one must recognize that certain errors may be involved. First of all those frequency components of ground acceleration which are comparable to or higher than the natural frequency of the seismometer will not be measured accurately due to the dynamic response characteristics of the instrument. This type of error may be classified as a recoverable error since the accelerogram can be corrected if one knows the natural frequency and percent of critical damping of the measuring instrument. A method for making this correction is discussed in a subsequent section of this report.

Among the unrecoverable errors of importance are the starting delay error, the sensitivity error, and the base line error.

The starting delay error is caused when the seismometer depends upon a certain level of ground acceleration to initiate recording. This error is usually present in earthquake accelerograms but need not be present in accelerograms resulting from planned nuclear underground explosions since the recorders in this case can be turned on just prior to detonation. The importance of missing the initial portion of the accelerogram lies in the fact that it does not allow, as demonstrated later, a proper base line correction.

The sensitivity error is directly related with the slow speed at which the recording paper advances during recording of the ground acceleration. In recording earthquakes, this paper speed is commonly set at one-half inch per second which results in very large slopes on the accelerogram. When digitizing such a record, these large slopes lead to important unrecoverable errors due to the fact that very small unpreventable errors in the time scale can produce large errors in the recorded accelerations. This type of error is herein referred to as the sensitivity error.

The base line error results from the fact that usually no axis of reference is drawn on the accelerogram record by the instrument and in some cases when a reference axis is drawn its position does not coincide with the position of zero acceleration. One might at first think that only a simple translation of the reference axis is required to eliminate a base line error, but this type of correction does not always work. Further discussion of the base line correction will be presented subsequently in more detail.

While the above mentioned errors influence to a certain extent the final results of any type of characterization study, it is not the main

purpose of this investigation to consider these effects. Rather the main objective of this investigation is to study the various ways of characterizing measured ground motion accelerograms (assuming they are free of the type of errors mentioned above) with an emphasis on the fact that maximum dynamic structural response is of primary concern. Of course, for a given structure subjected to a given base acceleration one can easily calculate structural response, but it must be remembered that structural response predictions must be made for future events. It is necessary therefore that general characterizations be established which can serve as a guide in predicting damage to an infinite variety of structures which may be built in the future and which could be subjected to a wide variety of earthquake or blast ground motions.

The discussion which follows will be concerned with three different characterizations, namely (1) the response spectra which characterizes ground motions from the viewpoint of their effects on a single degree of freedom linear system, (2) the Fourier spectra which characterizes ground motions according to their resolution into harmonic functions which have a continuous frequency distribution and (3) the power spectral density function which is based on a probabilistic approach assuming ground motions as a stationary, ergodic, Gaussian process.

B. Response Spectra - All response spectra are obtained from a transformation of the form

$$R_a(\omega) = \operatorname*{Sup}_t \left| \int_{-\infty}^{t} a(\tau)\, h\,(\omega,\, t-\tau)\, d\tau \right| \qquad (2.1)$$

which assigns to every ground acceleration function $a(t)$ a function $R_a(\omega)$ where $h(\omega,t)$ is the unit impulse response function for a single degree of

freedom system with natural frequency ω. Since, for example,

$$R_a(\omega) = R_{-a}(\omega) \tag{2.2}$$

a single function $R_a(\omega)$ does not uniquely define a single function of $a(t)$, in fact, many different functions of $a(t)$ could produce exactly the same function $R_a(\omega)$ through the transformation given by Eq. (2.1). Consequently, this transformation is not invertible. Also, noticing that

$$R_{a+b}(\omega) \leq R_a(\omega) + R_b(\omega) \tag{2.3}$$

shows this same transformation to be non-linear.

Since the dynamic response of a linear structural system in any one of its normal modes can be determined by a single degree of freedom system, the above spectra can be used in predicting ultimate response of such systems when subjected to ground motions produced by blasts or earthquakes. The structural properties of the system are implied in the function $h(\omega,t)$ which might represent the unit impulse response in terms of relative displacement, relative velocity, or absolute acceleration. The word "relative" implies the response is measured with respect to the moving support.

Three basic response spectra have been generated in this investigation, namely, relative displacement spectrum $RD(\omega)$, relative velocity spectrum $RV(\omega)$, and absolute acceleration spectrum $AA(\omega)$. These spectra represent the greatest values of relative displacement, relative velocity, and absolute acceleration, respectively, reached during the time history of the acceleration input $a(t)$. Two additional response spectra have been generated, namely, pseudo relative velocity spectrum $PSRV(\omega)$ and

pseudo absolute acceleration spectrum PSAA(ω) which are defined in terms of the relative displacement spectrum as follows:

$$PSRV(\omega) \equiv \omega_D \, RD(\omega) \tag{2.4}$$

$$PSAA(\omega) \equiv \omega^2 \, RD(\omega) \tag{2.5}$$

The pseudo relative velocity as given by Eq. (2.4) will be compared against RV(ω). The similitude between RV and PSRV for all ground motions has been used in previous investigations. The pseudo absolute acceleration represents the greatest value of the elastic spring force per unit of mass reached during the time history of the input motion.

C. Fourier Spectra - All Fourier spectra are obtained from a transformation of the form

$$F_a(\omega) = \int_{-\infty}^{\infty} a(\tau) \, e^{-i\omega\tau} \, d\tau \tag{2.6}$$

which assigns to every time function a(t) a frequency function $F_a(\omega)$. This transformation is, of course, linear and invertible; therefore, the original time function a(t) could be recovered from the frequency function $F_a(\omega)$. This invertible property means that all physical properties present in the function a(t) must also be present in the function $F_a(\omega)$. A characterization of the ground motion a(t) through this transformation does not include any structural characteristics since no structural function is included in its definition. $F_a(\omega)$ is a complex function whose real and imaginary parts are, respectively, the cosine and sine transforms. The modulus of this transform will be referred to herein as the amplitude spectrum and its argument as the phase spectrum.

D. Power Spectral Density - The power spectral density $PSDY_a(\omega)$ is defined by the transformation

$$PSDY_a(\omega) = \lim_{T \to \infty} \frac{\left| \int_{-T}^{T} a(\tau)\, e^{-i\omega\tau}\, d\tau \right|^2}{2\pi T} \qquad (2.7)$$

which is not invertible since the same power spectral density function can be obtained from an infinite number of different a(t) functions. Because of its definition, this function does not contain any information regarding the phase angles of the individual frequency components contained in the function a(t).

Since ground motions as produced by earthquakes or blast are of finite duration, the power spectral density functions of the ground accelerations will degenerate to zero in accordance with the strict definition given by Eq. (2.7) as $T \to \infty$. However, in those cases where the power spectral density function tends to a constant function as the value of T is increased within the time duration of the ground motion, it is proper to select in a restricted sense this function as representative of the power spectral density function. The acceptance of such a restricted power spectral density to describe the statistical properties of ground motion must, of course, be limited to angular frequencies ω substantially greater than $2\pi/T_o$ where T_o is the duration of the ground motion. This restriction is a consequence of the fact that strong motion earthquakes and underground nuclear blasts produce ground motions that are in the strict sense non-stationary processes. The error introduced by assuming a stationary, ergodic random process in this case is hard to evaluate but it is directly related to how well the power spectral density function tends to a constant function as T is increased towards T_o.

III. ANALYTICAL OUTLINE AND NUMERICAL PROCEDURE

All previously defined analytical expressions can be organized in a way to make all of the proposed ground motion characterizations depend on the same basic functions. The advantages of such a procedure is reflected in terms of computer time since the Fourier spectra and power spectral density can be obtained along with the various response spectra with little additional computer time required.

The relative displacement function is given by the expression

$$RD(t) = \frac{1}{\omega_D} \int_{-\infty}^{t} a(\tau)\, e^{-\lambda\omega(t-\tau)} \sin \omega_D (t-\tau)\, d\tau$$

$$= \frac{1}{\omega_D} \left\{ C(t) \sin \omega_D t - S(t) \cos \omega_D t \right\} \tag{3.1}$$

where

$$C(t) = e^{-\lambda\omega t} \int_{-\infty}^{t} a(\tau)\, e^{\lambda\omega\tau} \cos \omega_D \tau\, d\tau \tag{3.2}$$

and

$$S(t) = e^{-\lambda\omega t} \int_{-\infty}^{t} a(\tau)\, e^{\lambda\omega\tau} \sin \omega_D \tau\, d\tau \tag{3.3}$$

Since the relative velocity function is simply the time derivative of RD(t), one can state

$$RV(t) = \left\{ C(t) \cos \omega_D t + S(t) \sin \omega_D t \right\} - \frac{\lambda}{\sqrt{1-\lambda^2}} \left\{ C(t) \sin \omega_D t - S(t) \cos \omega_D t \right\} \tag{3.4}$$

The pseudo relative velocity is by definition

$$PSRV(t) = \omega_D\, RD\,(t) \tag{3.5}$$

The absolute acceleration is given by

$$AA(t) = -\, 2\lambda\omega\, RV(t) - \omega^2\, RD\,(t) \tag{3.6}$$

and the pseudo absolute acceleration is by definition

$$PSAA(t) = -\omega^2 \, RD(t) \tag{3.7}$$

The response spectra functions, as derived from the above mentioned time functions, are given by the least upper bound or supremum of these functions with respect to the variable t within the time history interval under consideration.

Defining Fourier cosine and sine transforms as

$$CT(\omega) = C(T_o)_{\lambda=0} \tag{3.8}$$

$$ST(\omega) = S(T_o)_{\lambda=0} \tag{3.9}$$

the amplitude and phase spectrum are respectively

$$AS(\omega) = (CT^2(\omega) + ST^2(\omega))^{1/2} \tag{3.10}$$

and

$$PHS(\omega) = \tan^{-1} \frac{ST(\omega)}{CT(\omega)} \tag{3.11}$$

In the above equations T_o represents the time at which the ground motion terminates.

The restricted power spectral density function is calculated for several increasing time durations with the formula

$$PSDY_t(\omega) = \frac{C^2(t)_{\lambda=0} + S^2(t)_{\lambda=0}}{2\pi t} \tag{3.12}$$

The calculation of the functions C(t) and S(t) required the use of an integration formula for which Simpson's rule was chosen. Since they are indefinite integrals it is convenient to use the following recurrence formula:

$$\left.\begin{matrix} C(t) \\ S(t) \end{matrix}\right\} = e^{\lambda\omega 2h} \left\{\begin{matrix} C(t-2h) \\ S(t-2h) \end{matrix}\right\} + e^{-\lambda\omega t} \int_{t-2h}^{t} a(\tau) e^{\lambda\omega\tau} \left\{\begin{matrix} \cos \omega_D \tau \\ \sin \omega_D \tau \end{matrix}\right\} d\tau \tag{3.13}$$

Application of Simpson's rule to the last integral evaluation and substitution of the continuous variable t by discrete equal spaced values given by

$$t = (m-1)h \quad ; \quad m = 1,3,5,7,---$$

yields for m = 1

$$C(o) = 0 \tag{3.14}$$

and for m = 3,5,7,---

$$\begin{Bmatrix} C((m-1)h) \\ S((m-1)h) \end{Bmatrix} = e^{-2\lambda\omega} \begin{Bmatrix} C((m-3)h) \\ S((m-3)h) \end{Bmatrix} + \frac{h}{3} \left[a((m-3)h)\, e^{-2\lambda\omega h} \begin{Bmatrix} \cos \omega_D ((m-3)h) \\ \sin \omega_D ((m-3)h) \end{Bmatrix} + 4\, a((m-2)h)\, e^{-\lambda\omega h} \begin{Bmatrix} \cos \omega_D ((m-2)h) \\ \sin \omega_D ((m-2)h) \end{Bmatrix} + a((m-1)h) \begin{Bmatrix} \cos \omega_D ((m-1)h) \\ \sin \omega_D ((m-1)h) \end{Bmatrix} \right] \tag{3.15}$$

Since digitized values of the acceleration function a(t) are not generally available at equal spaced time intervals, an interpolation procedure must be used. Two kinds of interpolation have been considered, namely, a linear and a sinusoidal interpolation. The linear interpolation can be used in tabulating accelerations when the time intervals are sufficiently small so that the true acceleration function is closely represented by such linear segments. The sinusoidal interpolation should be used for those acceleration records where the digitized values have been tabulated using essentially only the maximum and minimum points on the records. This latter interpolation method provides a better approximation in such cases since it fits a sinusoidal segment of curve between the maxima and minima points having zero slope at both extremums and neglecting the intermediate points.

IV. ACCELERATION CORRECTIONS

A. Dynamical Instrumental Correction - Generally when accelerogram records are interpreted, one assumes the seismograph displacement $x(t)$ at time t is directly proportional to the ground acceleration $a(t)$ with, of course, a scale factor being involved. This assumption is valid when measuring those components of acceleration whose frequencies are much lower than the natural frequency of the seismometer, but becomes considerably in error when measuring components whose frequencies are of the same order of magnitude or higher than the natural frequency of the seismometer. The error involved in making this assumption can be eliminated when generating standard response and Fourier spectra by incorporating the seismometer characteristics into the analytical procedures as developed in the following discussion.

The differential equation relating seismograph displacement $x(t)$ to ground acceleration $a(t)$ may be expressed as

$$\ddot{x}(t) + 2\rho\ p\ \dot{x}(t) + p^2\ x(t) = -V_s\ a(t) \qquad (4.1)$$

where ρ is percent of critical damping of the seismometer, p is the undamped natural frequency of the seismometer, and V_s is a dimensionless scale factor. For those frequency components of $a(t)$ which are small compared to the natural frequency p, the first two terms in Eq. (4.1) are small compared with the other two terms and therefore can be neglected. However, for higher frequencies, these two terms must be retained. Introducing the change of variable

$$A(t) \equiv -\ (p^2/V_s)\ x(t) \qquad (4.2)$$

which converts the measured seismograph record ordinates into units of

acceleration for purposes of tabulation, Eq. (4.1) becomes

$$\frac{\ddot{A}(t)}{p^2} + \frac{2\rho}{p}\dot{A}(t) + A(t) = a(t) \tag{4.3}$$

If the resulting accelerogram records A(t) are reduced in terms of percent of gravity, Eq. (4.3) is still used; however, the final acceleration values a(t) are also expressed in terms of percent of gravity.

The calculation of $\ddot{A}(t)$ having A(t) in tabulated form, is extremely difficult to perform with accuracy since seismograph recording paper moves rather slowly resulting in poorly defined local curvatures. Any numerical method of calculating the second derivative of A(t) by means of finite differences leads to such large errors that this method is impractical. Because of this difficulty, a completely different approach was used to correct for the instrumental error. In developing this approach, first, combine integrals (3.2) and (3.3) into a single complex function f(t), namely

$$f(t) \equiv c(t) + i\,S(t) = e^{-\lambda\omega t}\int_o^t a(\tau)\, e^{(\lambda\omega - i\omega_D)\tau}\, d\tau \tag{4.4}$$

Letting the time origin coincide with the moment the seismograph record begins and substituting Eq. (4.3) into Eq. (4.4) gives

$$f(t) = \int_o^t \left(\frac{\ddot{A}}{p^2} + \frac{2\rho}{p}\dot{A} + A\right) e^{(\lambda\omega - i\omega_D)\tau}\, d\tau \tag{4.5}$$

Integrating by parts

$$\begin{aligned} f(t) = {} & \frac{1}{p^2}\left\{\left(\dot{A}(t)\, e^{(\lambda\omega - i\omega_D)t} - \dot{A}(o) - (\lambda\omega - i\omega_D)\left(A(t)\, e^{(\lambda\omega - i\omega_D)t} - A(o)\right)\right)\right\} \\ & + \frac{2\rho}{p}\left\{A(t)\, e^{(\lambda\omega - i\omega_D)t} - A(o)\right\} \\ & + \left\{\frac{(\lambda\omega - i\omega_D)^2}{p^2} - \frac{2\rho}{p}(\lambda\omega - i\omega_D) + 1\right\}\int_o^t A(\tau)\, e^{(\lambda\omega - i\omega_D)\tau}\, d\tau \end{aligned} \tag{4.6}$$

It is convenient here to introduce the following two time functions:

$$CA(t) = e^{-\lambda\omega t} \int_0^t A(\tau)\, e^{\lambda\omega\tau} \cos \omega_D \tau \, d\tau \tag{4.7}$$

$$SA(t) = e^{-\lambda\omega t} \int_0^t A(\tau)\, e^{\lambda\omega\tau} \sin \omega_D \tau \, d\tau \tag{4.8}$$

Multiplying Eq. (4.5) by $e^{-\lambda\omega t}$ and separating into its real and imaginary parts gives

$$C(t) = \left[\frac{\dot{A}(t)}{p^2} + \left(\frac{2\rho}{p} - \frac{\lambda\omega}{p^2}\right) A(t)\right] \cos \omega_D t + \frac{\omega_D}{p^2} A(t) \sin \omega_D t$$
$$- \left[\frac{\dot{A}(o)}{p^2} + \left(\frac{2\rho}{p} - \frac{\lambda\omega}{p^2}\right) A(o)\right] e^{-\lambda\omega t}$$
$$\left[1 - \frac{2\rho\lambda\omega}{p} + \frac{(\lambda\omega)^2 - \omega_D^2}{p^2}\right] CA(t) + 2\omega_D \left[\frac{\rho}{p} - \frac{\lambda\omega}{p^2}\right] SA(t) \tag{4.9}$$

and

$$S(t) = \left[\frac{\dot{A}(t)}{p^2} + \left(\frac{2\rho}{p} - \frac{\lambda\omega}{p^2}\right) A(t)\right] \sin \omega_D t - \frac{\omega_D}{p^2} A(t) \cos \omega_D t + \frac{\omega_D}{p^2} A(o)\, e^{-\lambda\omega t}$$
$$\left[1 - \frac{2\rho\lambda\omega}{p} + \frac{(\lambda\omega)^2 - \omega_D^2}{p^2}\right] SA(t) - 2\omega_D \left[\frac{\rho}{p} - \frac{\lambda\omega}{p^2}\right] CA(t) \tag{4.10}$$

These equations permit one to determine the functions C(t) and S(t) in terms of the seismometer constants p and ρ and the recorded function A(t) and its first derivative $\dot{A}(t)$. The functions CA(t) and SA(t) as defined by Eqs. (4.7) and (4.8) have exactly the same form as Eqs. (3.2 and (3.3).

One should observe that for an instrument having a natural frequency p considerably higher than the highest frequency component of interest contained in A(t) and $\dot{A}(t)$, it can be stated that

$$C(t) = CA(t) \tag{4.11}$$

and

$$S(t) = SA(t) \tag{4.12}$$

The effect of the instrumental correction on response and Fourier spectra has been determined for several earthquake and blast ground motion records with the aim of establishing the frequency range as well as instrumental parameters which are of significance. These results are presented in a subsequent section.

B. Base Line Correction - Earthquakes, as well as underground nuclear explosions, present the typical feature of a highly oscillatory type of accelerogram. This pattern, together with the fact that the acceleration function has essentially a zero mean value, makes the determination of the ground velocity function strongly dependent on the position of the zero acceleration line.

Since the ground velocity function has also a marked oscillatory character which involves a rather small area, the position of the acceleration base line affects very strongly the determination of the ground displacement function.

The physical fact that ground velocity is zero, before the earth motion begins as well as after it ends, requires the total area under the true acceleration curve a(t) to be zero.

In the following discussion, it will be assumed that the accelerogram function A(t) represents the true ground acceleration. As previously pointed out, this assumption is valid only when the measuring instrument has a sufficiently high natural frequency p.

Because of the starting delay error, the beginning of the earthquake acceleration is not recorded; therefore, the condition of zero total area need not be satisfied exactly for the record obtained.

A base line correction of the accelerogram based on a parallel shift of the zero acceleration axis has been studied. The amount of shift

permitted is determined by the condition of zero total area under the acceleration function. This type of correction will not yield by integration the true ground velocity and displacement; however, it will give an estimate of the influence this correction has on structural response calculations. It has been applied to the ground motion characterizations as described in Chapter II.

In order to visualize how this correction affects structural behavior, one may notice that the least upper bound of the absolute value of the ground displacement curve is also a point in the relative displacement spectrum. It corresponds to the relative displacement for zero frequency and zero damping. One must expect that the influence of this correction will propagate through the spectrum with greatest effect on the low frequency range.

So far as the Fourier spectra is concerned, letting A_1 represent the acceleration correction, this influence can be determined easily. Noting that the sine and cosine transforms are, respectively,

$$ST(\omega) = \int_0^{t_1} A_1 \sin \omega t \, dt = A_1 \frac{(1 - \cos \omega t_1)}{\omega}$$

$$CT(\omega) = \int_0^{t_1} A_1 \cos \omega t \, dt = A_1 \frac{\sin \omega t_1}{\omega}$$

which are bounded by

$$\left| ST(\omega), CT(\omega) \right| \leq \begin{cases} \dfrac{2|A_1|}{\omega} & \text{for } \omega \geq \dfrac{2}{t_1} \\ |A_1| t_1 & \text{for } \omega < \dfrac{2}{t_1} \end{cases}$$

one observes that the base line correction affects the Fourier spectra predominately at the lower frequencies.

Studies of the base line correction effect on spectra have been made using several measured ground motion accelerograms by comparing the spectra obtained with and without the zero final velocity base line correction. The results of this study are presented in a subsequent section.

V. COMPUTER PROGRAM DESCRIPTION

A. General - All computations were performed by an IBM 7090 digital computer and the desired results were recorded in graphical form using a CALCOMP plotter. To carry out this procedure, a program was first written in Fortran language for the IBM 7090 which enabled the computer to calculate all spectral quantities and store them on magnetic tape. Next, a second program was written which would permit a transfer of the above spectral data to a second tape to be used by an IBM 1401 computer in activating a CALCOMP plotter.

B. Flow Scheme - The IBM 7090 computer program consisted of the following:

1. Initialization - A set of control cards containing all commands are first read into the computer.
2. Input data - All input data can be read into the computer either from punched cards or from magnetic tape, as desired.
3. Interpolation - Four different procedures have been made available for interpolating the input ground acceleration data a(t), namely 1) no interpolation used when the input data is digitized at equal time intervals, 2) linear interpolation used for the normal case of well defined functions, 3) sinusoidal interpolation

used when functions are digitized only at their consecutive maxima and minima points, and 4) sinusoidal interpolation after an atuomatic elimination of all digitized data between consecutive maxima and minima points.

4. Base line correction - The computer program permits two possibilities in regard to base line correction, i.e. no base line correction at all or a parallel shifting of the base line sufficiently to enforce a zero final ground velocity.

5. Ground velocity and displacement - The generation of ground velocity and displacement functions is optional and is set by proper selection of the control cards.

6. Spectral calculations - The convolution and Fourier integrals are calculated by the procedure outlined in Chaps. III and IV. By dividing the input function a(t) into j equal time intervals, the power spectral density function can be generated using only the initial portion of the input function starting at time zero and ending with any one of these intervals. Thus by inspection, the stationary property of the input can be checked.

7. Instrumental correction - The computer program will permit the instrumental correction to be made by simply punching the seismometer undamped natural period and its damping coefficient into the last data card. If the instrumental correction is not desired, the last data card is left unpunched.

8. Time history of response - The computer program has been written so that one can obtain the entire time history response of a single degree of freedom system to any input, if so desired.

Several additional options are permitted by the IBM 7090 program as written. These options, along with the Fortran listing of the program, are given in Appendix 2.

The plotting program is not included in this report since it is adaptable only to the specific computer installation available on the University of California campus.

C. Program Check - To check the accuracy of the computer results, a simple transient ground acceleration which could be expressed analytically was used as the input function. This transient input consisted of a single half sine wave of unit amplitude in the region $0 \leq t \leq 0.1$ sec. and zero in the region $.1 < t \leq .6$. The sinusoidal function was digitized to 5 significant figures every 0.001 seconds. The various spectral quantities were calculated by a direct analytical solution and compared with these same quantities generated by the computer. This comparison, as given by Table I for damping ratios of zero and 20 percent and for frequencies of $10\pi/4$, $20\pi/4$, and $30\pi/4$, shows agreement general to 5 significant figures. In a few cases an error of $\pm$ 1 appears in the last digit. The first value shown in each case was obtained by direct solution.

TABLE I

Damping Ratio = 0	S(ω)	C(ω)	RD(ω)	RV(ω)	AA(ω)
W=10 $\frac{\pi}{4}$	0.24008E-01 0.24008E-01	0.57962E-01 0.57961E-01	0.79880E-02 0.79879E-02	0.62737E-01 0.62737E-01	0.49274E 00 0.49273E 00
W=20 $\frac{\pi}{4}$	0.42441E-01 0.42441E-01	0.42441E-01 0.42441E-01	0.38211E-02 0.38211E-02	0.60021E-01 0.60021E-01	0.94281E 00 0.94281E 00
W=30 $\frac{\pi}{4}$	0.51447E-01 0.51447E-01	0.21310E-01 0.21310E-01	0.23634E-02 0.23634E-02	0.55685E-01 0.55685E-01	0.13121E 01 0.13121E 01
Damping Ratio = .2	S(ω)	C(ω)	RD(ω)	RV(ω)	AA(ω)
W=10 $\frac{\pi}{4}$	0.10078E-01 0.10078E-01	0.24482E-01 0.24482E-01	0.60400E-02 0.60399E-02	* 0.51160E-01	0.40450E 00 0.40450E 00
W=20 $\frac{\pi}{4}$	0.76322E-02 0.76322E-02	0.75206E-02 0.75206E-02	0.28894E-02 0.28894E-02	* 0.38654E-01	0.77402E 00 0.77402E 00
W=30 $\frac{\pi}{4}$	0.39422E-02 0.39421E-02	0.14984E-02 0.14984E-02	0.17878E-02 0.17877E-02	* 0.31843E-01	* 0.10743E 01

The instrumental error correction was also checked by direct solution using the above mentioned transient ground acceleration as input. For this check, a period of 0.1333 seconds and a damping ratio of 0.5 were assumed for the seismometer. The resulting acceleration time history, which would be recorded by this instrument, was then used as the acceleration input into 48 different single degree of freedom systems and their responses were compared with those which would result by using the original half sine wave transient acceleration as input. Of the 48 different systems used, one-half had zero damping; the other one-half had 20 percent of critical damping. The frequencies assumed for these single degree of freedom systems ranged from $10\pi/4$ to 60π. The check showed an increase in the computer error with an increase in frequency. For a frequency of $10\pi/4$, the error resulting in any response function was of the order unit in the 5th significant figure. For a frequency of 60π, i.e. a frequency

4 times greater than the seismometer frequency, the error increased to an order of about 5 units in the 4th significant figure.

It is worthwhile to metnion at this point that larger errors are observed in time response checks than in spectral response checks due to the fact that the latter does not involve phase errors.

Check similar to those described above were also made using other types of ground acceleration as input; however, the accuracies shown were of the same order of magnitude as those presented for the half sine wave input and therefore will not be discussed herein.

The accuracy of the general computer program as demonstrated above is considered sufficient for intended uses.

VI. RESULTS

A total of 29 accelerograms (19 produced by underground nuclear explosions and 10 by earthquakes) were analyzed in the general investigation reported herein. Table II summarizes some of the basic data associated with each event, namely 1) peak acceleration during the period of ground motion, 2) source and receiver media, 3) magnitude of event measured in kilotons for the nuclear explosions and in Richter scale for the earthquakes, 4) seismometer characteristics in terms of period and damping coefficient, and 5) the persons or group from whom the basic ground motion accelerogram data was obtained.

Table III lists the results which are presented in graphical form in Appendix 3.

TABLE II

ANALYZED RECORDS

Case No.	Event	Peak acc. (%g)	Epic. Dist. (km)	Medium		Magn. (*)	Ins. Char.		Vrs.
				Sor.	Rec.		T (sec)	∈	
1.	Gnome 2T	.74	1.6	S	A	3.1	.061	10	L
2.	" 3T	.23	3.2	S	A	3.1	.112	10	"
3.	" 4R	.05	6.5	S	A	3.1	.140	7	"
4.	" 4T	.02	6.5	S	A	3.1	.141	7	"
5.	" 6T	.03	1.6	S	A	3.1	.059	9	"
6.	" 7T	.16	3.2	S	A	3.1	.111	10	"
7.	Dannyboy D5R	.09	1.2	B	B	.4	.070	8	"
8.	" D8R	.03	2.1	B	B	.4	.110	8	"
9.	Mississippi 1777T	.05	8.9	T	A	-	.111	9	P
10.	" 8228T	.04	6.1	T	A	-	.056	12	"
11.	7245R	.45	2.0	T	A	-	.030	10	"
12.	9537R	.98	1.0	T	A	-	.017	13	"
13.	4074T	.25	3.1	T	A	-	.039	8	"
14.	4074R	.30	3.1	T	A	-	.040	7	"
15.	Hard Hat 1091T	.52	1.2	G	L	5.	.034	9	"
16.	" 4496T	.29	6.3	G	A	5.	.146	9	"
17.	Aardvark 3773T	.74	1.1	A	A	37.	.056	15	"
18.	" 1437T	.05	7.5	A	A	37	.101	13	"
19.	Sedan R3	.15	1.1	A	A	110	.017	5	L
20.	Taft 52 N21E	.18	64	-	-	7.7	.081	8	B
21.	" "	.18	64	-	-	7.7	.081	8	H
22.	" "	.18	64	-	-	7.7	.081	8	V
23.	" "	.18	64	-	-	7.7	.081	8	C
24.	El Centro 40 NS	.32	48	-	-	6.7	.099	8	B
25.	" EW	.23	48	-	-	6.7	.100	7	B
26.	" 34 NS	.26	54	-	-	6.5	.098	8	B
27.	Olympia 49 N80E	.32	72	-	-	7.1	.080	9	B
28.	S. F. 57 S80E	.13	12	-	-	5.3	.078	10	V
29.	Ferndale 41 S45E	.12	32	-	-	6.6	.099	10	V

Tabulation Versions:
L - Lawrence Radiation Lab.
P - Planetary Sciences Inc.
B - Berg
C - Clough
H - Hudson
V - Veletsos

Medium Characterization:

A - Alluvium
S - Salt
B - Basalt
L - Limestone
G - Granite
T - Wether Tuff

(*) Magnitude in kilotons for blasts, in Richter magnitude for earthquakes.

TABLE III

Summary of Results

Case No.	A	Integr. V	Integr. D	Response Spectra RD	Response Spectra RV	Response Spectra PSRV	Response Spectra AA	Response Spectra PSAA	Fourier Spectra ST	Fourier Spectra CT	Fourier Spectra AS	Fourier Spectra PHS	PSDY	RUN
1	t	t	t											290
1				ωT	ωT		ωT				ω			247
1	t)	t)	t)											297
1				ω)										318
1							(ω							260
2	t	t	t											290
2				ωT	ωT		ωT				ω			247
2	t)	t)	t)											297
2				ω)										318
2							(ω							260
3	t	t	t											290
3				ωT	ωT		ωT				ω			247
3	t)	t)	t)											297
3				ω)										318
3				(ω	(ω		(ω				(ω			260
4	t)	t)	t)											376
4				ωT	ωT		ωT				ω			247
5	t)	t)	t)											376
5				ωT	ωT		ωT				ω			247
5									ω	ω	ω	ω	ω	187
6	t)	t)	t)											376
6				ωT	ωT		ωT				ω			247
7	t	t	t											552
7	t)	t)	t)											552
7				ωT	ωT		ωT				ω			386
8	t	t	t											552
8	t)	t)	t)											552
8				ω	ω	ω	ω	ω			ω			486
9	t	t	t											532
9	t)	t)	t)											532
9				ω	ω	ω	ω	ω			ω			538
10	t	t	t											532
10	t)	t)	t)											532
10				ω	ω	ω	ω	ω			ω			538
11	t	t	t											532
11	t)	t)	t)											532
11				ω	ω	ω	ω	ω			ω			538

TABLE III - Continued

Case No.	Integr. A	Integr. V	Integr. D	Response Spectra RD	Response Spectra RV	Response Spectra PSRV	Response Spectra AA	Response Spectra PSAA	Fourier Spectra ST	Fourier Spectra CT	Fourier Spectra AS	Fourier Spectra PHS	PSDY	RUN
12	t	t	t											532
12	t)	t)	t)											532
12				ω	ω	ω	ω	ω			ω			555
13	t	t	t											532
13	t)	t)	t)											532
13				ω	ω	ω	ω	ω			ω			555
14	t	t	t											532
14	t)	t)	t)											532
14				ω	ω	ω	ω	ω			ω			555
15	t	t	t											532
15	t)	t)	t)											532
15				ω	ω	ω	ω	ω			ω	ω		555
16	t	t	t											532
16	t)	t)	t)											532
16				ω	ω	ω	ω	ω			ω			555
16					(ω	(ω	(ω	(ω			(ω			555
17	t	t	t											532
17	t)	t)	t)											532
17				ω	ω	ω	ω	ω			ω			555
18	t	t	t											532
18	t)	t)	t)											532
18				ω	ω	ω	ω	ω			ω	ω		555
18					(ω	(ω	(ω	(ω			(ω	(ω		555
19	t)	t)	t)											376
19				ωT	ωT		ωT				ω			338
20	t	t	t											369
20	t)	t)	t)											372
20	t													545
21	t	t	t											369
21	t)	t)	t)											372
21	t													545
22	t	t	t											369
22	t)	t)	t)											372
22	t													545
23	t	t	t											369
23	t)	t)	t)											372
23	t													545
23				ωT	ωT		ωT				ω			350
23									ω	ω	ω	ω	ω	89

TABLE III - Continued

Case No.	A	Integr. V	Integr. D	Response Spectra RD	RV	PSRV	AA	PSAA	Fourier Spectra ST	CT	AS	PHS	PSDY	RUN
24	t)	t)	t)											376)
24				ωT	ωT		ωT				ω			361
25	t)	t)	t)											376)
25				ωT	ωT		ωT				ω			341
25					(ωT		(ωT				(ω			348)
26	t)	t)	t)											376
26				ωT	ωT		ωT				ω			344
27	t)	t)	t)											376
27					ωT		ωT				ω			359
28	t	t	t											552
28	t)	t)	t)											552
28				ω	ω	ω	ω	ω			ω	ω		555
29	t	t	t											552
29	t)	t)	t)											552
29				ω	ω	ω	ω	ω			ω			555

Conventions:
- t: graph versus time
- ω: graph versus angular frequency
- T: graph versus period
-): graphs at the left calculated with instrumental correction
- (: graphs at the right calculated with instrumental correction

- A: ground acceleration
- V: ground velocity
- D: ground displacement

Graphs of ground acceleration, ground velocity, and ground displacement versus time are presented with and without base line corrections in accordance with Table III.

All response spectra calculations were obtained for five different damping ratios (0, 0.02, 0.05, 0.10 and 0.20) with frequencies ranging from 1 to 120 radians per second. Values were calculated at frequency intervals of 1 radian per second. Fourier spectra and power spectral density were calculated over the same domain.

Power spectral density functions were obtained for input durations ending after each of the 3 sub intervals in which the time domain was divided.

VII. DISCUSSION OF RESULTS

A. General - The discussion of results which follows is presented for the purposes of (1) demonstrating the importance of the base line correction, with special emphasis placed on its effect on response spectra in the low frequency range, (2) demonstrating the importance of the dynamical instrumental correction on the evaluation of response spectra and Fourier spectra, (3) comparing the various response spectra, their similarities, and differences and showing the errors involved when generating these spectra by approximate methods directly from velocity spectra, (4) explaining the difficulties encountered in getting suitable Fourier spectra for accelerograms, (5) showing evidence that power spectral density functions cannot be used as a meaningful statistical description of ground motion accelerograms, (6) demonstrating which of the various types of response spectra can be used most effectively in characterizing ground motion, (7) summarizing possible correlations which appear to exist between the spectral results and the geophysical parameters of ground motion accelerograms such as epicentral distance, geology, and source magnitude, and (8) showing the magnitude of errors to be expected in the basic results, giving a time estimate formula which may be used to indicate the efficiency of the Fortran program, and finally discussing the advantages of the method used.

Most of the basic spectral results presented in Appendix III have been plotted as ordinates with frequency as the abscissa. In some cases, these same results were plotted with the reciprocal of frequency, i.e. period as the abscissa. However, it is readily apparent that plotting these data against frequency is considerably more effective in revealing the important characteristics. For example, when plotting against frequency the peaks

on the spectral curves are more evenly distributed than when plotting against period which forces most of the peaks into a narrow region of the graph. Thus, the following discussion will refer mainly to the frequency plots.

B. Base Line Correction - Consider first the effect of the base line correction on the evaluation of ground velocity and displacement. For each of the 29 cases studied in the general investigation, plots of the recorded ground acceleration along with its first and second integrals, i.e. velocity and displacement, respectively, are shown in Appendix III. In many of these cases, the velocity and displacement functions generated both with and without the base line corrections are included.

Inspection of the velocity and displacement functions generated without base line correction shows a tendency for these functions to drift away from the base line, especially in the case of displacement where the drift tends to be of the parabolic type. Comparing these functions with those generated with the base line correction, one finds little noticeable change in the acceleration function; however, the corrected velocity function is zero at the end of the ground motion and the corrected displacement function shows on the average smaller displacements.

It should be realized that the corrected ground displacement functions are still considerably in error. This fact may be due to the following reasons: 1) the zero final velocity condition may have been imposed at times when the true velocities were not actually zero, 2) the functional character of the applied correction, i.e. a parallel shifting of the base lines, may not be sufficient for its intended purpose, and 3) the digitized acceleration function may itself contain significant tabulation errors.

Since the net area under the acceleration function is nearly zero, the above mentioned tabulation errors may be of major importance. To check this possibility, one component of the Taft 1952 earthquake accelerogram which was digitized by 4 different individuals was integrated twice, thus leading to 4 different ground velocity and 4 different ground displacement functions. A discussion of the differences involved due to the tabulation errors in this case is presented in a subsequent section dealing with errors. No further efforts were spent on improving base line correction for purposes of getting more realistic ground displacements, since its effects on response spectra was of major interest.

As previously mentioned, the base line correction affects spectral results principally in the lower frequency range. A comparison of the numerical results for Cases 1, 2, and 3 (with and without base line correction) shows that this correction influences the results noticeably below about 10 radians/second. This comparison can be seen in Table IV where ratios of corrected to uncorrected response and amplitude spectra are presented for three different frequencies using 20 percent of critical damping in each case.

TABLE IV

INFLUENCE OF BASE LINE CORRECTION ON SPECTRA
(λ = 20% of critical)

Case No.	Event	ω rad/sec	$\frac{RDc}{RD}$	$\frac{RVc}{RV}$	$\frac{AAc}{AA}$	$\frac{ASc}{AS}$
1	Gnome 2T	3	0.64	0.98	0.67	0.71
		6	0.85	1.02	0.89	1.17
		10	0.92	1.02	0.92	1.28
2	Gnome 3T	3	0.88	0.97	0.90	1.05
		6	0.93	0.99	0.94	0.95
		10	0.96	1.00	0.97	1.02
3	Gnome 4R	3	0.73	0.96	0.84	0.94
		6	1.07	1.00	1.05	1.06
		10	1.03	1.00	1.02	1.00
	Deviations average	3	.25	.03	.20	.13
		6	.10	.01	.07	.09
		10	.05	.01	.04	.10

The deviation averages given in Table IV show the base line correction to be more important when generating RD and AA functions than when generating RV functions. For example, in the case of ω = 3 rad./sec., deviation averages of 25, 20, and 3 percent, respectively, are obtained. The reason for the larger deviation averages for RD and AA resides in the fact that both have the same type of functional dependence on the acceleration function a(t), i.e. an integral versus essentially a sinusoidal function relationship. Whereas, RV has a different functional relationship since the above sinusoidal function is replaced by a cosine.

The base line corrections used in this investigation have shown that RD and AA spectra are sensitive to the magnitude of the correction in the low frequency range. Further, these studies have shown that these spectra are usually reduced in the low frequency range as a result of the base line correction. It is expected that the true base line correction would reduce the spectral response even more.

C. Dynamical Instrumental Correction - The instrumental correction affects ground motion spectra over the entire frequency range but is most noticeable for the higher frequencies. The most sensitive quantity to this correction is PHS which starts showing noticeable differences at frequencies as low as 1/10 of the instrument frequency (see Case 18). It is followed in order of sensitivity by ST, CI, PSDY and then by AS, RV, AA, and RD for which the instrumental correction becomes apparent at frequencies as low as 1/2 the instrument frequency (see AA Cases 1, 2, 3, 16, 18, 25). It is natural that the instrumental correction does not show up starting at the same percentage of instrument frequency since such correction depends on the frequency content of the accelerogram in each case.

The above correction can be observed better by first re-writing the relative displacement function given by Eq. (3.1) in terms of time dependent amplitude and phase functions $A(t,\omega)$ and $\phi(t,\omega)$, respectively, defined as:

$$A(t,\omega) \equiv (C^2(t) + S^2(t))^{1/2} \tag{7.1}$$

$$\phi(t,\omega) \equiv \tan^{-1} \frac{S(t)}{C(t)} \tag{7.2}$$

thus, obtaining

$$RD(t) = \frac{A(t,\omega)}{\omega_D} \sin (\omega_{Dt} - \phi(t,\omega)) \tag{7.3}$$

It is now apparent from Eqs. (3.10 and (3.11) that

$$PHS(\omega) = \phi(T_o,\omega)_{\lambda=0} \tag{7.4}$$

$$AS(\omega) = A(T_o,\omega)_{\lambda=0} \tag{7.5}$$

Therefore, PHS represents the phase angle at the end of the record ($t = T_o$) of the sinusoidal function describing relative displacement.

These same considerations hold for AS in relation to the defined amplitude function.

The fact that the influence of instrumental correction on PHS shows for frequencies as low as 1/5 of the frequency that affects AS means that it affects the instantaneous phase function $\phi(t,\omega)$ more than amplitude function $A(t,\omega)$. This observation indicates the importance of the instrumental correction when determining the time history response of multi-degree of freedom systems since correctness of phase is essential when including several modes.

The effects of the instrumental correction on response and amplitude spectra are shown in Table V for the six cases to which this correction

TABLE V

EFFECTS OF DYNAMIC INSTRUMENTAL CORRECTION

ω = 100 rad./sec.

Case No.	Event	Inst. Freq. (rad/sec)	Damping Ratio = 0.0				Damp. Ratio = 0.2		
			RDc/RD	RVc/RV	AAc/AA	ASc/AS	RDc/RD	RVc/RV	AAc/AA
1	Gnome 2T	103	1.20	1.14	1.20	1.15	0.75	1.17	0.82
2	Gnome 3T	56	2.21	2.84	2.21	3.17	1.31	1.95	1.41
3	Gnome 4R,	45	3.94	4.53	3.94	4.57	2.08	4.05	2.31
16	Hard Hat 4496T	43	4.91	5.09	4.91	4.93	1.65	3.93	1.58
18	Aardvark 1437T	62	1.67	2.34	1.67	2.89	1.01	1.75	1.06
25	El Centro 40-EW	63	2.04	2.19	2.04	2.22	1.01	1.54	1.02

was applied at a frequency of 100 rad./sec. and damping ratios of zero and 0.2. It is clear from this table, the effects of the instrumental correction are smaller for the damped response spectra than for the undamped spectra.

However, in making this comparison, one should notice the frequency range in which the comparison is being made and compare the frequencies in this range with the natural frequency of the measuring seismometer. In the frequency range above the instrument frequency (see AA, Cases 2, 3, 16, 18, 25), the effect of the correction decreases in general when the damping ratio increases. For these same cases, it is noticeable in Table V that the most sensitive of the various response spectra is RV followed by AA and RD which show similar effects. This observation is opposite to that found in the case of the base line correction previously discussed and may also be attributed to the closer functional character existing between RD and AA as compared with RV.

For frequencies lower than the instrumental frequency (see AA, Case 1), the effects of instrumental correction are not too noticeable except that frequency shifts of the spectral peaks appear. This latter observation is directly associated with the observation previously made showing the manner in which PHS and AA are affected for frequencies below the instrument frequency and means that phase angles are modified but amplitudes remain essentially constant.

Comparing the effects of instrumental correction on spectral results derived from earthquake ground motions versus those derived from underground nuclear explosions show practically the same characteristic features. For example, compare Cases 18 and 24 which have almost identical instrument frequencies.

Note, the instrument frequency is indicated for each corrected case on the graphs by a vertical line between the abscissa axis and adjacent parallel line.

The effect of tabulation errors on instrumental correction is commented upon briefly in a subsequent section on errors.

D. Response Spectra - By definition any single response spectrum value represents the greatest ordinate (without regard to sign) of its corresponding time history response function. This value is usually reached at either a maximum or minimum point in the range $0 < t < T_o$. However, in some cases for an undamped system, it may appear at the end of the interval, i.e. at $t = T_o$. The ground motion accelerogram must be truncated, i.e. T_o must be selected of sufficient magnitude so that the supremum is reached at a maximum or minimum point within the time interval $0 < t < T_o$.

The most quickly observed characteristic of response spectra curves is the fact that an increase in damping readily damps out the rather random oscillatory character which is so evident in the case of zero damping. The sharp peaks which are observed in the undamped case are due to the existance of nearly pure harmonic components of limited duration within the acceleration function a(t) which tend to build up temporary resonant conditions. One will observe also that similar peaks are present on the graphs of Fourier amplitude spectra which represent the decomposition of the acceleration functions into their harmonic components. In the case of highly damped systems, the temporary resonant conditions are not influential on response because of the ability of the system to dissipate energy.

The ultimate objective of this investigation as well as others is to provide average characteristics of ground motions for the purposes of predicting the dynamic behavior of well designed structures, i.e. structures which have high energy dissipation capabilities. It is generally known

that the energy dissipation capabilities of structures is the consequence of numerous phenomena such as those associated with Coulomb friction, cracking of materials, inelastic deformations, etc. Of major importance in limiting maximum structures response is the ability of a structure to dissipate energy during its oscillatory motion. In the following discussion it will be assumed for comparison purposes that this energy absorbing capability can be represented by an equivalent viscous damping factor of 20 percent.

Inspection of all results show that they follow the general asymptotic trends which can be established analytically by assuming ground acceleration, velocity, and displacement functions satisfy homogeneous initial conditions. Based on this assumption it follows that when $\omega \longrightarrow 0$

$$RD(\omega) = \frac{PSRV(\omega)}{\omega_D} = \frac{PSAA(\omega)}{\omega^2} \longrightarrow \underset{t}{\text{Sup}} \left|d(t)\right| \tag{7.6}$$

$$RV(\omega) \longrightarrow \underset{t}{\text{Sup}} \left|v(t)\right| \tag{7.7}$$

$$\frac{AA(\omega)}{\omega} \longrightarrow \underset{t}{\text{Sup}} \left|2\lambda\, v(t) + \omega(1 - 2\lambda^2)\, d(t)\right| \tag{7.8}$$

Moreover, since ground acceleration functions satisfy Dirichlet's conditions regarding maxima and minima and discontinuities, it can be proved that when $\omega \longrightarrow \infty$

$$RD(\omega) = \frac{PSRV(\omega)}{\omega_D} = \frac{PSAA(\omega)}{\omega^2} \longrightarrow \frac{1}{\omega^2} \underset{t}{\text{Sup}} \left|a(t)\right| \tag{7.9}$$

$$RV(\omega) \longrightarrow \frac{1}{\omega^2} \underset{t}{\text{Sup}} \left|\dot{a}(t)\right| \tag{7.10}$$

$$AA(\omega) \longrightarrow \sup_t \left|a(t)\right| \qquad (7.11)$$

On all graphs of acceleration spectra presented in Appendix III, a short horizontal mark has been placed by the right hand border line of each graph to indicate the intensity of the peak ground acceleration, i.e. $\sup_t \left|a(t)\right|$. In most cases, the spectral values at these borders are coincident or very near the marked peak ground accelerations which is in agreement with Eq. (7.11). Good agreement means that essentially all frequency components within the ground acceleration functions fall within the frequency band 0-120 rads./sec. Poor agreement on the other hand means significant frequency components are present above 120 rads/sec.

In the following discussion comparisons are made for the 20 percent damped case. Table VI shows the similarities existing between AA and PSAA as a function of frequency, for four cases associated with underground nuclear explosions. The results given in this Table reveal the contribution of the damping force (when added to the elastic spring force) to the total inertia force for the 20% damping case.

TABLE VI

RATIO OF ABSOLUTE ACCELERATION TO PSEUDO ABSOLUTE ACCELERATION
(λ = 20% of critical)

	Case No.	Event	ω = 6 (T=1.05)	ω = 10 (T=1.63)	ω = 20 (T=0.31)	ω = 40 (T=0.16)
Underground Nuclear Expls.	7	Mississippi 1777T	1.08	1.06	1.04	1.00
	10	Mississippi 8228T	1.20	1.10	1.04	1.01
	16	Hard Hat 4496T	1.05	1.07	1.03	1.01
	18	Aardvark 1437T	1.12	1.08	1.04	1.02
		Average	1.11	1.08	1.04	1.01
Earthquakes	24	El Centro 40 NS	1.09	1.10	1.04	1.06
	25	El Centro 40 EW	1.09	1.09	1.03	1.09
	26	El Centro 34 NS	1.11	1.07	1.01	1.02
	27	Olympia 49 N80E	1.08	1.19	1.05	1.03
		Average	1.09	1.11	1.03	1.05

It is observed that the damping force contribution to the absolute acceleration spectra ranges from 1% to 11%, on the average, as frequency varies from 40 to 6 radians per second. For frequencies lower than those given in Table VI the base line errors can be so significant that the spectral results contain substantial errors. Therefore, values in this low frequency range are not included. Table VII shows the differences existing between RV and PSRV for the same eight cases. The results of this Table shows the magnitude of errors introduced if displacement and acceleration spectra for 20 percent damping are obtained from velocity spectra in the traditional way as stated by Eqs. (2.6) and (2.7) using the approximation RV $\cong$ PSRV.

TABLE VII

RATIO OF RELATIVE VELOCITY TO PSEUDO RELATIVE VELOCITY
(λ = 20% of critical)

	Case No.	Event	ω = 6 (T=1.05)	ω = 10 (T=0.63)	ω = 20 (T=0.31)	ω = 40 (T=0.16)
Underground Nuclear Expls.	9	Mississippi 1777T	1.10	0.82	0.90	0.41
	10	Mississippi 8228T	1.71	1.05	0.79	0.83
	16	Hard Hat 4496T	1.05	1.09	0.66	0.50
	18	Aardvark 1437T	1.25	0.97	0.75	0.63
		Average	1.28	0.98	0.77	0.59
Earthquakes	24	El Centro 40 NS	1.27	1.19	1.02	0.77
	25	El Centro 40 EW	1.96	1.11	0.72	0.87
	26	El Centro 34 NS	1.70	1.05	0.70	0.56
	27	Olympia 49 N80E	1.54	1.16	0.69	0.89
		Average	1.62	1.13	0.78	0.77

It may be noticed that PSRV $\cong$ RV involves two approximations: a) neglecting the sine function form in the definition of RV, see Appendix I, and b) replacing the term cos $\omega_D (t-\tau)$ by ω_D sin $\omega_D(t-\tau)$. By using Eqs. (7.6) and (7.7) and letting $\omega \longrightarrow 0$, one gets

$$\frac{RV}{PSRV} = \frac{\text{Sup } |V(t)|}{\omega_D \text{ Sup } |d(t)|} \longrightarrow \infty \qquad (7.12)$$

and using Eqs. (7.9) and (7.10) as $\omega \longrightarrow \infty$, one obtains

$$\frac{RV}{PSRV} = \frac{\text{Sup } |\dot{a}(t)|}{\omega_D \text{ Sup } |a(t)|} \longrightarrow 0 \qquad (7.13)$$

Therefore, it follows that since the ratio RV/PSRV is a continuous function of ω, it must take on the value 1 at some value of ω, say ω_1. At this frequency the functions RV and PSRV must cross. This crossing point occurs on the average in the interval $6 \leq \omega_1 \leq 10$ for those underground nuclear explosions and in the interval $10 \leq \omega_1 \leq 20$ for those earthquakes represented in Table VII. This crossing frequency ω_1 may vary substantially, as can be observed for other cases, for example see the curves of $RV_{\lambda=0.2}$ and $PSRV_{\lambda=0.2}$ given in Appendix III. The assumption that PSRV $\cong$ RV can be made over a frequency range in the vicinity of ω_1. For zero damping, this range is much wider than for the case of a highly damped system accepting the same magnitude of error in each case.

It is of interest to compare some of the results obtained in this general investigation with those given by Housner. The cases in which such comparisons can be made are the above four earthquakes and in addition Case 29. Since plots of data against period are available only for the first 4 cases, the comparison made herein will be restricted to these cases. Housner's relative velocity spectrum for 20 percent damping is plotted for discrete points on the corresponding relative velocity graphs. Comparisons will show some general dispersion of values of indeterminable nature. The differences observed in the asymptotic behavior with increasing period is due possibly to errors related to base line correction or to differences in the acceleration digitized data which modify ground velocity.

A comparison of the absolute acceleration spectra (Appendix III) for the above cases with Housner's acceleration spectra shows Housner's results to be on the average lower for periods smaller than approximately 0.6 seconds and higher for periods greater than 0.6 seconds. This observation is in agreement with the results of Table VII.

E. Fourier Spectra - As mentioned in Chap. II, Sect. C and in Chap. III, there are two ways of representing the Fourier spectra: 1) The amplitude and phase spectra (AS, PHS), and 2) the Fourier sine and cosine transforsm (ST, CT). Consider first the (AS, PHS) representation. By inspection of the graphs, it can be noticed that AS resembles RV. This resemblance is a consequence of their mathematical definitions. From Eq. (3.4) and for $\lambda = 0$, one gets

$$\underset{\lambda=0}{RV(t)} = \underset{\lambda=0}{C(t)} \cos \omega t + \underset{\lambda=0}{S(t)} \sin \omega t \qquad (7.12)$$

Using the time dependent amplitude and phase functions as defined by Eqs. (7.1) and (7.2), Eq. (7.12) becomes

$$\underset{\lambda=0}{RV(t)} = \underset{\lambda=0}{A(t,\omega)} \cos (\omega t - \underset{\lambda=0}{\phi(t,\omega)}) \qquad (7.13)$$

For $t \geq T_o$, $\underset{\lambda=0}{A(t,\omega)}$ and $\underset{\lambda=0}{\phi(t,\omega)}$ are independent of t so

$$\underset{t \geq T_o}{\text{Sup}} \left| \underset{\lambda=0}{RV(t)} \right| = \underset{\lambda=0}{A(T_o,\omega)} = AS(\omega) \qquad (7.14)$$

But from the definition of $RV(\omega)$

$$\underset{t \geq T_o}{\text{Sup}} \left| \underset{\lambda=0}{RV(t)} \right| \leq \underset{\lambda=0}{RV(\omega)} \qquad (7.15)$$

Therefore,

$$AS(\omega) \leq \underset{\lambda=0}{RV(\omega)} \tag{7.16}$$

which shows that $A(\omega)$ is uniformly bounded by $\underset{\lambda=0}{RV(\omega)}$.

By comparing the graphs of $AS(\omega)$ and $\underset{\lambda=0}{RV(\omega)}$, one can see that the points of coincidence of $AS(\omega)$ and $\underset{\lambda=0}{RV(\omega)}$ seldom occur. It can therefore be concluded that the spectral relative velocity is seldom reached, even for zero damping, at a time t greater than or equal to T_o. For extremely low frequencies the graphs show that AS may exceed $RV_{\lambda=0}$ which is in contradiction with Eq. (8.5). This apparent discrepancy will be clarified in a later section devoted to errors.

The graphs for PHS represent the principal value of the function defined by Eq. (3.11). Since there was no practical way of writing the plotter program so that the discontinuities of magnitude π could be represented, the plot came out as a continuous curve. This would not make too much difference for smooth PHS because these discontinuities could be recognized. However, typical ground motion accelerograms produce PHS spectra having very steep slopes which make it impossible to distinguish between phase discontinuities and the true values of the function. This fact restricts tremendously the value of the first Fourier spectral representation (AS, PHS). For this reason only 4 PHS graphs are presented in Appendix III.

It is more convenient to use the second of the above mentioned Fourier sine and cosine transforms, since it avoids the above difficulty. To illustrate the differences between the two representations, Cases 5 and 23 for the spectral results for both representations are given in

Appendix III. These results were obtained for the frequency range 0.4 - 30 using a time increment of .01 seconds and a frequency increment of .02 radians/sec.

It would be very desirable to have available a digital computer program which would generate the inverse Fourier transform. With such a program one could investigate completely the feasibility of using the Fourier spectral representation of ground motion accelerograms.

F. Power Spectral Density - Power spectral density plots have been obtained, together with the Fourier transforsm for Cases 5 and 23. For each of these two Cases, three PSDY functions were obtained using those portions of the accelerogram between t = 0 and t = 1/3 T_o, 2/3 T_o, 3/3 T_o, respectively. These three functions were then used to check the stationarity property of the accelerogram. Making this check for each of the above cases, reveals that the three functions do not approach asymptotically a unique function. It will be noted that when using 1/3 T_o, large intensities of PSDY are observed in the relatively high frequency ranges while for 3/3 T_o large intensities are observed in the low frequency ranges. This predominance of frequencies in the high range in one case and in the low range in the other can be observed directly in the two accelerograms where high frequency components are apparent in the earlier portion of the accelerogram and diminish in the latter.

Because of the non-stationary property demonstrated above, the power spectral density method of characterizing ground motions produced by earthquakes or underground nuclear explosions is considered inappropriate.

G. Selection of a Single Representative Spectrum - It would be very helpful from a practical point of view if the necessary information to characterize ground motion could be obtained from a single type of spectrum. At this point, therefore, the question is raised, "Is any one of the 5 spectra described herein adequate to describe the important ground motion characteristics for structural response purposes?".

To answer the above question, one must of course be aware of the different kinds of information which the various spectra yield. In the discussion which follows, any two spectra which cannot be related by a simple algebraic operation, such as dividing or multiplying by ω, will be regarded as algebraically independent functions and algebraically dependent spectra will hereafter be assumed to contain the same ground motion information. According to the definitions stated in Chap. II, Sect. B, among the 5 spectra only 3 are algebraically independent, say RD, RV, and AA. Algebraically dependent spectra are RD, PSRV, and PSAA. Accepting the point of view that RV is not directly associated with any design criterion, one can eliminate it as a possible choice for the one standard spectra desired. RD represents the greatest relative displacement that a one degree of freedom system will undergo when submitted to a given ground motion. As such, it could be used as a standard if maximum structural deformation is a sound design criterion. If, however, maximum total force within a structural system is considered a better criterion, then AA should be used as it displays the analog function.

RV spectrum represents the relative velocities induced in a structural system which cannot be interpreted directly in terms of their effect on the system. Further, there is no experimental evidence to indicate higher relative velocities produce greater damage. As previously

discussed, RV cannot be used as a medium for calculating other spectra when damping is important since the errors introduced by using the usual approximation (PSRV $\cong$ RV) may be greater than one can permit. Consequently, RV is disregarded as a possible standard spectra to be used in characterizing ground motion from a structural response point of view. This elimination reduces the number of independent spectra to two.

Now consider establishing an appropriate failure theory for structural materials. In the dynamic problem of concern here, a velocity dependent force is usually present; therefore, the total inertia or dynamic load is not algebraically dependent upon displacement. Consequently, maximum inertia force and maximum displacement may not occur at the same instant; thus, they represent different physical quantities.

If a dynamic failure theory is chosen no possibility exists of reducing more the number of independent spectra; RD and AA will consitute important independent information. The quasi static failure theory assumes that elastic force, and not inertia force, is the basic cause of damage. Since elastic force and relative displacement are algebraically dependent they both constitute a measure for the same fact. The RD spectra represents the greatest relative displacement and PSAA the greatest elastic force, both maximums occurring at the same time. This viewpoint requires one to consider the inertia forces when establishing equations of motion but arrives at the design of systems by limiting the magnitude of the elastic forces. If this theory is chosen, one needs only one spectrum, namely, RD to characterize ground motion, and AA will be irrelevant to the problem.

The quasi static criterion is in agreement with the fact that there is no experimental evidence which supports the fact that failure depends

on total force (inertia + damping force) at least during short time phenomena such as earthquake or blast. Moreover, all mechanical properties of structural materials available to the designer are obtained by quasi static test procedures. So, it is reasonable to chose the last viewpoint which reduces the number of algebraically independent spectra to one.

Previously in this section the number of independent spectra from which a standard might be chosen was stated as 3, namely, RD, PSRV, and PSAA. However, the previous discussion eliminated RV which automatically eliminates PSRV as a possible choice. Comparing RD and PSAA spectra, it is obvious that PSAA is the logical choice.

General properties of $PSAA_{\lambda = 0.2}$ can be stated as follows:

A. For increasing frequencies, it tends asymptotically to the peak ground acceleration, i.e. $\sup_t |a(t)|$.

B. For zero frequency, its value is zero.

C. RD can be obtained from PSAA by division by ω^2.

D. PSAA represents seismic coefficient of a single degree of freedom system (elastic force).

E. A clear correlation with epicentral distance is evident (see Sec. H).

H. Correlation Between Geophysical and Spectral Parameters - It would be helpful if correlations could be established between certain geophysical parameters (such as epicentral distance, event magnitude, and types of propagation media) and the important spectral parameters. However, insufficient ground motion accelerogram data exist at the present time to permit a complete correlation study based on statistical concepts;

therefore, only a few crude observations suggesting possible trends can be made based on the data presented herein. Only one of these observations, namely, the correlation between epicentral distance and spectra will be discussed. To establish this correlation, the AA spectrum has been used because of its characteristic feature of maintaining significant values over the entire frequency range. A damping ratio of 20 percent has been used since it reflects average ground motion characteristics.

Considering some characteristic frequency as the parameter of the spectrum which is to be correlated with epicentral distance, first one must define this frequency. For those cases where a single maximum occurs in the frequency range $0 < \omega < 120$ radians/sec., the characteristic frequency is taken as that frequency corresponding to the maximum point. For those cases where the maximum spectral value occurs at a frequency equal to or greater than 120 radians/sec., the characteristic frequency is taken as 120 rads./sec. For those cases which do not fit either of the above, the characteristic frequency is selected as that frequency corresponding to the greatest maximum value.

Characteristic frequencies based on the above definitions along with corresponding epicentral distances are shown in Tables VIII and IX for underground nuclear blasts and earthquakes, respectively. Observing the values shown in Tables VIII and IX a correlation is apparent, namely that with decreasing frequencies epicentral distances are increasing.

TABLE VIII

CORRELATION FREQUENCY - EPICENTRAL DISTANCE

UNDERGROUND NUCLEAR EXPLOSIONS

Case No.	Event	Charact. Freq. (rad/sec)	Epic. Dist. (km)
15	Hard Hat 1091T	120	1.2
1	Gnome 2T	100	1.2
12	Mississippi 9537R	87	1.0
5	Gnome 6T	80	1.6
11	Mississippi 7245 R	80	2.0
6	Gnome 7T	70	3.2
13	Mississippi 4074T	66	3.1
2	Gnome 3T	63	3.2
17	Aardvark 3773T	58	(1.1)
7	Dannyboy D5R	49	(1.2)
4	Gnome 4T	48	6.5
16	Hard Hat 4496T	45	6.3
3	Gnome 4R	45	6.5
19	Sedan R3	33	(1.1)
8	Dannyboy D8R	15	(2.1)
14	Mississippi 4074R	13	(3.1)
10	Mississippi 8228T	13	6.1
9	Mississippi 1777T	8	8.9

TABLE IX

CORRELATION FREQUENCY - EPICENTRAL DISTANCE

EARTHQUAKES

Case No.	Event	Charact. Freq. (rad/sec)	Epic. Dist. (km)
28	San Francisco 57 S80E	54	12
29	Ferndale 41 S45E	26	33
33	Taft 52 N21E	19	(64)
27	Olympia 49 NE	18	(72)
24	El Centro 40 NS	14	48
25	El Centro 40 EW	13	48
26	El Centro 34 NS	12	54

I. Errors, Computer Time Estimate and Advantages of Method

A. Tabulation Errors - base line correction error and instrumental correction error. The Taft 1952 earthquake component N21E was tabulated in this investigation from a contact copy of the original record using unequal spaced intervals to define maxima and other intermediate significant points. The tabulation was made, using a milimeter scale, by measuring abscissas on ordinates to the nearest 1/10 of a milimeter. The first 60 second portion of this record was tabulated and defined by 696 values with a density of 16 values per second at the beginning and 6 values per second near the end. Similar contact copies of the Taft 1952 earthquake were tabulated with the same procedure by three other investigators using 748, 812, 818 points (Event Nos. 20, 21, and 22, respectively) for defining this same 60 second portion of the record.

All four of the above versions were integrated with and without base line correction giving the results shown in Appendix III. By inspection of these results, one may notice that 1) uncorrected ground acceleration graphs look practically alike for all four cases, 2) uncorrected ground velocities for Cases 20 and 22 are quite similar but they differ considerably with the uncorrected ground velocities of Cases 21 and 23, and 3) uncorrected ground displacements of all four Cases 20, 21, 22, and 23 differ considerably, not only at particular time values but also in their functional character. Observations 1, 2 and 3 prove that, though ground accelerations may appear practically alike, displacements are strongly affected by tabulation errors. Moreover, these errors have such a functional character that it is impossible to find a base line correction method which can yield the same ground displacement function for all four tabulated accelerations. This proves, in effect, that some of the four tabulations,

all supposedly tabulated with the same procedure, have substantial errors which cannot be eliminated by using the same correction method.

Consider now the effect of base line correction on spectra. Inspection of the used base line correction effects on the four tabulations shows that this base line correction 1) changes the magnitude of ground accelerations very little, 2) affects ground velocities considerably more than ground accelerations, and 3) affects ground displacements considerably more than ground velocities. Eqs. (7.6) and (7.7) show that supremums of the absolute value of ground velocity and ground displacement are equal to the magnitude of RV and RD spectra, namely defined by the abscissa $\omega = 0$. The small variation effects in RV and the considerably greater variation effects in RD as shown in Table IV can be explained in terms of the above observations regarding base line correction.

Ground acceleration, velocity, and displacement functions are shown in Appendix III for all 29 cases studied in this investigation. It is quite apparent by observing these functions that important errors due to inaccurate tabulations are present.

Instrumental correction requires one to know the time derivative of the acceleration record; therefore, the tabulation of the accelerogram must accurately represent the function itself and also its time derivative. The accuracy of the numerical results obtained using instrumental corrections depends on the ability of corresponding ground acceleration tabulations to represent the first derivative. It should be noticed that when checking the base line correction effects, RD should be selected since it is the most sensitive spectra with regard to this correction. However, when checking the instrumental correction effects, RV should be selected for the same reason.

It must be kept in mind that, unless the seismometer equation (Eq. 4.3) is used which requires first and second derivatives of the record, only approximate ground velocities and displacements are found. As a consequence, the tabulation of acceleration cannot contain the complete ground acceleration description unless records are improved to evidence curvature characteristics. To this end it has to be noticed that usual earthquake recording velocities of 1/2" per second are inadequate.

Moreover, it would be convenient to tabulate records at equal time intervals to avoid interpolation procedures. It is suggested that time increments be equal to or smaller than .005 seconds for typical earthquake and underground nuclear explosion records.

B. Interpolation Errors - Linear interpolation was used in all results presented in Appendix III. In choosing a time interval a compromise between computer time and accuracy of calculations was resolved using 5 points per cycle for the highest frequency to be analyzed. As analysis was restricted to frequencies in the interval $0 < \omega \leq 120$ rads./sec., the time interval was chosen as .01 seconds. $\frac{20}{2\pi} = 20 \text{ cps}$ $T = .05$

C. Plotter Error and Truncation Error - All plots in Appendix III have a resolution of .01 inch which is the minimum pitch of the digital CALCOMP plotter.

Response spectra analysis was made by truncating acceleration functions at time T_o where ordinates become "negligible", i.e. the supremum is taken with respect to t over the interval $0 < t < T_o$. This procedure does not include possible, but remote, spectral values reached at $t > T_o$. After some practice, one learns to truncate acceleration functions at a proper place with considerably economy in computer time. The risk in

truncating ground motions amounts to the fact that some calculated spectral values, in the very low frequency range, may occur at $t > T_o$. However, this possibility can be checked by comparing AS with $RV_{\lambda=0}$ since by Eq.(7.16), one has $AS \leq RV$. This criterion allows one to recognize if the supremum really occurs at a t greater than T_o. In case it does, the above chosen T_o is too small, and if spectral values are required in this low frequency range the calculations must be repeated using a greater T_o. Since the low frequency values in this range are always affected by base line type errors, repeated calculations of this type were not made.

D. Computer Time Estimate - The following formula allows one to estimate the IBM 7090 computer time required for spectra calculations. Time in minutes is given approximately by

$$\frac{N \cdot I \cdot T_o}{80000 \cdot DT}$$

where

N = number of different damping ratios

I = " " " frequencies

T_o = lengths of function in seconds

DT = integration interval in seconds

If instrumental correction is used, the estimated time must be increased by about 30%. For example, to analyze 10 seconds of ground motion acceleration and plot graphs of 7 spectra such as RD, RV, PSRV, AA, PSAA, ST, and CT, it will take about 9 minutes of IBM 7090 computer time per 120 spectral points using 5 damping ratios and a time interval of .01 sec.

E. Advantages of Digital Method

(1) All spectral functions can be obtained in practically the same time as required for getting a single response spectrum.

(2) Digital computer programming has greater flexibility compared to other methods since by simply changing some cards the computer program can be modified.

(3) High efficiency and accuracy are characteristics of the method. Once acceleration function is read into the computer, all of the work leading to the graphs themselves are done automatically.

VIII. CONCLUSIONS AND RECOMMENDATIONS

Based on the data obtained in this investigation and a careful study of their significance, the following general conclusions have been deduced:

(1) The base line correction is important and must not be ignored when generating spectral values in the low frequency range.

(2) The instrumental correction is significant when generating spectral and time response values in the high frequency range, i.e. for frequencies which are high compared with the natural frequency of the seismometer.

(3) The approximation often made which assumes that pseudo relative velocity is equal to relative velocity may be considerably in error for highly damped systems.

(4) Typical ground motion acceleration functions resulting from earthquakes and underground nuclear explosions are non-stationary in character.

(5) Pseudo absolute acceleration spectrum most effectively, of all the spectra, characterizes ground motion accelerograms.

(6) The acceleration spectra show that a correlation exists between epicentral distance and the frequencies at which large spectral values are obtained. This correlation shows a decrease in the frequencies with increasing epicentral distances.

(7) The digital computer programs developed in this investigation for computing response and Fourier spectra of ground motion accelerograms have proved to be accurate and efficient.

(8) Response spectra for accelerograms resulting from underground nuclear explosions should be interpreted and used by structural engineers in the same sense as they now interpret and use earthquake response spectra.

In the interest of aiding future research the following recommendations are made:

(1) Studies should be made for the purpose of establishing whether or not an equivalent viscous damping approach can be used to predict spectral response of a single degree system with high non-viscous energy dissipation.

(2) If the equivalent viscous damping factor approach could be shown to be feasible for the single degree system, further study would then be needed to extend this approach to multi-degree structural systems and to establish correct equivalent damping factors.

(3) It has been shown in this investigation that the generation of accurate response spectra is sensitive in the relatively high and low frequency ranges to the accuracy of the digitized

accelerogram data used; therefore, every effort should be made to improve digitizing procedures.

(4) Recording techniques should be improved to obtain better descriptions of ground motion accelerations, i.e. better definitions of slopes and curvatures of the recorded function are needed.

(5) Research on base line correction methods should be undertaken to minimize spectral response at low frequencies.

(6) For establishing correlations between spectra, magnitude of event, and geology more planned-accelerogram data should be obtained.

ACKNOWLEDGEMENT

The authors wish to express their appreciation and sincere thanks to those individuals who contributed to the completion of this investigation, especially to Glen Worth, Lou Caulthen, and Ted Cherry of the Lawrence Radiation Laboratory for their advise and encouragement, to William Adams and Nancy Nuhn of Planetary Sciences Inc. who supplied most of the digitized accelerogram data for underground nuclear blasts, and to A. S. Veletsos, University of Illinois, D. Hudson, California Institute of Technology, and G. Berg, University of Michigan, who supplied most of the digitized earthquake accelerogram data.

Finally, the authors wish to thank the Lawrence Radiation Laboratory, Livermore, California for the financial assistance which made this investigation possible.

X. BIBLIOGRAPHY

1. Biot, M., "Theory of Vibrations of Buildings During Earthquakes", Zeit. Ang. Math. und Mech., Vol. 14, No. 4, Aug. 1934, pp. 213 - 223.

2. Biot, M., "A Mechanical Analyzer for the Prediction of Earthquake Stresses", Bull. Seism. Soc. of Amer., Vol. 31, No. 2, 1941, pp. 151 - 171.

3. Alford, J. L., Housner, G. W., and Martel, R. R., "Spectrum Analysis of Strong-Motion Earthquakes", Tech. Rep., Cal. Inst. Tech., Aug. 1951.

4. Blume, John A., "Structural Dynamics in Earthquake-Resistant Design", Proc. ASCE, Vol. 84, No. ST4, July 1958, pp. 1695, 1-25.

5. Hudson, D. E., "Some Problems in the Application of Spectrum Techniques to Strong-Motion Earthquake Analysis", Bull. Seism. Soc. of Amer., Vol. 52, No. 2, 1962, pp. 417 - 432.

6. Berg, G. V., and Housner, G. W., "Integrated Velocity and Displacement of Strong Earthquake Ground Motion", Bull. Seism. Soc. Amer., Vol. 51, 1961, pp. 175 - 189.

7. Zemanian, A. H., "An Approximate Method of Evaluating Integral Transforms", Journ. Appl. Phys., Vol. 25, No. 2, 1964, pp. 262 - 266.

8. Caughey, T. K. and Stump, H. J., "Transient Response of a Dynamic System Under Random Excitation", Journ. Appl. Mech., Dec. 1961, pp. 563 - 566.

APPENDIX 1

SUMMARY OF FORMULAS

$$RD(\omega) = \sup_t \left| \frac{1}{\omega_D} \int_0^t a(\tau)\, e^{-\lambda\omega(t-\tau)} \sin \omega_D (t-\tau)\, d\tau \right|$$

$$RV(\omega) = \sup_t \left| \int_0^t a(\tau)\, e^{-\lambda\omega(t-\tau)} (\cos \omega_D (t-\tau) - \lambda' \sin \omega_D (t-\tau))\, d\tau \right|$$

$$AA(\omega) = \sup_t \left| \omega_D \int_0^t a(\tau)\, e^{-\lambda\omega(t-\tau)} ((1-\lambda'^2) \sin \omega_D (t-\tau) + 2\lambda' \cos \omega_D (t-\tau))\, d\tau \right|$$

$$\lambda' = \frac{\lambda}{\sqrt{1-\lambda^2}}$$

APPENDIX 2

RESPONSE PROGRAM - RESP 3F/ FORTRAN II

I. DESCRIPTION

Given the acceleration function, the program allows the calculation of:

1. The velocity and displacement of ground motion.
2. The Fourier spectra of the acceleration function (sine transform, cosine transform, amplitude spectra, phase spectra), the power spectral density, and the response spectra of the acceleration function (relative displacement, relative velocity, pseudo-relative velocity, absolute acceleration, pseudo-absolute acceleration).
3. The time response of a single-degree of freedom system to be given acceleration function (relative displacement, relative velocity, absolute acceleration).

II. OPERATION

Initialization

First, the computer reads a control card which allows different modes of operation. The second data card specifies the input FORMAT. The third data card specifies the output FORMAT both on BCD tape and the print statements of the first part of the program. The fourth card contains a Hollerith field for identification purposes and a numerical field which specifies the number of points of the input function. After the fourth card, the function is read into the computer. There are three ways in which the input function can be specified, namely:

A. Function may be punched on cards giving abscissas and ordinates consecutively (control card NF = 1).

B. Function may be punched on cards giving the consecutive ordinates only for those functions defined at constant time increments. (Control card NF = 2.) In this case an extra card must be placed in front of the function deck to specity the origin of ordinates, scale of ordinates, and size of the increment. In this case the input cards are printed using output format.

C. Function given in BCD tape by its abscissas and ordinates (control card NF = 3). A call to the position subroutine allows the computer to select the tape unit, the files that must be skipped before the record at which the function begins (control card NQ = logical tape unit, N1 = files to be skipped, N2 = records to be skipped).

In all three cases the function is printed. (Called reduced function).

The program then proceeds to check for illegal abscissas (non strictly monotonically increasing abscissas). In case of illegality, it prints a message specifying the point at which the error occurs and calls exit.

Next, the computer calculates the supremum of the given function and prints it together with the point number at which it occurs.

Now one has the option of reducing the function to maximal points (maximums and minimums only, throwing the rest away), (control card NA = 2). Then, the reduced function is printed.

The next card specifies the time interval, the initial velocity, the initial displacement, initial Fourier cosine and initial Fourier sine. Usually, the four last quantities are zero, so that the time interval is the only number to be specified leaving the rest of the card blank.

Interpolation Procedure

There are four options for the interpolation procedures:

A. Linear interpolation: Control card NA = 0.

B. No interpolation: Can be used only if the acceleration function is specified according to the second procedure (i.e. case B above), (control card NA = -1).

C. Sinusoidal interpolation:

   1. Sinusoidal interpolation of the given acceleration function (control card NA = 1).

   2. Sinusoidal interpolation of the reduced function to maximal points (control card NA = 2). So the option of reduced function to maximal points always requires sinusoidal interpolation.

Correction Procedure

There is provision for correcting the given acceleration function for zero final velocity. This correction performs a parallel displacement of the ordinates axis of the acceleration function such that the total net area of the function is zero. Whenever this correction is implied (control card NC = 1) it prints out the acceleration error = Vfinal/(tfinal - tinitial). Next, the computer calculates the supremum of the interpolated acceleration and prints the supremum.

Double Integration Option

The velocity and displacement functions are calculated by trapezoidal and Simpson's rule respectively, and the supremum of each are calculated and printed. Provision is made for printing the two integrated functions if desired (NP = 1 or NP = 3 on control card. See description of control

card at the end). Provision is also made for writing on tape the two integrated functions (control card NW = 1 or NW = 2).

Response Calculation

The computer calculates the Fourier and response spectra (control card ND = 1) or the time response (control card ND = 2). The next card specifies the printing FORMAT following by a card specifying the tape FORMAT. The next card specifies the number of and their values of the different damping ratios. When calculating only Fourier spectra and power spectral densities, the damping ratio is zero. Only one damping value is used in this case. Next card specifies the initial angular frequency, the increment of angular frequency, the number of different angular frequencies and the number of points at which the time response is desired. This last value is set equal to 1 for spectral response. In the case of time response, this number (equal to N) indicates the number of points at which the response is desired and divides the time domain of the given acceleration function into N equal intervals.

Next card specifies the instrument period and instrument damping coefficient if instrumental correction is desired. If instrumental correction is not required, this card should contain blanks. When using the instrumental correction, the control card allows one to choose a 2 point formula (NO = 1) or a 5 point formula (NO = 2) for calculating the initial derivative of the acceleration function which is needed for the instrumental correction. If the given acceleration function has zero initial derivative this parameter can be set equal to zero (NO = 0). Options for printing the response are NP = 2 or NP = 3, see control card. If one wishes to write the response on tape, let NT = 1. A provision is

made for repeating the entire program as many times as desired with different data (control card parameter RE). If a new function is to be read in, its value should be 2. If new calculations with the same function are required then its value should be 1. Exit is provided by placing a minus (-) sign in front of the numerical value of RE.

Control Card Description

NF = { 1 Cards (see IIA)
       2 Cards (see IIB)
       3 Tape (see IIC)

NQ = { 0 (no input tape is used)
       L (where L is the logical number of input tape)

N1 = Number of files to be skipped in input tape

N2 = Number of records to be skipped in desired file

NT = { 0 (if no output tape is used)
       M (where M is the logical number of output tape)

Functions of the first part of the program when written on output tape are controlled by:

NW =	Given function	Interpolated function	1st integral	2nd integral
0	no	no	no	no
1	yes	no	yes	yes
2	yes	yes	yes	yes

Functions of the second part of the program when written on output tape are controlled by:

NW2 = { 0 Does not write on output tape
        1 It writes on tape M the spectral response or the time response

NP =
- 0 No print
- 1 Prints integration (works only if NI = 1)
- 2 Prints spectral response or time response
- 3 Prints both

NA =
- -1 No interpolation (works only for NF = 2)
- 0 Linear interpolation
- 1 Sinusoidal interpolation
- 2 Same but using only maxima and minima

NC =
- 0 No correction
- 1 Zero final velocity correction

NI =
- 0 Does not integrate to give 1st integral and second integral of accelerogram
- 1 Calculates both first and second integrals

ND =
- 0 Does not calculate response spectra or time response
- 1 Calculates response spectra
- 2 Calculates time response

NO =
- 0 Zero initial derivative
- 1 2 point formula derivative
- 2 5 point formula derivative

Works only if instrumental correction is used.

RE =
- -2 Reads a new function and does not repeat
- -1 Does not read a new function and does not repeat
- 0 Call exit
- 1 Does not read a new function and repeat
- 2 Reads a new function and repeats

NTI =
- 0 No time given
- 1 Time printed

```
*     FORTRAN
(RESP3F 11/01/67 VICTOR JENSCHKE - RESPONSE PROGRAM

C     GIVEN THE ACCELERATION FUNCTION IT CALCULATES,
C     1.- THE VELOCITY AND DISPLACEMENT OF THE MOTION
C     2.- THE FOURIER SPECTRA OF THE ACCELERATION FUNCTION (SINE TRANSFORM, COSI
C     NE TRANSFORM, AMPLITUDE SPECTRUM, PHASE SPECTRUM, POWER SPECTRAL DENSITY)
C     AND THE RESPONSE SPECTRA OF THE ACCELERATION FUNCTION (RELATIVE DISPLACE-
C     MENT, RELATIVE VELOCITY, PSEUDORELATIVE VELOCITY, ABSOLUTE ACCELERATION,
C     PSEUDOABSOLUTE ACCELERATION)
C     3.- TIME RESPONSE OF A SINGLE DEGREE FREEDOM SYSTEM TO THE GIVEN ACCELE-
C     RATION FUNCTION (RELATIVE DISPLACEMENT, RELATIVE VELOCITY, ABSOLUTE ACCE-
C     LERATION)

      DIMENSION
     1U(40000),T(40000),A(16000),V(16000),D(16000),EMAA(6000),EMAV(6000),
     2EMAD(6000),Y(6000),UU(3000),TT(3000),
     3RD(1000),RV(1000),PSDY(1000),AA(1000),ST(1000),CT(1000),FTM(1000),
     4FTP(1000),W(1000),,TDIV(3000),
     5FMI(14),FMOP(14),FMOT(14),FMO(14),R(10)
      COMMON
     1U,T,A,
     2V,EMAA,EMAD,RD,RV,PSDY,AA,ST,CT,
     3D,EMAV,Y,UU,TT,FTM,FTP,W,TDIV,
     4FMI,FMOP,FMOT,FMO,R
      EQUIVALENCE
     1(V,EMAA),(V,EMAD),(V,RD),(V(1001),RV),(V(2001),PSDY),(V(3001),AA),
     2(V(4001),ST),(V(5001),CT),
     3(D,EMAV),(D,Y),(D,UU),(D(3001),TT),(D,FTM),(D(1001),FTP),(D(2001),
     4W),(D(3001),TDIV)

      NT1=0

C     INITIALIZATION
   91 READ 209,NF,NO,N1,N2,NT,NW,NW2,NP,NA,NC,NI,ND,NO,NRE,NT1
      PRINT209,NF,NO,N1,N2,NT,NW,NW2,NP,NA,NC,NI,ND,NO,NRE,NT1
  209 FORMAT(4H1    I1,4H    I1, 3H   I2, 3H   I2,4H    I1,4H    I1,4H
     1 I1,4H    I1,3H   I2 ,4H    I1,4H    I1,4H    I1,4H    I1,3H   I2,
     24H    I1)
      CALL TIMED(NT1)
  100 FORMAT(66H
     1                I4)
      NREP=XABSF(NRE)
      IF(NREP-1)1701,709,105
  105 READ 803,(FMI(I),I=1,14)
  803 FORMAT(14A6)
      PRINT1134,(FMI(I),I=1,14)
 1134 FORMAT(1X14A6)

      READ 803,(FMO(I),I=1,14)
      PRINT 1134,(FMO(I),I=1,14)
      READ 100,NMAX
      PRINT 100,NMAX

C     INPUT SELECTION
      GO TO (730,797,801),NF
  801 REWIND NO
      CALL POSITT(NO,N1,N2)
      READ INPUT TAPE NO,FMI,(T(N),U(N),N=1,NMAX)
      CALL TIMED(NT1)
      GO TO 208
  796 FORMAT(5H     E15.8,5H     E15.8,5H     E15.8)
  797 READ 796,Y0 ,SCL,DTN
      PRINT 796,Y0,SCL,DTN
      READ FMI,(Y(I),I=1,NMAX)
      PRINT FMO,(Y(I),I=1,NMAX)
      DO 794 I=1,NMAX
      Y(I)=Y(I)-Y0
      U(I)=Y(I)
      U(I)=SCL*U(I)
      EI=I
  794 T(I)=(EI-1.0)*DTN
      PRINT 793
  793 FORMAT (18H1 REDUCED FUNCTION)
      GO TO 208
  730 READ FMI,(T(N),U(N),N=1,NMAX)
  208 PRINTFMO,(T(N),U(N),N=1,NMAX)

C     CHECK FOR REPEATED ABCISAS
      B=-1.0
      DO 10 N=2,NMAX
      IF (T(N)-T(N-1))11,11,10
   11 PRINT 103,N,T(N),T(N-1)
  103 FORMAT(12H ERROR AT T(I4,2H)=F6.2/19H PREVIOUS TIME WAS F6.2)
      B=1.0
   10 CONTINUE
      IF(B)13,12,12
   12 CALL EXIT

C     SUP(U)
   13 SUPU=0.0
      NSUPU=1
      DO 7 N=1,NMAX
      IF(ABSF(U(N))-SUPU) 7,7,267
  267 SUPU=ABSF(U(N))
      NSUPU=N
    7 CONTINUE
      PRINT 556,SUPU,NSUPU
  556 FORMAT(10H0  SUP(A)=E20.6/10H    AT  N =I20)

C     WOT T(N),U(N)
      IF(NT)94,94,96
   96 IF(NT)95,95,94
   95 REWIND NT
      NT1=1
   94 IF(NW-1)709,700,700
  700 CONTINUE
      WRITE OUTPUT TAPE NT,100,NMAX
      WRITE OUTPUT TAPE NT,FMO,(T(N),U(N),N=1,NMAX)
      END FILE NT

C     REDUCTION TO MAXIMAL POINTS
  709 IF(NA-1)710,710,572
  572 K=1
      N=1
      UU(1)=U(1)
      TT(1)=T(1)
  573 IF((U(N+2)-U(N+1))*(U(N+1)-U(N)))574,574,575
  574 K=K+1
      UU(K)=U(N+1)
      TT(K)=T(N+1)
  575 N=N+1
      IF(NMAX-N-1)576,576,573
  576 NMAX=K
      K=1
      DO 577 N=1,NMAX
      U(N)=UU(K)
      T(N)=TT(K)
      K=K+1
  577 CONTINUE
      PRINT 97
   97 FORMAT(42H1 REDUCED FUNCTION TO MAX, AND MIN, POINTS)
      PRINT FMO,(T(N),U(N),N=1,NMAX)
  102 FORMAT( 4H    E16.9,3H   E12.5,3H   E12.5,3H   E12.5,3H   E12.5)

C     INTERPOLATION
  710 READ 102,DT,V1,DI,FC,FS
      PRINT 102,DT,V1,DI,FC,FS
      CALL TIMED(NT1)
      IF(NA)1016,1019,1019

C     AVOID INTERPOLATION
 1016 DO 1017 M=1,NMAX
      A(M)=U(M)
 1017 CONTINUE
      MMAX=NMAX
      GO TO 1020

C     LINEAR AND SINUSOIDAL INTERPOLATION
 1019 MMAX=(T(NMAX)-T(1))/DT+1.0
      N=1
      DO 20 M=1,MMAX
      EM=M
      IF(T(N)-T(1)-(EM-1.0)*DT)22,23,25
   22 N=N+1
      IF(T(N)-T(1)-(EM-1.0)*DT)22,23,24
   23 A(M)=U(N)
      GO TO 20
   24 IF(NA-1)824,924,924
  824 W=(U(N)-U(N-1))/(T(N)-T(N-1))
      GO TO 25
  924 UM=(U(N)+U(N-1))/2.0
      UL=(U(N)-U(N-1))/2.0
      TM=(T(N)+T(N-1))/2.0
      TL=(T(N)-T(N-1))
   25 IF(NA-1)825,925,925
  825 A(M)=((EM-1.0)*DT-(T(N-1)-T(1)))*W+U(N-1)

      GO TO 20
  925 A(M)=UM+UL*SINF(((EM-1.0)*DT-TM)*3.1415927/TL)
   20 CONTINUE

C     ZERO FINAL VELOCITY CORRECTION
 1020 IF(NC-1)731,721,731
  721 CONTINUE
      V(1)=0.0
      XDT=DT/2.0
      DO 30 M=2,MMAX
   30 V(M)=V(M-1)+XDT*(A(M-1)+A(M))
  104 FORMAT(29H FINAL EARTHQUAKE VELOCITY V(I4,2H)=E12.5)
      PRINT 104,MMAX,V(MMAX)
      EMMAX=MMAX
      DA=V(MMAX)/((EMMAX-1.0)*DT)
  114 FORMAT (23H ACCELERATION ERROR DA=E12.5)
      PRINT 114,DA
      SUPA=0.0
      MSUPA=1
      DO 29 M=1,MMAX
   29 A(M)=A(M)-DA
  731 DO 31 M=1,MMAX
      IF(ABSF(A(M))-SUPA)31,31,269
  269 SUPA=ABSF(A(M))
      MSUPA=M
   31 CONTINUE
      IF(NP-1)951,950,1950
 1950 IF(NP-2)951,951,950
  126 FORMAT(30H1          EQUIDIVIDED FUNCTION)
  950 PRINT 126
      DO 1400 M=1,MMAX
      EM=M-1
 1400 EMAA(M)=EM*DT
      PRINTFMO,(EMAA(M),A(M),M=1,MMAX)
  951 PRINT 557,SUPA,MSUPA
  557 FORMAT(10H0  SUP(A)=E20.6/10H    AT  M =I20)
      IF(NW-2)761,701,701
  701 CONTINUE
   26 WRITE OUTPUT TAPE NT,126
      DO 1500 M=1,MMAX
      EM=M-1
 1500 EMAA(M)=EM*DT
      WRITE OUTPUT TAPE NT,FMO,(EMAA(M),A(M),M=1,MMAX)
      END FILE NT

C     DOUBLE INTEGRATION OF GIVEN FUNCTION
  761 IF(NI-1)713,711,713
  711 V(1)=V1
      XDT=DT/2.0
      SUPV=0.0
      MSUPV=1
      DO 32 M=2,MMAX
      V(M)=V(M-1)+XDT*(A(M-1)+A(M))
      IF(ABSF(V(M))-SUPV)32,32,271
  271 SUPV=ABSF(V(M))
      MSUPV=M
   32 CONTINUE
      IF(NP-1)953,952,1952
 1952 IF(NP-2)953,953,952
```

```
      952 PRINT 148
          DO 1401 M=1,MMAX
          EM=M-1
     1401 EMAV(M)=EM*DT
          PRINTFMO,(EMAV(M),V(M),M=1,MMAX)
          PRINT 558,SUPV,MSUPV
      558 FORMAT(10H0  SUPV(V)=E20.6/10H    AT  M =I20)
          IF(NW-11712,702,702
      702 CONTINUE
       39 WRITE OUTPUT TAPE NT,148
      148 FORMAT(24H1           FIRST INTEGRAL)
          DO 1501 M=1,MMAX
          EM=M-1
     1501 EMAV(M)=EM*DT
          WRITE OUTPUT TAPE NT,FMO,(EMAV(M),V(M),M=1,MMAX)
          END FILE NT
      712 D(1)=D1
          YDT=DT/3.0
          SUPD=0.0
          LSUPD=1
          DO 40 M=3,MMAX,2
          L=(M-1)/2
          D(L)=D(L-1)+YDT*(V(M-2)+4.0*V(M-1)+V(M))
          IF(ABSF(D(L))-SUPD)40,40,272
      272 SUPD=ABSF(D(L))
          LSUPD=L
       40 CONTINUE
          LMAX=L
          IF(NP-1)1955,954,1954
     1954 IF(NP-2)1955,955,954
      954 PRINT 149
          DO 1402 M=1,LMAX
          EM=M-1
     1402 EMAD(M)=2.0*DT*EM
          PRINTFMO,(EMAD(M),D(M),M=1,LMAX)
      955 PRINT 559,SUPD,LSUPD
      559 FORMAT(10H0  SUP(D)=E20.6/10H    AT  L =I20)
          IF(NW-11713,703,703
      703 CONTINUE
       48 WRITE OUTPUT TAPE NT,149
      149 FORMAT(25H1           SECOND INTEGRAL)
          DO 1502 M=1,LMAX
          EM=M-1
     1502 EMAD(M)=2.0*DT*EM
          WRITE OUTPUT TAPE NT,FMO,(EMAD(M),D(M),M=1,LMAX)
          END FILE NT
      713 CALL TIMED(NTI)

C         RESPONSE
          IF(ND-1)89,722,722
      722 READ  803,(FMOP(I),I=1,14)
          READ  803,(FMOT(I),I=1,14)
          PRINT1134,(FMOP(I),I=1,14)
          PRINT1134,(FMOT(I),I=1,14)
      122 FORMAT(8H          I2,3H    F7.4,3H    F7.4,3H    F7.4,3H    F7.4,
         13H    F7.4,3H    F7.4)
          READ  122,NRMAX,(R(NR),NR=1,NRMAX)
          PRINT 122,NRMAX,(R(NR),NR=1,NRMAX)
      132 FORMAT( 4H     E16.9, 4H     E16.9,5H      I5,5H      I5)
```

```
          READ  132,WMIN,DW,IMAX,JMAX
          PRINT 132,WMIN,DW,IMAX,JMAX
      133 FORMAT(5H      E15.8,5H      E15.8)
          READ 133,TS,ES
          PRINT133,TS,ES
          IF(TS)602,602,601
      601 PS=6.2831853/TS
          AO=LOGF(ES)
          RS=AO/SQRTF(9.8696044+AO*AO)
      602 MMAX=((MMAX-1)/2)*2+1
          D2=24.0*DT
          IF(NO-1)1,2,3
        1 DERA1=0.0
          GO TO 4
        2 DERA1=(A(2)-A(1))/DT
          GO TO 4
        3 DERA1=(-50.0*A(1)+96.0*A(2)-72.0*A(3)+32.0*A(4)-6.0*A(5))/D2
        4 H=DT/3.0
          DO 89 NR=1,NRMAX
          RR=SQRTF(1.0-R(NR)*R(NR))
          RRR=R(NR)/RR
          R2=2.0*R(NR)
          W(1)=WMIN
          DO 88 I=1,IMAX
          EIA=(I-1)
          W(I)=W(1)+EIA*DW
          WD=W(I)*RR
          D1=WD*DT
          HW=H*W(I)
          RW=R(NR)*W(I)
          IF(TS)604,604,603
      603 PS2=PS*PS
          AAA=1.0-2.0*RS*RW/PS+(RW*RW-WD*WD)/PS2
          BBB=2.0*WD*(RS/PS-RW/PS2)
          D2PS2=D2*PS2*H
          CCC=(2.0*RS/PS-RW/PS2)/H
          DDD=WD/(PS2*H)
          EEE1=DERA1/(PS2*H)+CCC*A(1)
          EEE2=A(1)*DDD
      604 RWDT=RW*DT
          HI=H/WD
          EXP1=EXPF(RWDT)
          EXP2=EXPF(2.0*RWDT)
          J=1
          CC=FC/H
          SS=FS/H
          S1MAX=0.0
          RVHMAX=0.0
          AAHMAX=0.0
          COS3=1.0
          SIN3=0.0
          COSD1=COSF(D1)
          SIND1=SINF(D1)
          DD1=2.0*D1
          COSD2=COSF(DD1)
          SIND2=SINF(DD1)
          DO 85 M=3,MMAX,2
          EMA=M-1
          COS1=COS3
          SIN1=SIN3
          COS2=COS1*COSD1-SIN1*SIND1
          SIN2=SIN1*COSD1+COS1*SIND1
          COS3=COS1*COSD2-SIN1*SIND2
          SIN3=SIN1*COSD2+COS1*SIND2
          CC=(CC+A(M-2)*COS1)/EXP2+(A(M-1)*COS2)/EXP1+A(M)*COS3
          SS=(SS+A(M-2)*SIN1)/EXP2+(A(M-1)*SIN2)/EXP1+A(M)*SIN3
          IF(TS)690,690,691
      691 EEE1=EEE1/EXP2
          EEE2=EEE2/EXP2
          IF(M-MMAX)693,696,696
      693 FFF=12.0*A(M-2)-16.0*A(M-1)+16.0*A(M)-2.0*A(M-3)/EXP2+(CC*A(M)
          GO TO 695
      694 FFF=14.0*A(M-4)-32.0*A(M-3)+72.0*A(M-2)-96.0*A(M-1)+50.0*A(M)/
         1EXP2+CCC*A(M)
      695 GGG=DDD*A(M)
          CF=AAA*CC+BBB*SS+FFF*COS3+GGG*SIN3-EEE1
          SF=AAA*SS-BBB*CC+FFF*SIN3-GGG*COS3-EEE2
          GO TO 692
      690 CF=CC
          SF=SS
      692 S1=SIN3*CF-COS3*SF
          C1=COS3*CF+SIN3*SF
          RVH=C1-RRR*S1
          AAH=S1/RR+R2*RVH
          IF(MD-1)689,680,681
      681 S1MAX=S1
          RVHMAX=RVH
          AAHMAX=-AAH
          GO TO 86
      680 IF(ABSF(S1)-S1MAX)71,71,70
       70 S1MAX=ABSF(S1)
       71 IF(ABSF(RVH)-RVHMAX)73,73,72
       72 RVHMAX=ABSF(RVH)
       73 IF(ABSF(AAH)-AAHMAX)86,86,74
       74 AAHMAX=ABSF(AAH)
       86 IF(MD-1)89,986,987
      987 EJ=J
          EMHMAX=MMMAX
          EJMAX=JMAX
          IF(EJ*(EMHMAX-1.01)-EJMAX*EMA)80,80,85
      986 IF(J*(MMMAX-1)-JMAX*(M-1))80,80,85
       80 TDIV(J)=EMA*DT
          IJ=I+(J-1)*IMAX
          RD  (IJ)=W1*S1MAX
          RV  (IJ)=H*RVHMAX
          AA  (IJ)=HW*AAHMAX
          ST  (IJ)=SF*H
          CT  (IJ)=CF*H
          XXYY=ST(IJ)*ST(IJ)+CT(IJ)*CT(IJ)
          FTM(IJ)=SQRTF(XXYY)
          TTXX=6.2831853*TDIV(J)
          PSDY(IJ)=XXYY/TTXX
          FTP(IJ)=ATANF(ST(IJ)/CT(IJ))
       82 J=J+1
       85 CONTINUE
       88 CONTINUE

C         RESPONSE OUTPUT
```

```
          IF(ND-1)89,1660,1661
     1660 K11=JMAX
          L11=IMAX
          GO TO 660
     1661 K11=IMAX
          L11=JMAX
      660 DO 505 K=1,K11
          DO 506 L=1,L11
          IF(ND-1)89,1760,1761
     1760 J=K
          I=L
          GO TO 1750
     1761 I=K
          J=L
     1750 IJ=I+(J-1)*IMAX
          PER=6.2831853/W(I)
          PSRV=RR*W(I)*RD(IJ)
          PSAA=W(I)*PSRV
          IF(NP-2)1700,213,213
      213 IF(L-1)89,997,998
      997 PRINT 211,NR,R(NR)
      211 FORMAT(20H1   DAMPING RATIO R(I2,2H)=F7.4,61H TDIV, PER, W, RD, RV
         1, PSRV, AA, PSAA, PSDY, ST, CT, FTM, FTP)
      998 PRINT FMOP,TDIV(J),PER,W(I),RD(IJ),RV(IJ),PSRV    ,AA(IJ),PSAA,
         1PSDY(IJ),ST(IJ),CT(IJ),FTM(IJ),FTP(IJ)
     1700 IF(NW2-1)506,333,333
      333 IF(L-1)89,500,504
      500 WRITE OUTPUT TAPE NT,211,NR,R(NR)
      504 WRITE OUTPUT TAPE NT,FMOT,TDIV(J),PER,W(I),RD(IJ),RV(IJ),PSRV
         1AA(IJ),PSAA,PSDY(IJ),ST(IJ),CT(IJ),FTM(IJ),FTP(IJ)
      506 CONTINUE
          IF(NW2-1)505,334,334
      334 END FILE NT
      505 CONTINUE
       89 CONTINUE
          CALL TIMED(NTI)

C         ENDING
          IF(NRE)90,90,91
       90 IF(NW+NW2-1)716,706,706
      706 CONTINUE
          CALL REWUNL (NT)
      716 CONTINUE
          IF(NO)1701,1701,1702
     1702 CALL REWUNL(NO)
     1701 CONTINUE
          CALL TIMED(NTI)
          CALL EXIT
          END


*         FORTRAN
          SUBROUTINE TIMED(N)

          IF(N1)1,1,2
        2 CALL TIME(A)
          B=(A-A1)*60.0
          PRINT 3,A,B
        3 FORMAT(12H0ABS. TIME =F8.2,21H MIN       REL. TIME =F8.2,4H SEC/)
```

```
      A1=A
    1 RETURN
      END

C     SAMPLE PROBLEM

*     DATA
INF=1NO=  N1=  N2=  NT=  NW=  NW2= NP= 3NA=  NC=  NI= 1NO= 1NO=  RE=-2NT1=1
(E25.8,3E15.8)
(8E15.8)
0HALF SINE FUNCT, CHECK - AMPLIT=1.0,LENGTH=0.1,FREE ERA=0.6          102
          0.00000000E 00 0.00000000E 00 0.10000000E-02 0.31410000E-01
          0.20000000E-02 0.62790000E-01 0.30000000E-02 0.94110000E-01
          0.40000000E-02 0.12533000E 00 0.50000000E-02 0.15643000E 00
          0.60000000E-02 0.18738000E 00 0.70000000E-02 0.21814000E 00
          0.80000000E-02 0.24869000E 00 0.90000000E-02 0.27899000E 00
          0.10000000E-01 0.30902000E 00 0.11000000E-01 0.33874000E 00
          0.12000000E-01 0.36812000E 00 0.13000000E-01 0.39715000E 00
          0.14000000E-01 0.42578000E 00 0.15000000E-01 0.45399000E 00
          0.16000000E-01 0.48175000E 00 0.17000000E-01 0.50904000E 00
          0.18000000E-01 0.53583000E 00 0.19000000E-01 0.56229000E 00
          0.20000000E-01 0.58779000E 00 0.21000000E-01 0.61271000E 00
          0.22000000E-01 0.63742000E 00 0.23000000E-01 0.66131000E 00
          0.24000000F-01 0.68455000E 00 0.25000000E-01 0.70711000E 00
          0.26000000E-01 0.72897000E 00 0.27000000E-01 0.75011000E 00
          0.28000000E-01 0.77051000E 00 0.29000000E-01 0.79015000E 00
          0.30000000E-01 0.80902000E 00 0.31000000E-01 0.82708000E 00
          0.32000000E-01 0.84433000E 00 0.33000000E-01 0.86074000E 00
          0.34000000E-01 0.87631000E 00 0.35000000E-01 0.89101000E 00
          0.36000000E-01 0.90483000E 00 0.37000000E-01 0.91775000E 00
          0.38000000E-01 0.92978000E 00 0.39000000E-01 0.94088000E 00
          0.40000000E-01 0.95106000E 00 0.41000000E-01 0.96029000E 00
          0.42000000E-01 0.96858000E 00 0.43000000E-01 0.97592000E 00
          0.44000000E-01 0.98229000E 00 0.45000000E-01 0.98769000E 00
          0.46000000E-01 0.99211000E 00 0.47000000E-01 0.99556000E 00
          0.48000000E-01 0.99803000E 00 0.49000000E-01 0.99951000E 00
          0.50000000E-01 0.10000000E 01 0.51000000E-01 0.99951000E 00
          0.52000000E-01 0.99803000E 00 0.53000000E-01 0.99556000E 00
          0.54000000E-01 0.99211000E 00 0.55000000E-01 0.98769000E 00
          0.56000000E-01 0.98229000E 00 0.57000000E-01 0.97592000E 00
          0.58000000E-01 0.96858000E 00 0.59000000E-01 0.96029000E 00
          0.60000000E-01 0.95106000E 00 0.61000000E-01 0.94088000E 00
          0.62000000E-01 0.92978000E 00 0.63000000E-01 0.91775000E 00
          0.64000000E-01 0.90483000E 00 0.65000000E-01 0.89101000E 00
          0.66000000E-01 0.87631000E 00 0.67000000E-01 0.86074000E 00
          0.68000000E-01 0.84433000E 00 0.69000000E-01 0.82708000E 00
          0.70000000E-01 0.80902000E 00 0.71000000E-01 0.79016000E 00
          0.72000000E-01 0.77051000E 00 0.73000000E-01 0.75011000E 00
          0.74000000E-01 0.72897000E 00 0.75000000E-01 0.70711000E 00
          0.76000000E-01 0.68455000E 00 0.77000000E-01 0.66131000E 00
          0.78000000E-01 0.63742000E 00 0.79000000E-01 0.61291000E 00
          0.80000000E-01 0.58779000E 00 0.81000000E-01 0.56229000E 00
          0.82000000E-01 0.53583000E 00 0.83000000E-01 0.50904000E 00
          0.84000000E-01 0.48175000E 00 0.85000000E-01 0.45399000E 00
          0.86000000E-01 0.42578000E 00 0.87000000E-01 0.39715000E 00
          0.88000000E-01 0.36812000E 00 0.89000000E-01 0.33874000E 00
          0.90000000E-01 0.30902000E 00 0.91000000E-01 0.27899000E 00
          0.92000000E-01 0.24869000E 00 0.93000000E-01 0.21814000E 00



          0.94000000E-01 0.18738000E 00 0.95000000E-01 0.15643000E 00
          0.96000000E-01 0.12533000E 00 0.97000000E-01 0.94110000E-01
          0.98000000E-01 0.62790000E-01 0.99000000E-01 0.31410000E-01
          0.10000000E 00 0.00000000E 00 0.60000000E 00 0.00000000E 00
ODT= 0.1          E-02
(XF2.0,10E12.5,2F1.0)
(XF2.0,10E12.5,2F1.0)
ONRMAX=  2R1= 0.0    R2= 0.20
0 W= 0.7853981633E 01 DW= 0.7853981633E 01IMAX=     3JMAX=     1
OTS=                  ES=
```

APPENDIX 3

List of Graphs

	Page
Ground Accelerations - Underground Nuclear Blasts (UNB)	67-75
- Earthquakes (EQ)	76-80
Ground Velocity - UNB	81-89
- EQ	90-93
Ground Displacement - UNB	94-102
- EQ	103-106
Relative Displacement Spectra - UNB (F*)	107-112
- EQ (F)	113-114
- UNB(P**)	115-116
- EQ (P)	117
Relative Velocity Spectra - UNB (F)	118-123
- EQ (F)	124-125
- UNB (P)	126-127
- EQ (P)	128-129
Pseudo Relative Velocity Spectra - UNB (F)	130-132
- EQ (F)	133
Absolute Acceleration Spectra - UNB (F)	134-139
- EQ (F)	140-141
- UNB (P)	142-143
- EQ (P)	144-145
Pseudo Absolute Acceleration Spectra - UNB (F)	146-148
- EQ (F)	149
Fourier Amplitude Spectra - UNB	150-155
- EQ	156-157
Fourier Phase Spectra - UNB, EQ	158
Sine Transform, Cosine Transform - UNB	159
Power Spectral Density - UNB	160
Fourier Spectra,- EQ	161-162

* Spectral quantities are plotted against frequency.
** Spectral quantities are plotted against period.

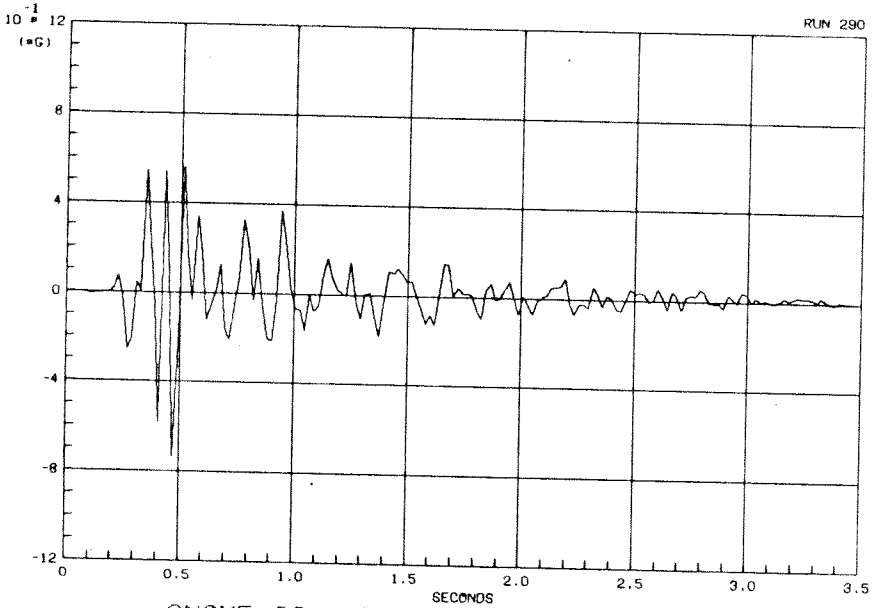

GNØME S2 - TRANSVERSE ACCELERATION

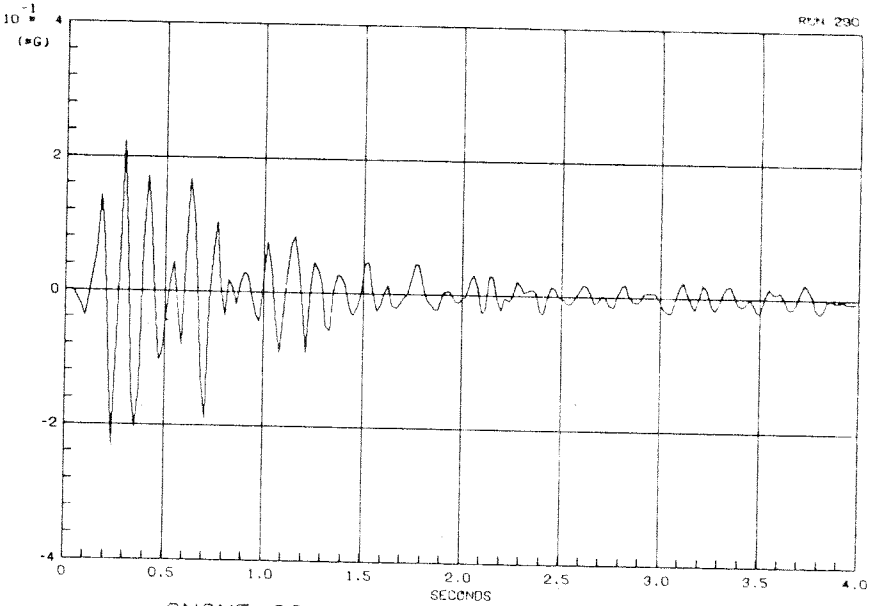

GNØME S3 - TRANSVERSE ACCELERATION

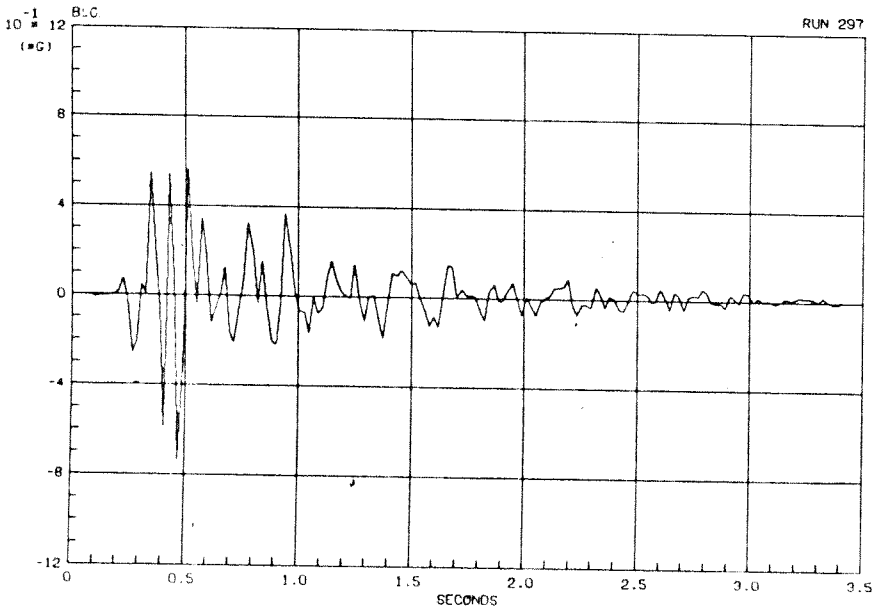

GNØME S2 - TRANSVERSE ACCELERATION

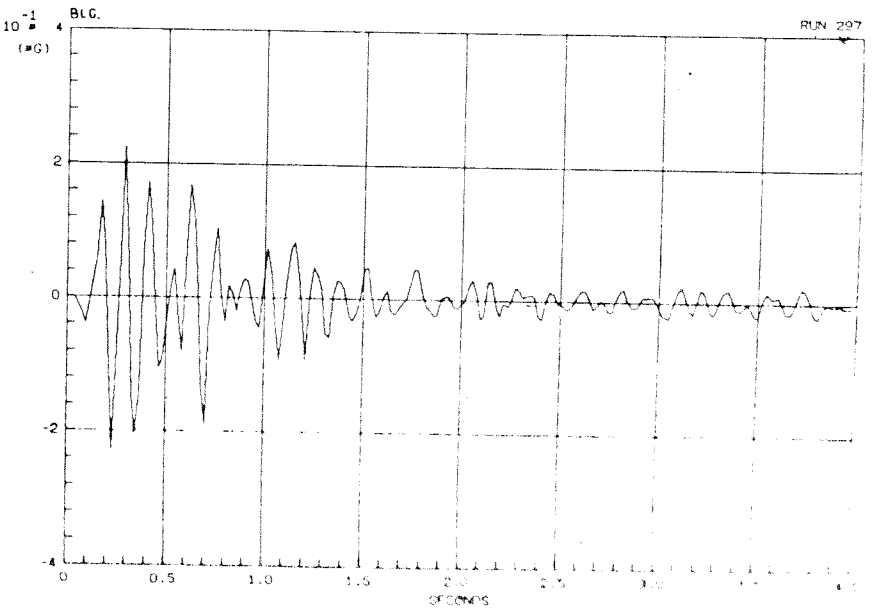

GNØME S3 - TRANSVERSE ACCELERATION

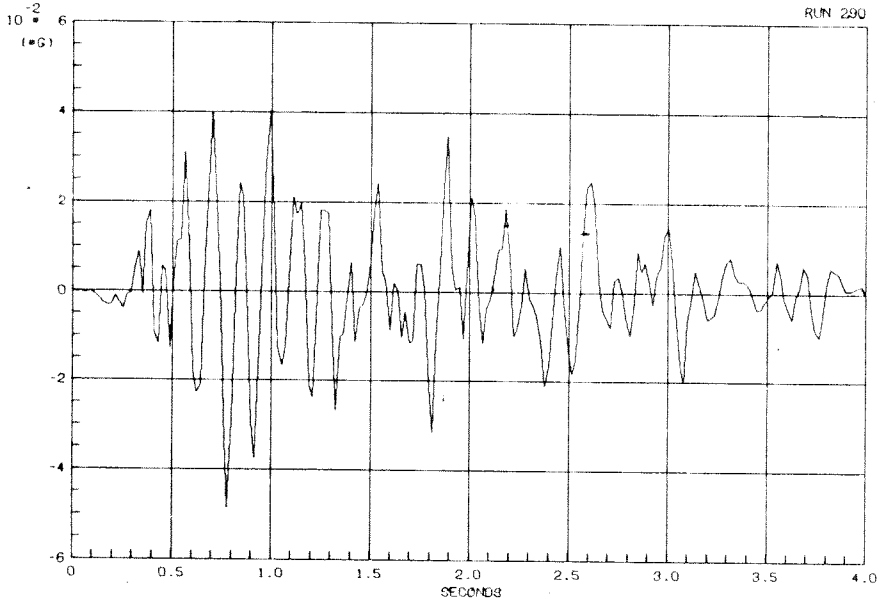

GNOME S4 - RADIAL ACCELERATION

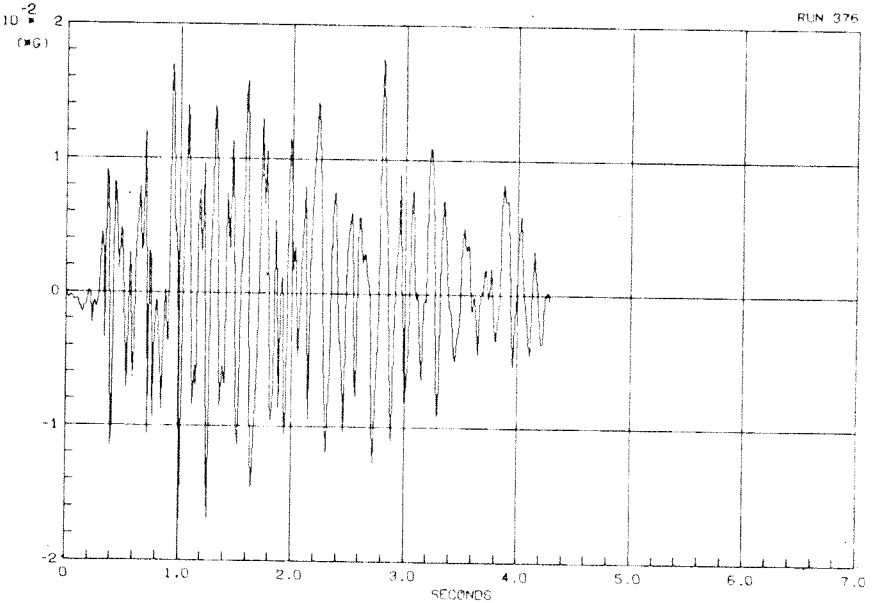

GNOME S4 - TRANSVERSE ACCELERATION

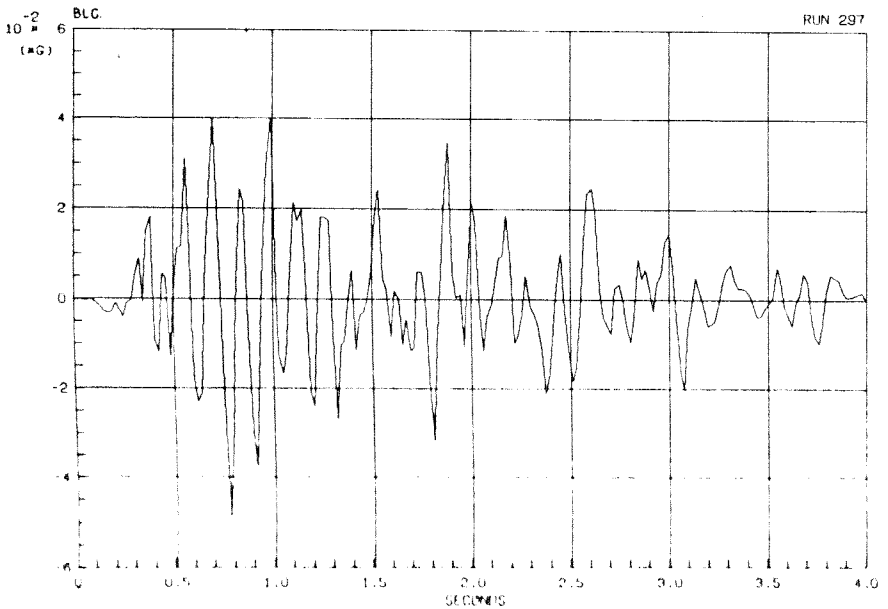

GNOME S4 - RADIAL ACCELERATION

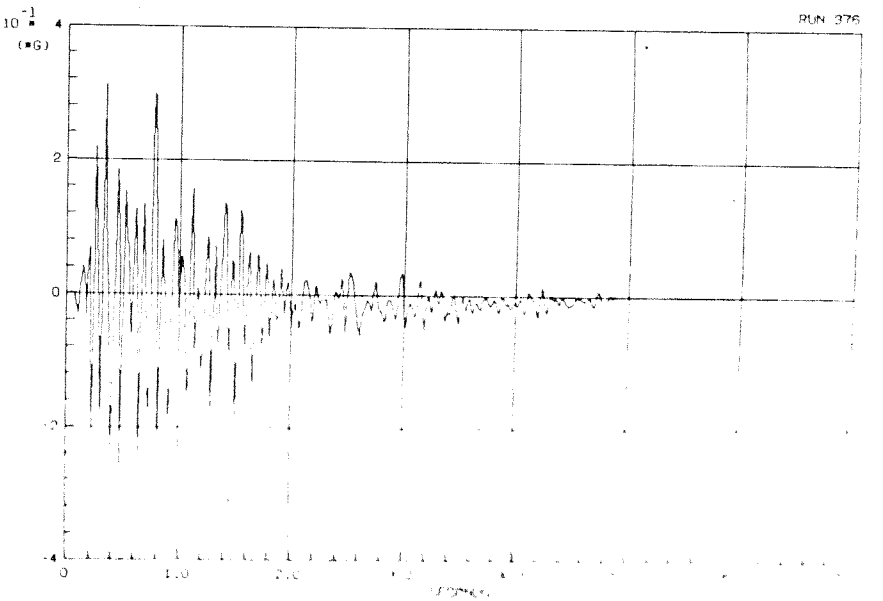

GNOME S4 - TRANSVERSE ACCELERATION

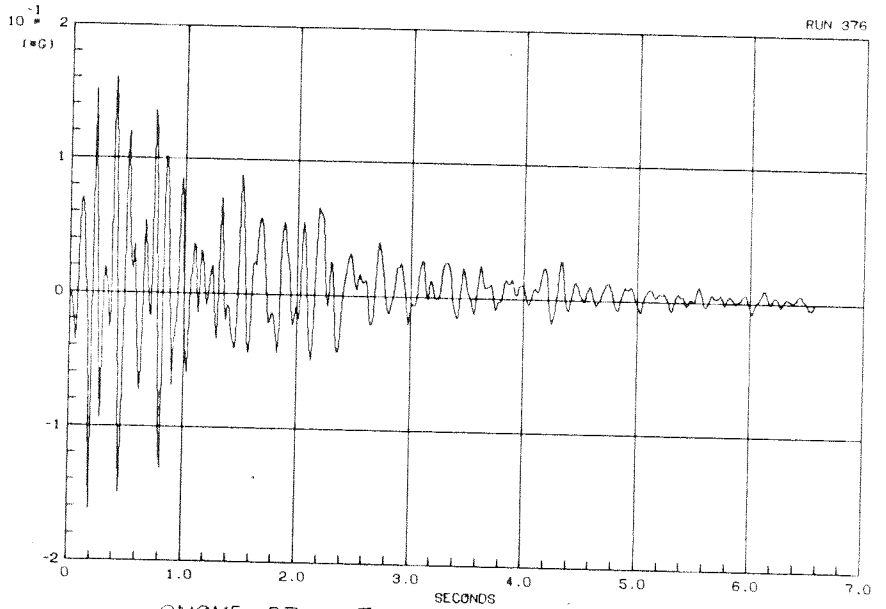

GNOME S7 TRANSVERSE ACCELERATION

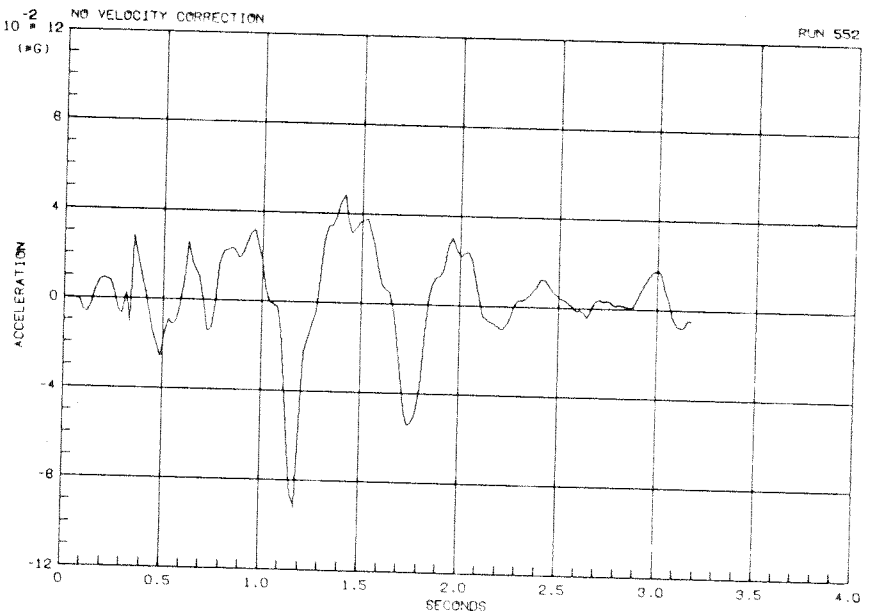

DANNYBOY D5 - RADIAL

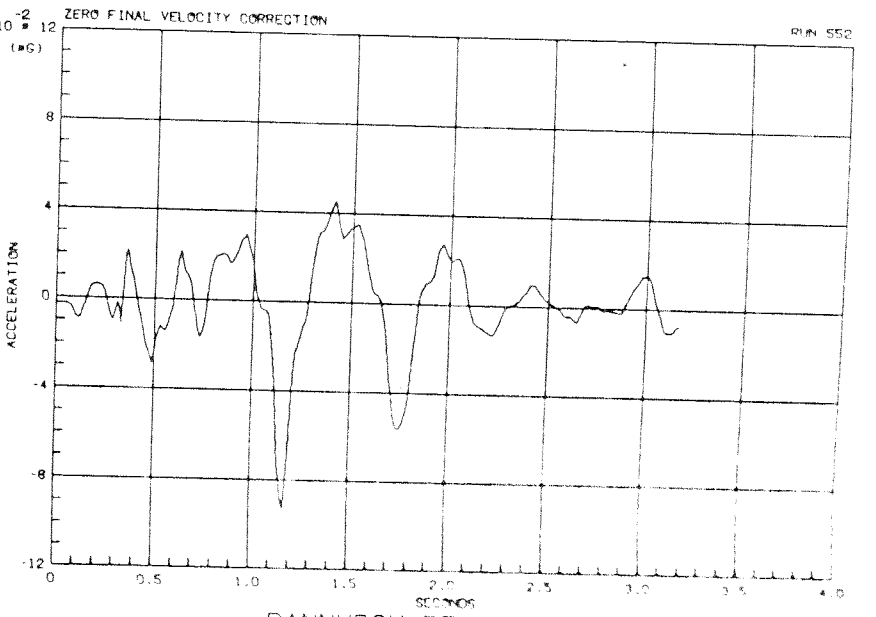

DANNYBOY D5 - RADIAL

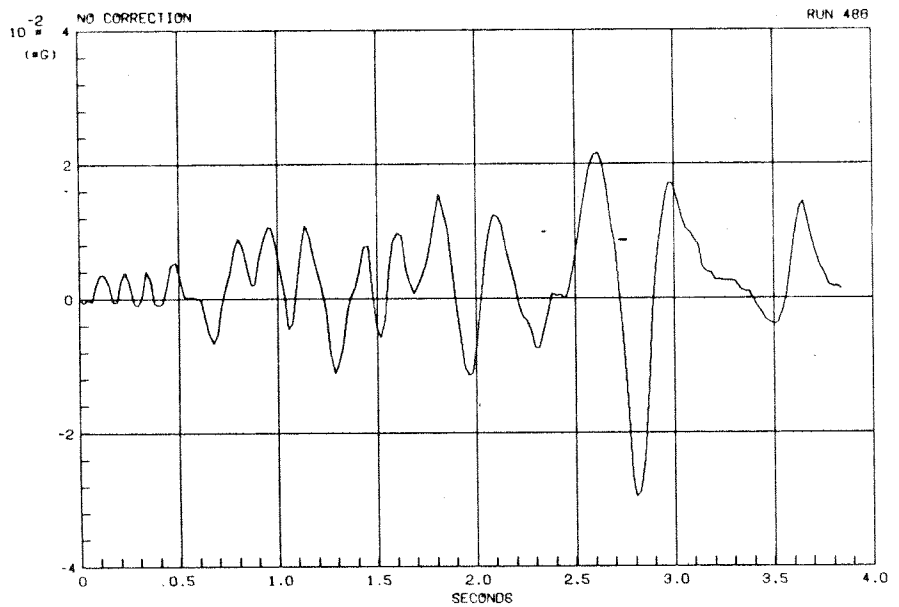

DANNYBØY D8 - RADIAL ACCELERATION

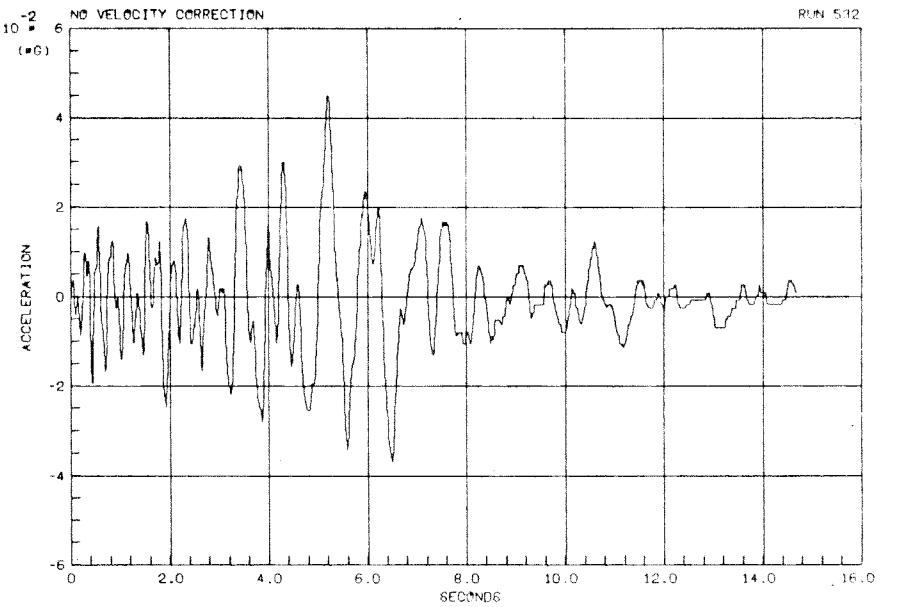

MISSISSIPPI 1777 - TRANSVERSE

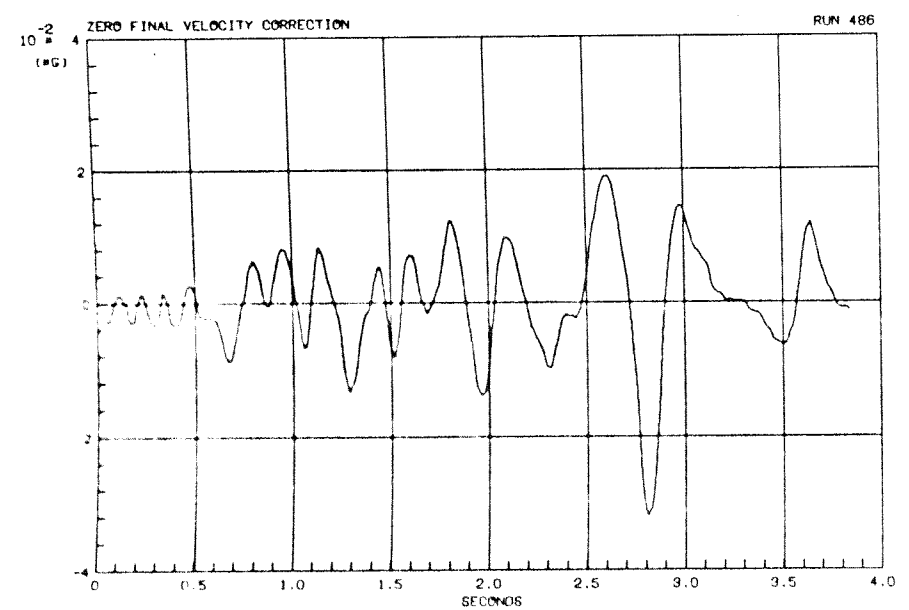

DANNYBØY D8 - RADIAL ACCELERATION

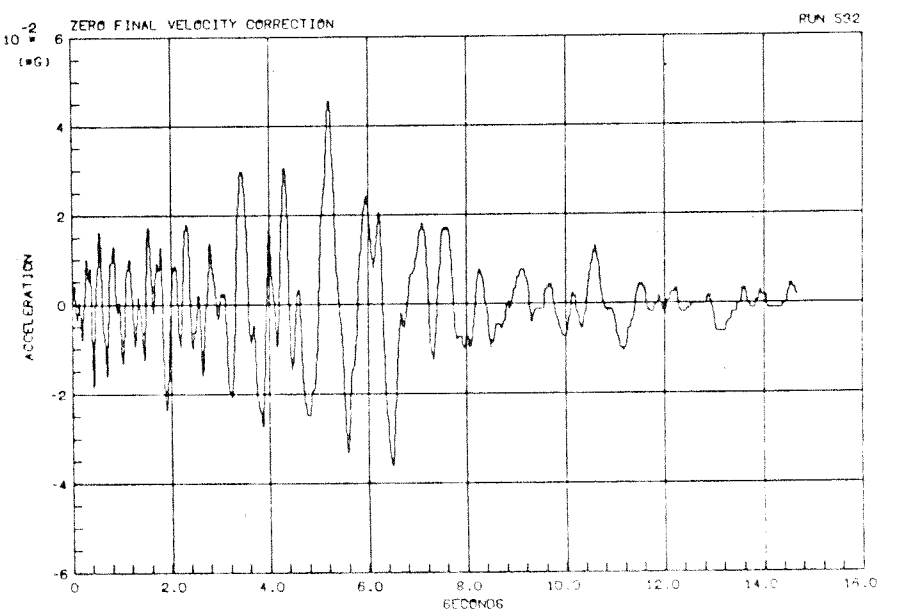

MISSISSIPPI 1777 - TRANSVERSE

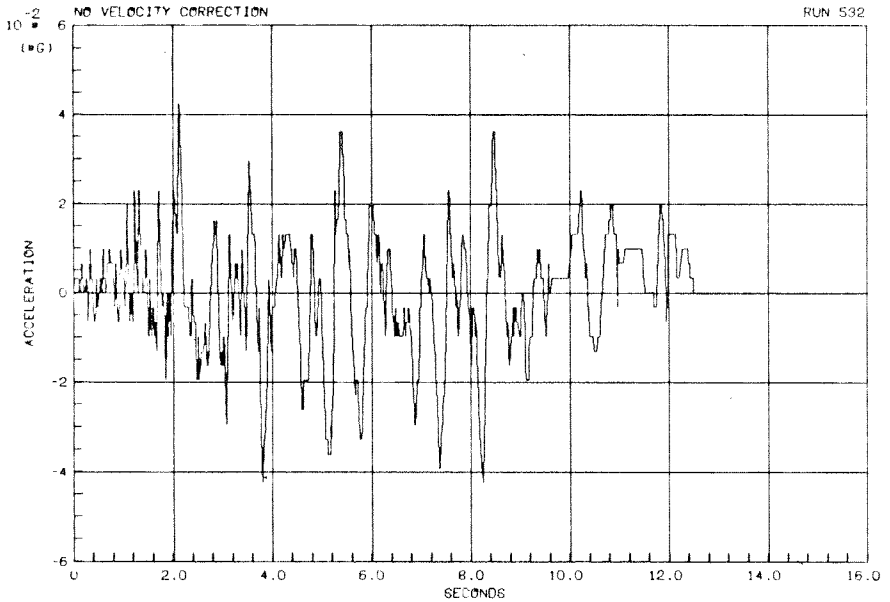

MISSISSIPPI 8228 - TRANSVERSE

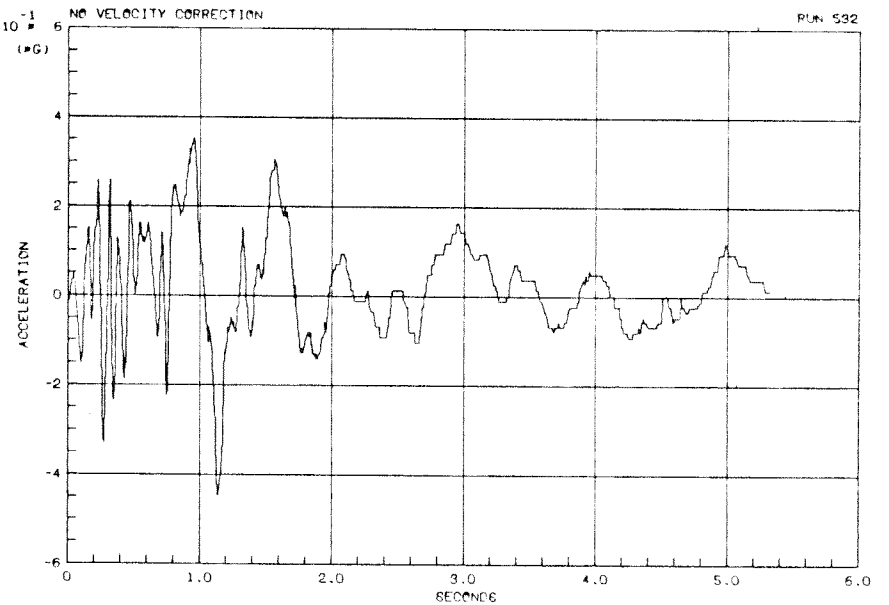

MISSISSIPPI 7245 - RADIAL

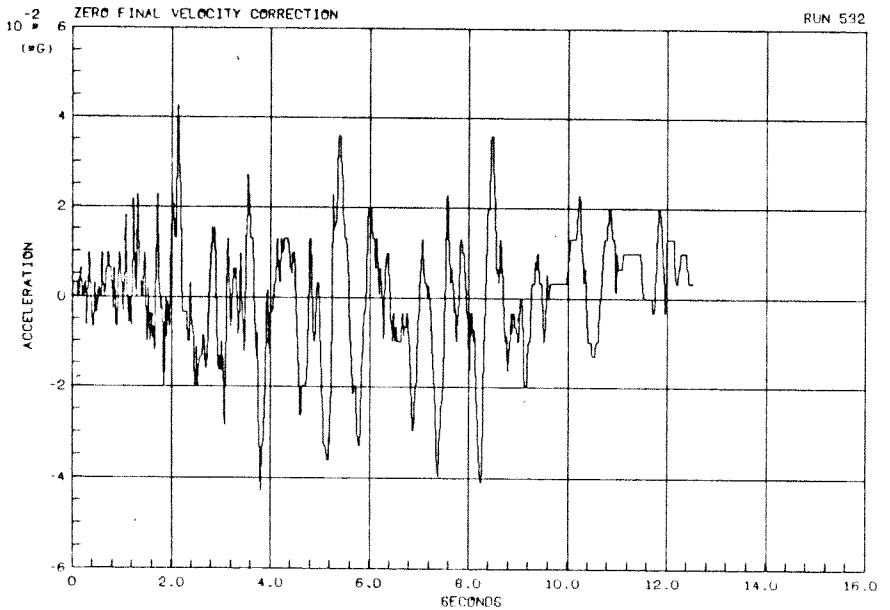

MISSISSIPPI 8228 - TRANSVERSE

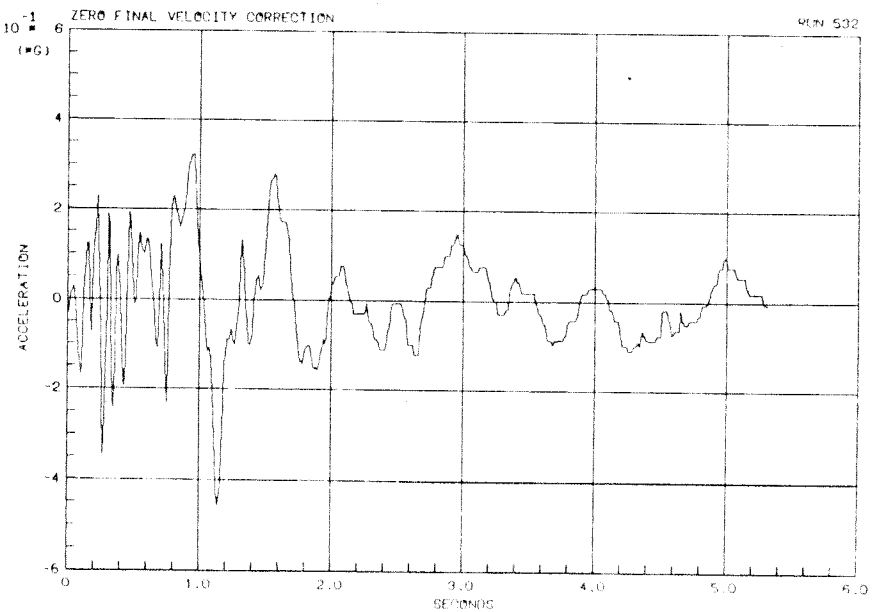

MISSISSIPPI 7245 - RADIAL

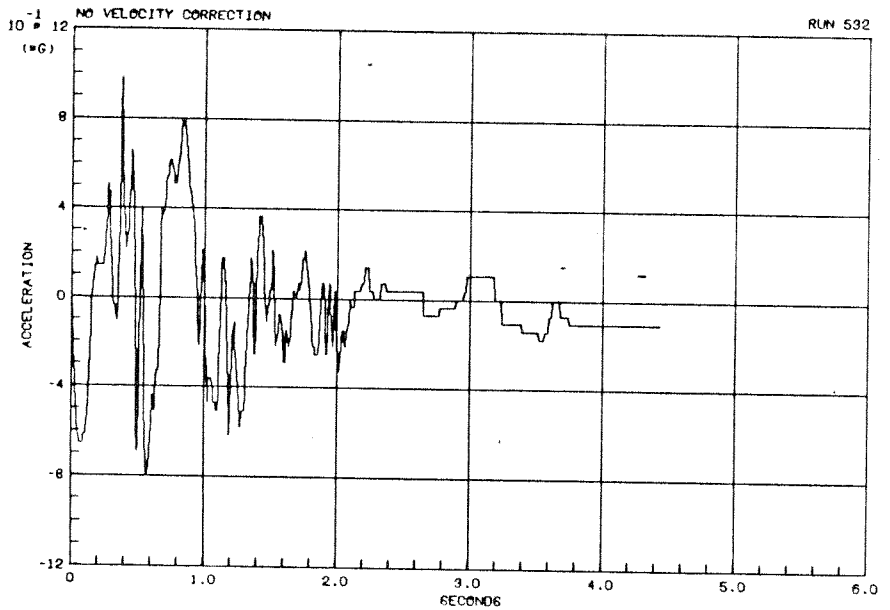

MISSISSIPPI 9537 - RADIAL

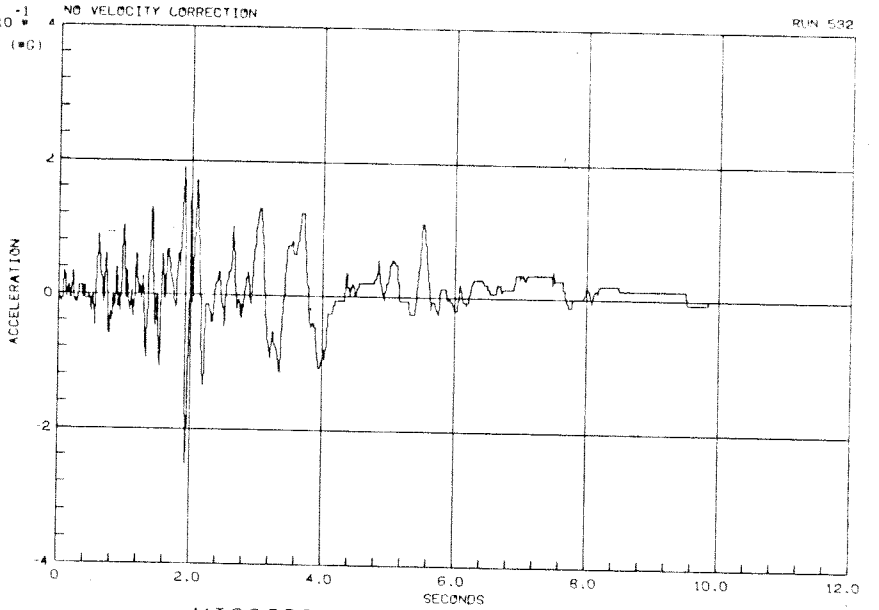

MISSISSIPPI 4074 - TRANSVERSE

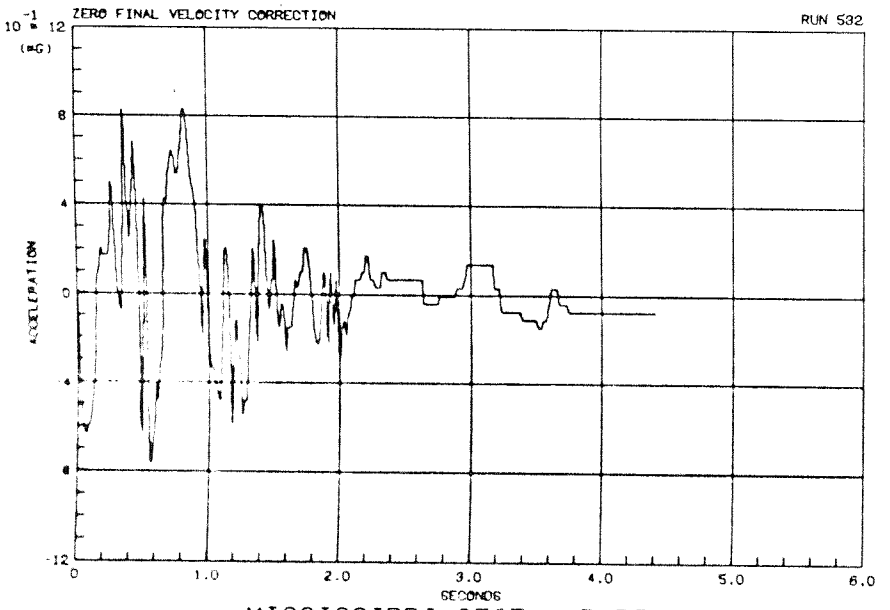

MISSISSIPPI 9537 - RADIAL

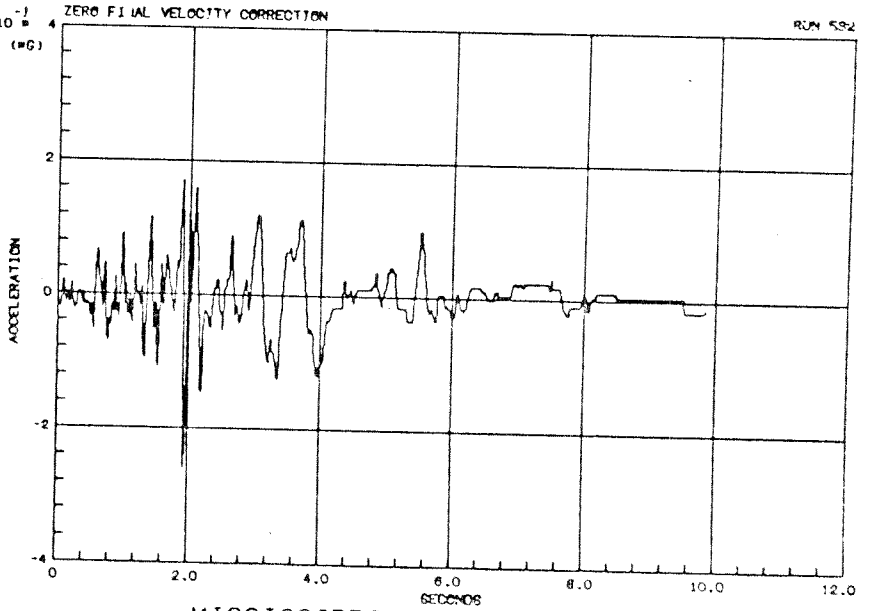

MISSISSIPPI 4074 - TRANSVERSE

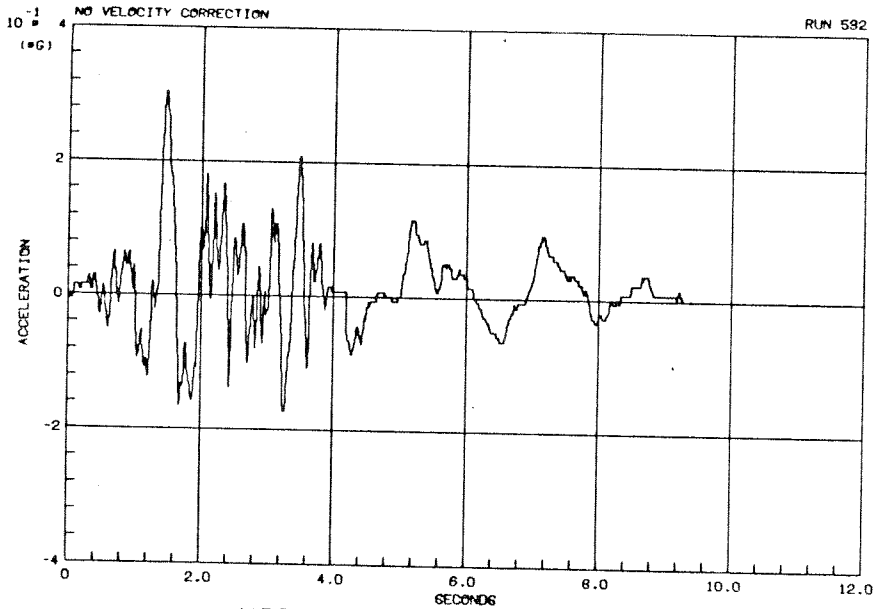

MISSISSIPPI 4074 - RADIAL

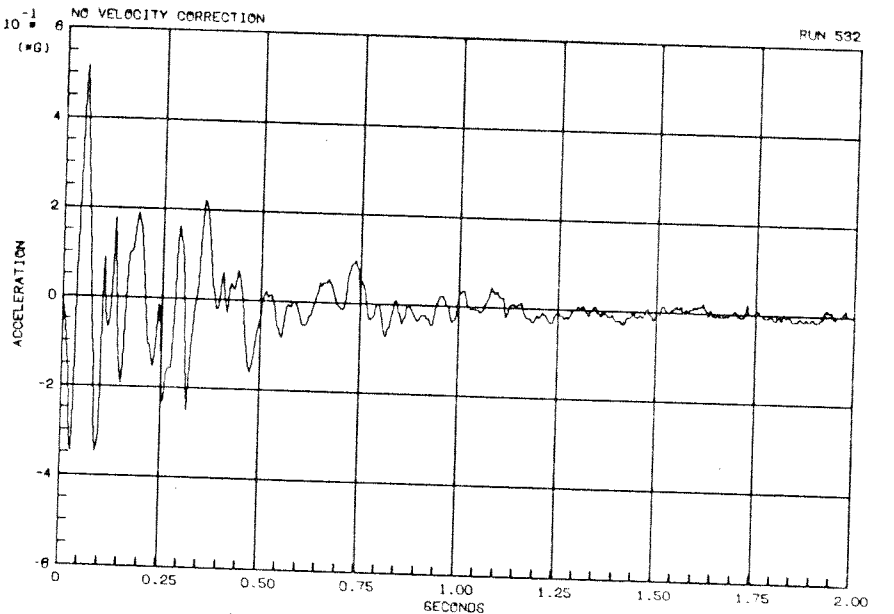

HARDHAT 1091 - TRANSVERSE

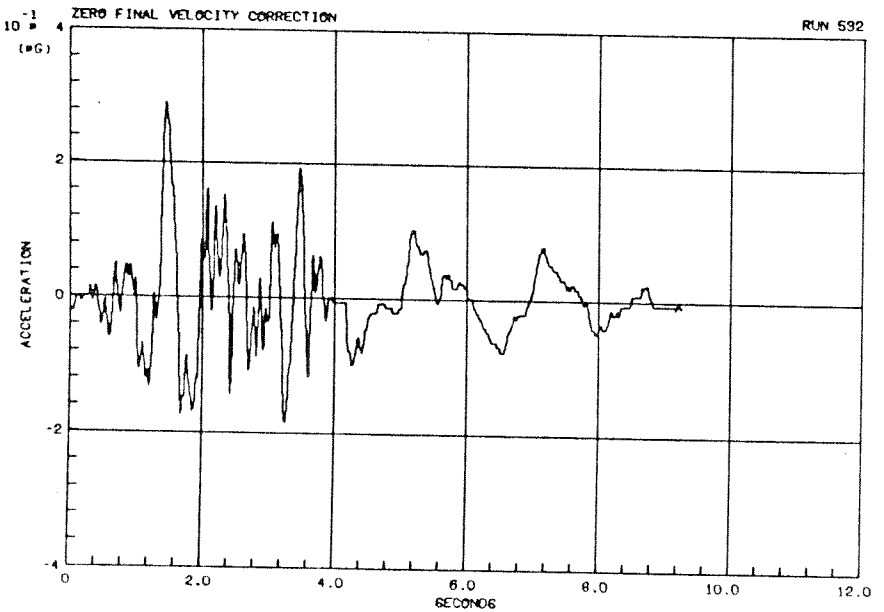

MISSISSIPPI 4074 - RADIAL

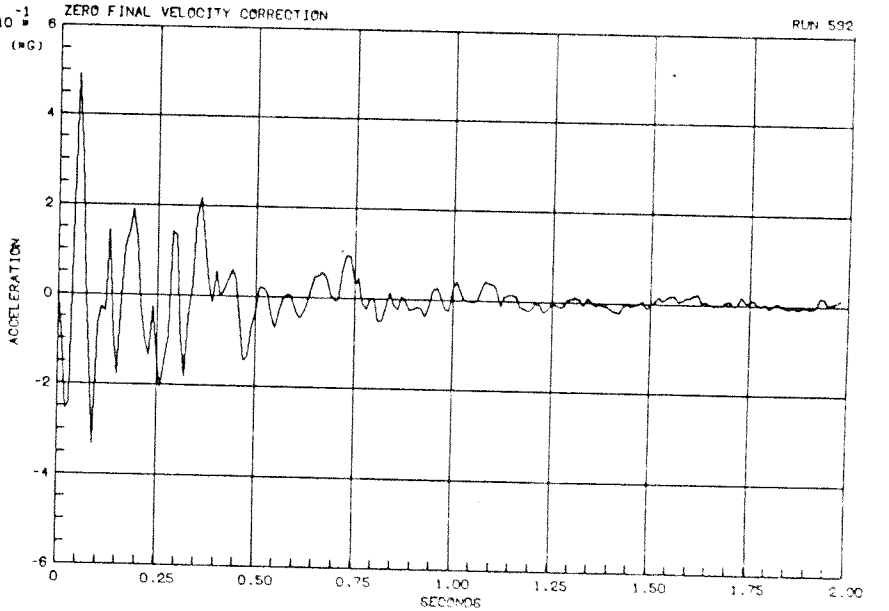

HARDHAT 1091 - TRANSVERSE

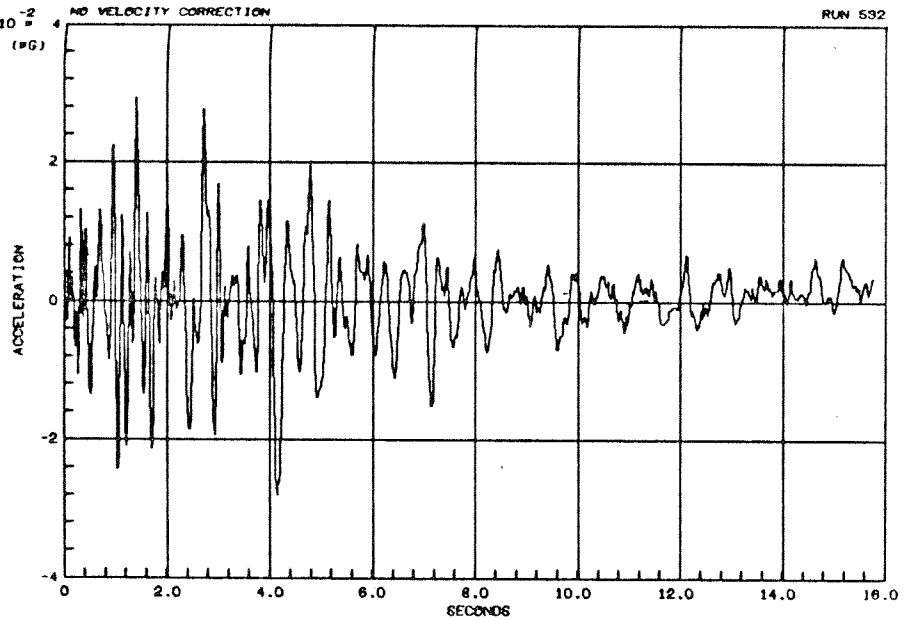

HARDHAT 4496 - TRANSVERSE

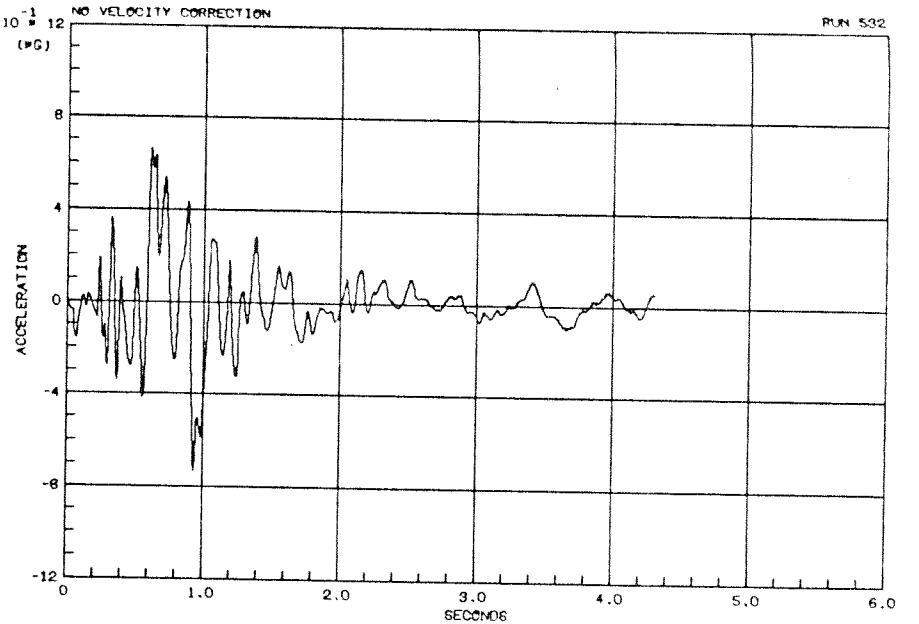

AARDVARK 3773 - TRANSVERSE

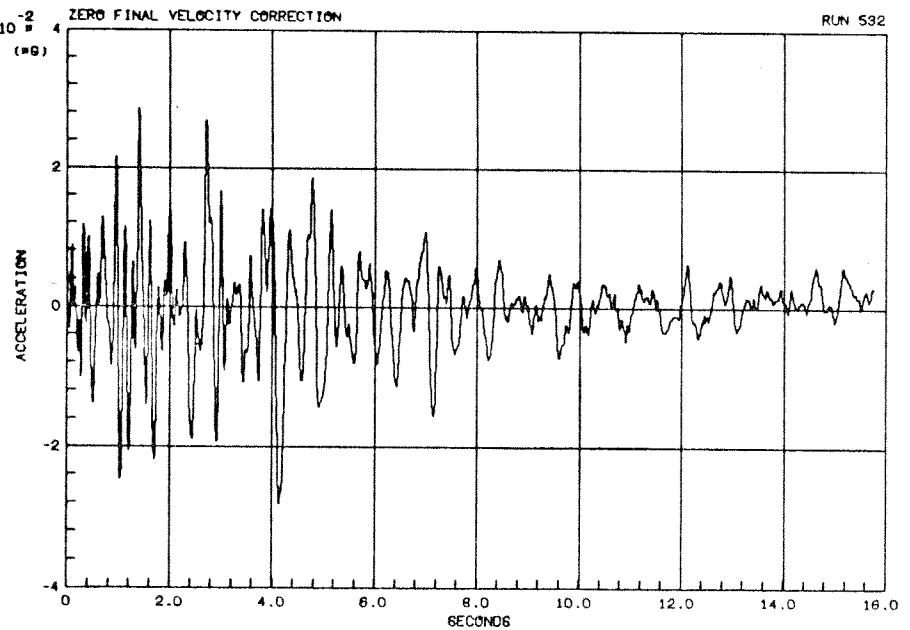

HARDHAT 4496 - TRANSVERSE

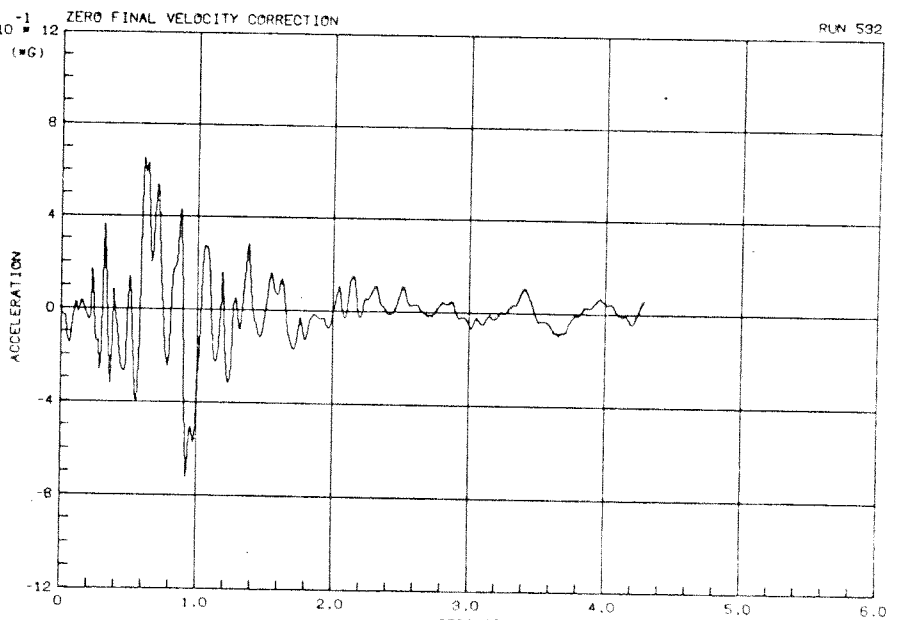

AARDVARK 3773 - TRANSVERSE

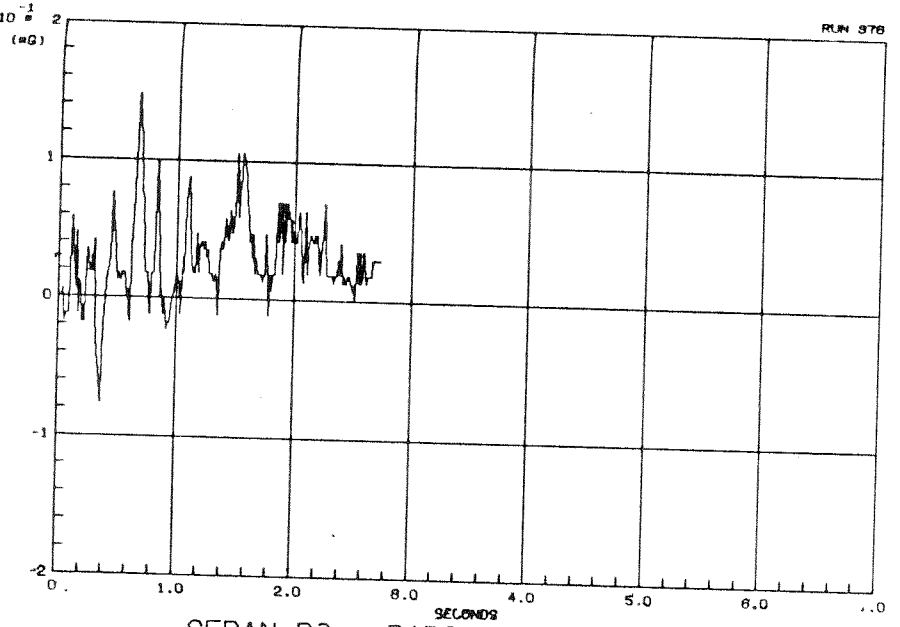

SEDAN R3 RADIAL ACCELERATION

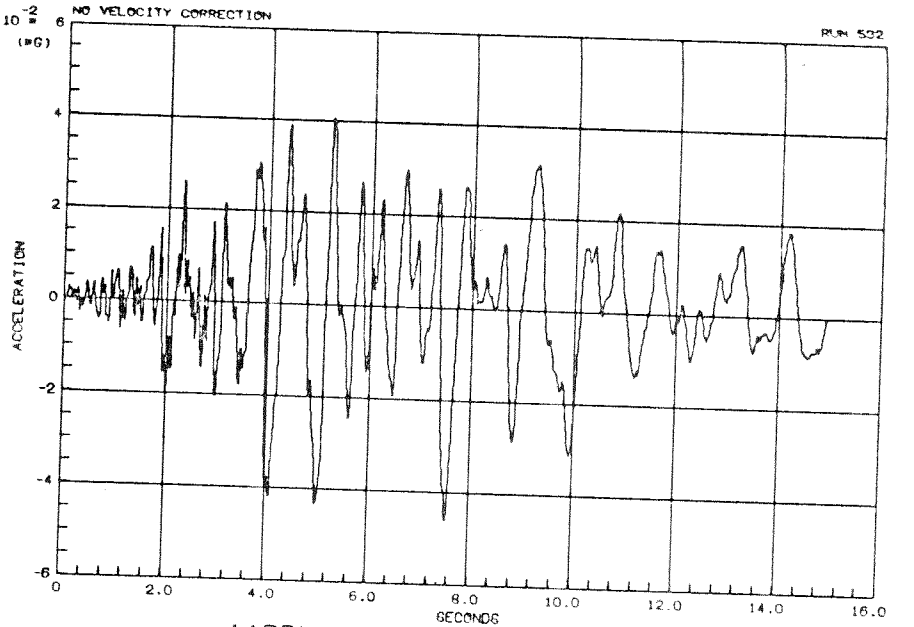

AARDVARK 1437 - TRANSVERSE

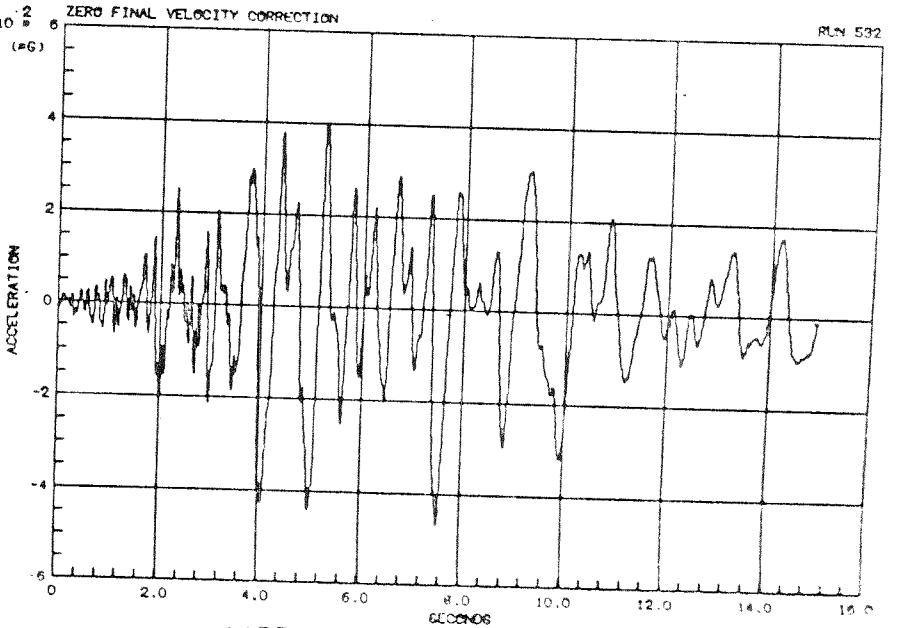

AARDVARK 1437 - TRANSVERSE

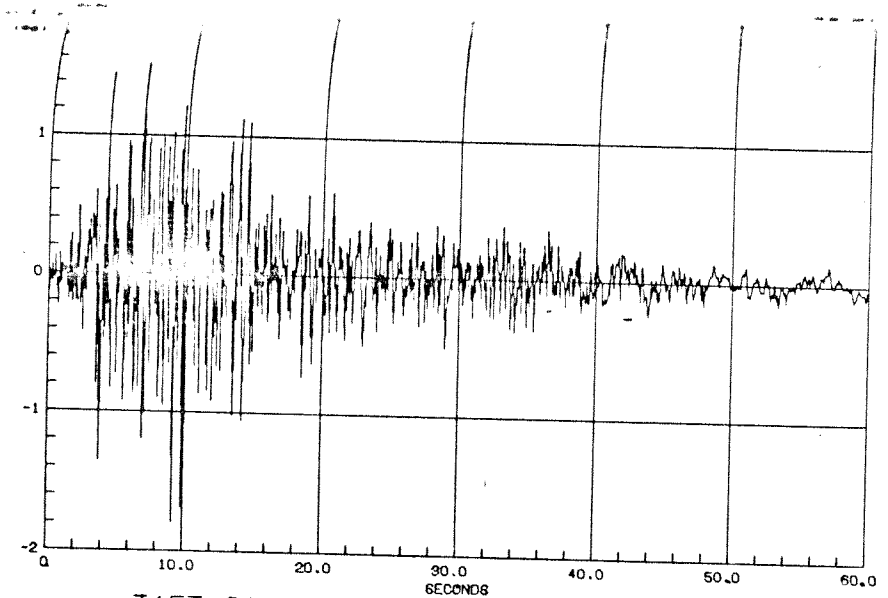

TAFT 21 JULY 1952 N21E ACCELERATION

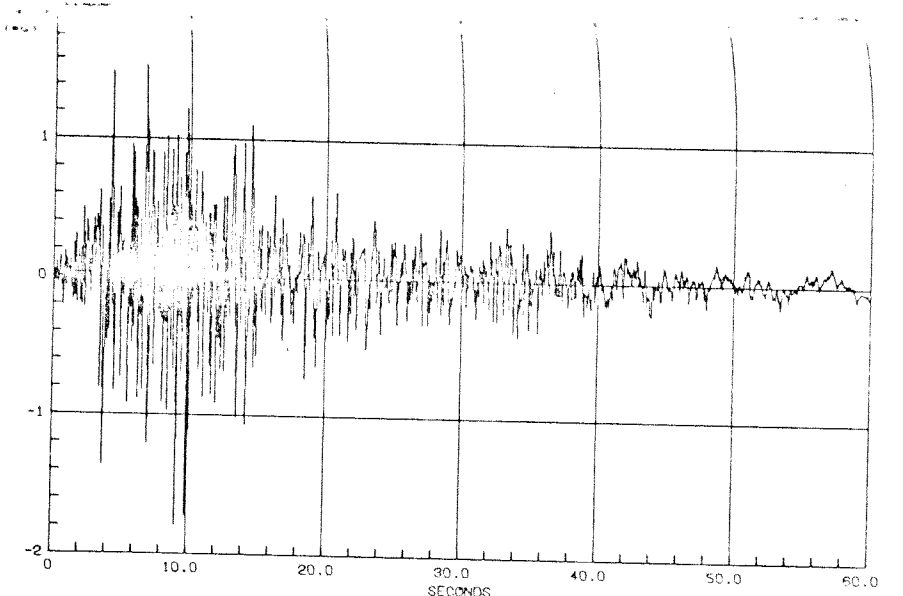

TAFT 21 JULY 1952 N21E ACCELERATION

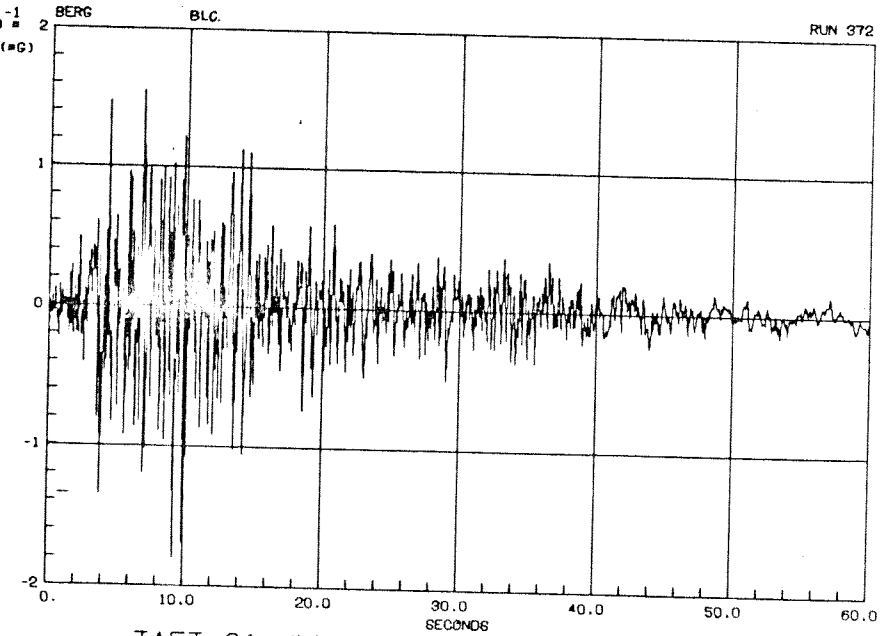

TAFT 21 JULY 1952 N21E ACCELERATION

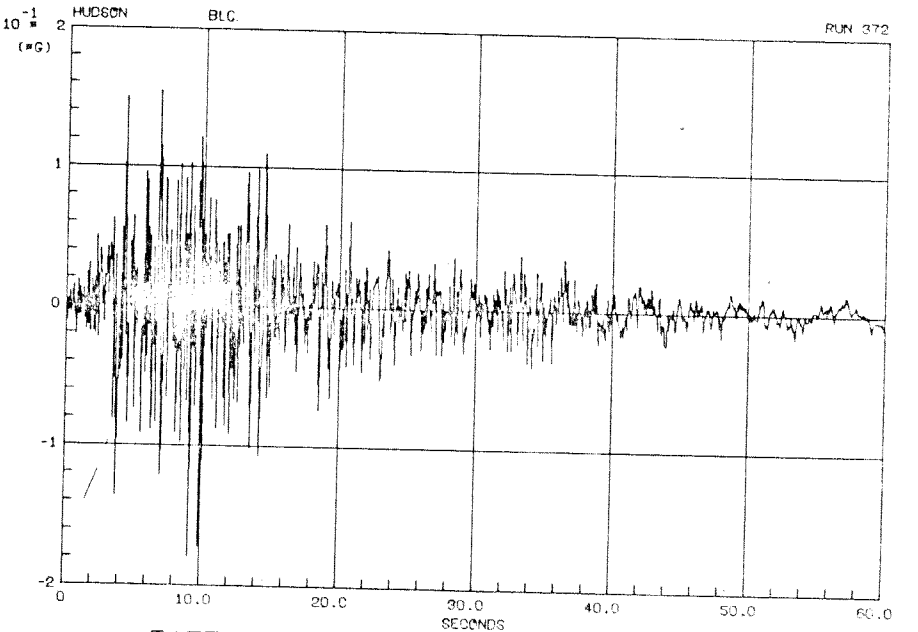

TAFT 21 JULY 1952 N21E ACCELERATION

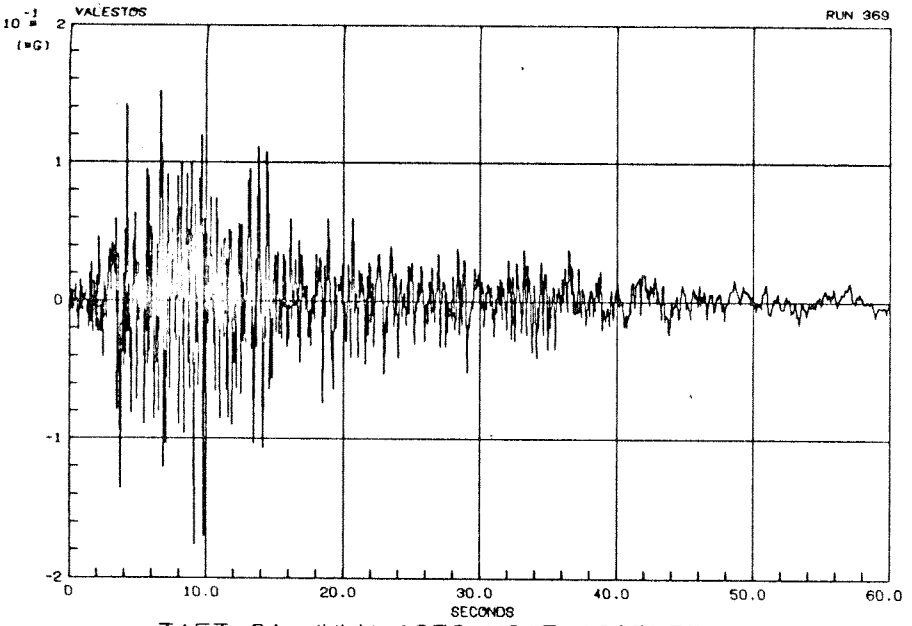

TAFT 21 JULY 1952 N21E ACCELERATION

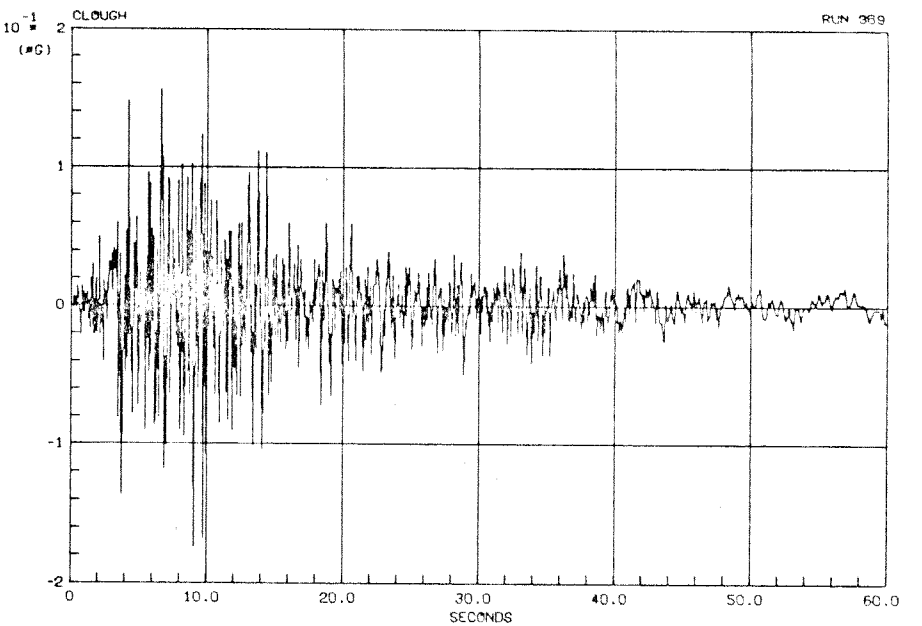

TAFT 21 JULY 1952 N21E ACCELERATION

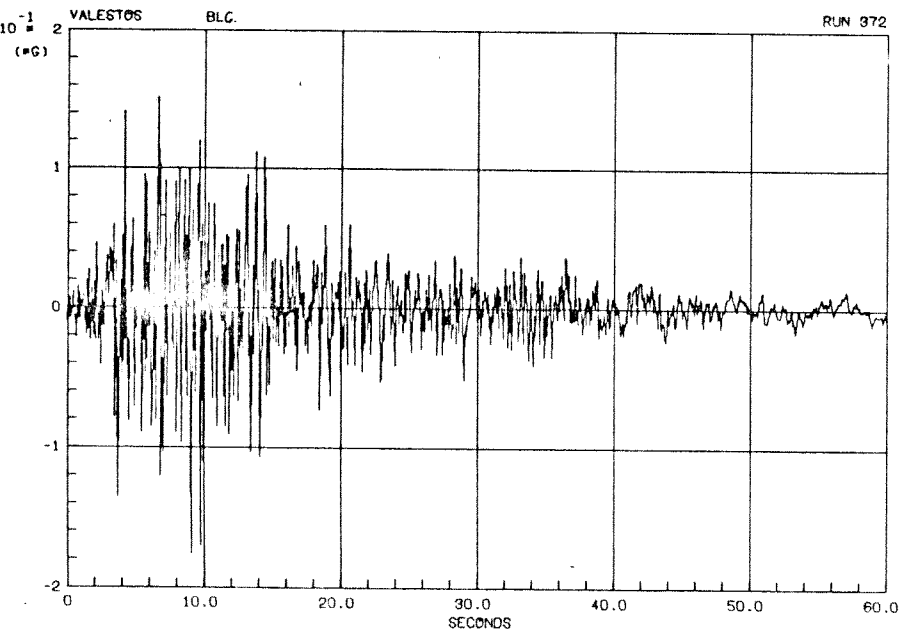

TAFT 21 JULY 1952 N21E ACCELERATION

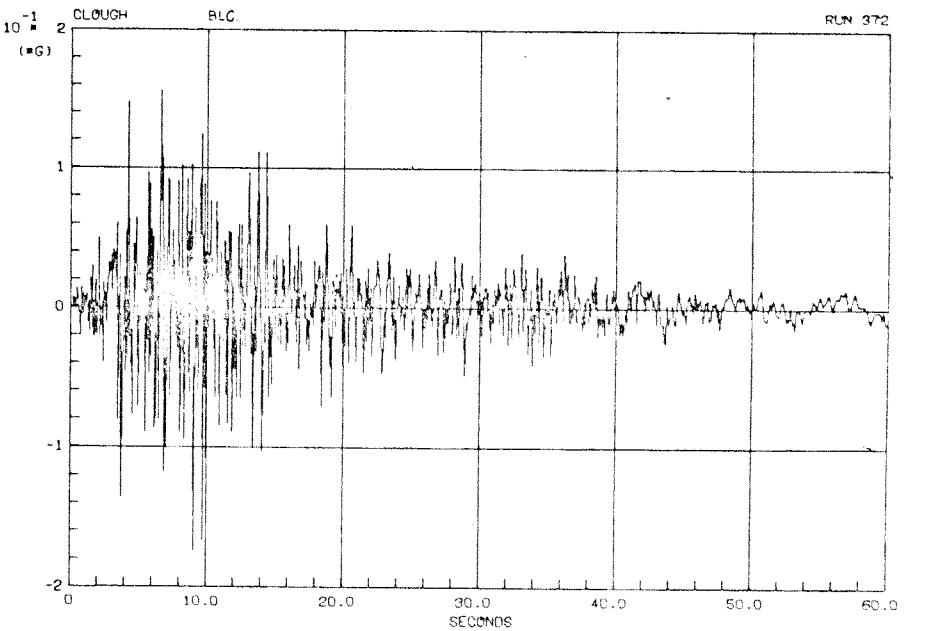

TAFT 21 JULY 1952 N21E ACCELERATION

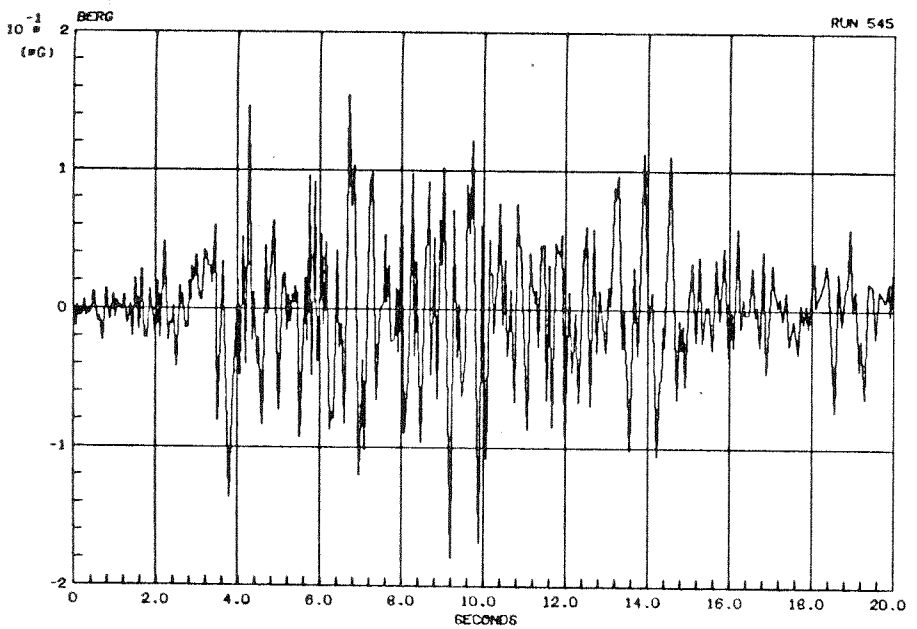

TAFT 1952, N21E - ACCELERATION

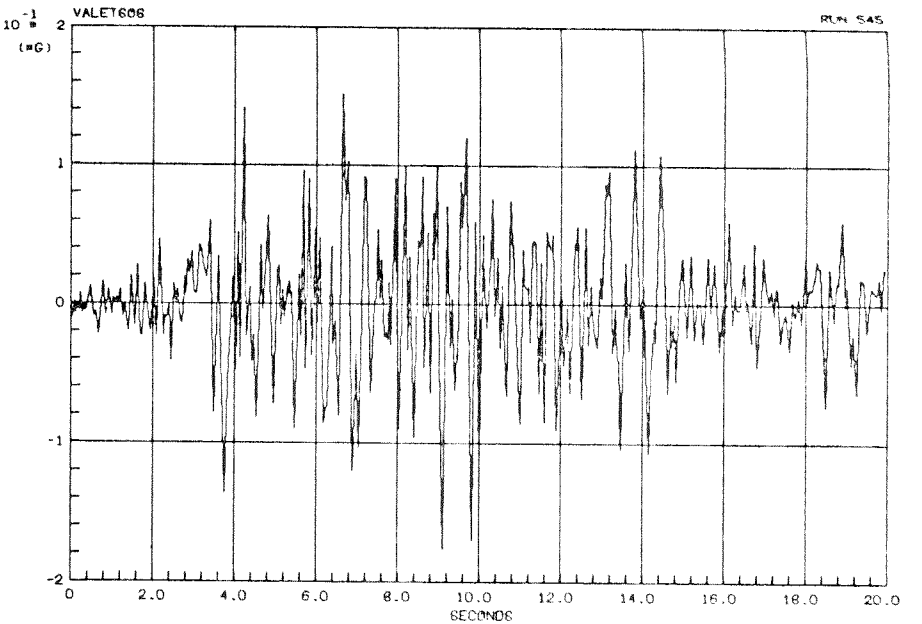

TAFT 1952, N21E - ACCELERATION

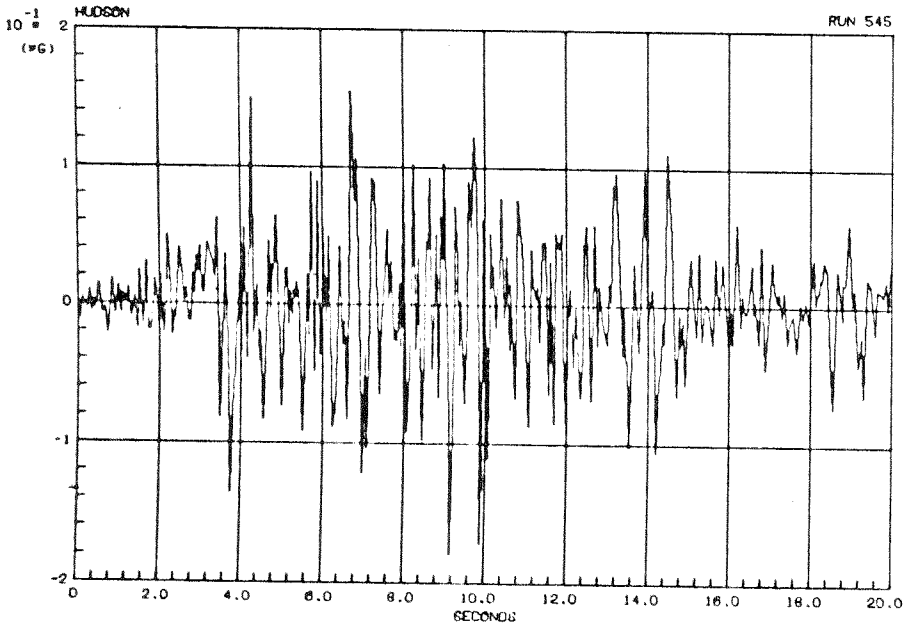

TAFT 1952, N21E - ACCELERATION

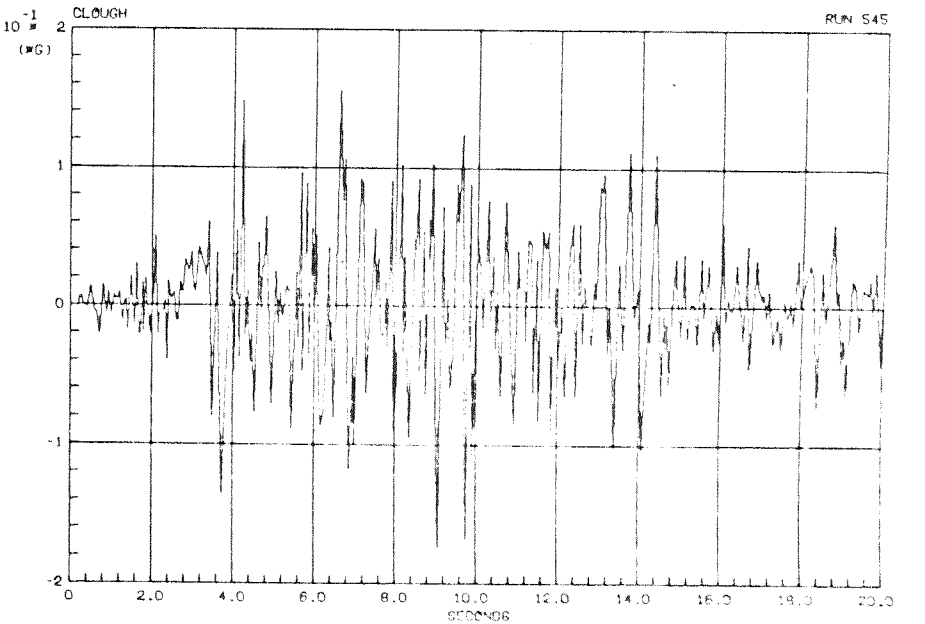

TAFT 1952, N21E - ACCELERATION

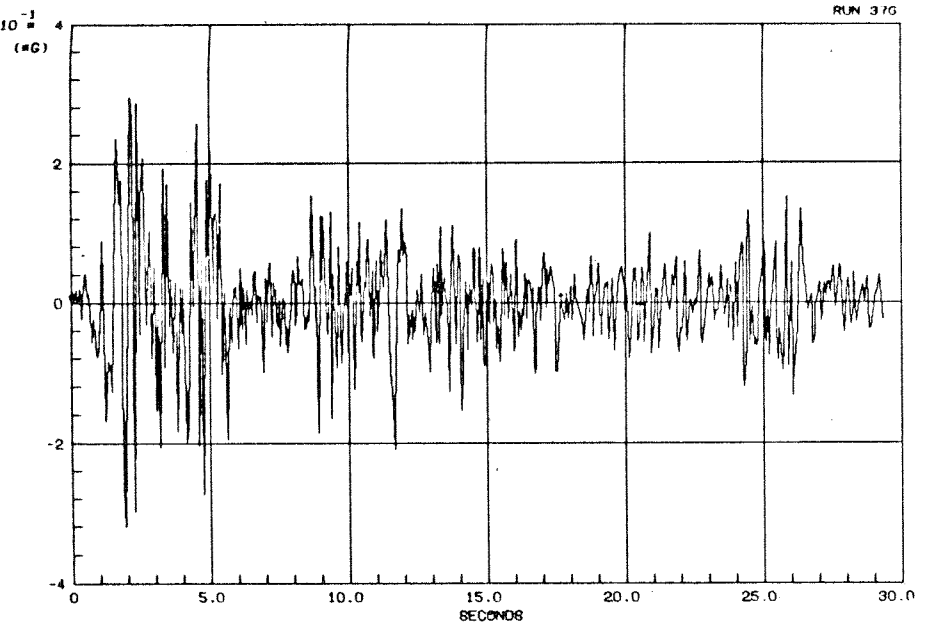

EL CENTRØ 1940 NS ACCELERATIØN

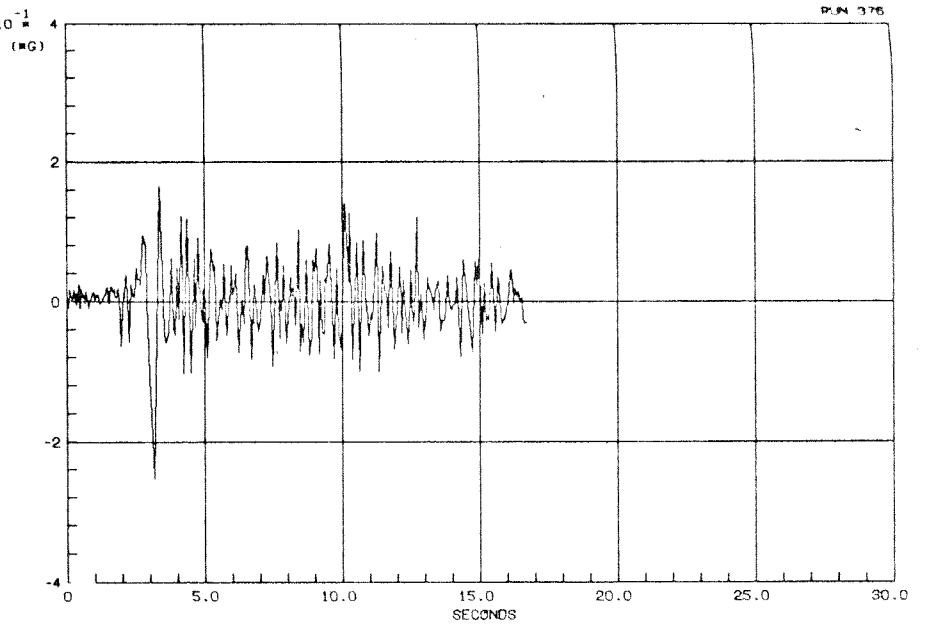

EL CENTRØ 1934 NS ACCELERATIØN

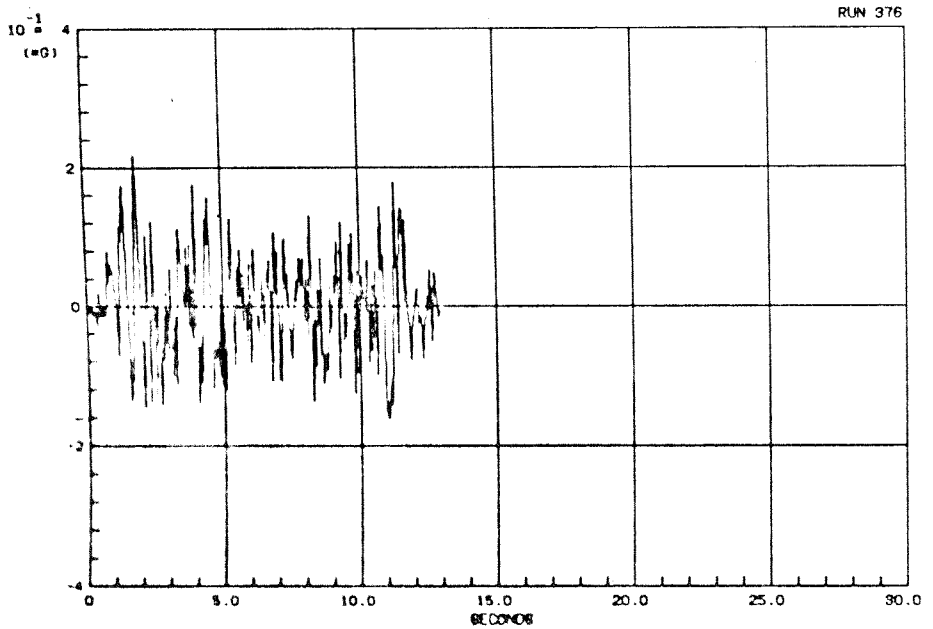

EL CENTRØ 1940 EW ACCELERATIØN

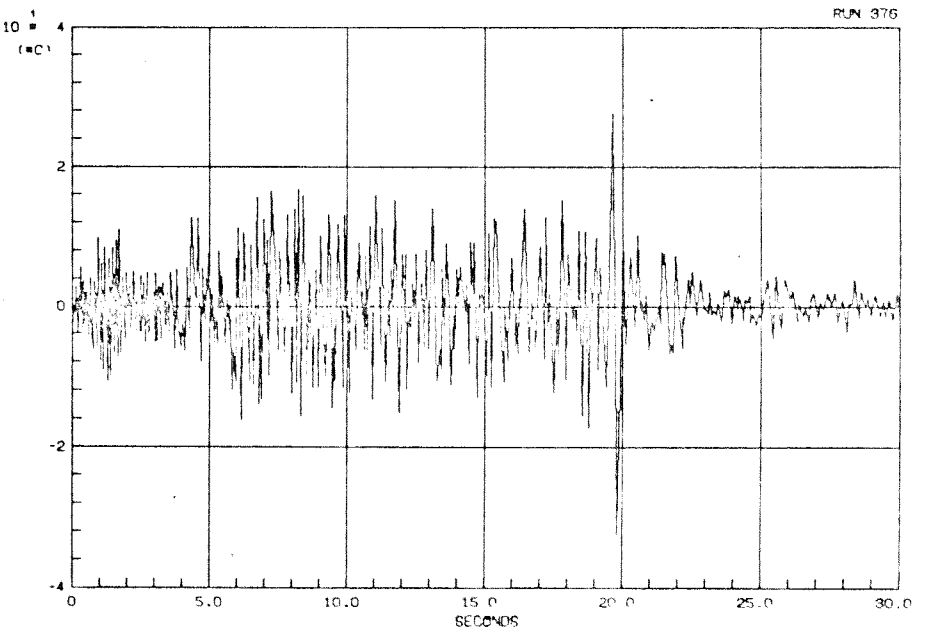

ØLYMPIA 1949 N8ØE ACCELERATIØN

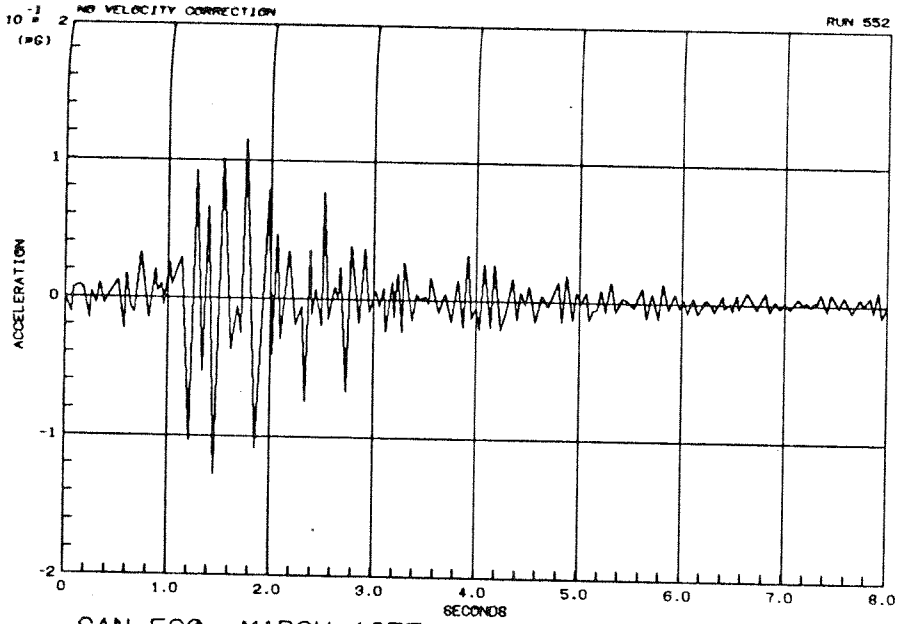

SAN FCO. MARCH 1957 - GOLDEN GATE PARK S80E

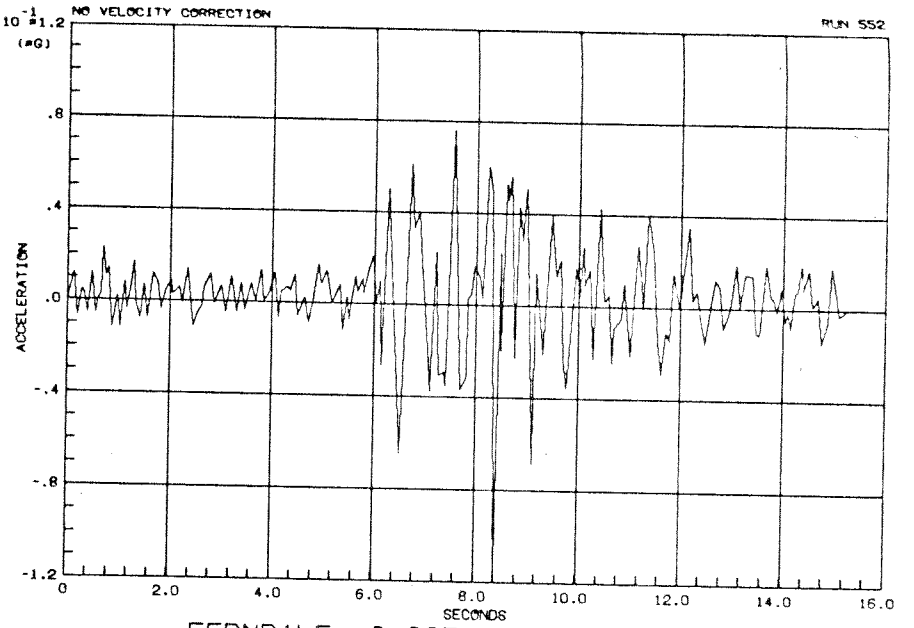

FERNDALE, 3 OCTOBER 1941 - S45E

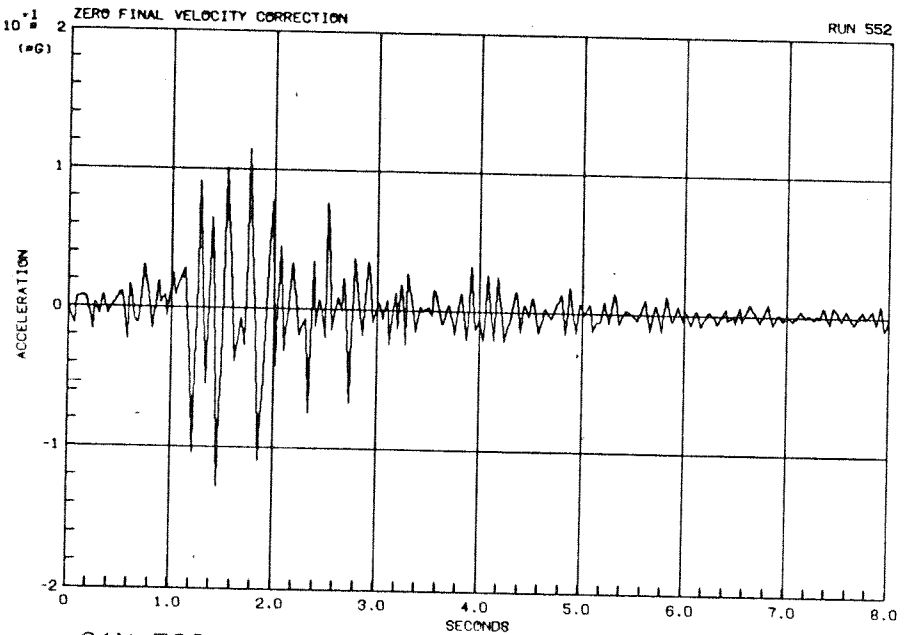

SAN FCO. MARCH 1957 - GOLDEN GATE PARK S80E

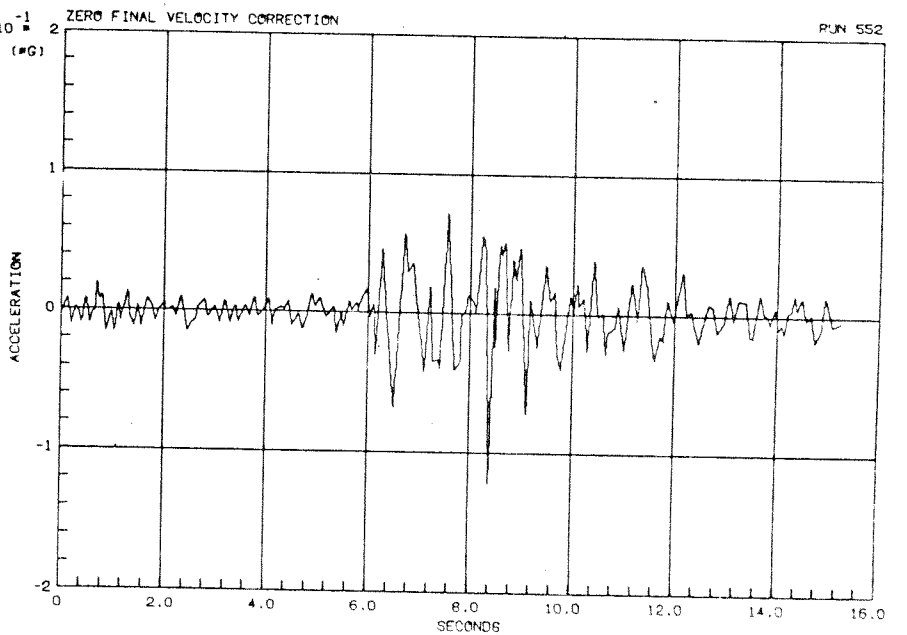

FERNDALE, 3 OCTOBER 1941 - S45E

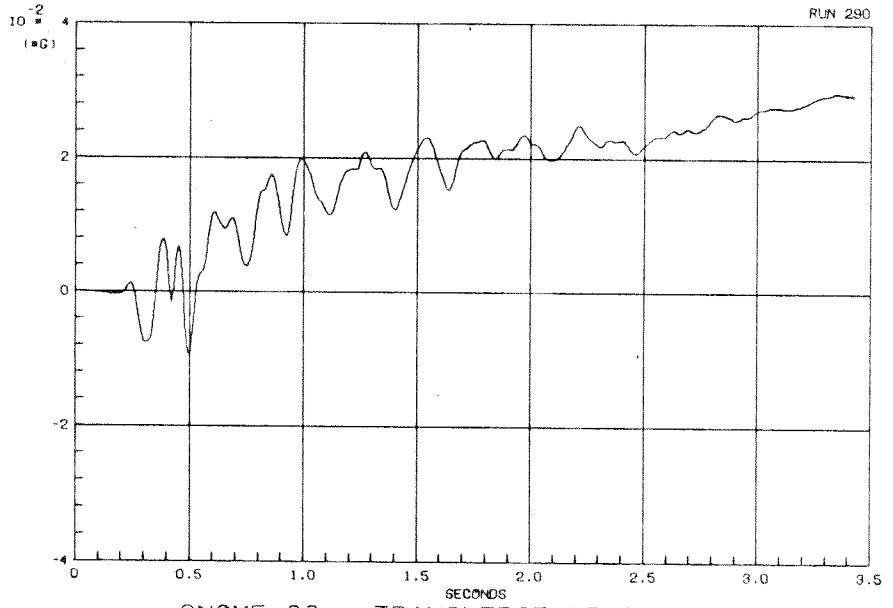

GNOME S2 - TRANSVERSE VELOCITY

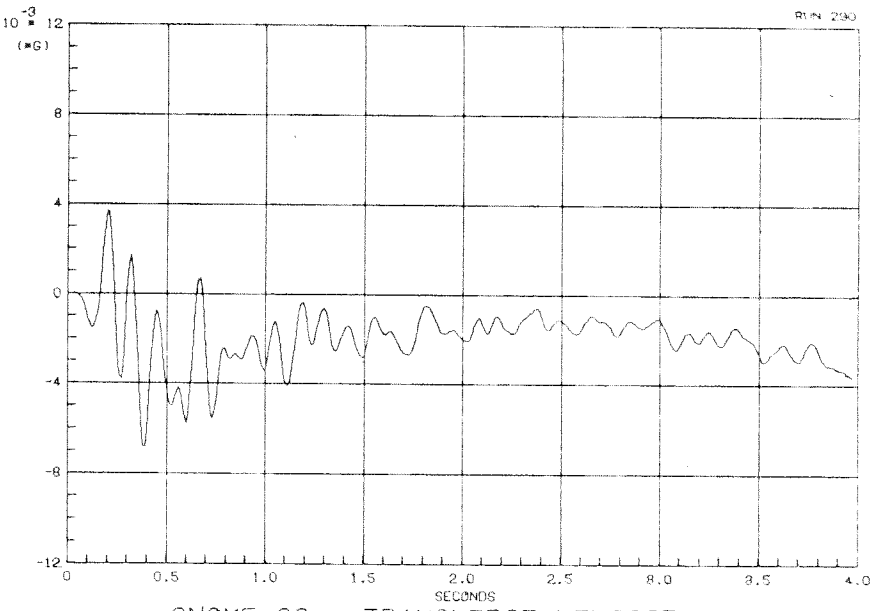

GNOME S3 - TRANSVERSE VELOCITY

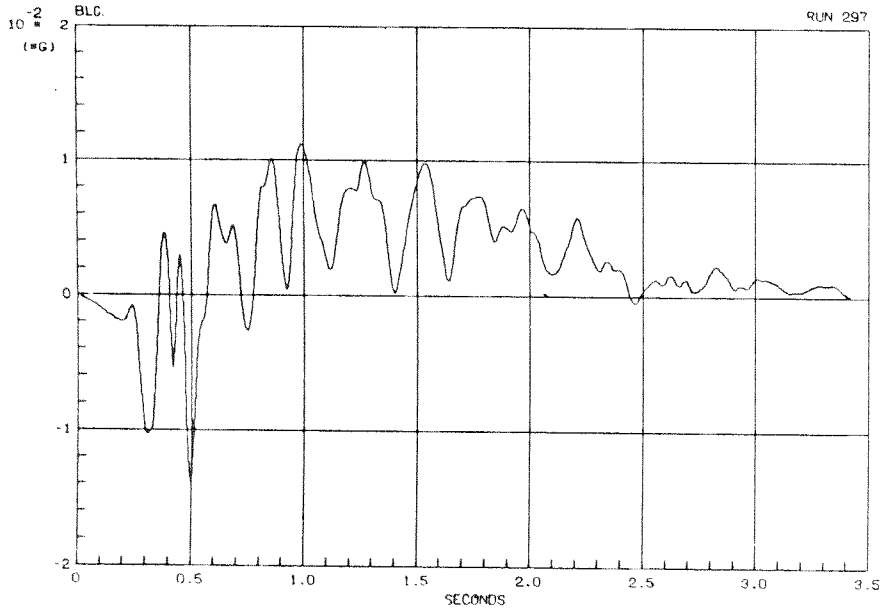

GNOME S2 - TRANSVERSE VELOCITY

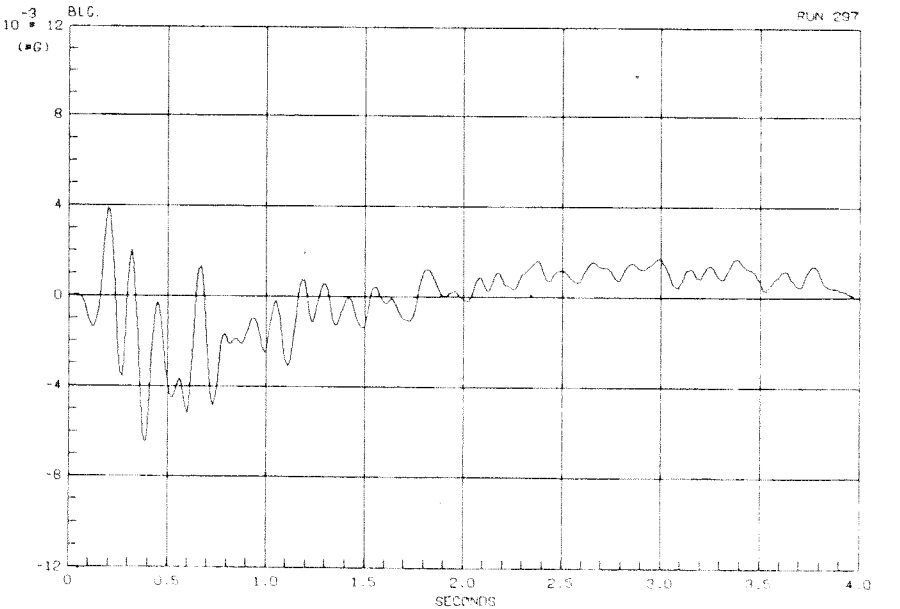

GNOME S3 - TRANSVERSE VELOCITY

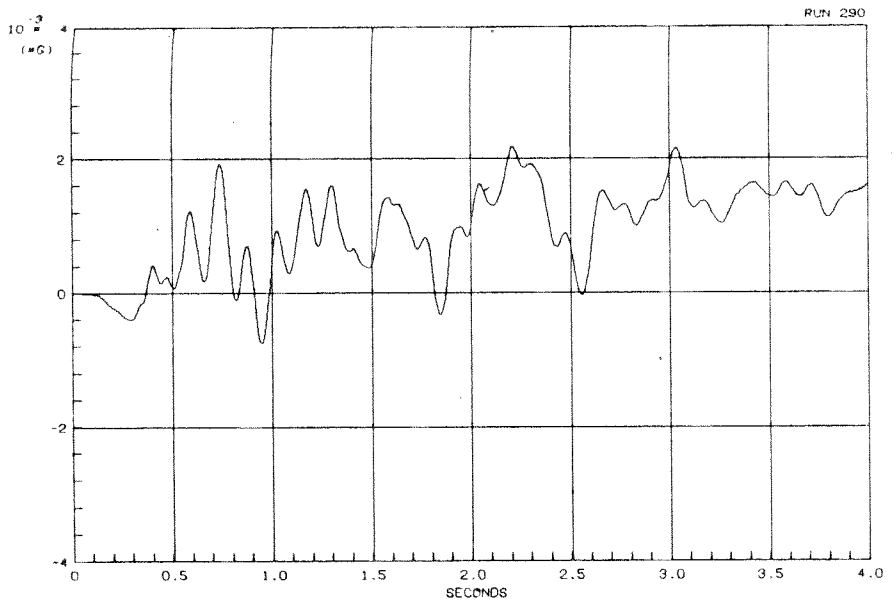

GNOME S4 - RADIAL VELOCITY

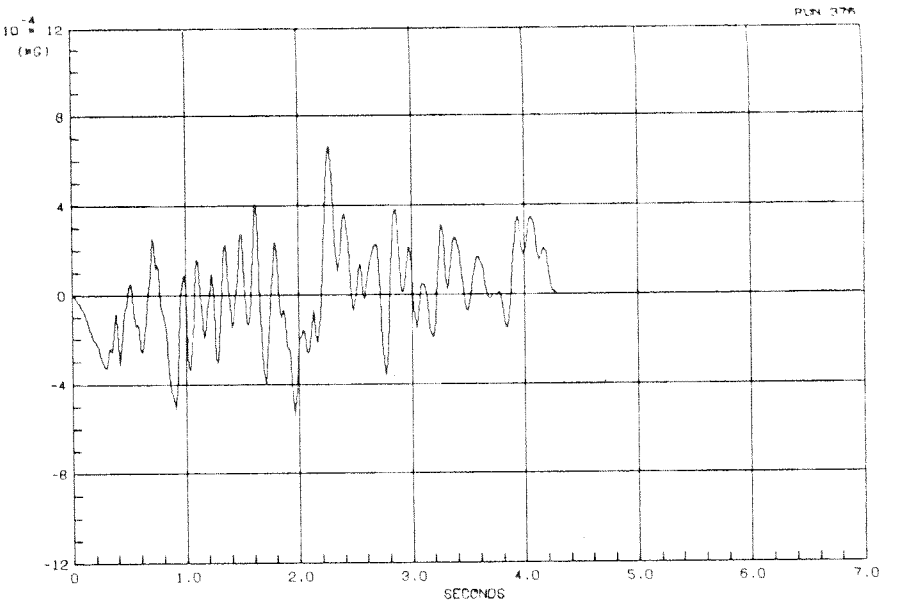

GNOME S4 - TRANSVERSE VELOCITY

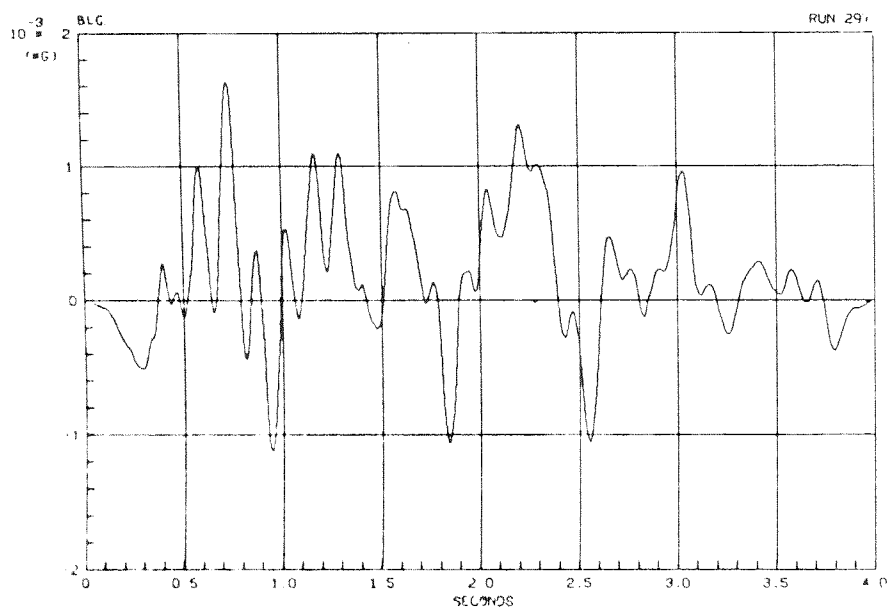

GNOME S4 - RADIAL VELOCITY

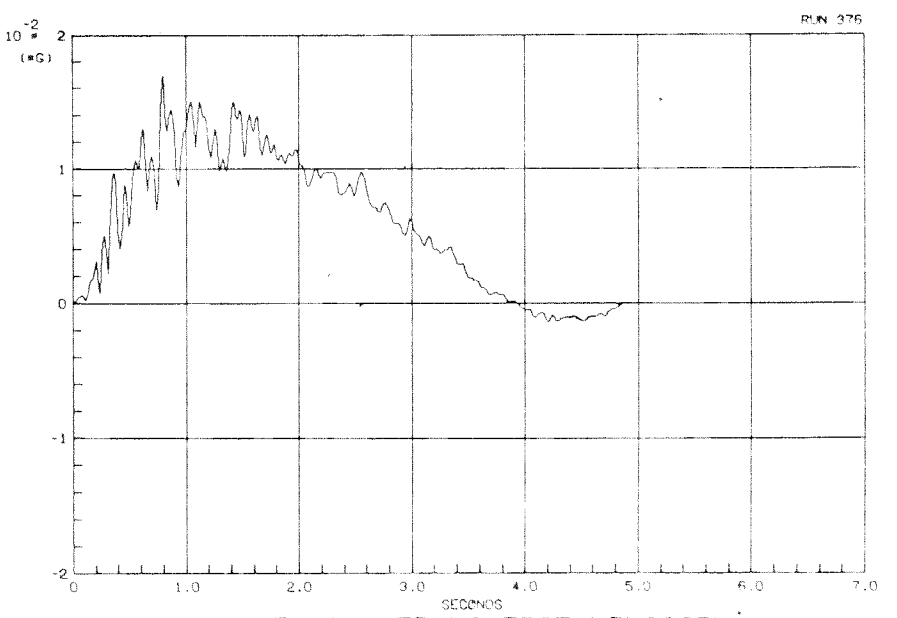

GNOME S6 - TRANSVERSE VELOCITY

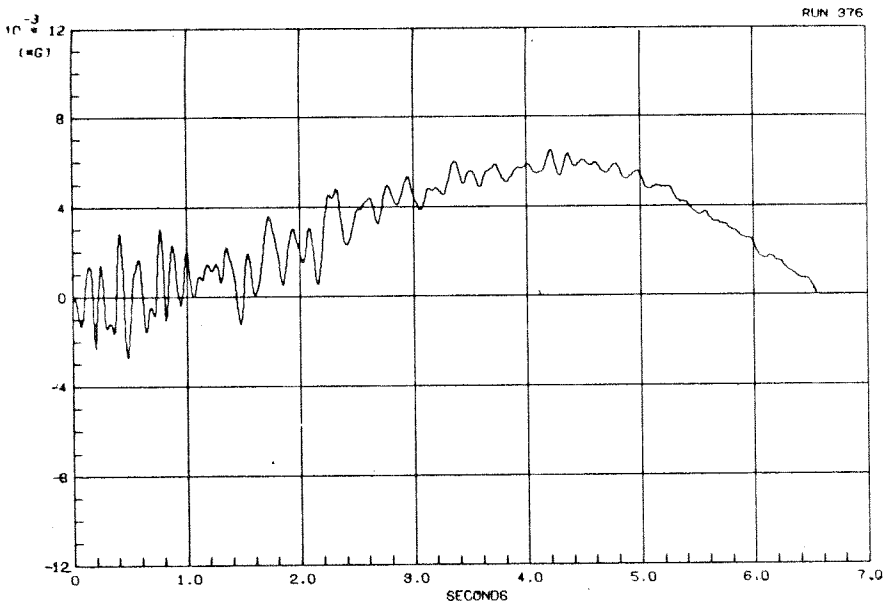

GNOME ST - TRANSVERSE VELOCITY

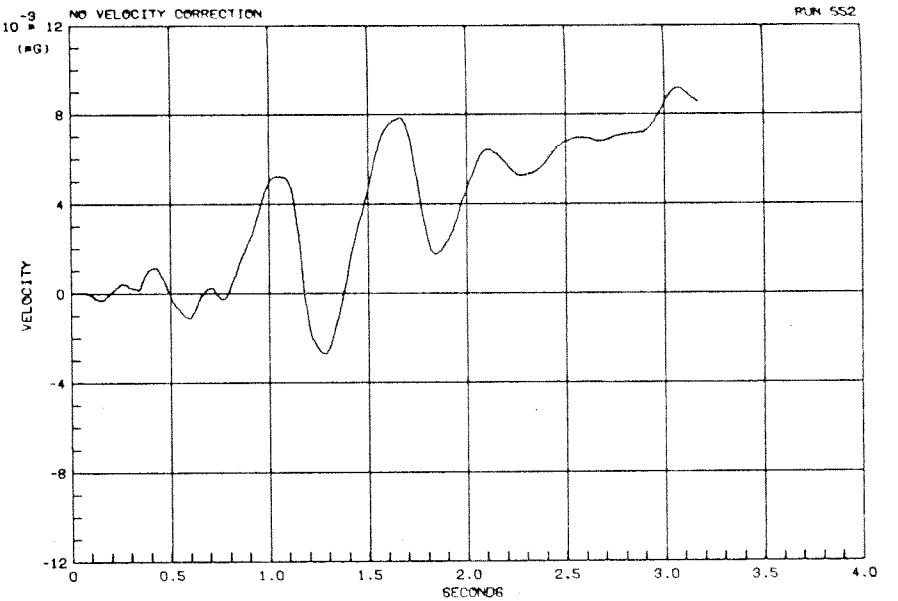

DANNYBOY D5 - RADIAL

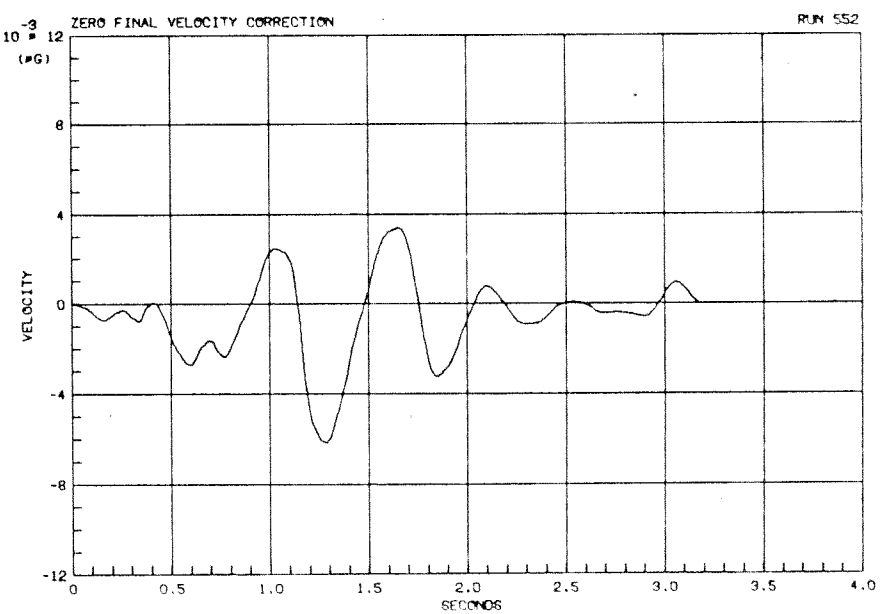

DANNYBOY D5 - RADIAL

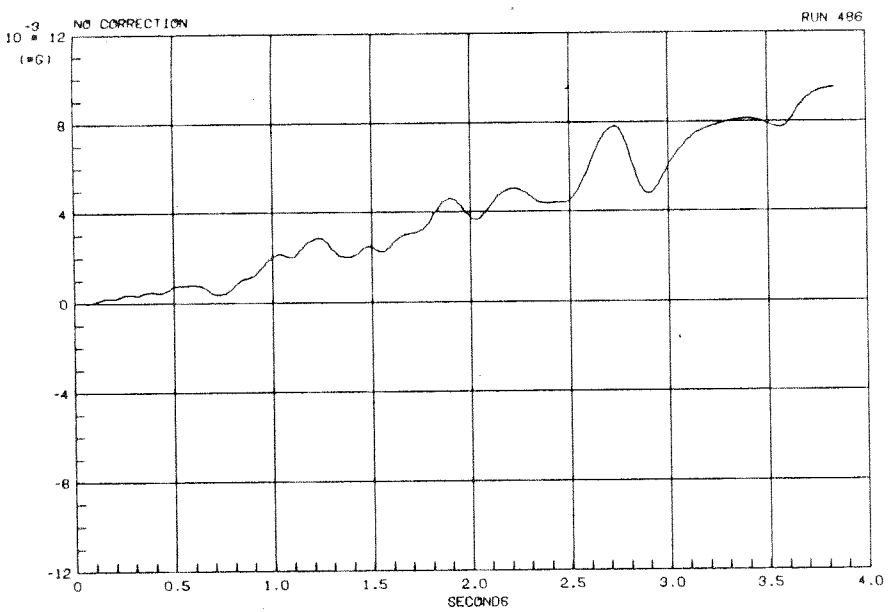

DANNYBØY D8 - RADIAL VELØCITY

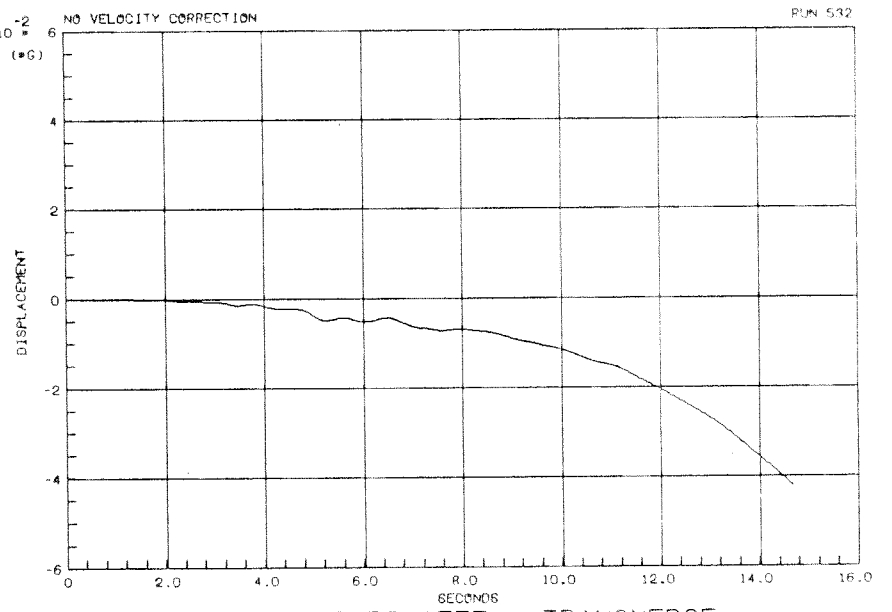

MISSISSIPPI 1777 - TRANSVERSE

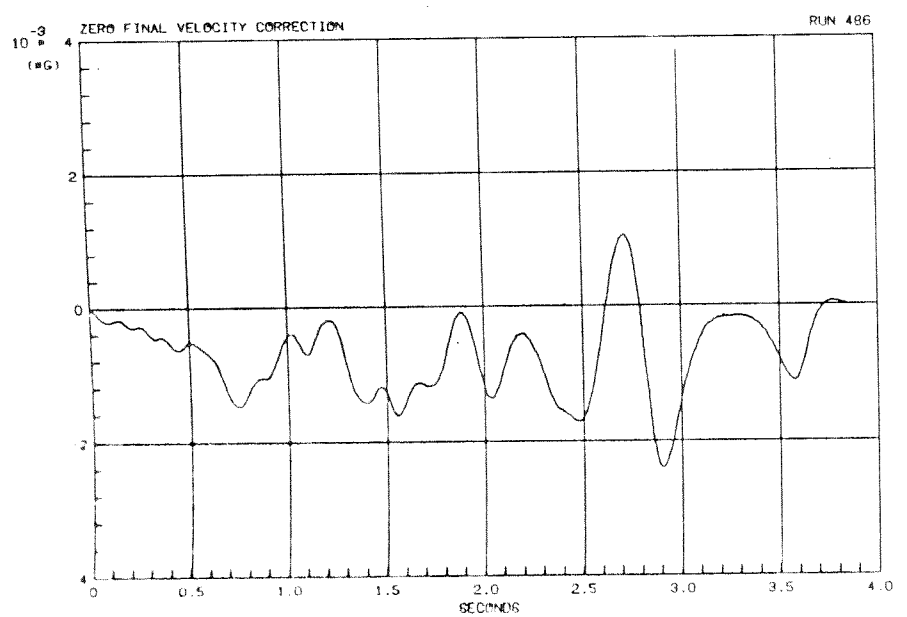

DANNYBØY D8 - RADIAL VELØCITY

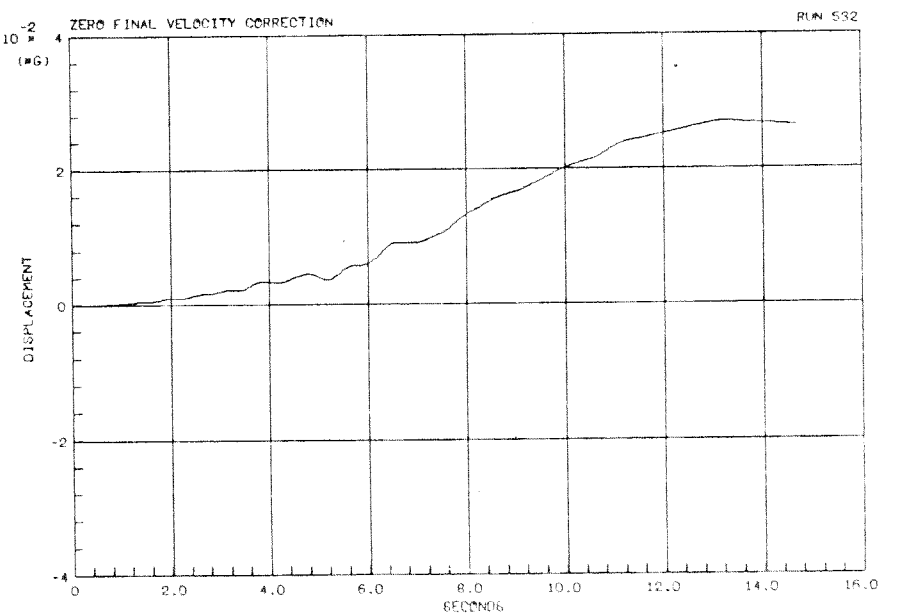

MISSISSIPPI 1777 - TRANSVERSE

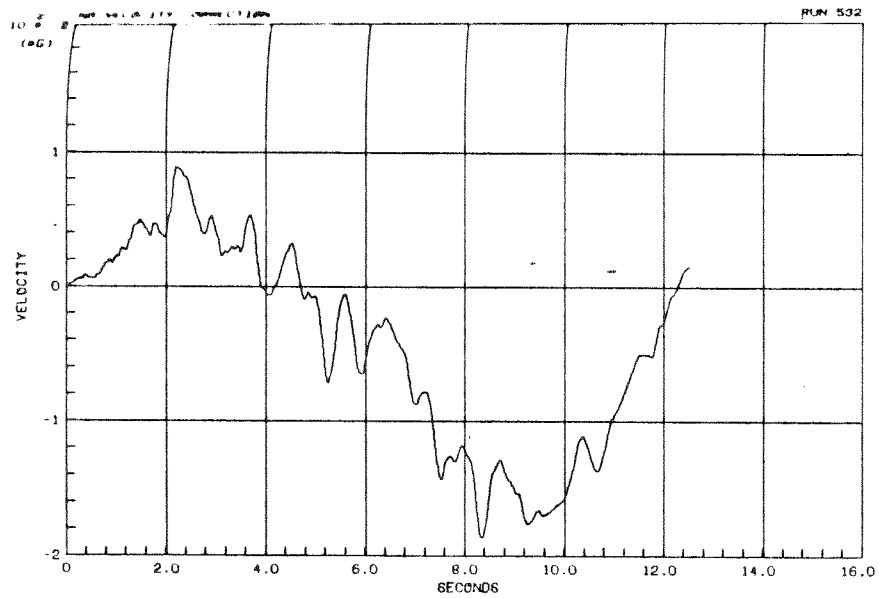

MISSISSIPPI 8228 - TRANSVERSE

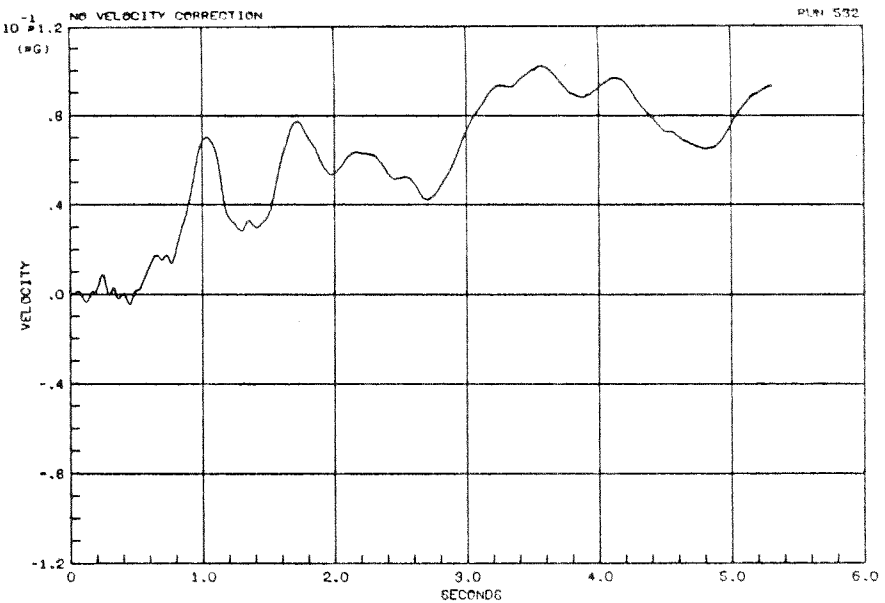

MISSISSIPPI 7245 - RADIAL

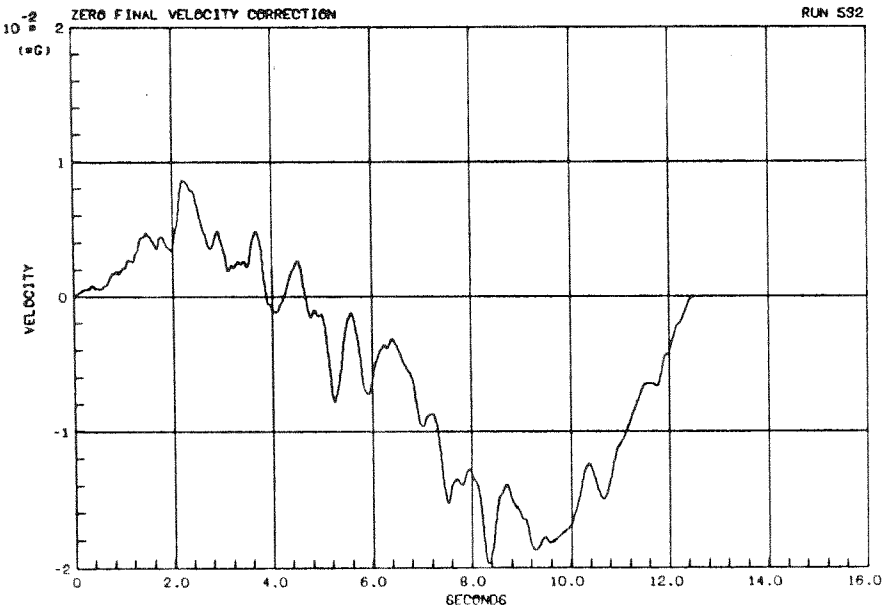

MISSISSIPPI 8228 - TRANSVERSE

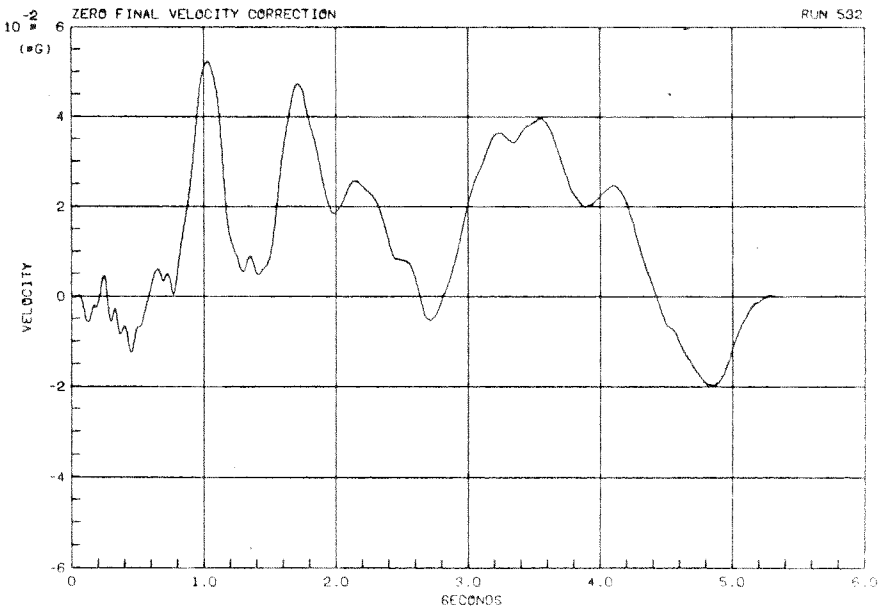

MISSISSIPPI 7245 - RADIAL

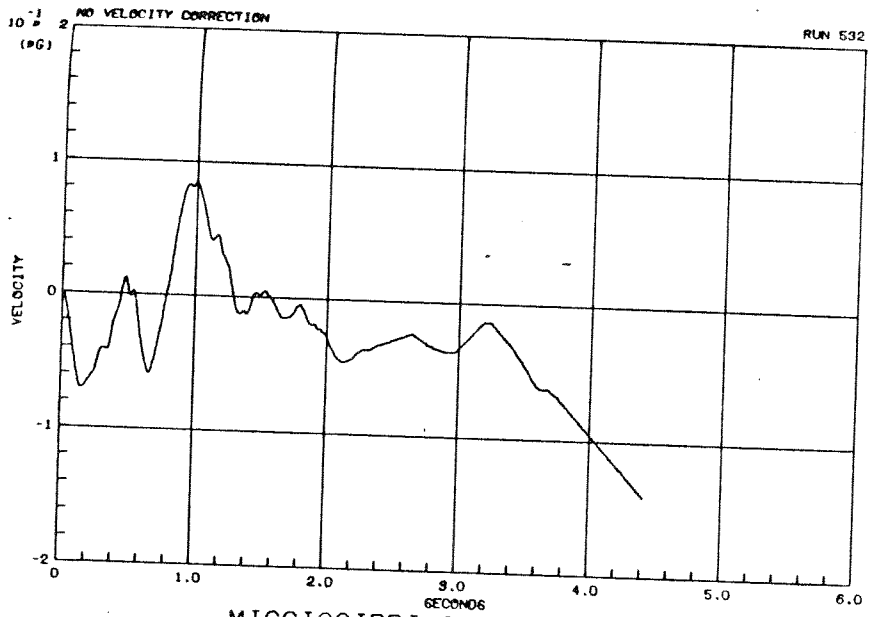

MISSISSIPPI 9537 - RADIAL

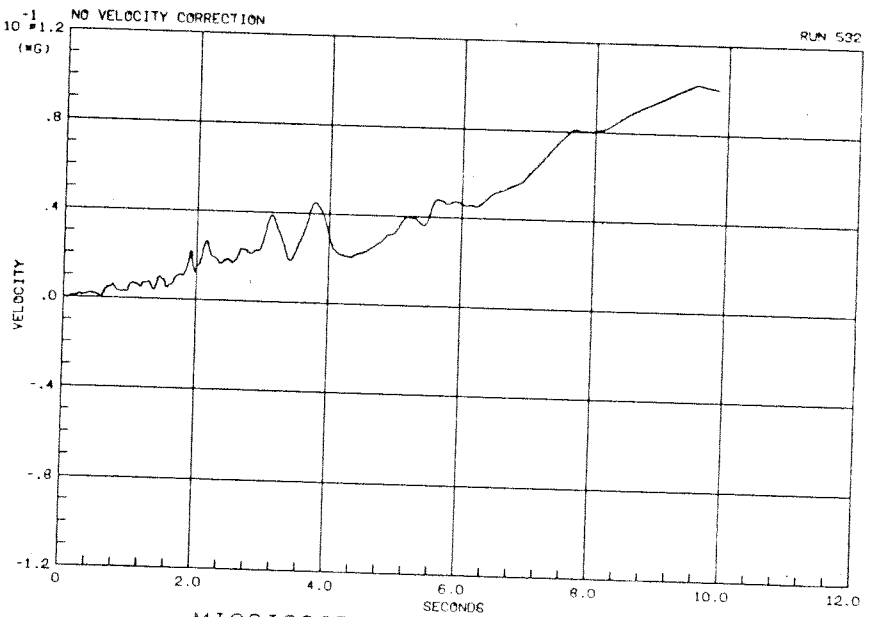

MISSISSIPPI 4074 - TRANSVERSE

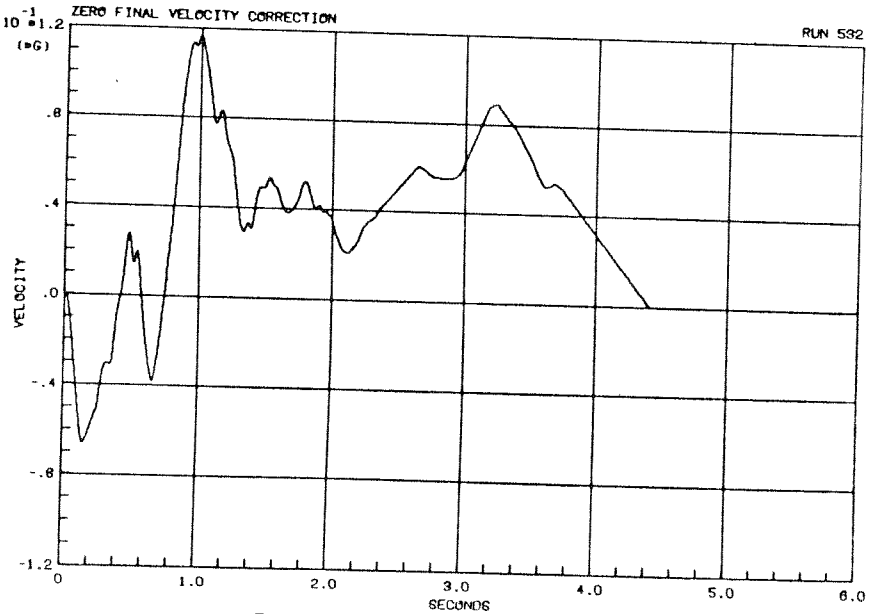

MISSISSIPPI 9537 - RADIAL

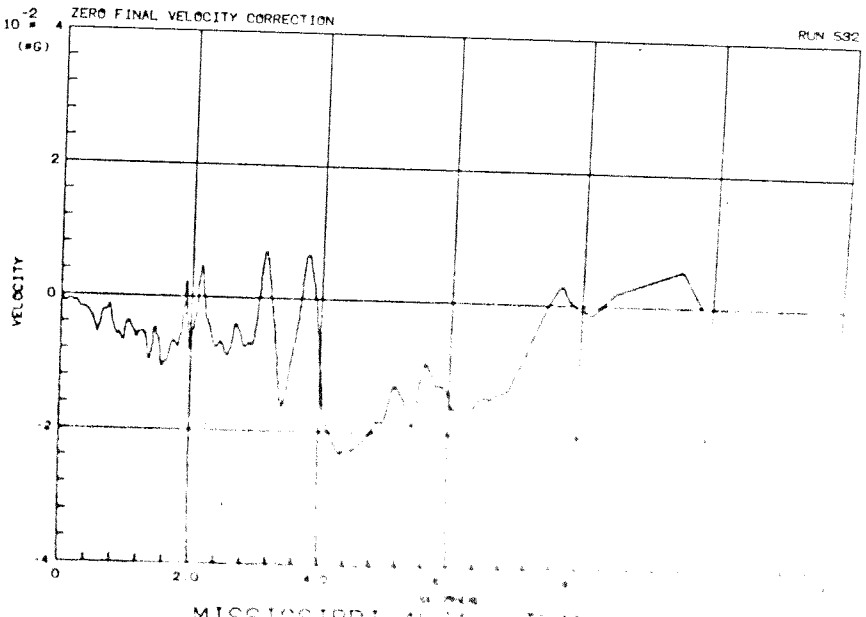

MISSISSIPPI 4074 - TRANSVERSE

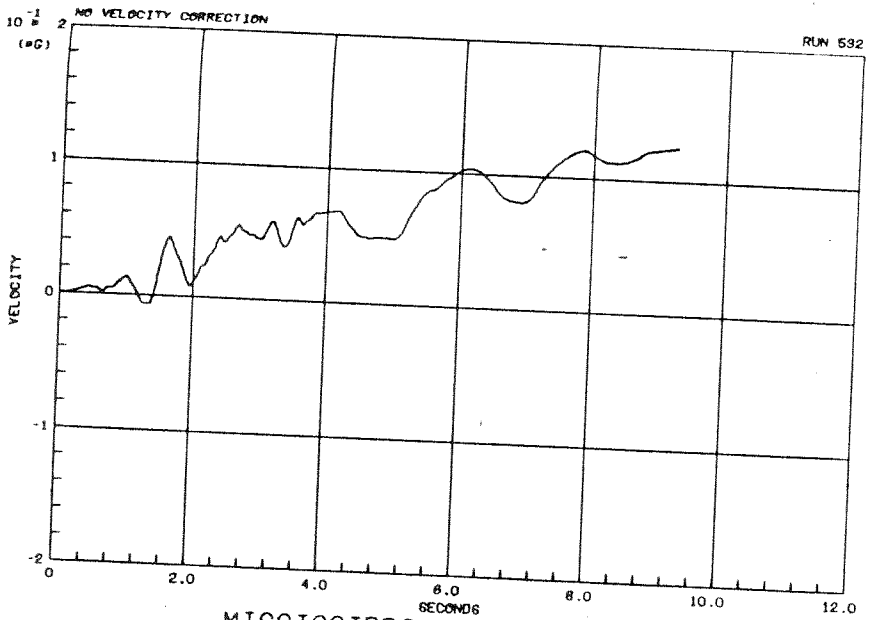

MISSISSIPPI 4074 - RADIAL

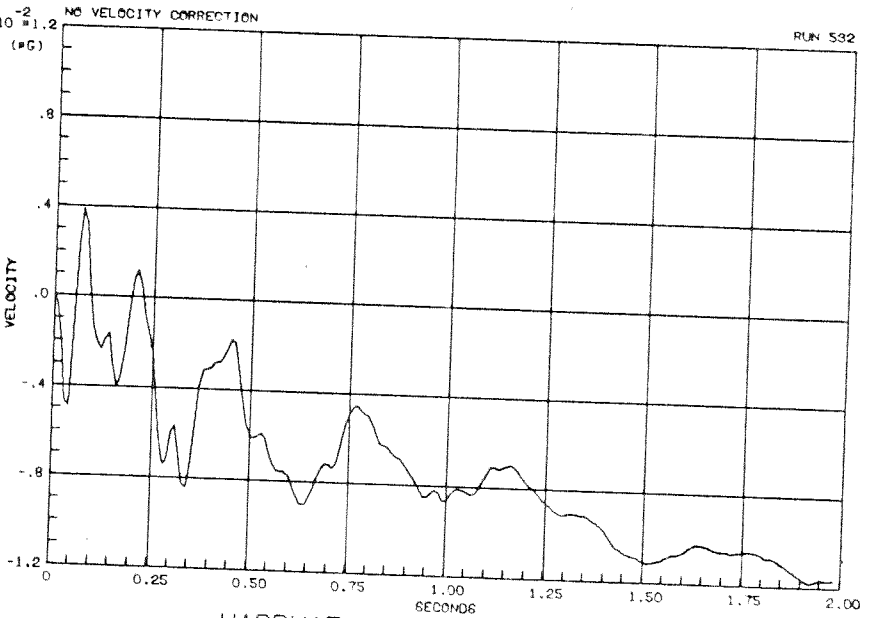

HARDHAT 1091 - TRANSVERSE

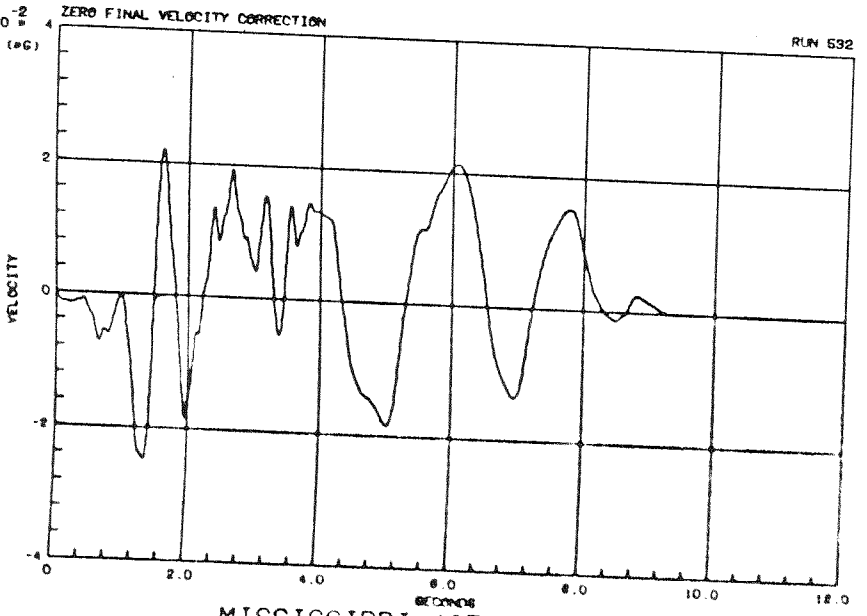

MISSISSIPPI 4074 - RADIAL

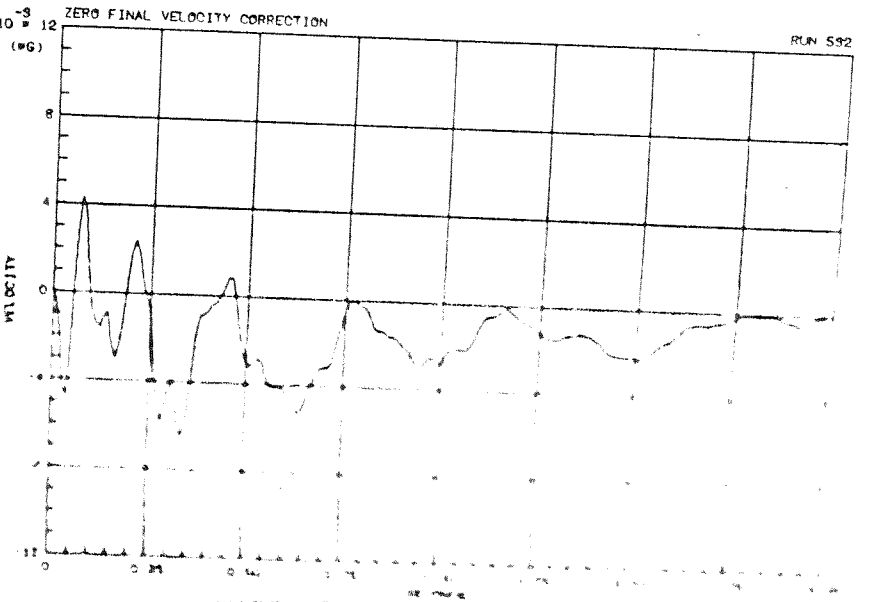

HARDHAT 1091 - TRANSVERSE

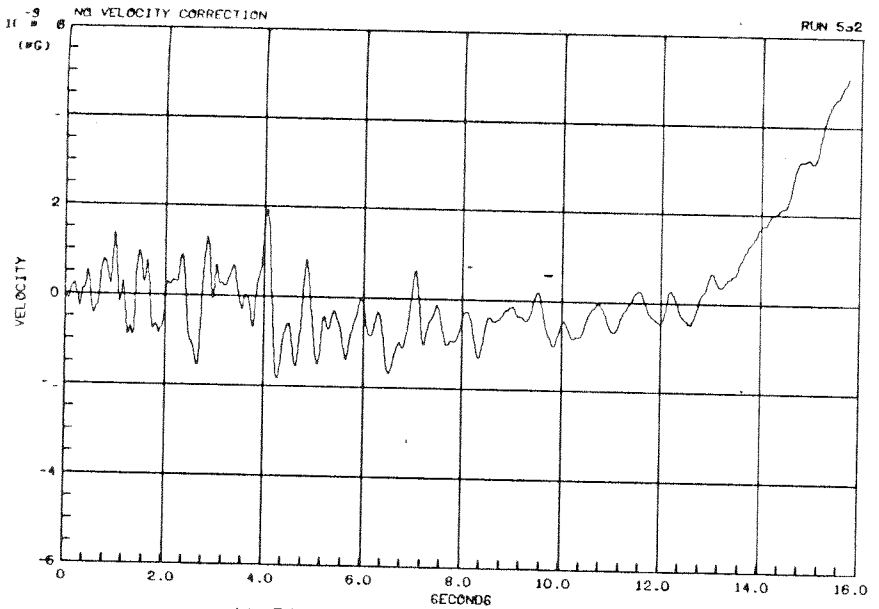

HARDHAT 4496 - TRANSVERSE

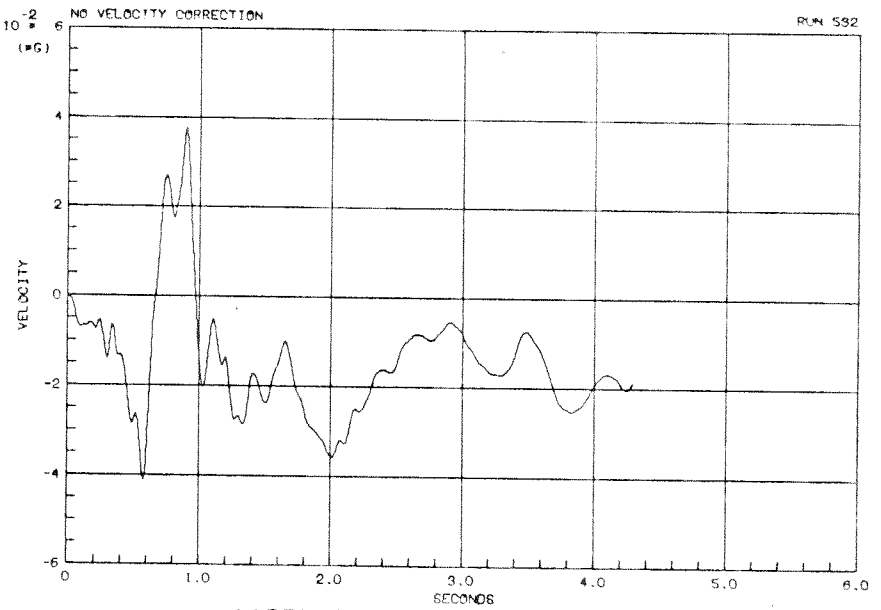

AARDVARK 3773 - TRANSVERSE

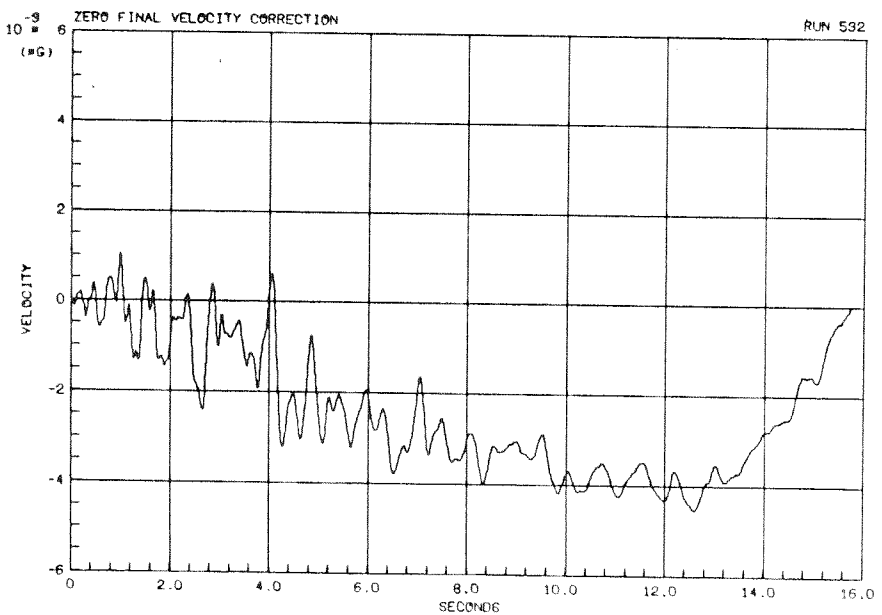

HARDHAT 4496 - TRANSVERSE

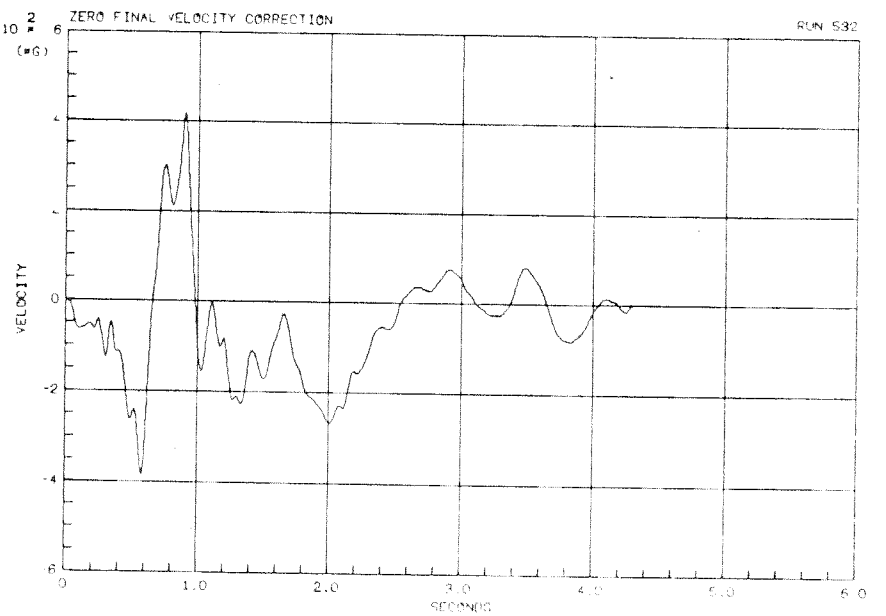

AARDVARK 3773 - TRANSVERSE

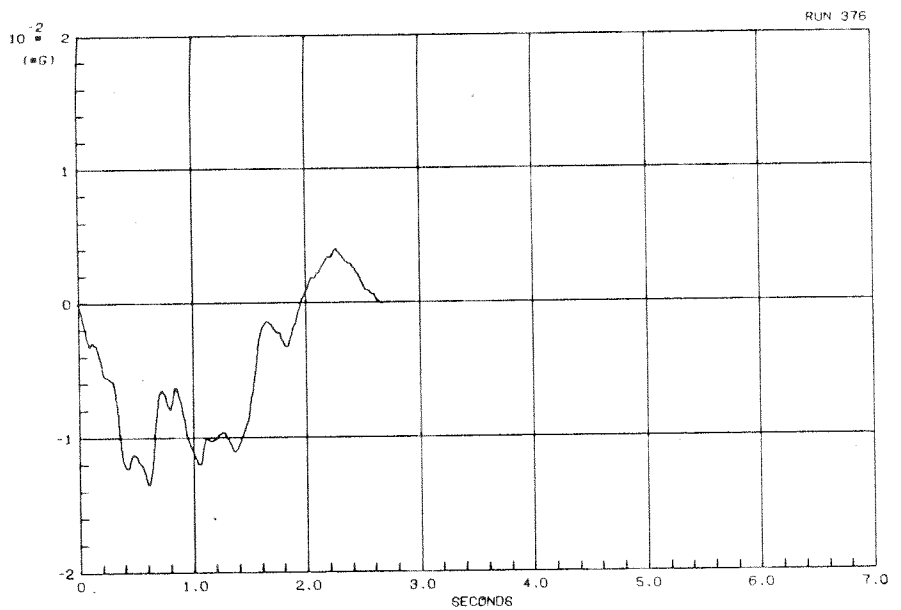

SEDAN R3 - RADIAL VELOCITY

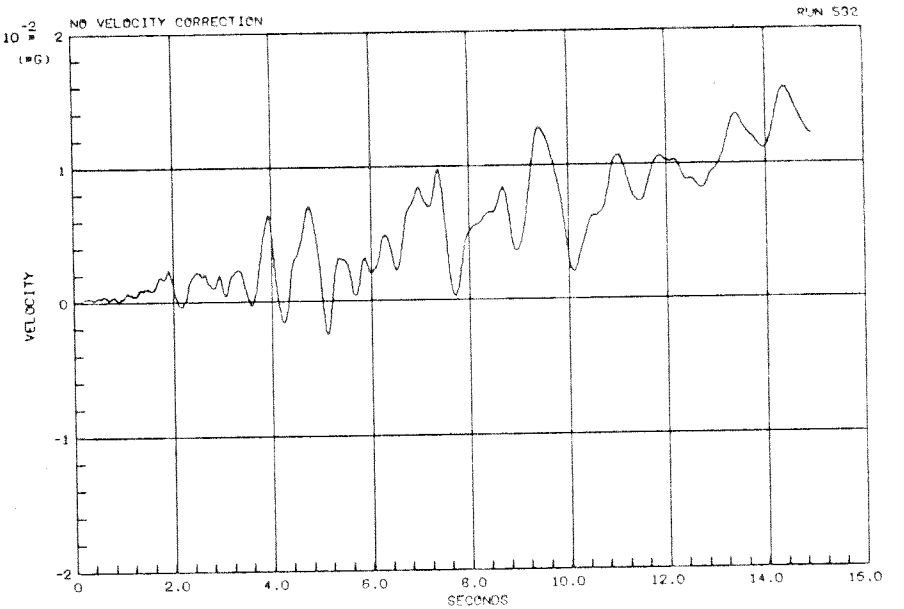

AARDVARK 1437 - TRANSVERSE

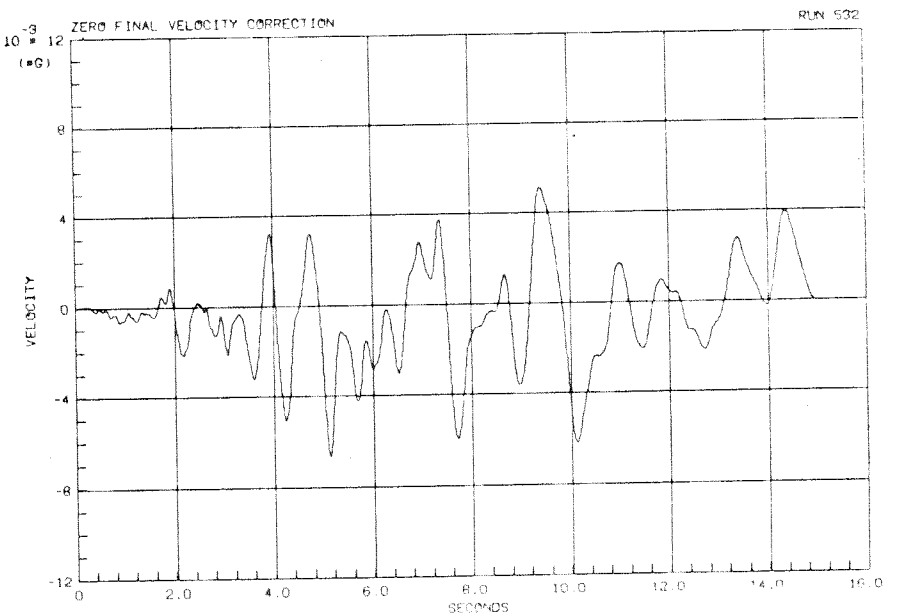

AARDVARK 1437 - TRANSVERSE

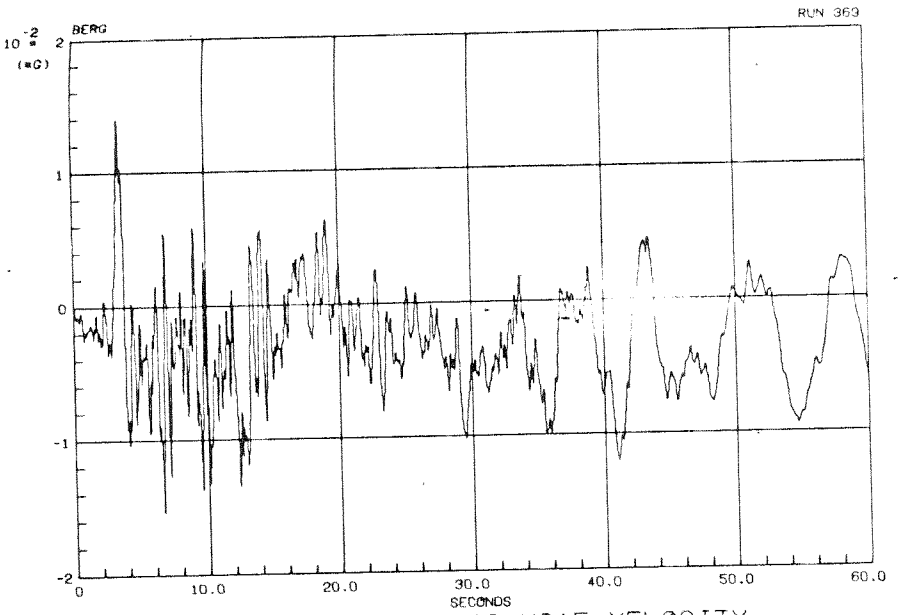

TAFT 21 JULY 1952 N21E VELOCITY

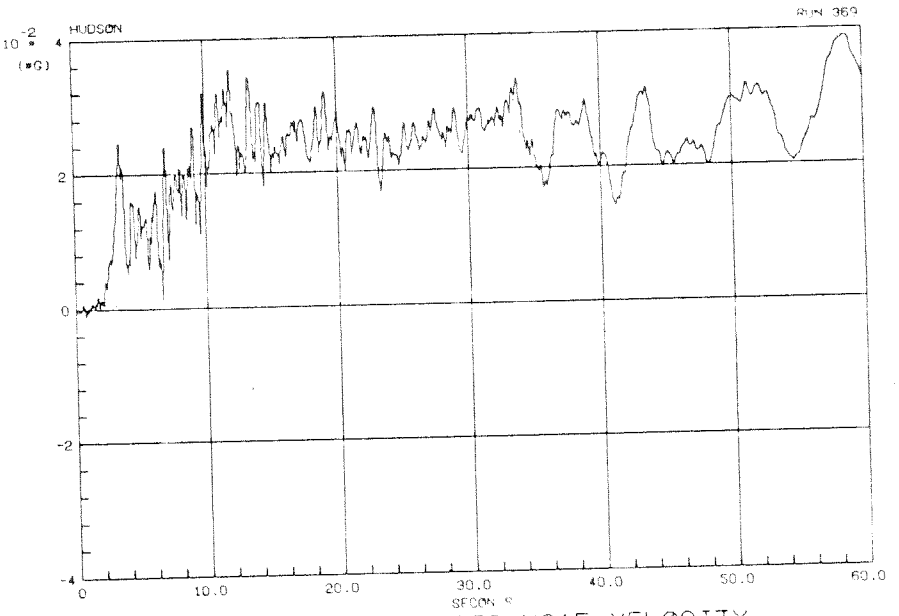

TAFT 21 JULY 1952 N21E VELOCITY

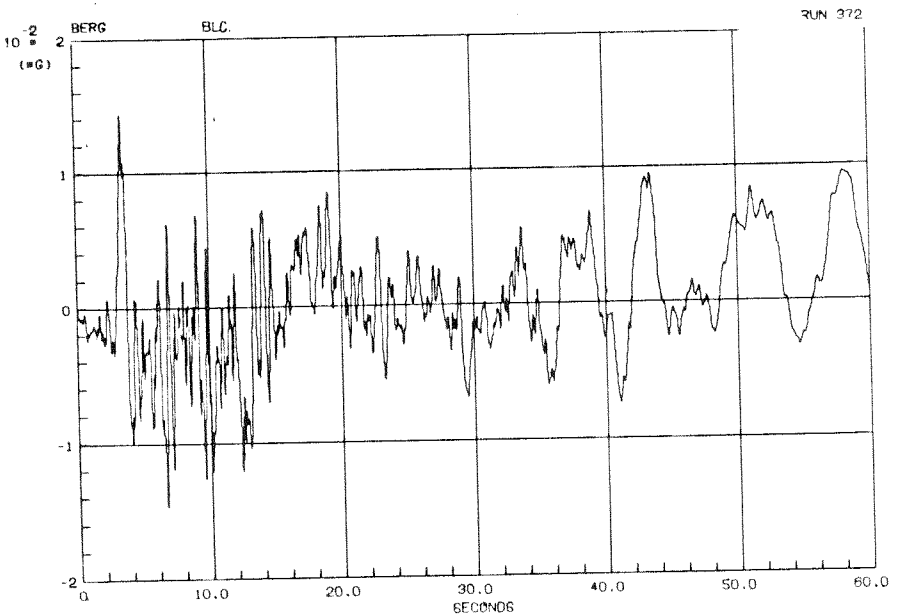

TAFT 21 JULY 1952 N21E VELOCITY

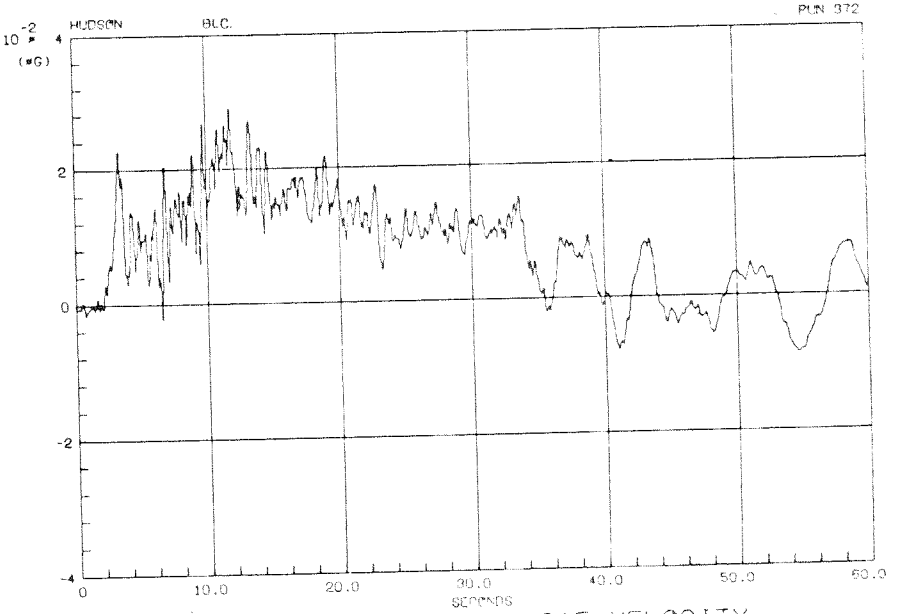

TAFT 21 JULY 1952 N21E VELOCITY

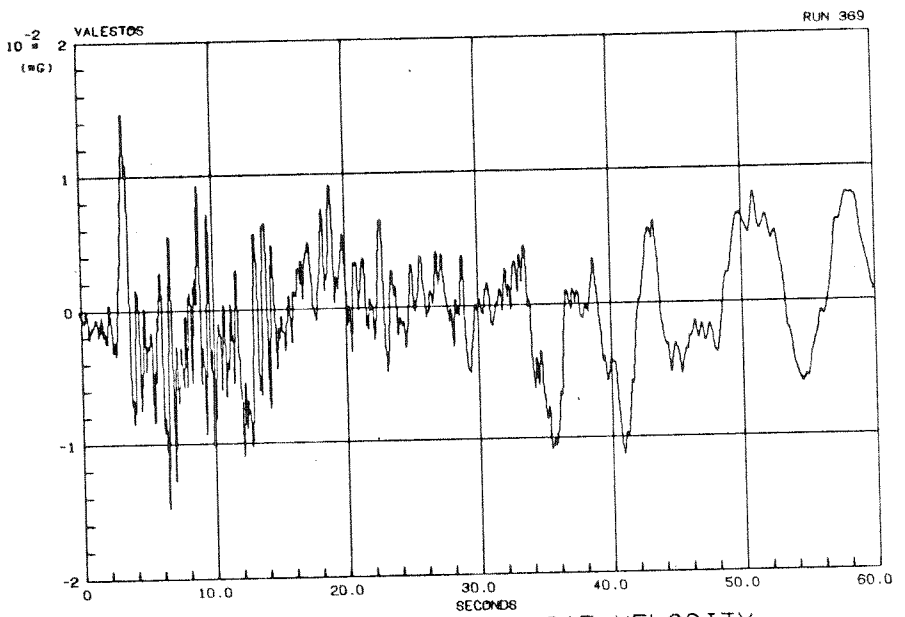

TAFT 21 JULY 1952 N21E VELOCITY

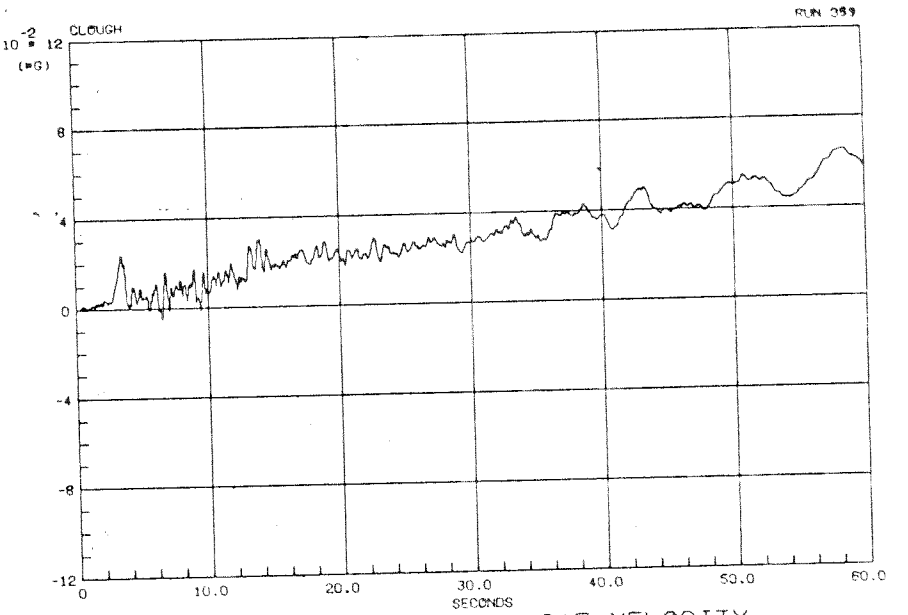

TAFT 21 JULY 1952 N21E VELOCITY

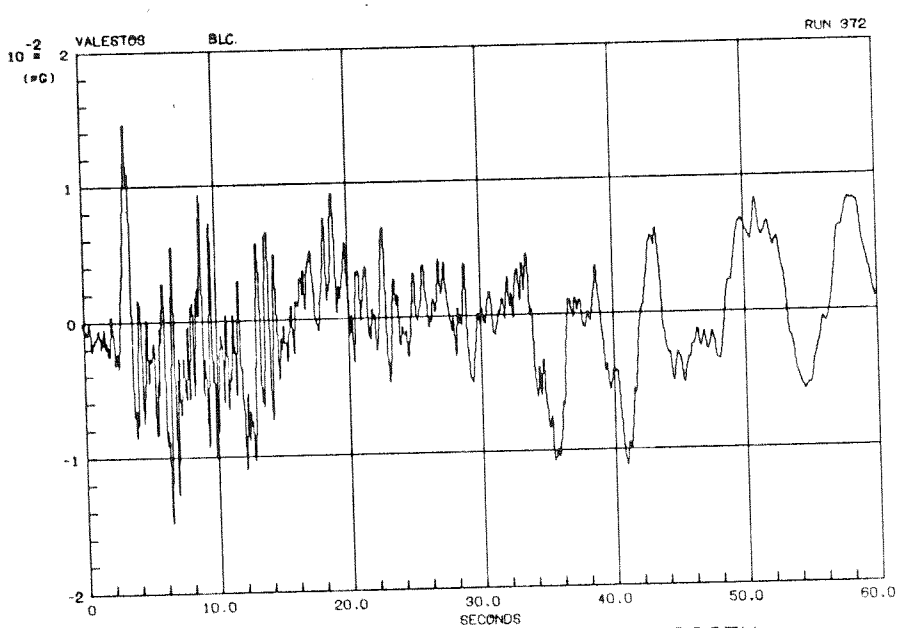

TAFT 21 JULY 1952 N21E VELOCITY

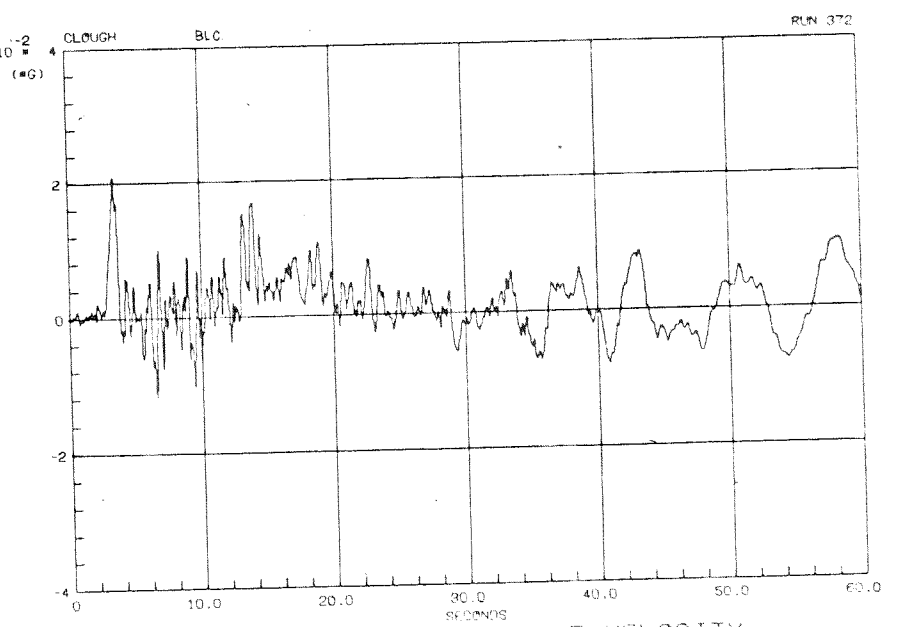

TAFT 21 JULY 1952 N21E VELOCITY

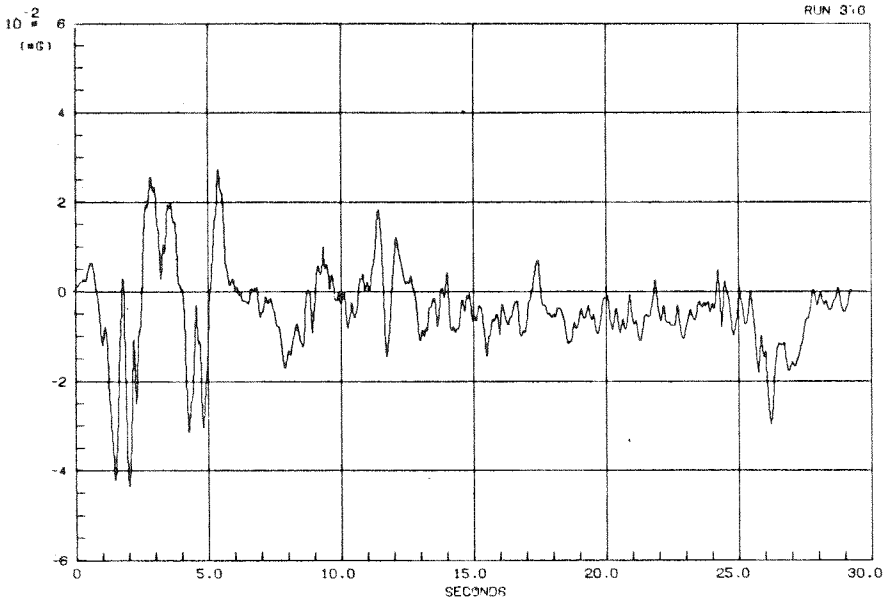

EL CENTRO 1940 NS VELOCITY

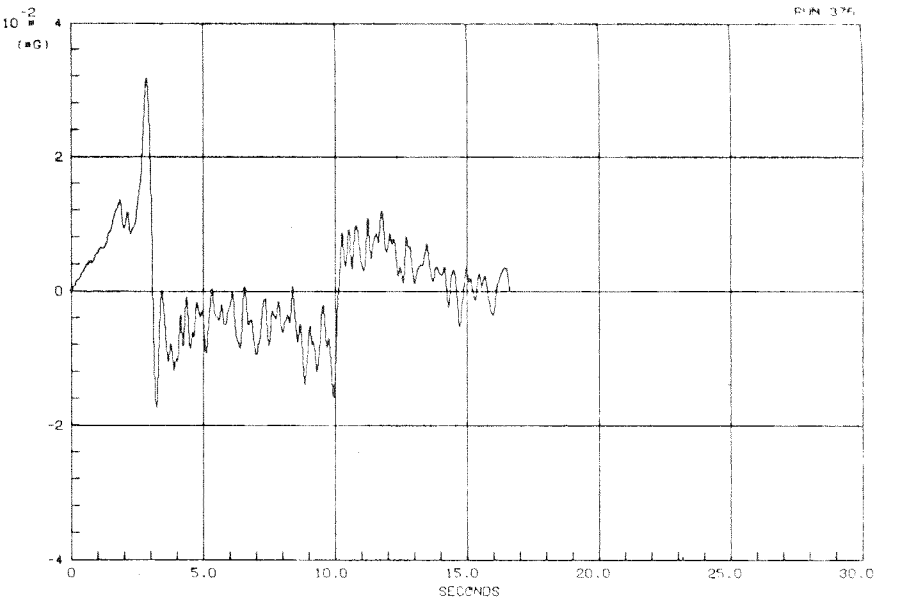

EL CENTRO 1934 NS VELOCITY

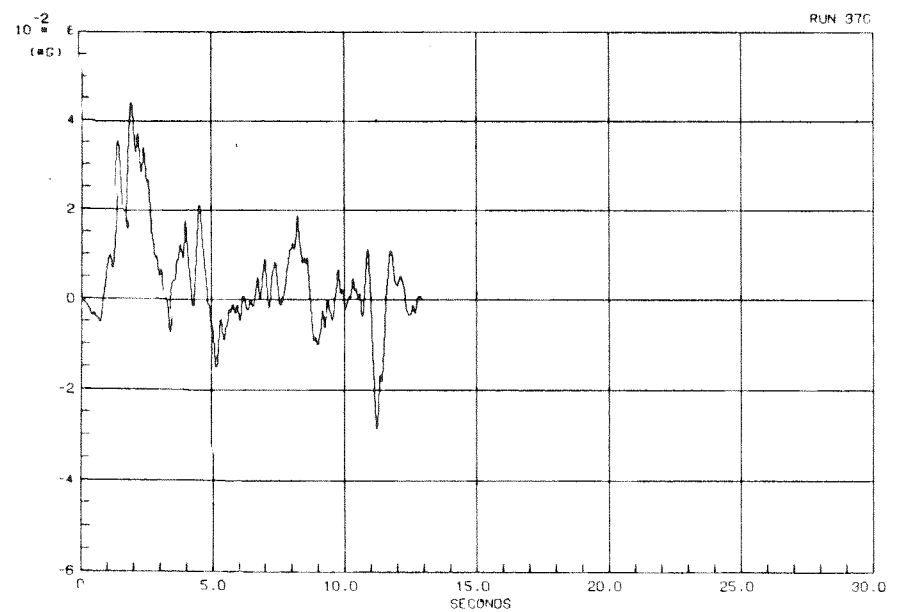

EL CENTRO 1940 EW VELOCITY

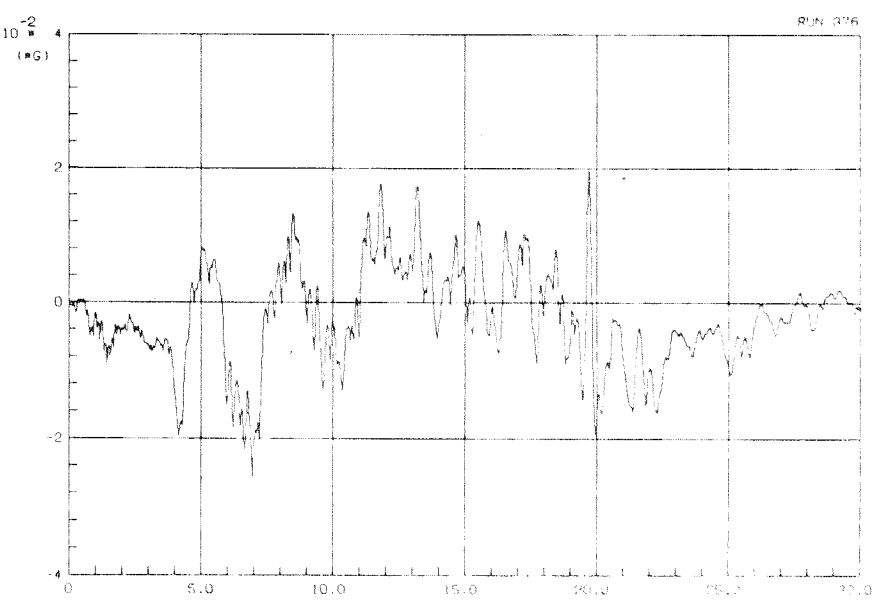

OLYMPIA 194 [illegible] VELOCITY

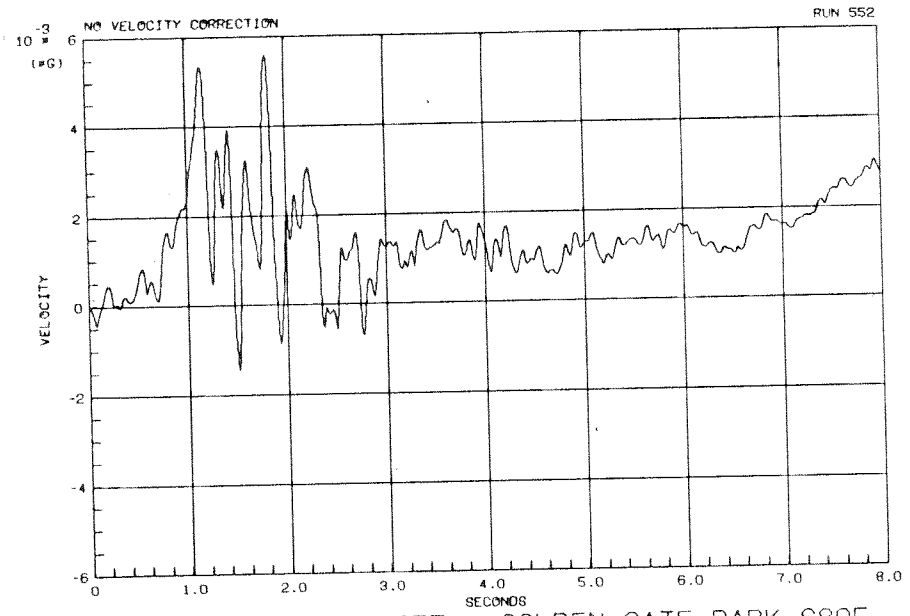

SAN FCO. MARCH 1957 - GOLDEN GATE PARK S80E

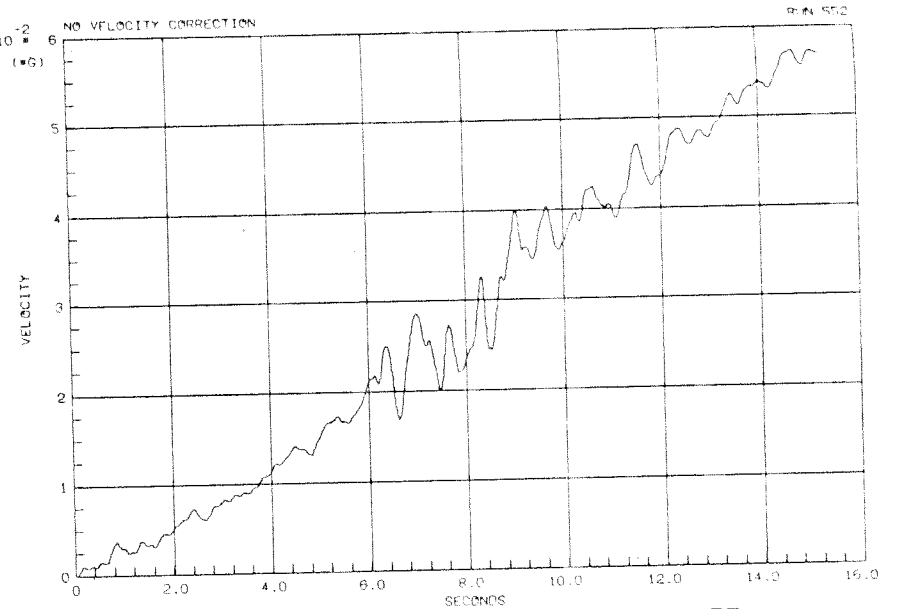

FERNDALE, 3 OCTOBER 1941 - S45E

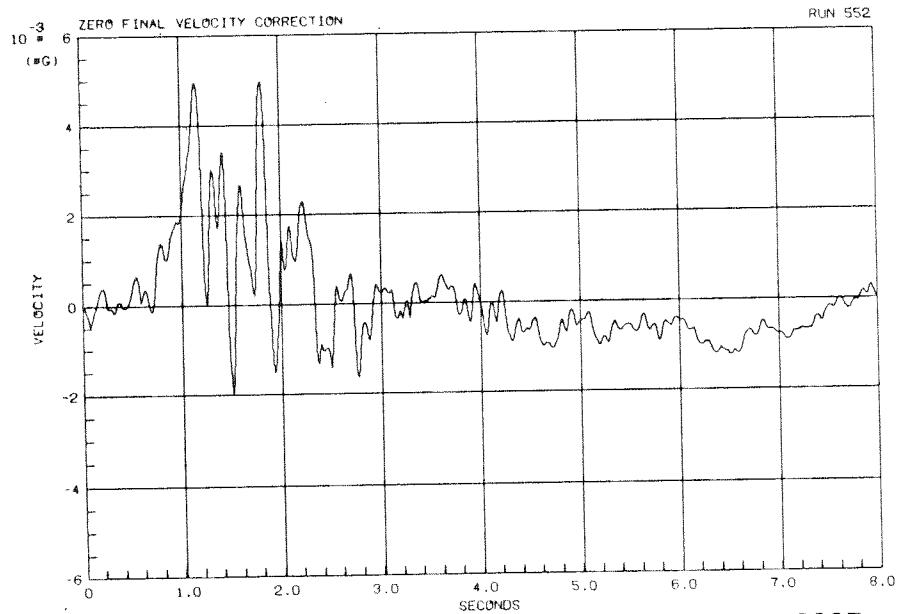

SAN FCO. MARCH 1957 - GOLDEN GATE PARK S80E

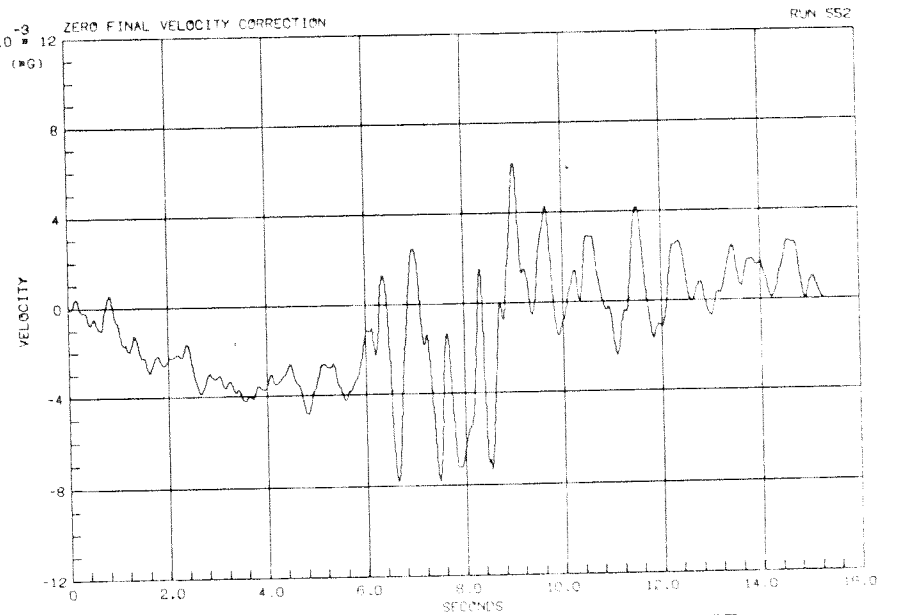

FERNDALE, 3 OCTOBER 1941 - S45E

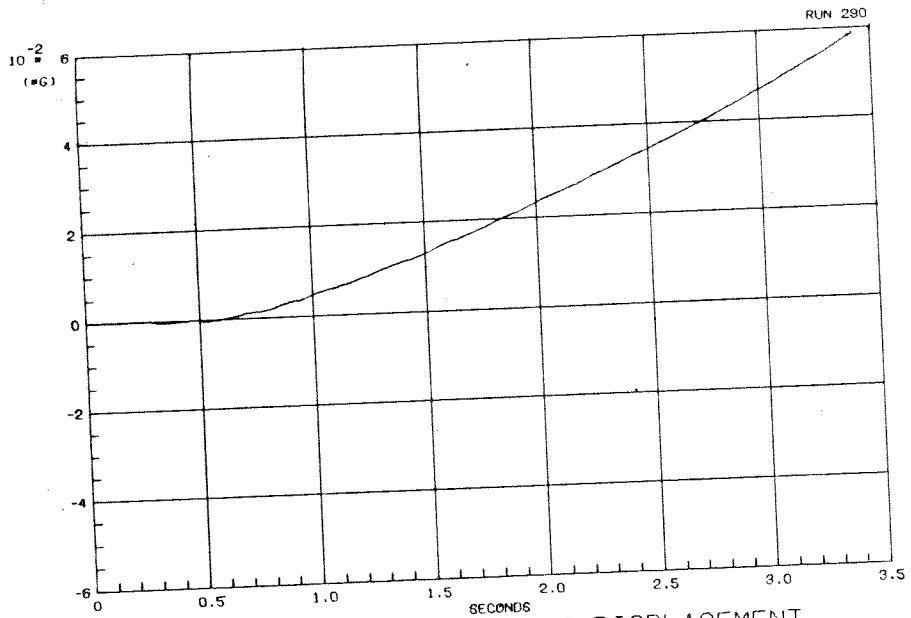

GNOME S2 - TRANSVERSE DISPLACEMENT

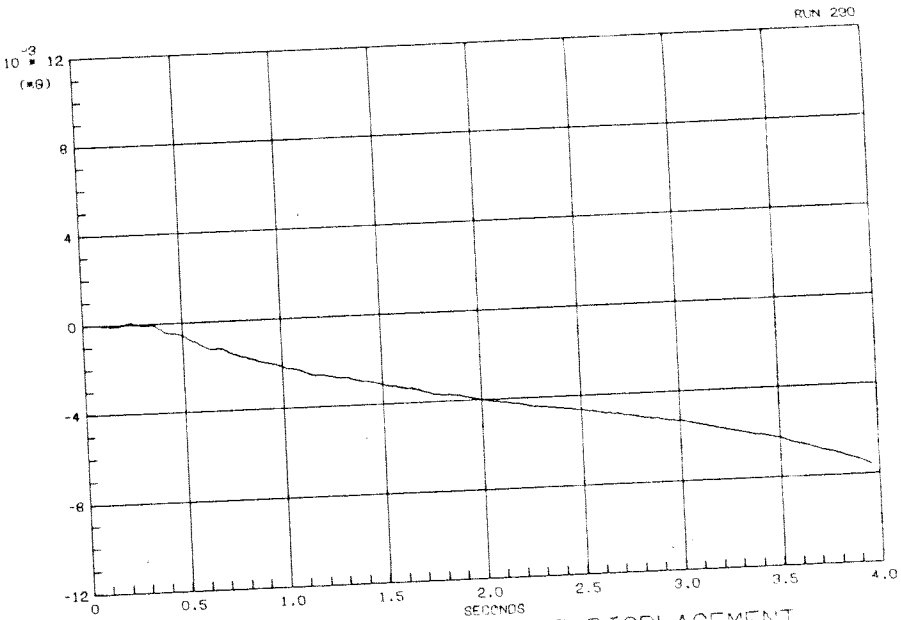

GNOME S3 - TRANSVERSE DISPLACEMENT

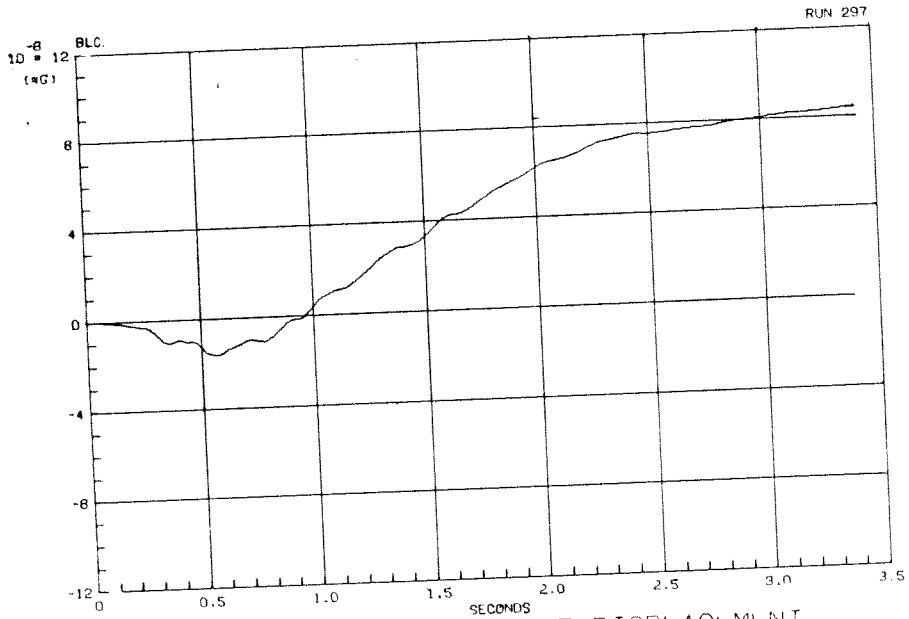

GNOME S2 - TRANSVERSE DISPLACEMENT

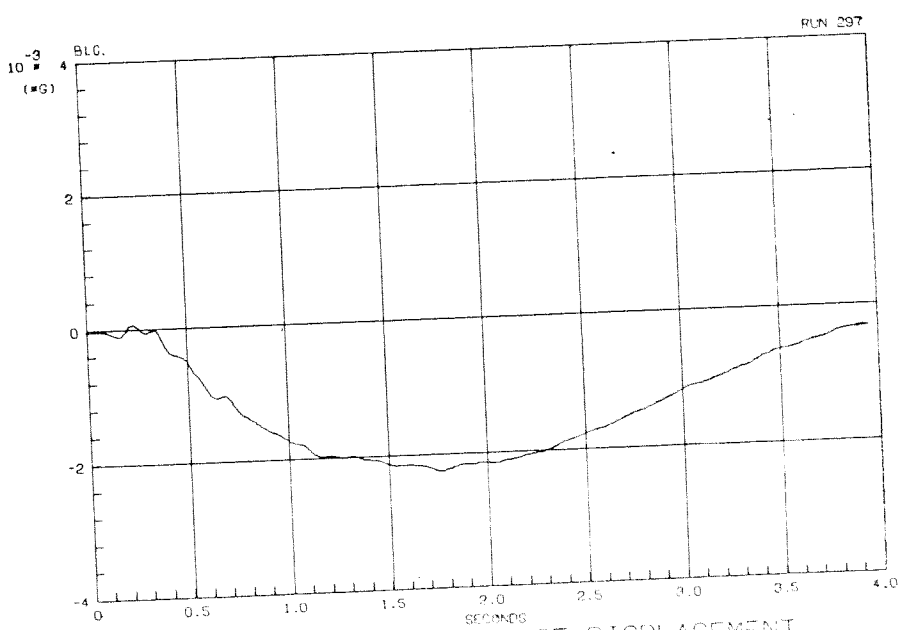

GNOME S3 - TRANSVERSE DISPLACEMENT

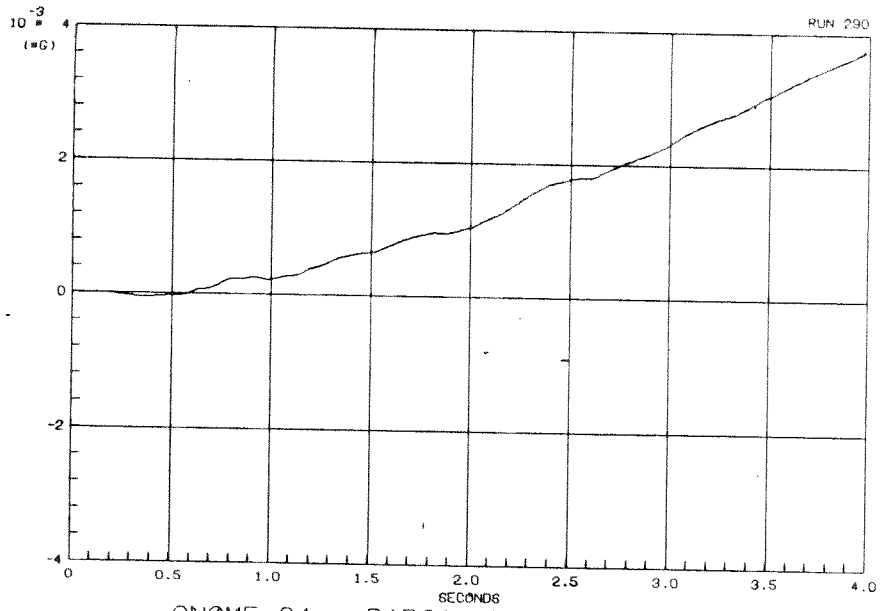

GNØME S4 - RADIAL DISPLACEMENT

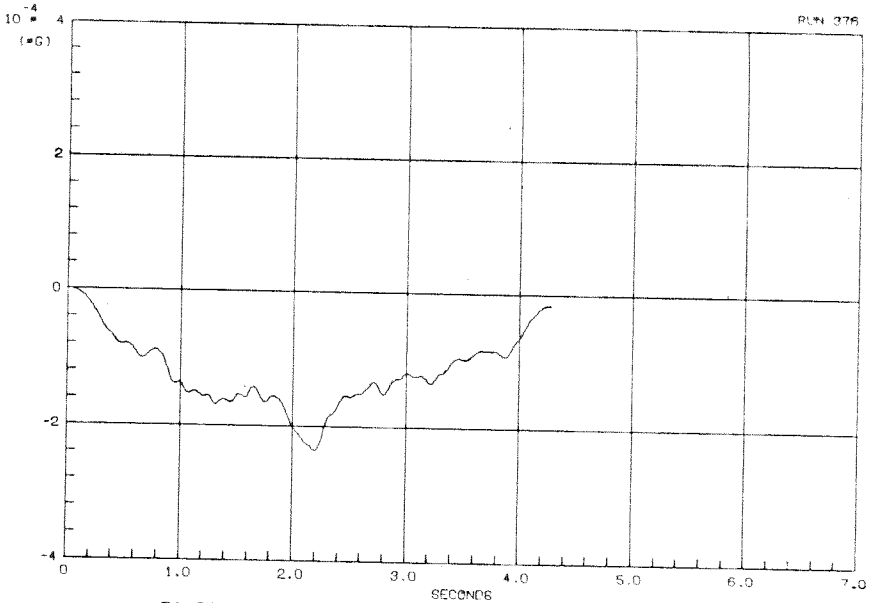

GNØME S4 - TRANSVERSE DISPLACEMENT

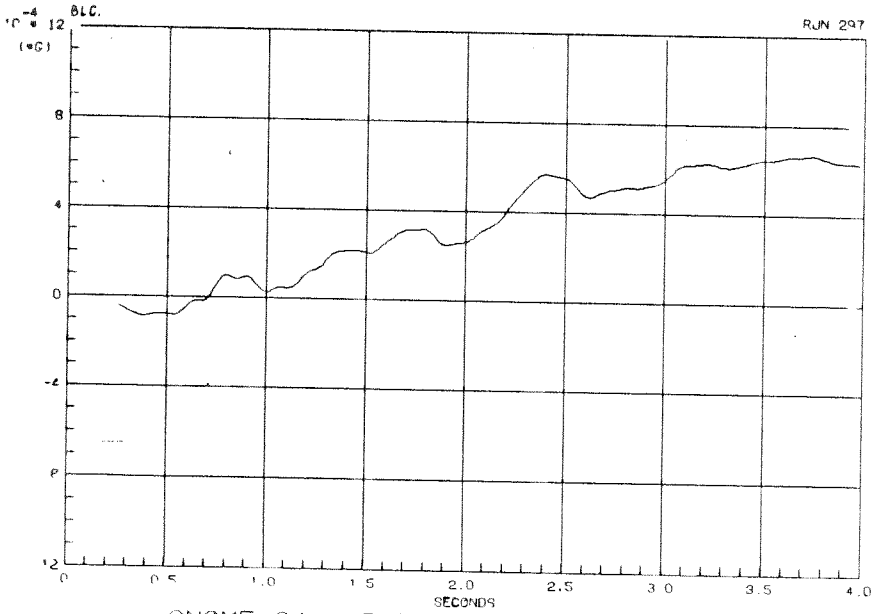

GNØME S4 RADIAL DISPLACEMENT

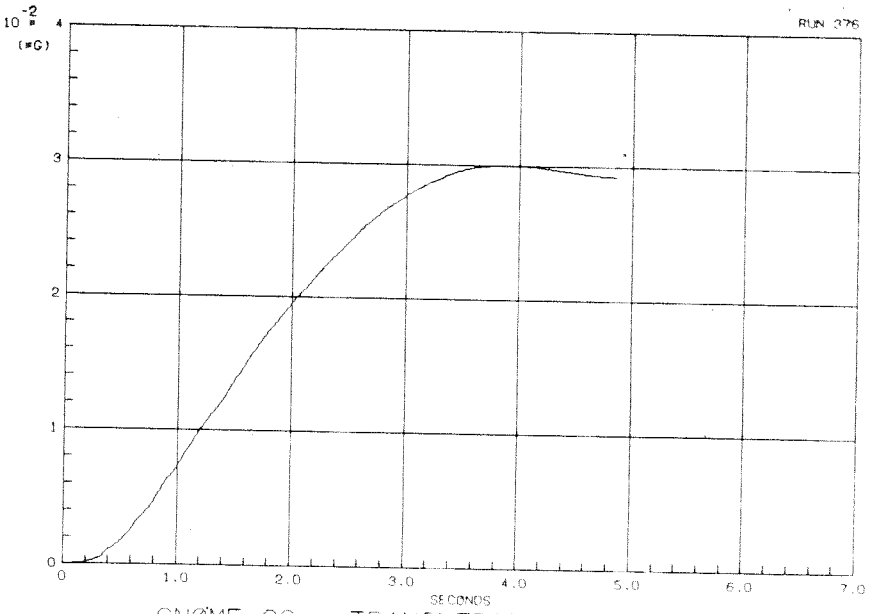

GNØME S6 - TRANSVERSE DISPLACEMENT

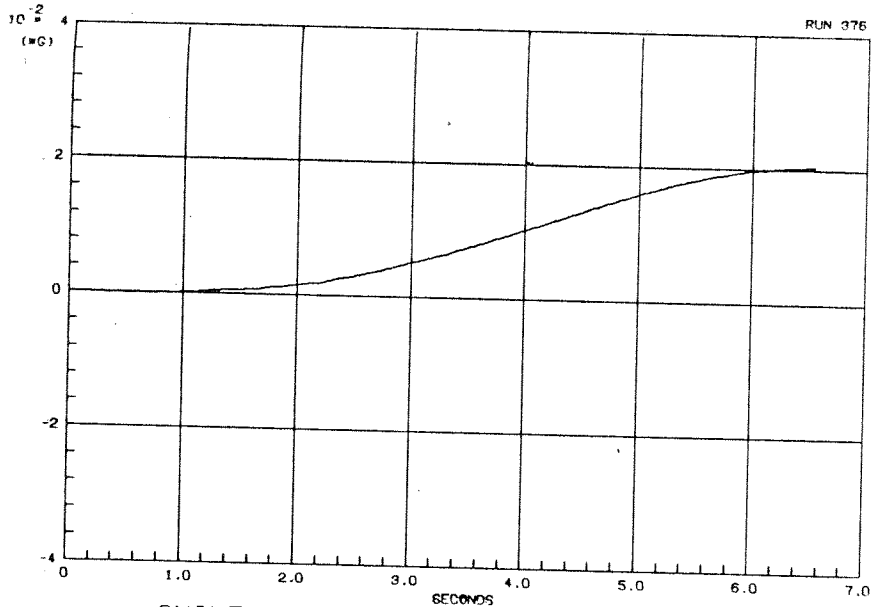

GNOME S7 - TRANSVERSE DISPLACEMENT

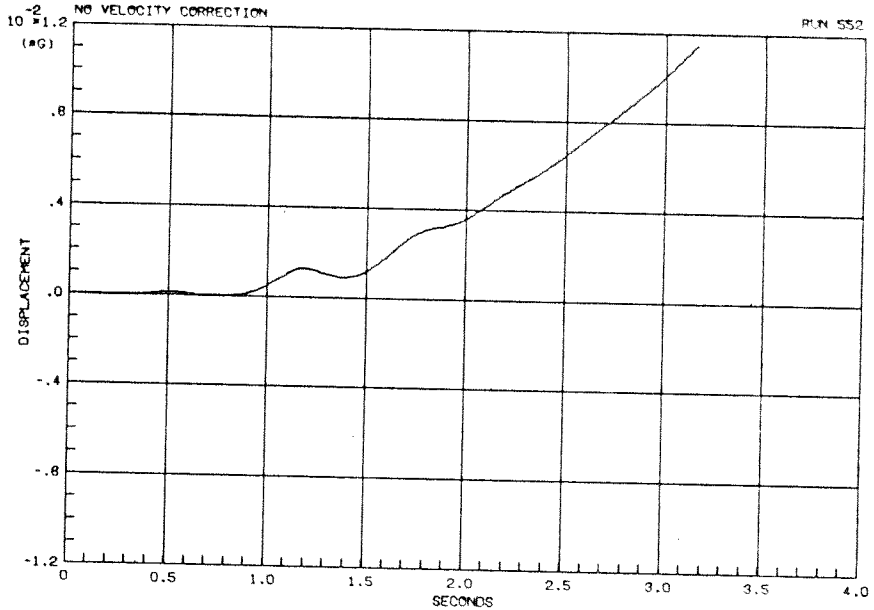

DANNYBOY D5 - RADIAL

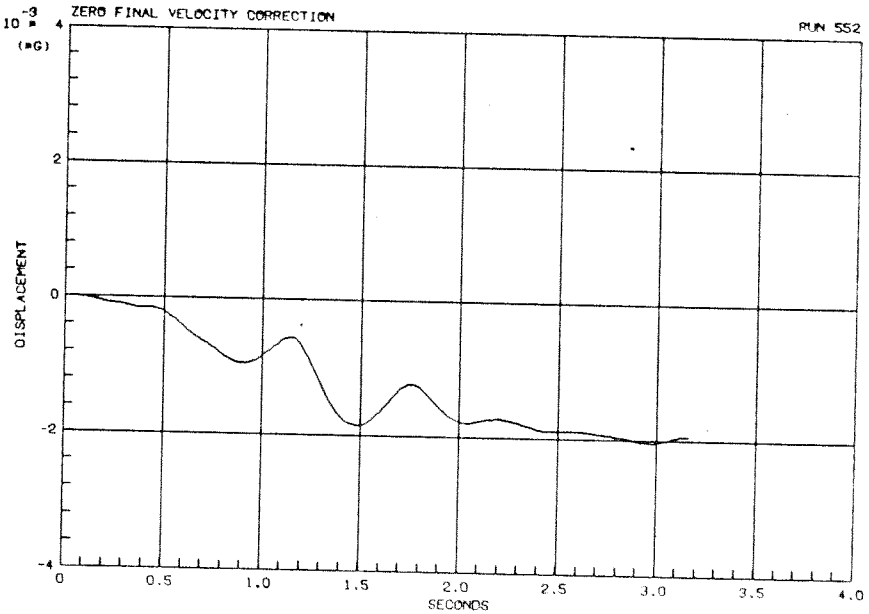

DANNYBOY D5 - RADIAL

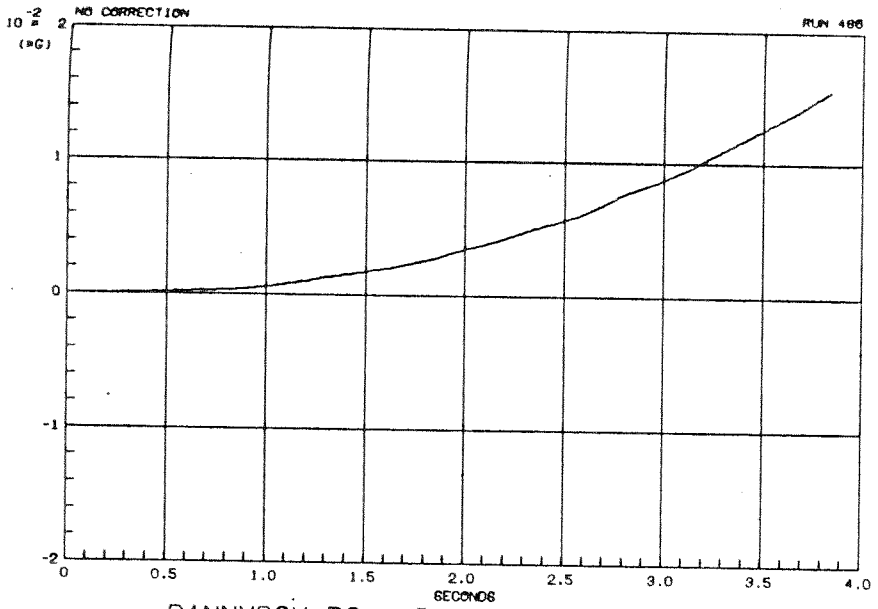

DANNYBOY D8 - RADIAL DISPLACEMENT

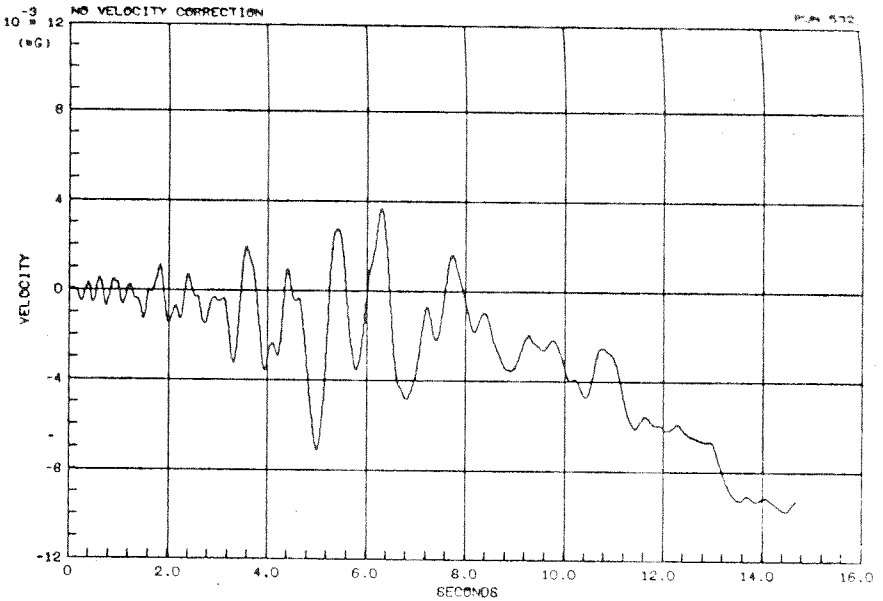

MISSISSIPPI 1777 - TRANSVERSE

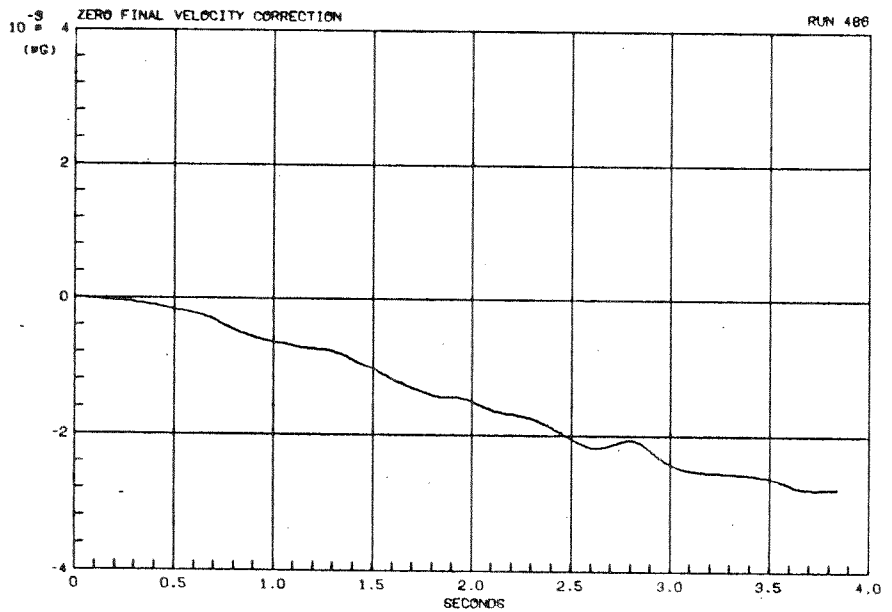

DANNYBOY D8 - RADIAL DISPLACEMENT

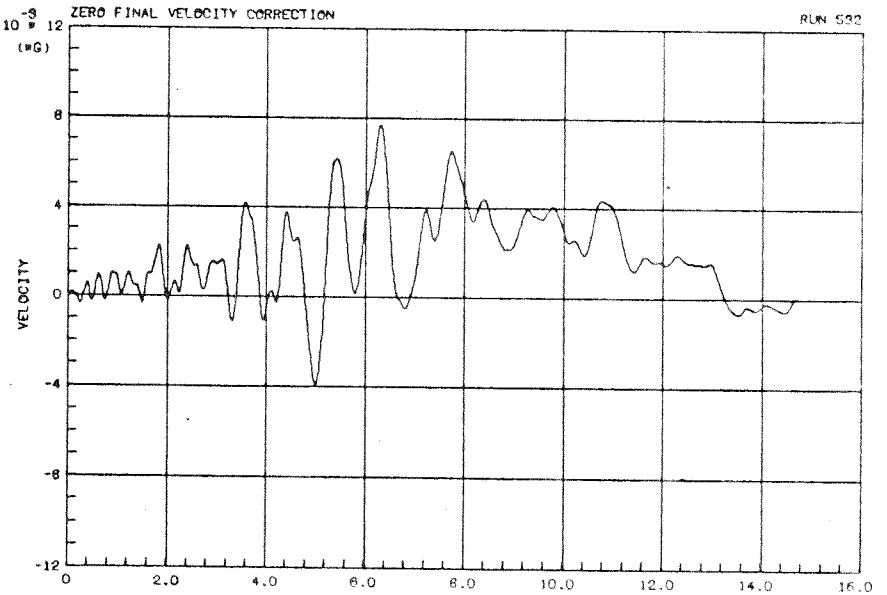

MISSISSIPPI 1777 - TRANSVERSE

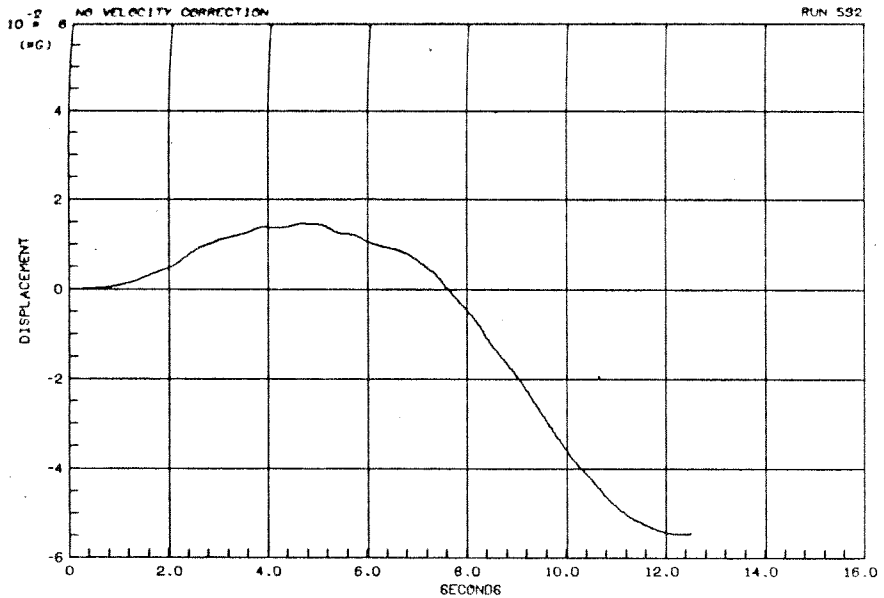

MISSISSIPPI 8228 - TRANSVERSE

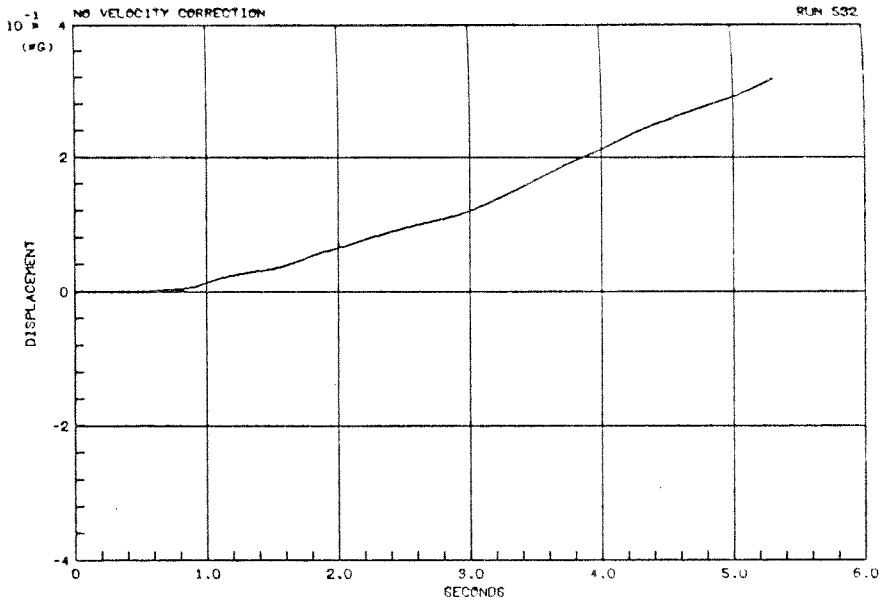

MISSISSIPPI 7245 - RADIAL

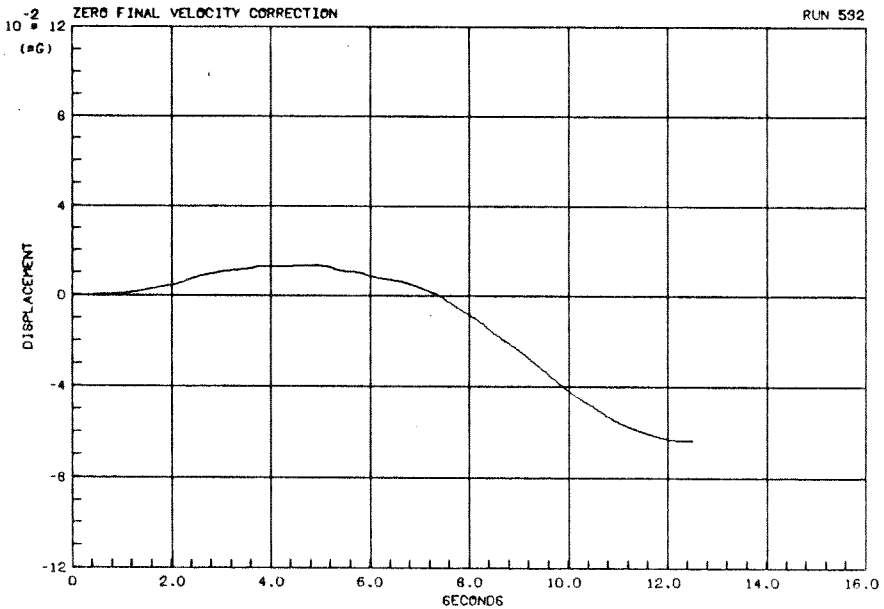

MISSISSIPPI 8228 - TRANSVERSE

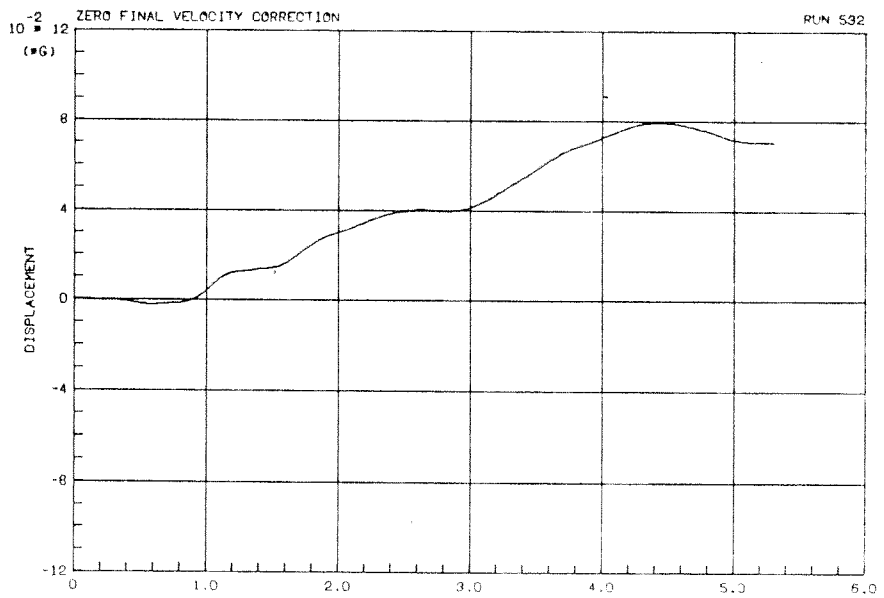

MISSISSIPPI 7245 - RADIAL

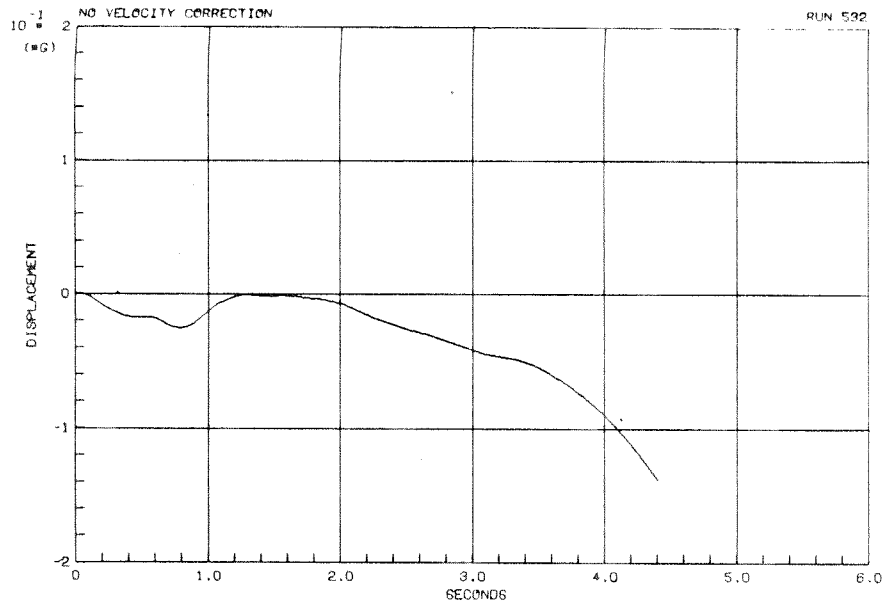

MISSISSIPPI 9537 - RADIAL

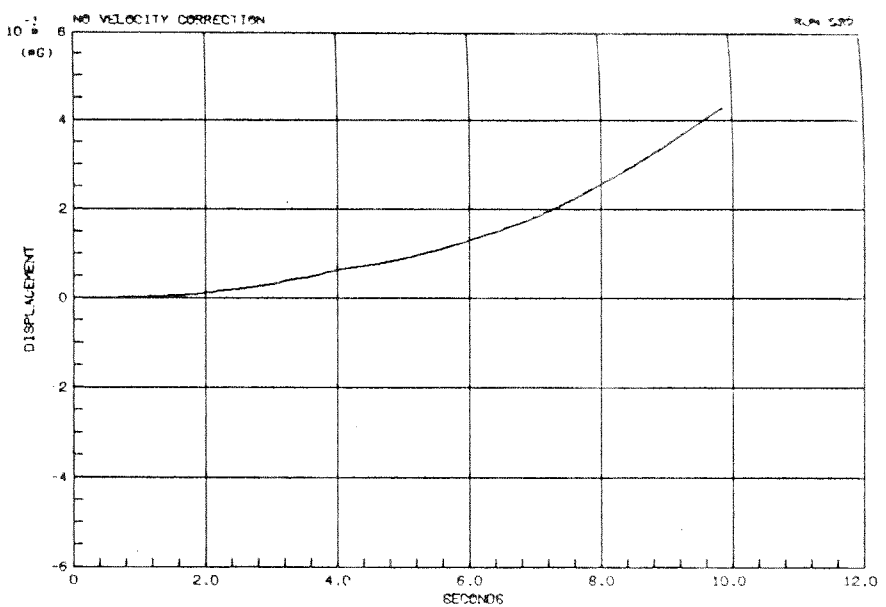

MISSISSIPPI 4074 - TRANSVERSE

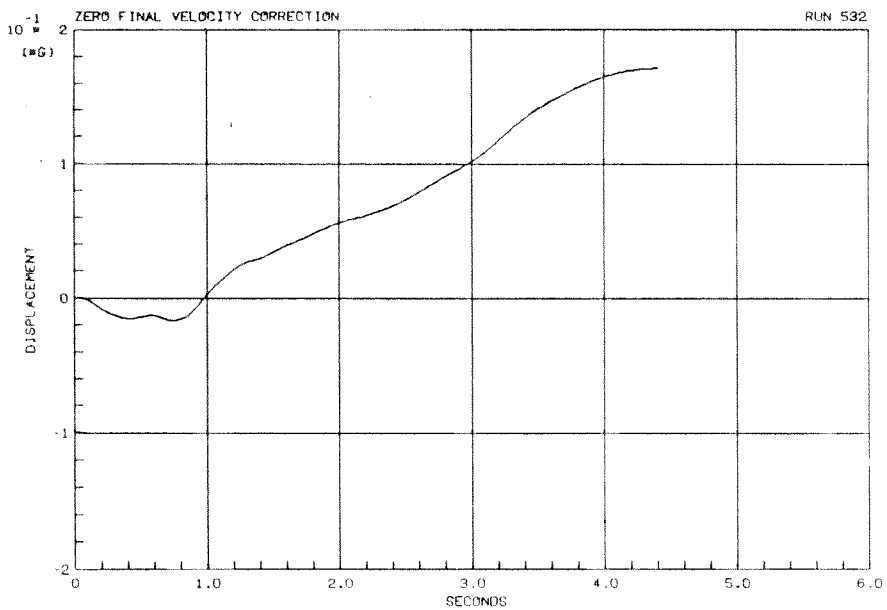

MISSISSIPPI 9537 - RADIAL

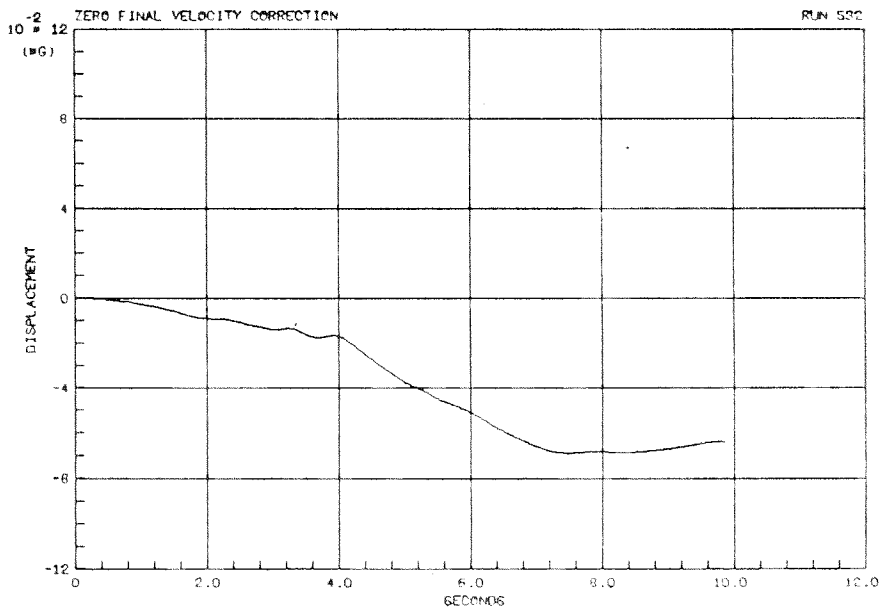

MISSISSIPPI 4074 - TRANSVERSE

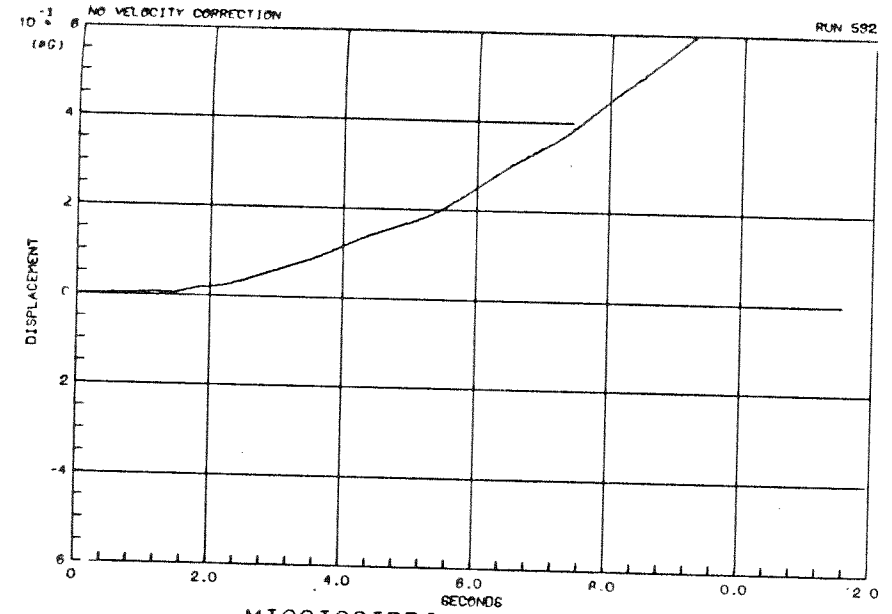

MISSISSIPPI 4074 - RADIAL

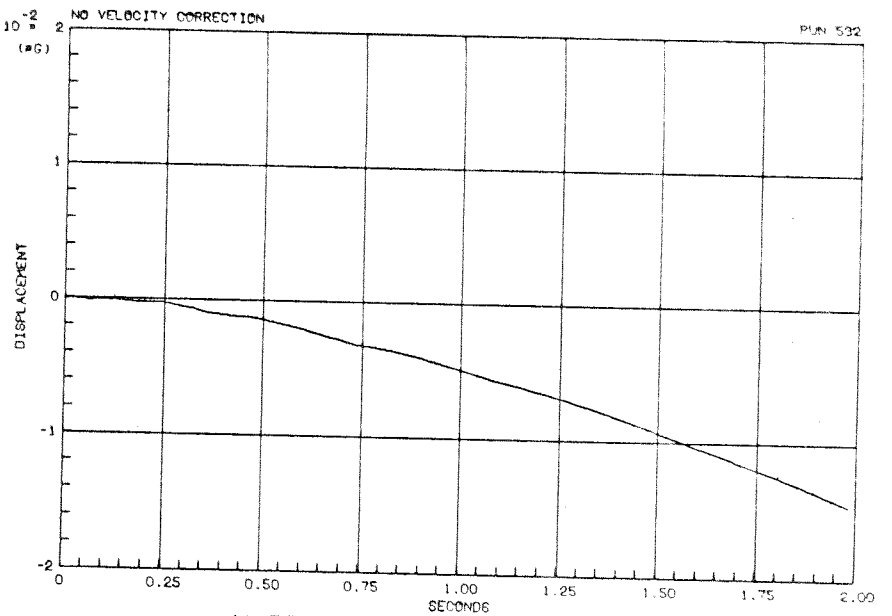

HARDHAT 1091 - TRANSVERSE

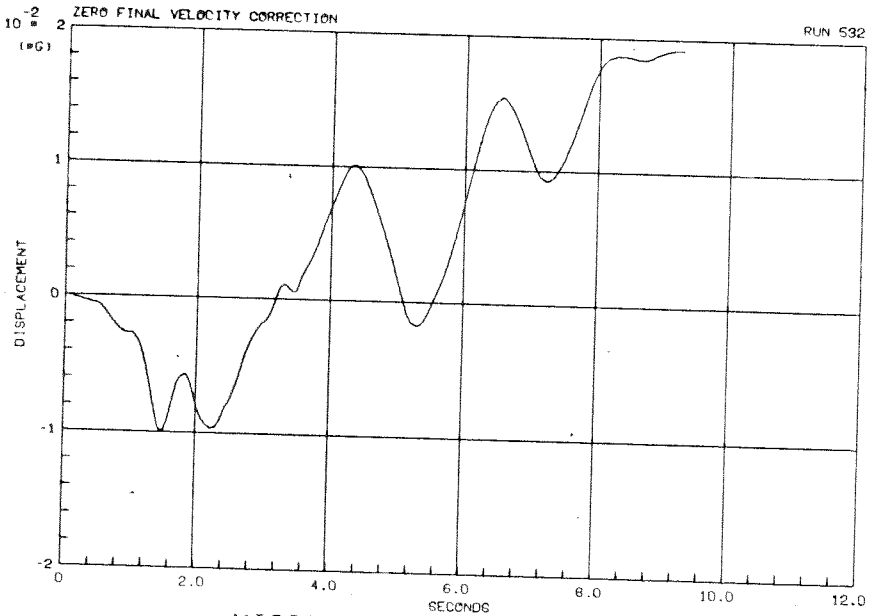

MISSISSIPPI 4074 - RADIAL

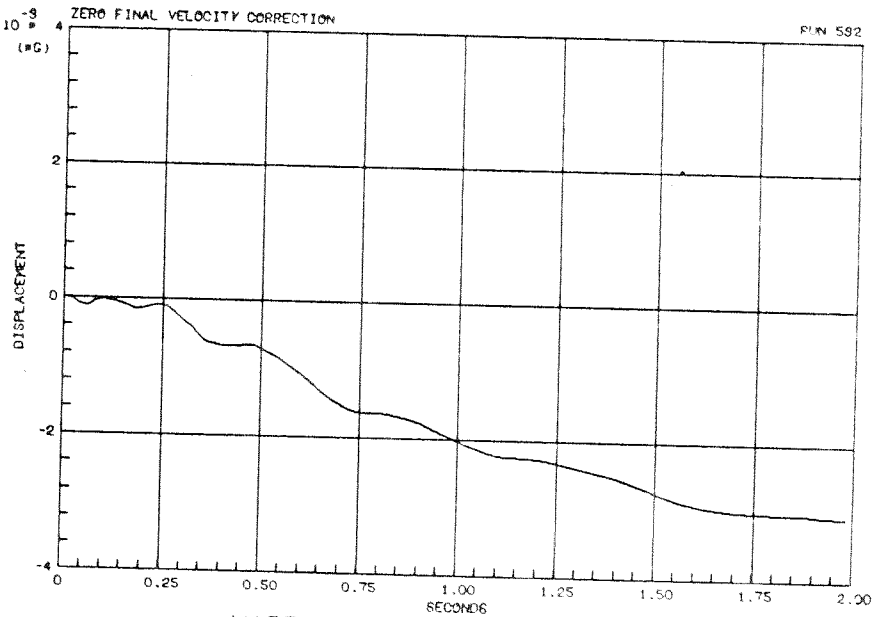

HARDHAT 1091 - TRANSVERSE

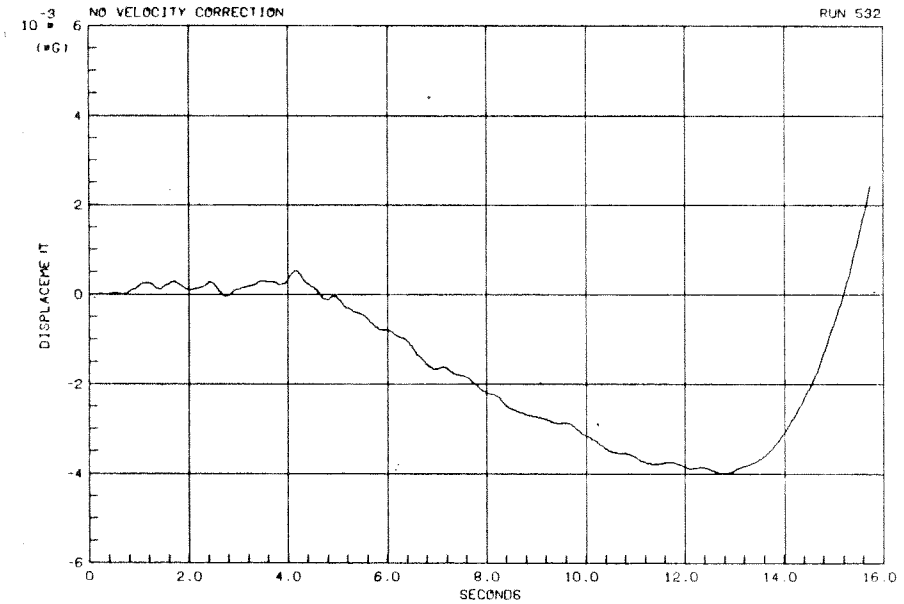

HARDHAT 4496 - TRANSVERSE

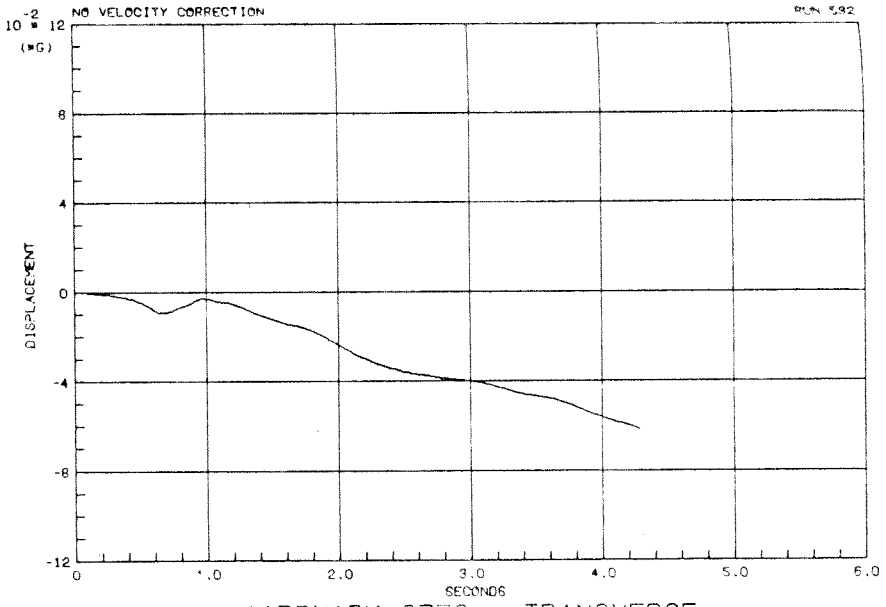

AARDVARK 3773 - TRANSVERSE

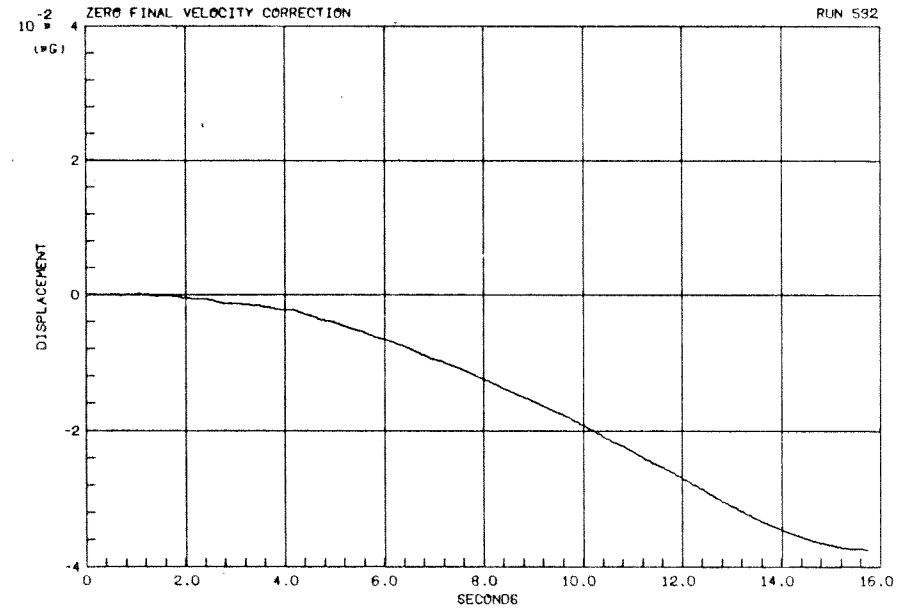

HARDHAT 4496 - TRANSVERSE

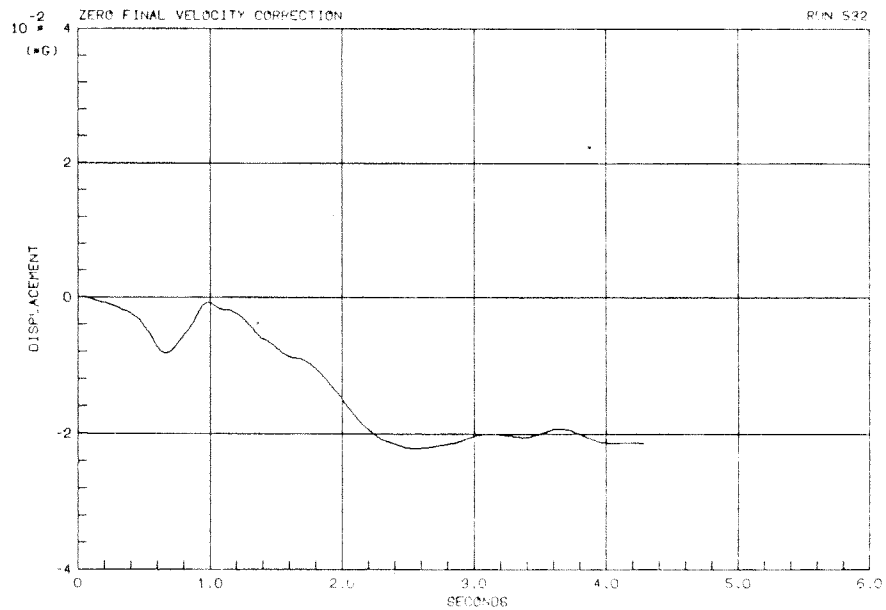

AARDVARK 3773 - TRANSVERSE

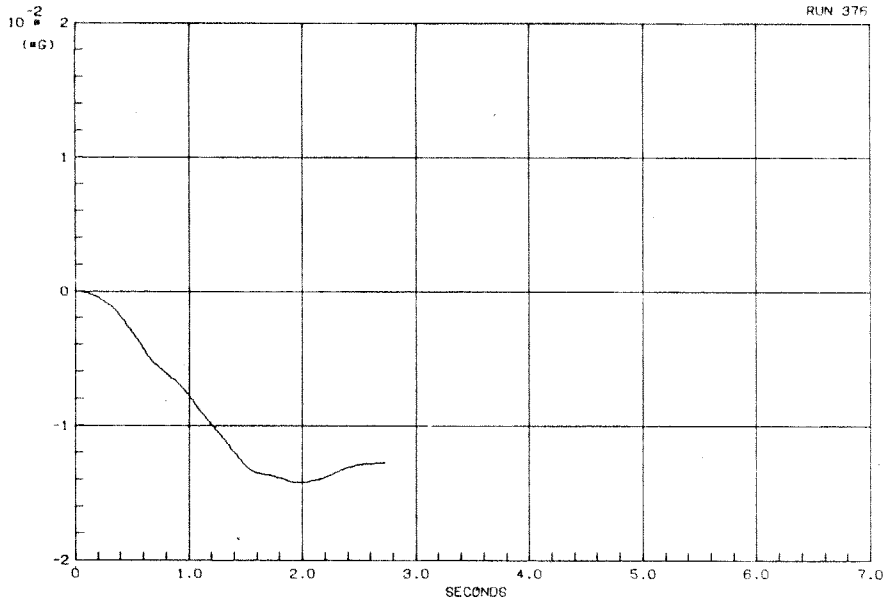

SEDAN R3 - RADIAL DISPLACEMENT

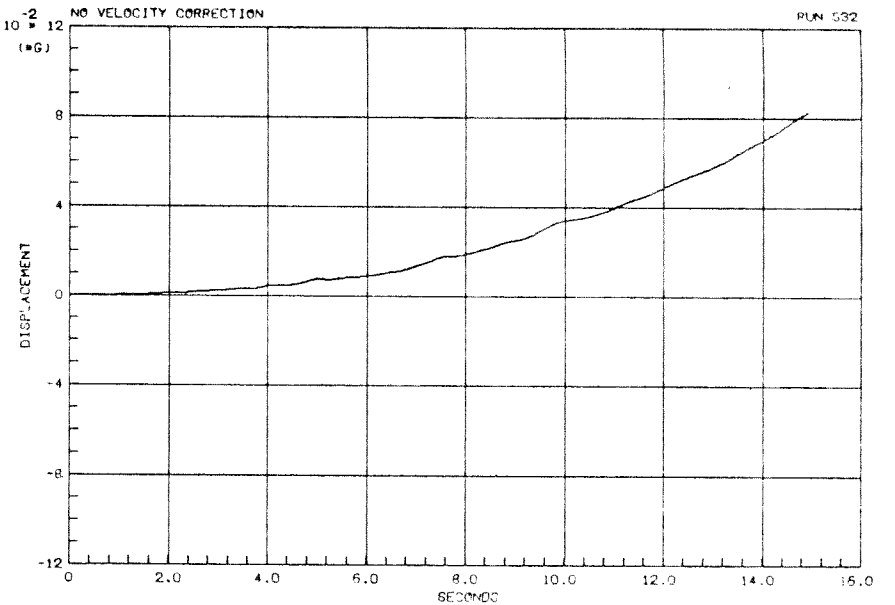

AARDVARK 1437 - TRANSVERSE

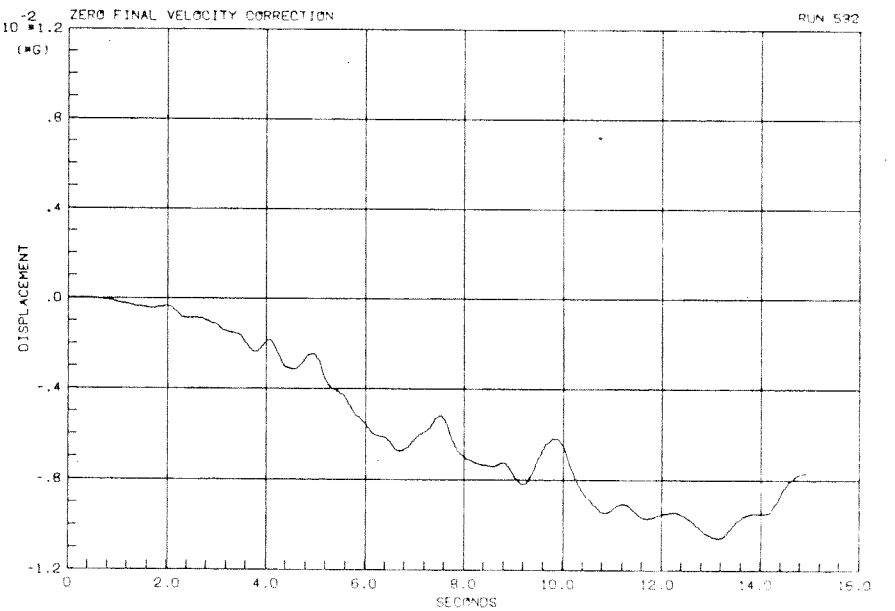

AARDVARK 1437 - TRANSVERSE

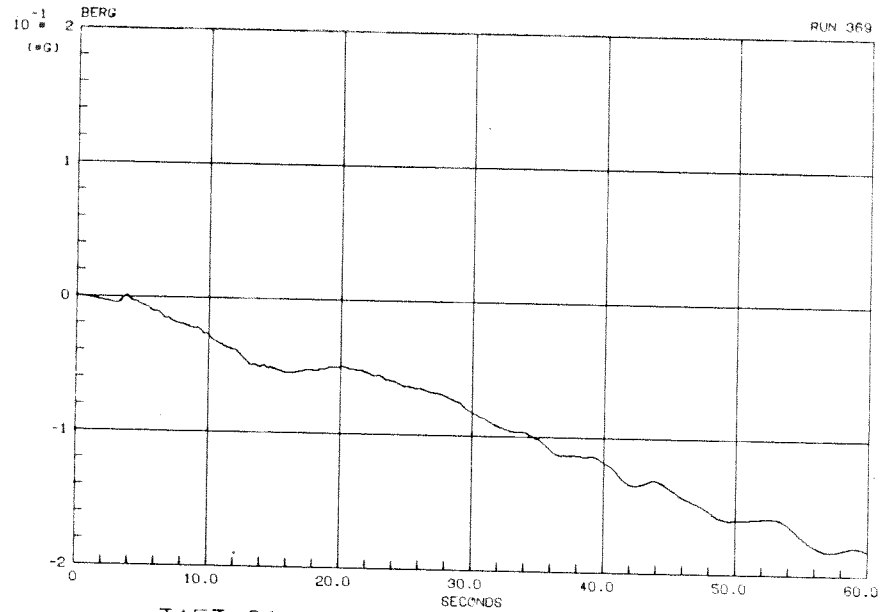

TAFT 21 JULY 1952 N21E DISPLACEMENT

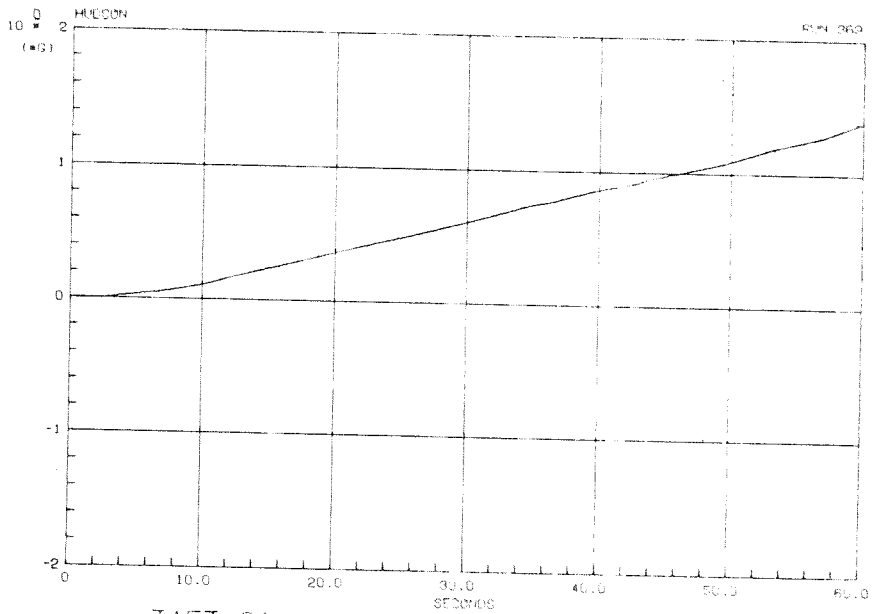

TAFT 21 JULY 1952 N21E DISPLACEMENT

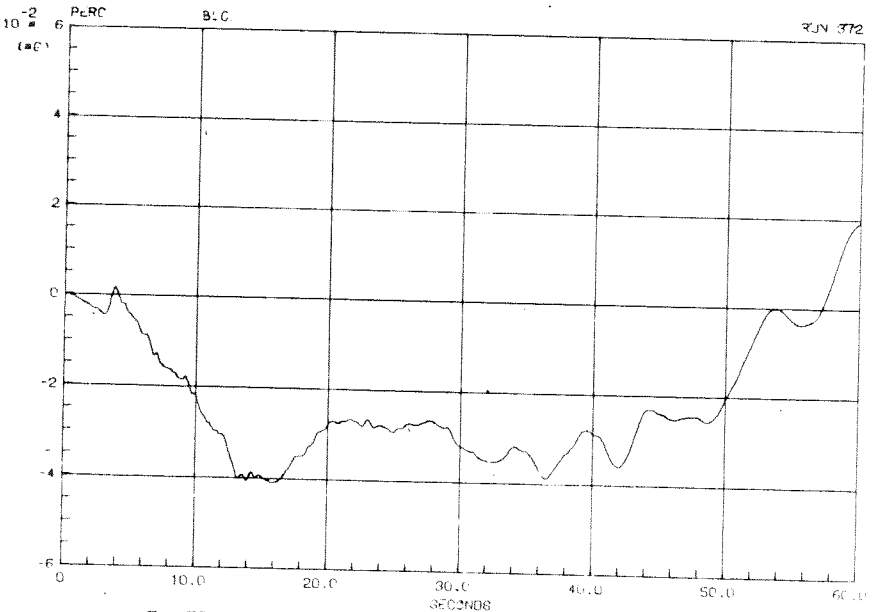

TAFT 21 JULY 1952 N21E DISPLACEMENT

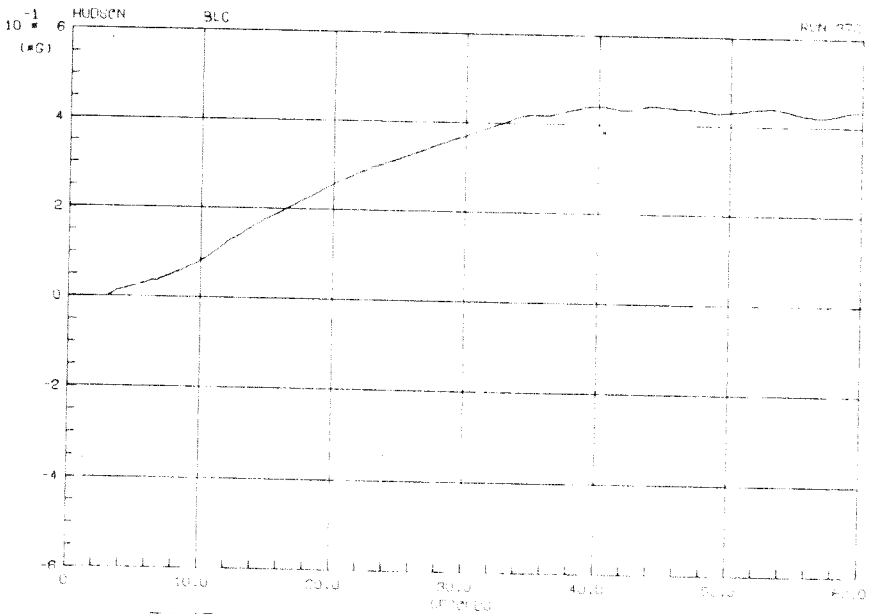

TAFT 21 JULY 1952 N21E DISPLACEMENT

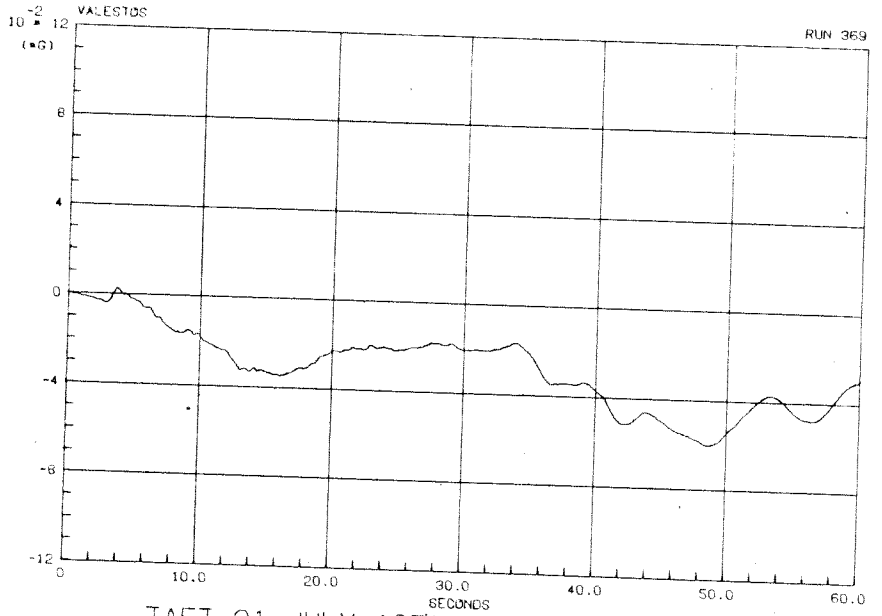

TAFT 21 JULY 1952 N21E DISPLACEMENT

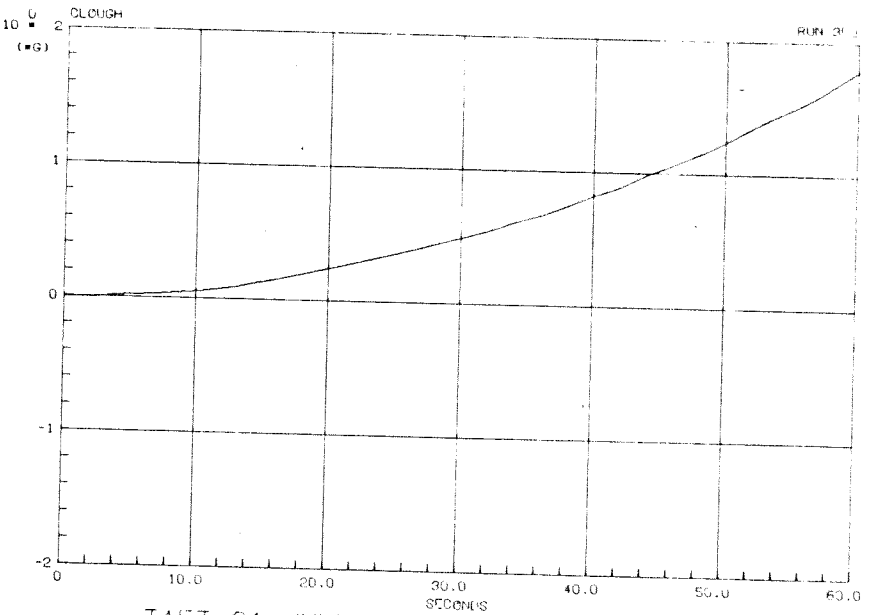

TAFT 21 JULY 1952 N21E DISPLACEMENT

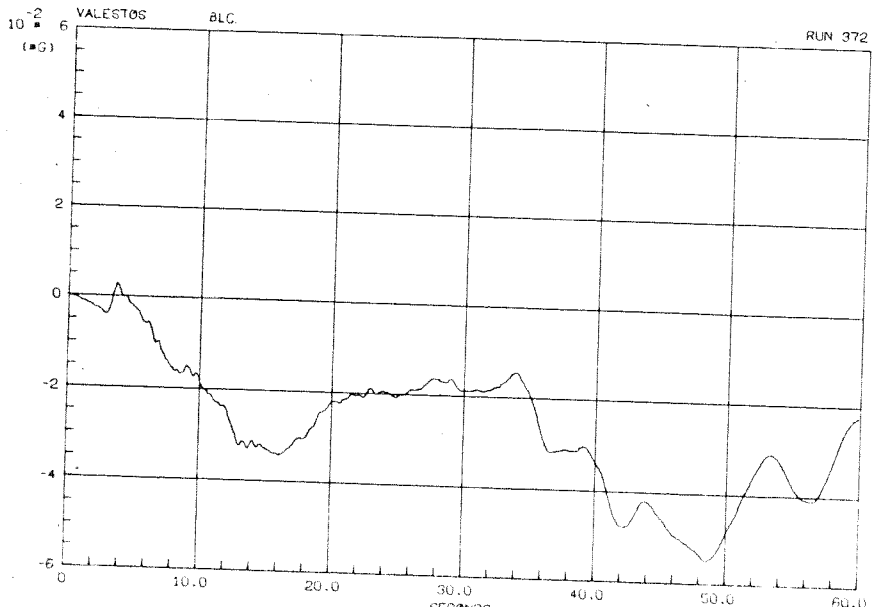

TAFT 21 JULY 1952 N21E DISPLACEMENT

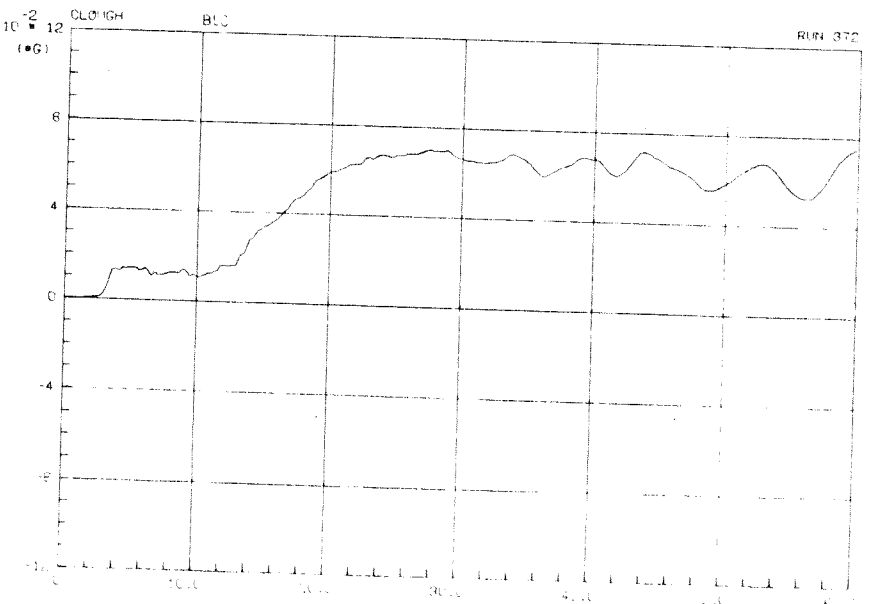

TAFT 21 JULY 1952 N21E DISPLACEMENT

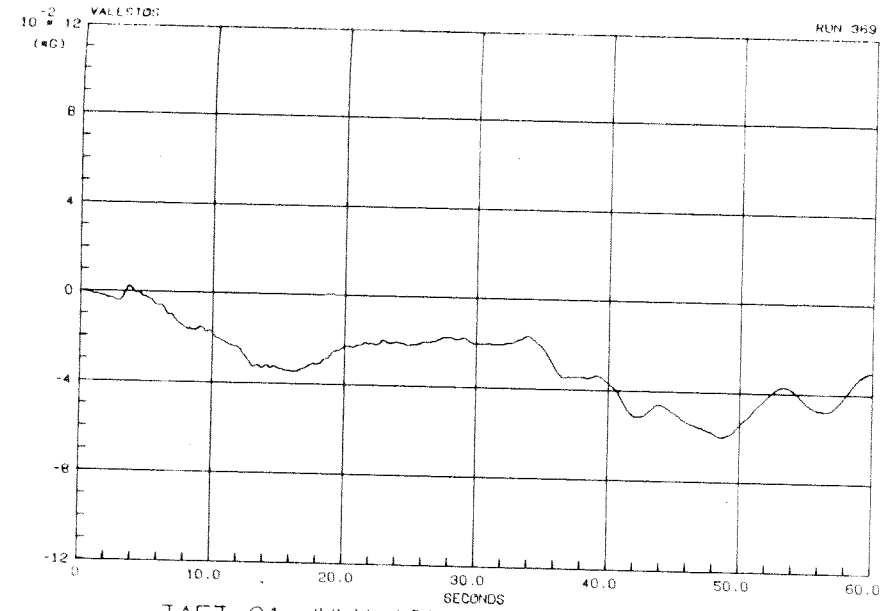

TAFT 21 JULY 1952 N21E DISPLACEMENT

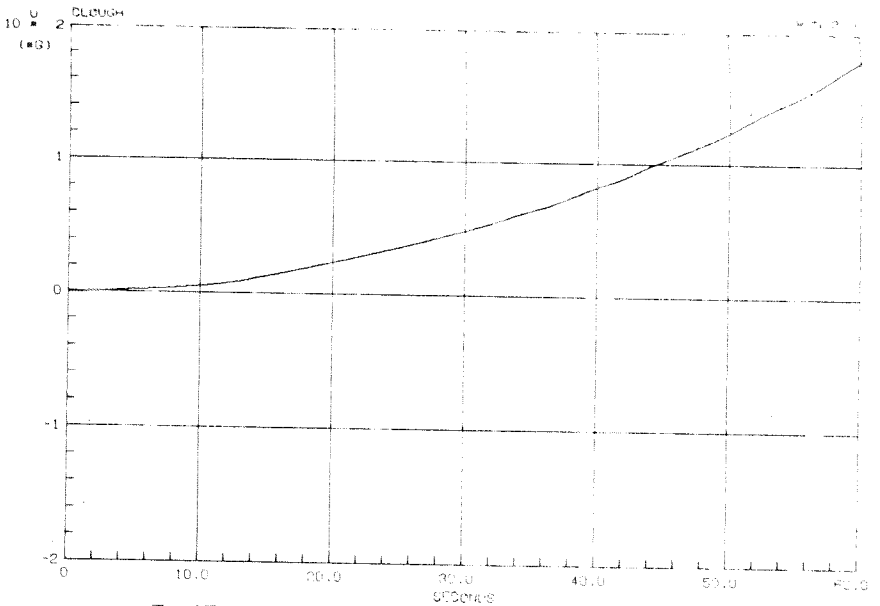

TAFT 21 JULY 1952 N21E DISPLACEMENT

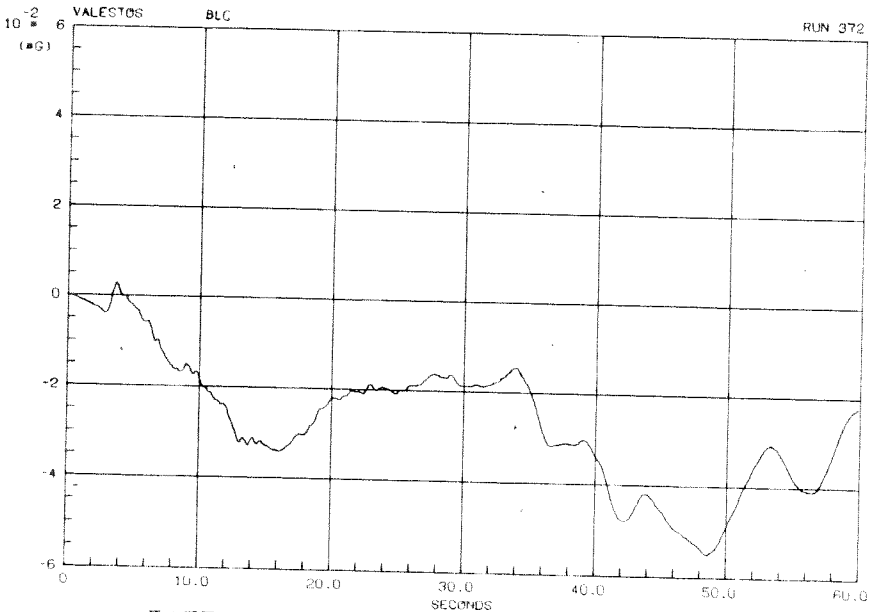

TAFT 21 JULY 1952 N21E DISPLACEMENT

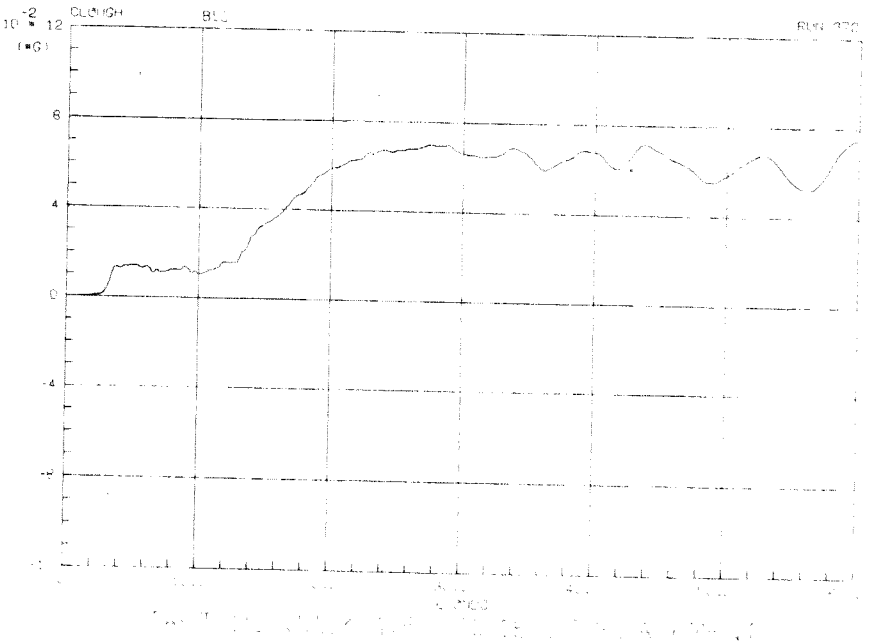

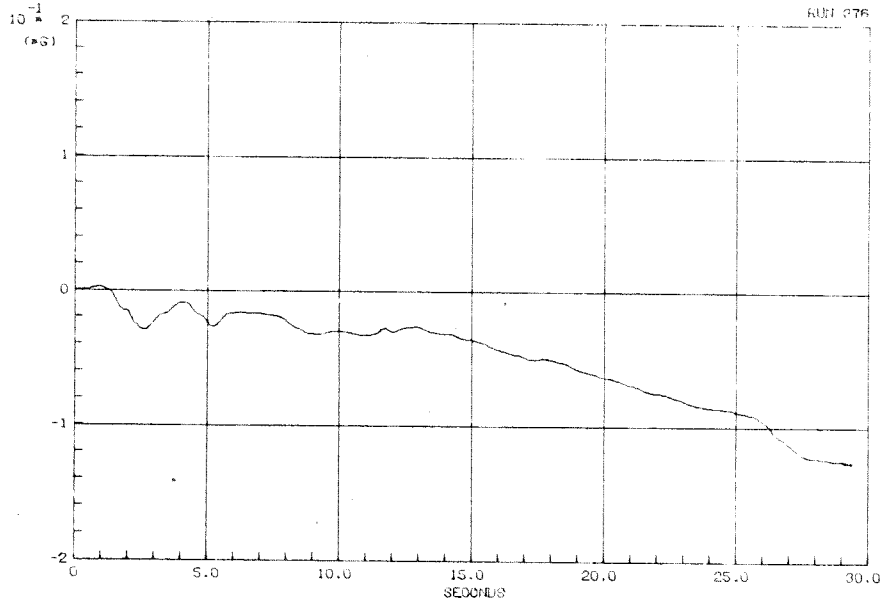

EL CENTRO 1940 NS DISPLACEMENT

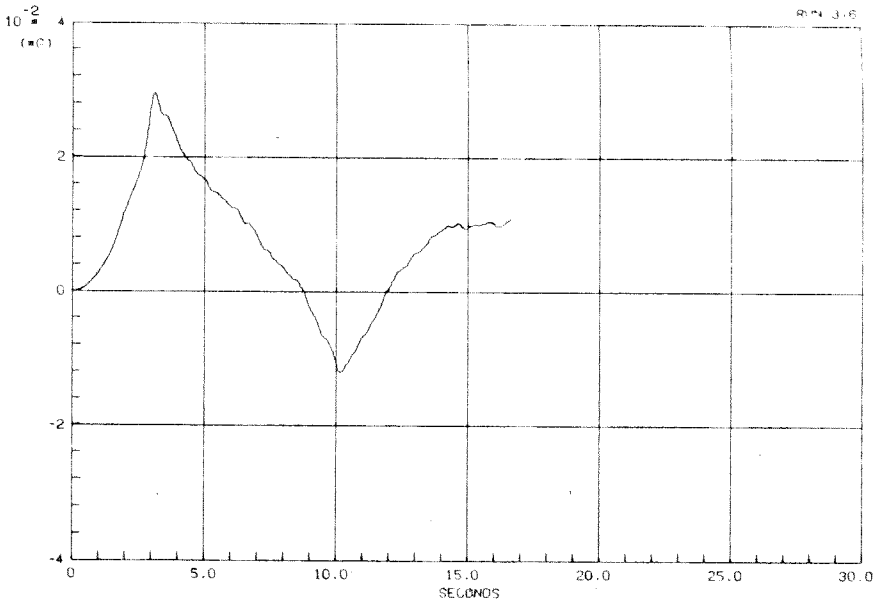

EL CENTRO 1934 NS DISPLACEMENT

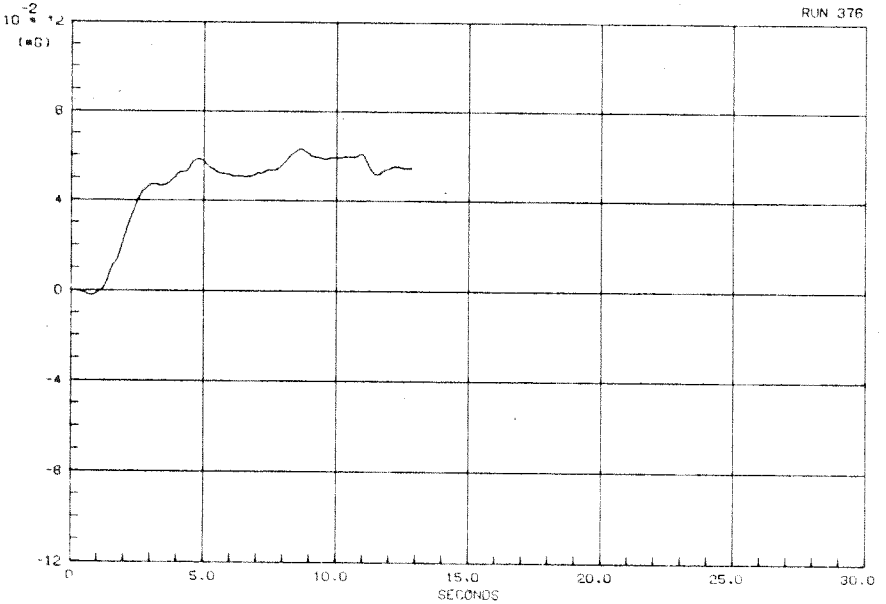

EL CENTRO 1940 EW DISPLACEMENT

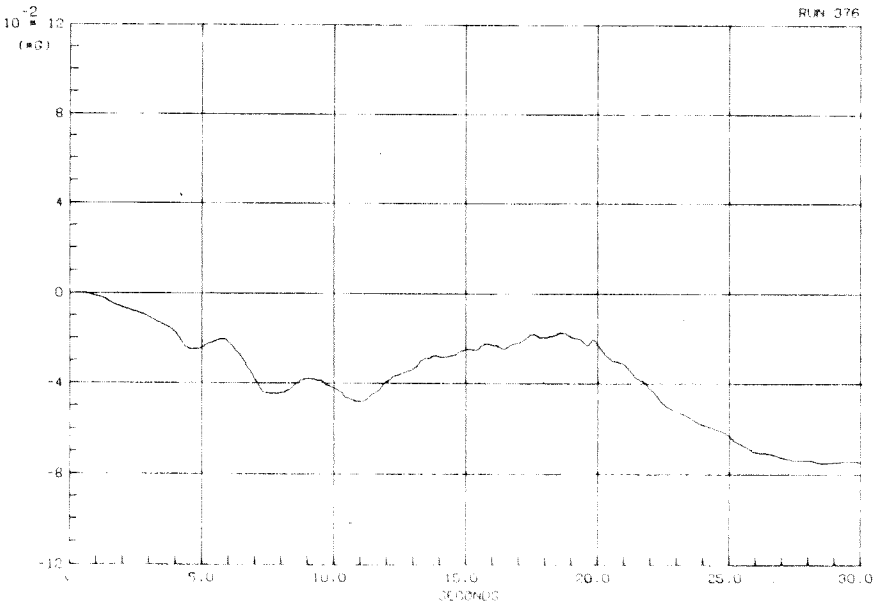

OLYMPIA 1949 NS DISPLACEMENT

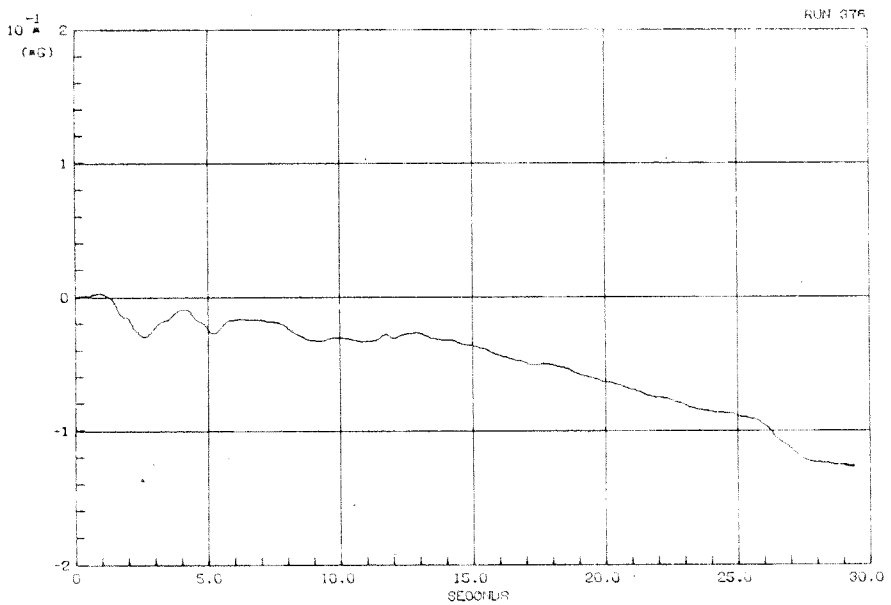

EL CENTRO 1940 NS DISPLACEMENT

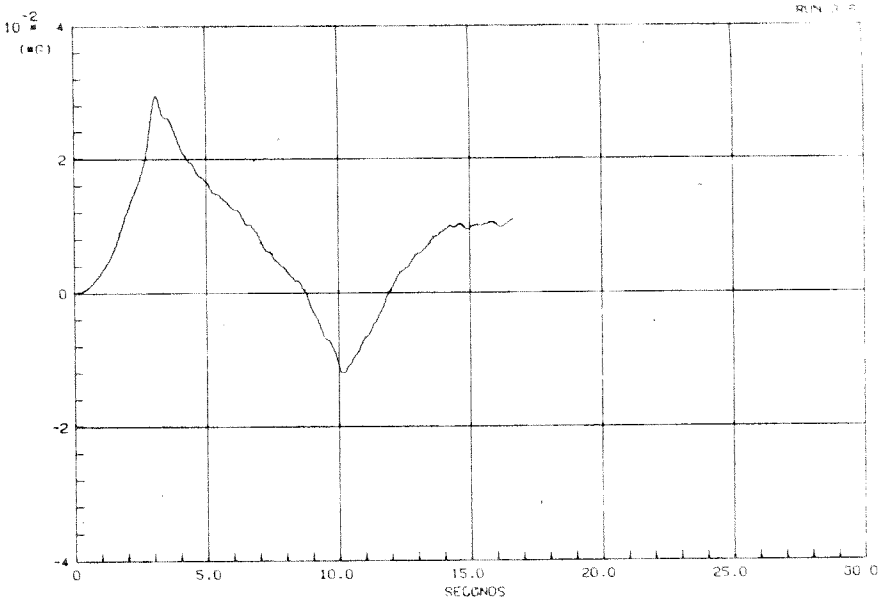

EL CENTRO 1934 NS DISPLACEMENT

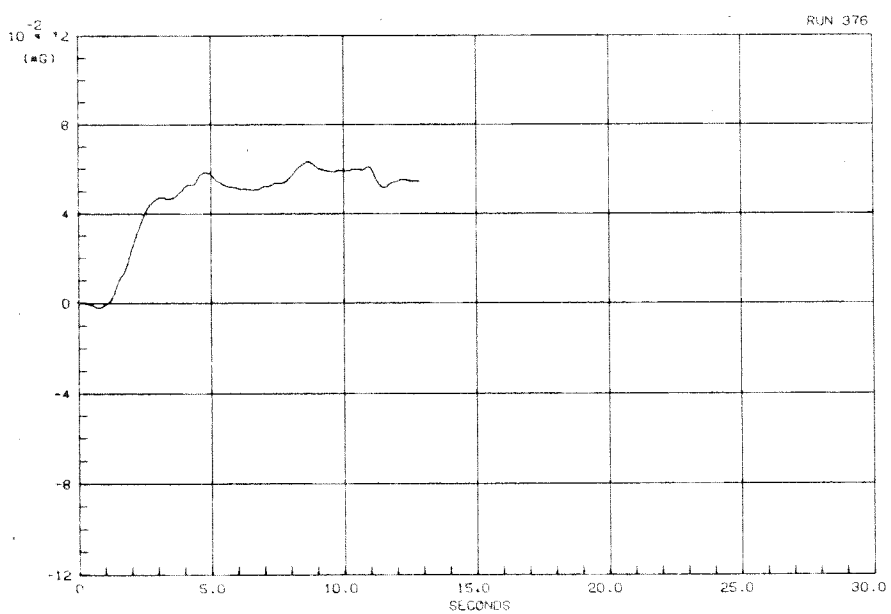

EL CENTRO 1940 EW DISPLACEMENT

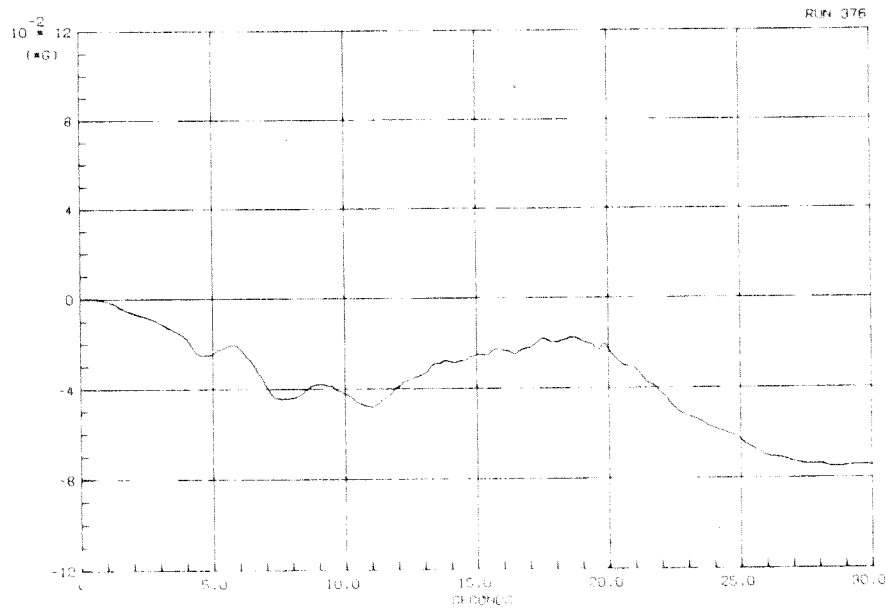

OLYMPIA 1949 NS DISPLACEMENT

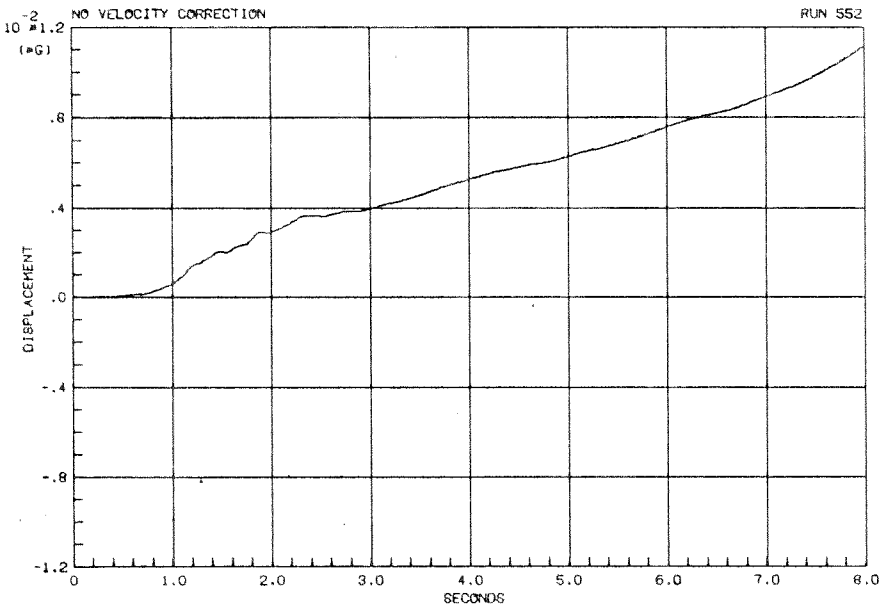

SAN FCO. MARCH 1957 - GOLDEN GATE PARK S80E

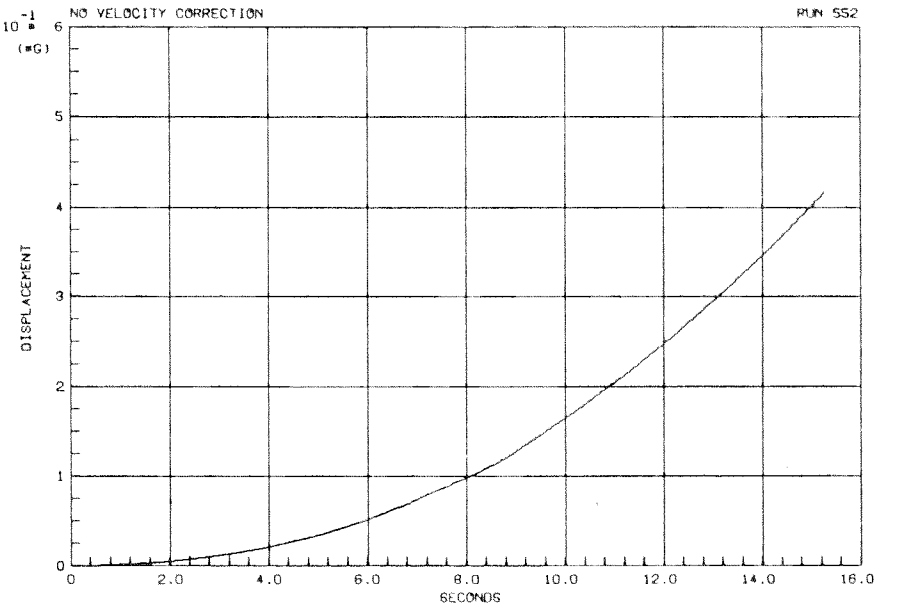

FERNDALE, 3 OCTOBER 1941 - S45E

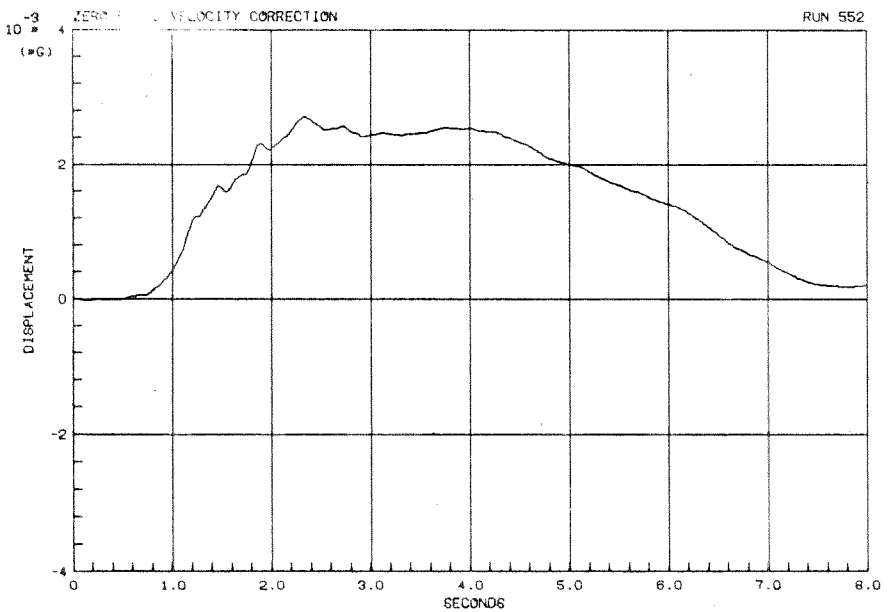

SAN FCO. MARCH 1957 - GOLDEN GATE PARK S80E

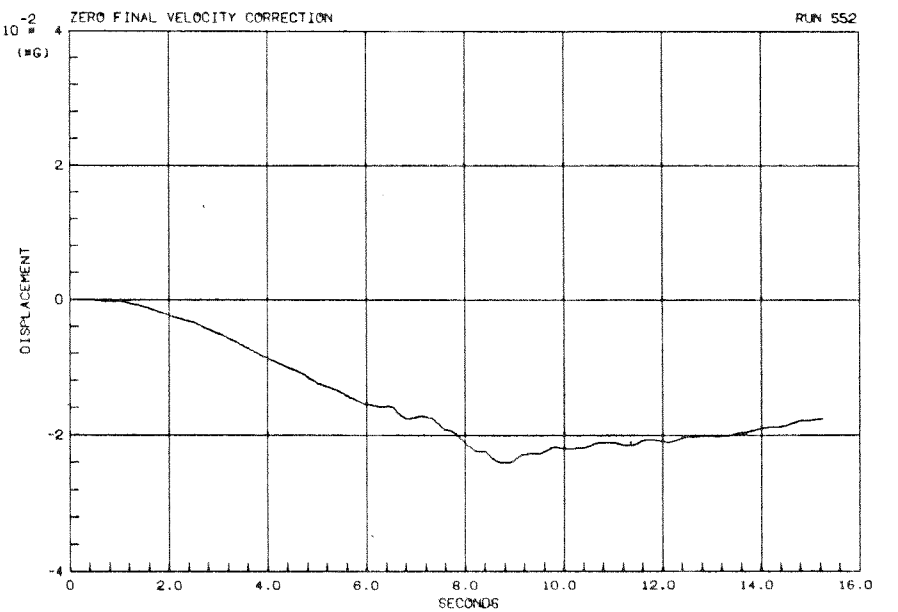

FERNDALE, 3 OCTOBER 1941 - S45E

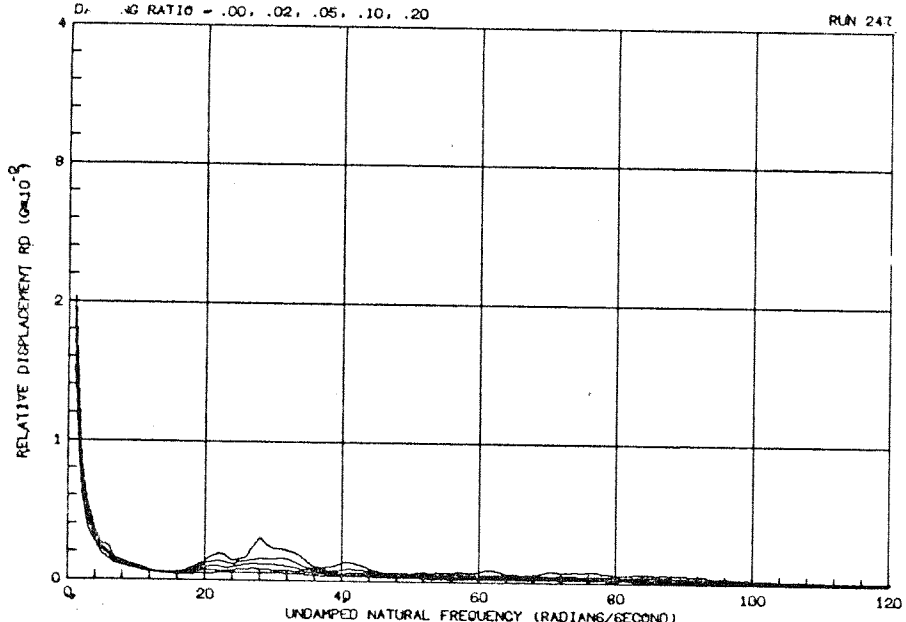

GNOME 10 DEC 1961 - S2 TRANSVERSE

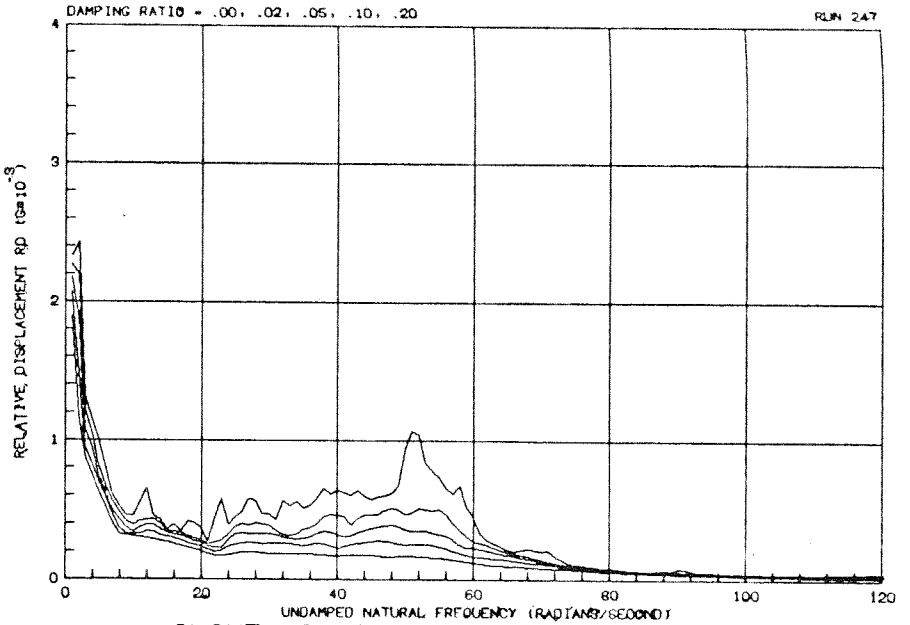

GNOME 10 DEC 1961 - S3 TRANSVERSE

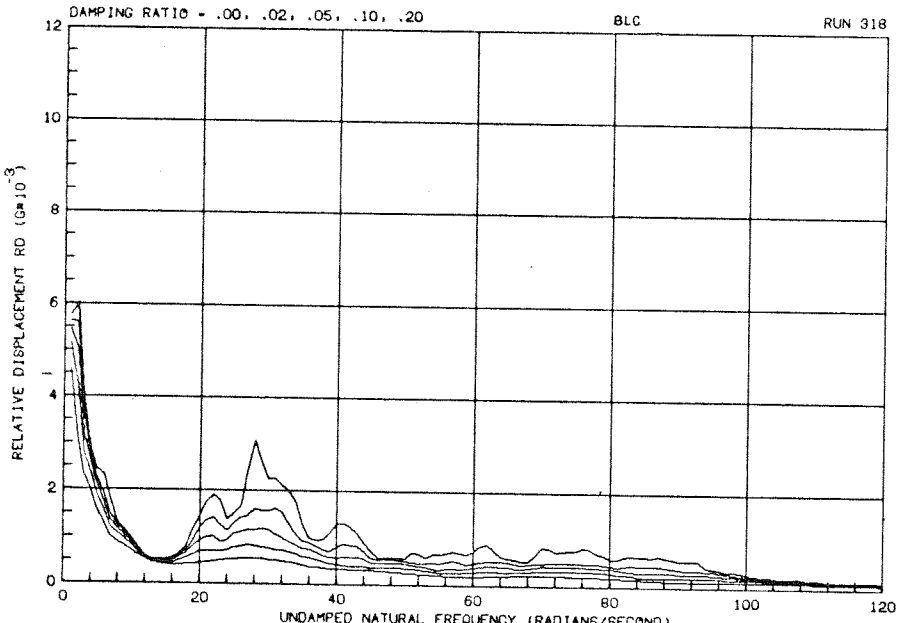

GNOME 10 DEC 1961 - S2 TRANSVERSE

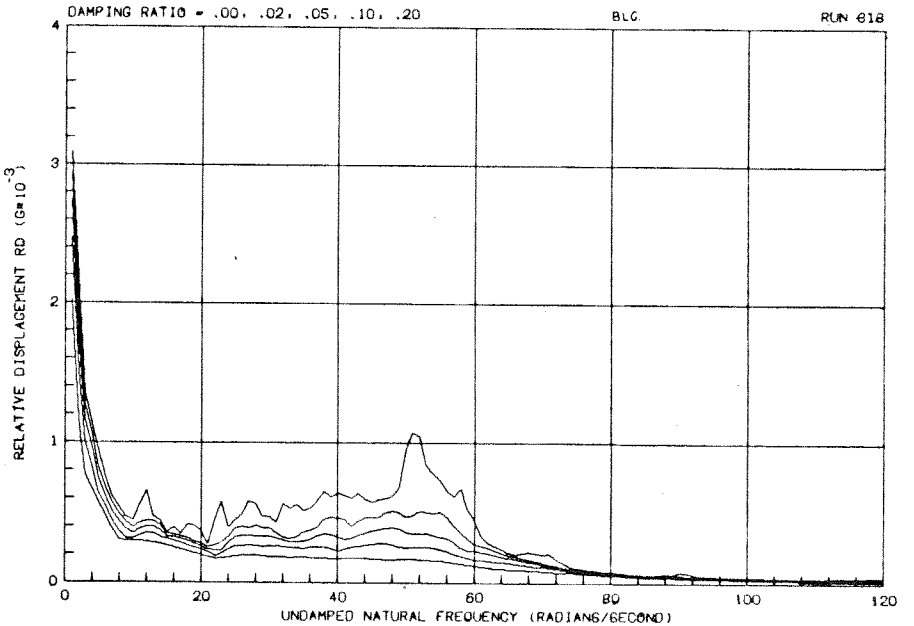

GNOME 10 DEC 1961 - S3 TRANSVERSE

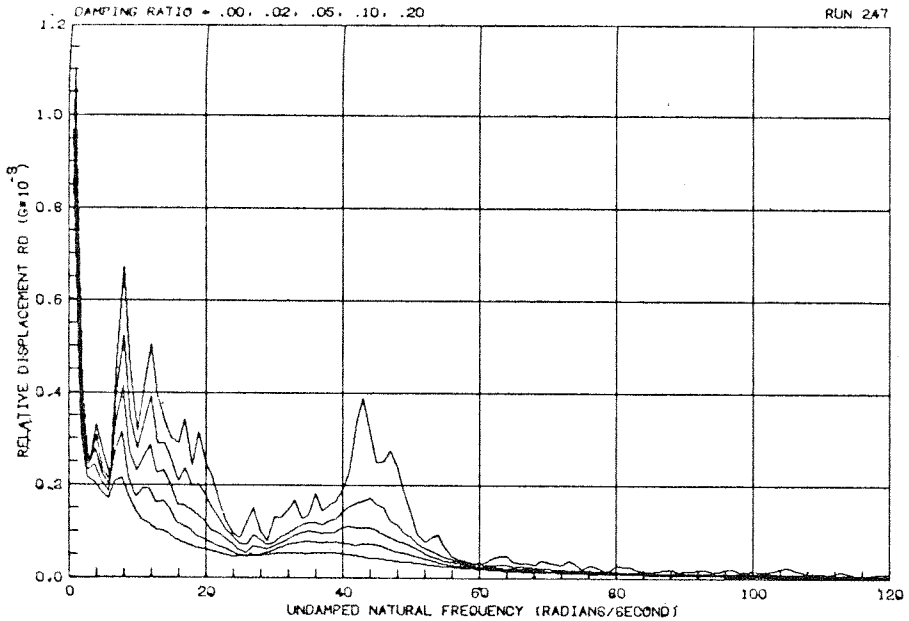

GNOME 10 DEC 1961 - S4 RADIAL

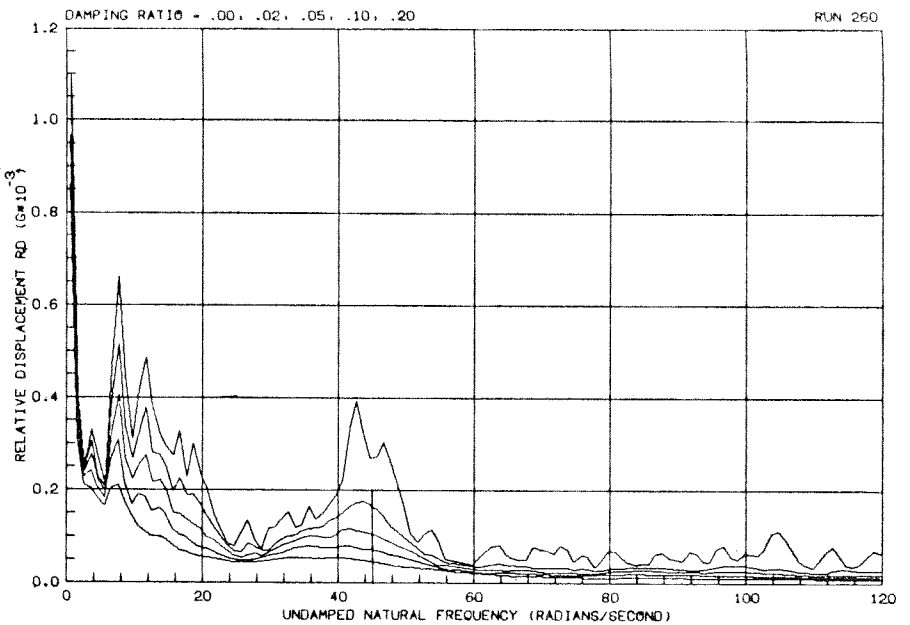

GNOME 10 DEC 1961 - S4 RADIAL

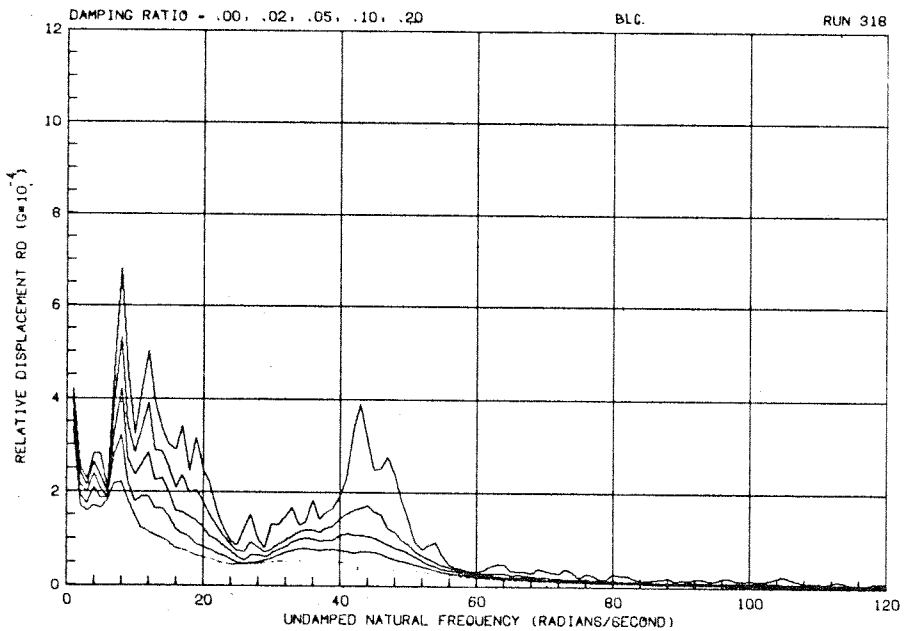

GNOME 10 DEC 1961 - S4 RADIAL

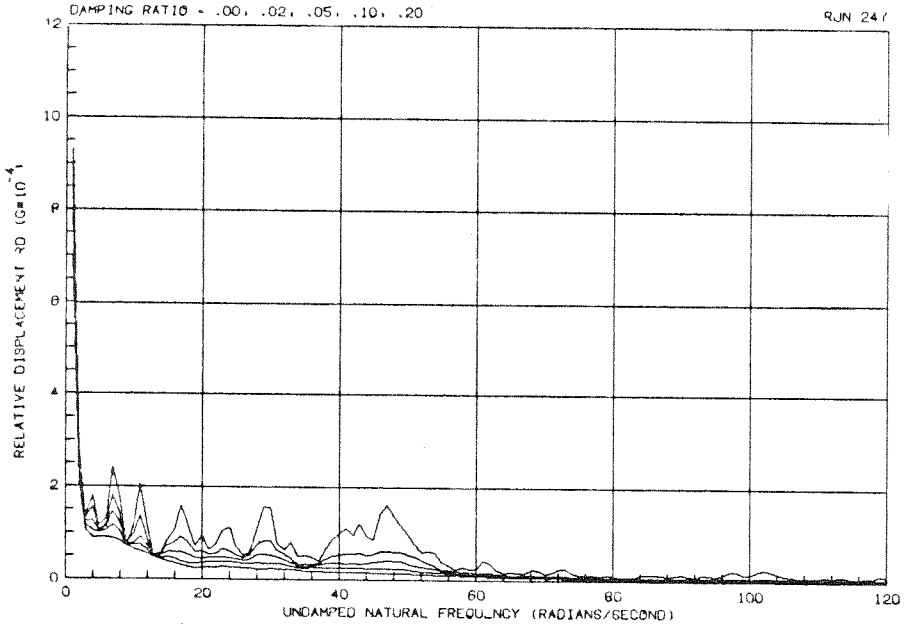

GNOME 10 DEC 1961 S4 TRANSVERSE

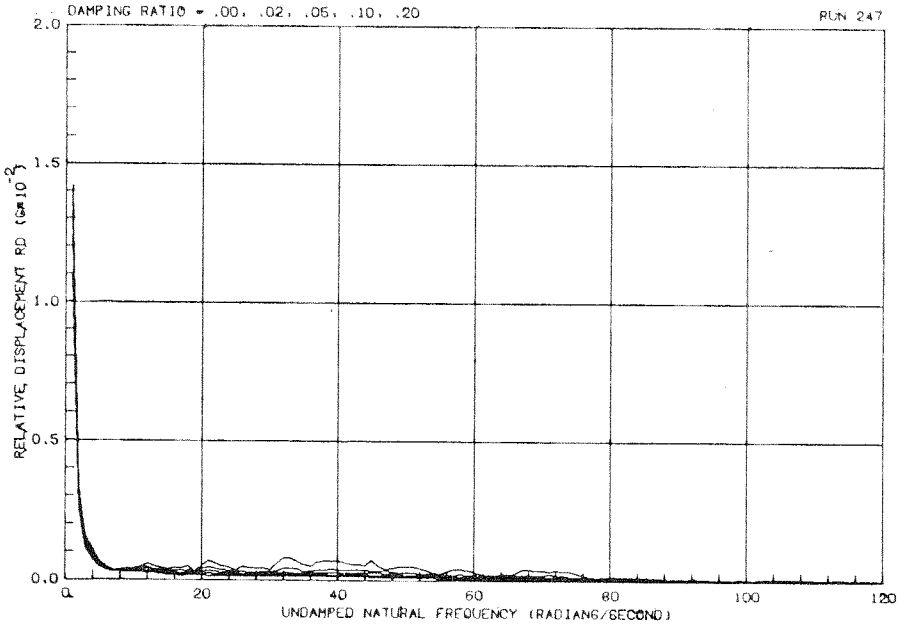

GNOME 10 DEC 1961 - S7 TRANSVERSE

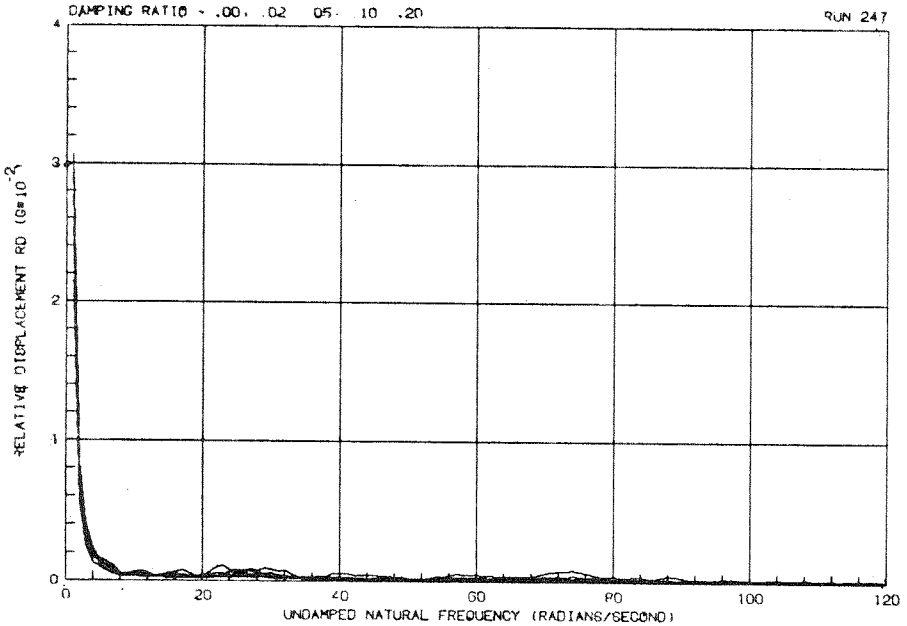

GNOME 10 DEC 1961 - S6 TRANSVERSE

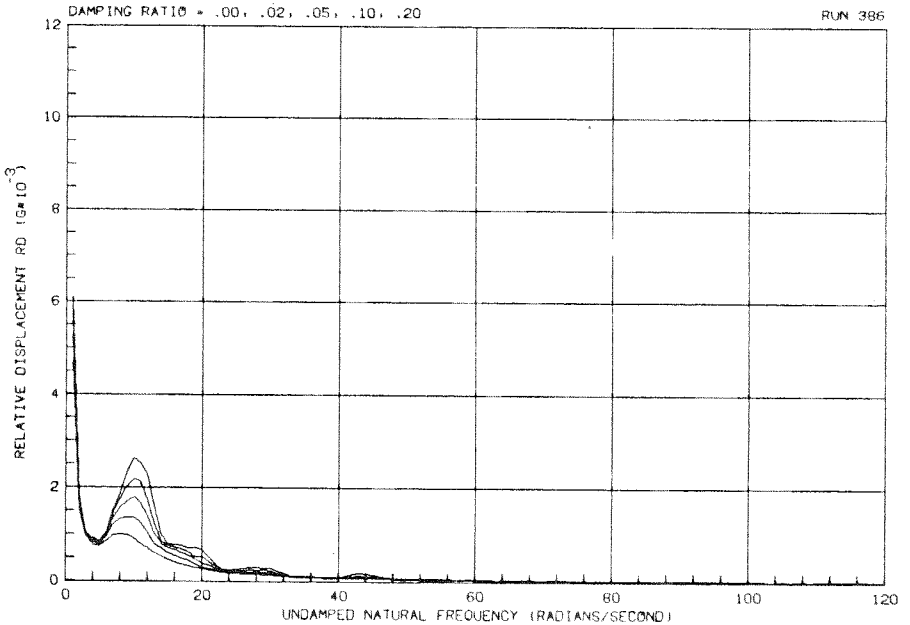

DANNYBOY D5 - RADIAL

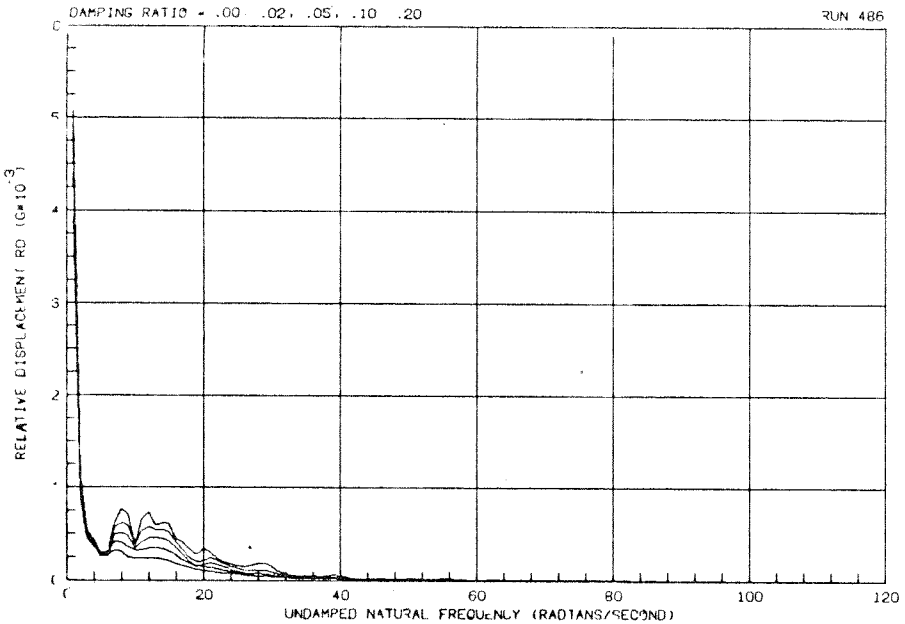

DANNYBOY D8 - RADIAL

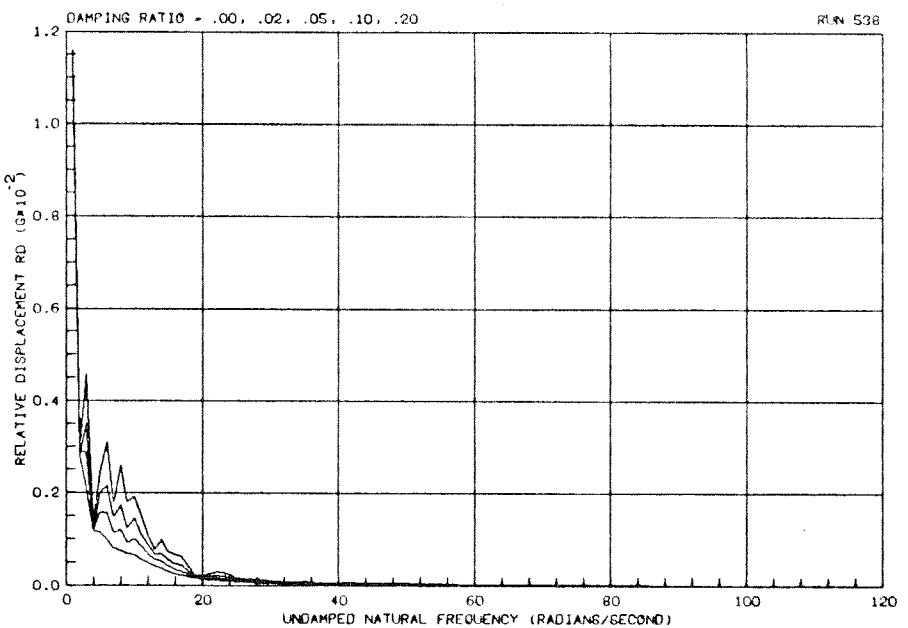

MISSISSIPPI 8228 - TRANSVERSE

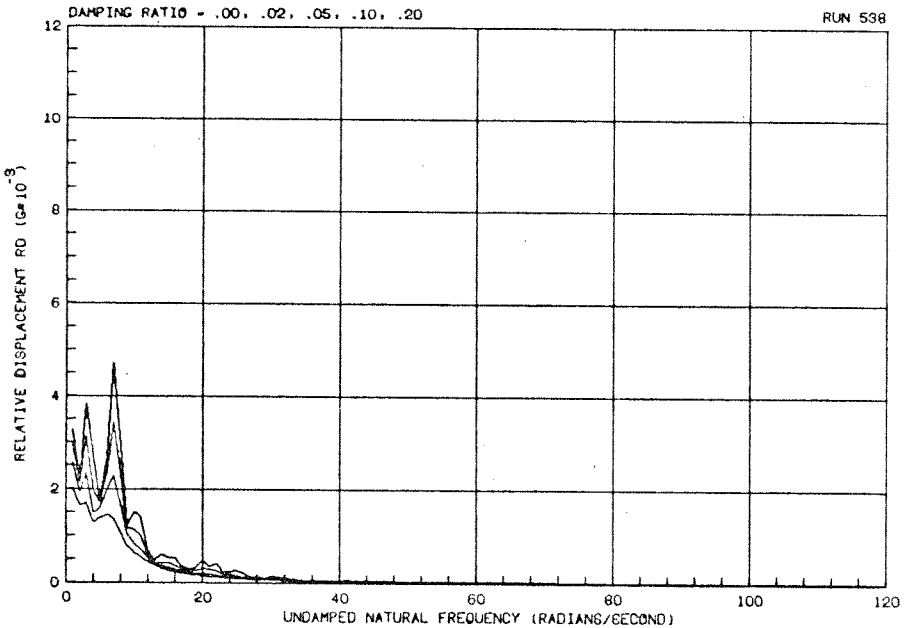

MISSISSIPPI 1777 - TRANSVERSE

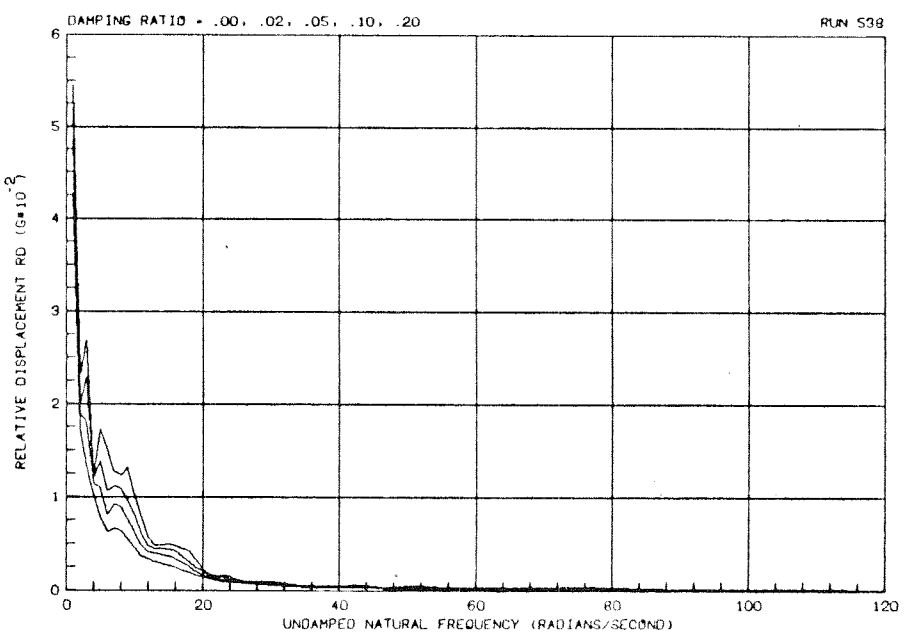

MISSISSIPPI 7245 - RADIAL

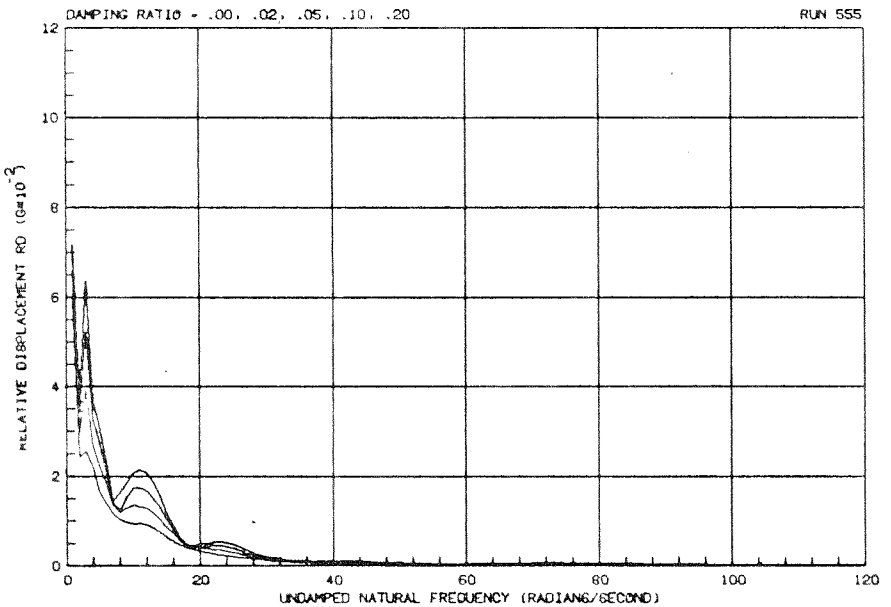

MISSISSIPPI 9537 - RADIAL

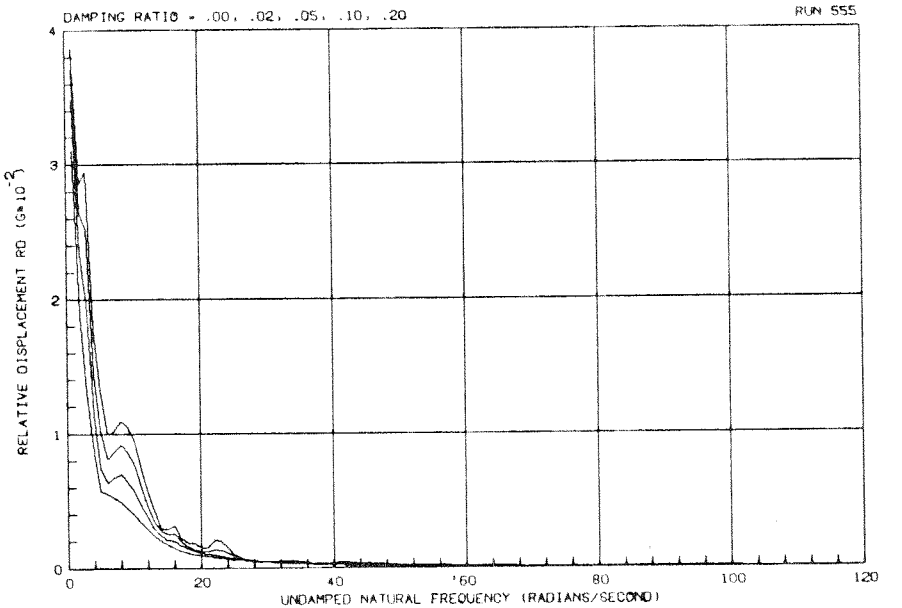

MISSISSIPPI 4074 - RADIAL

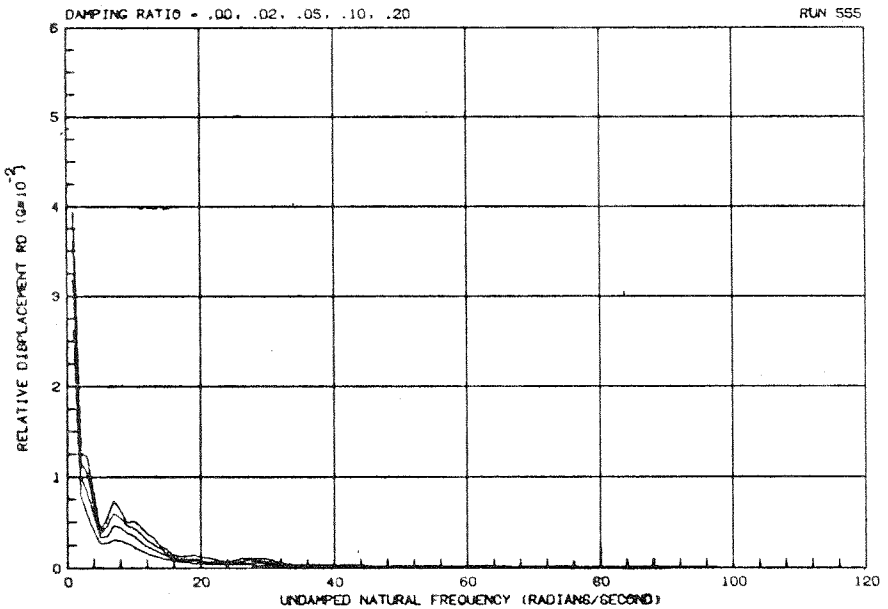

MISSISSIPPI 4074 - TRANSVERSE

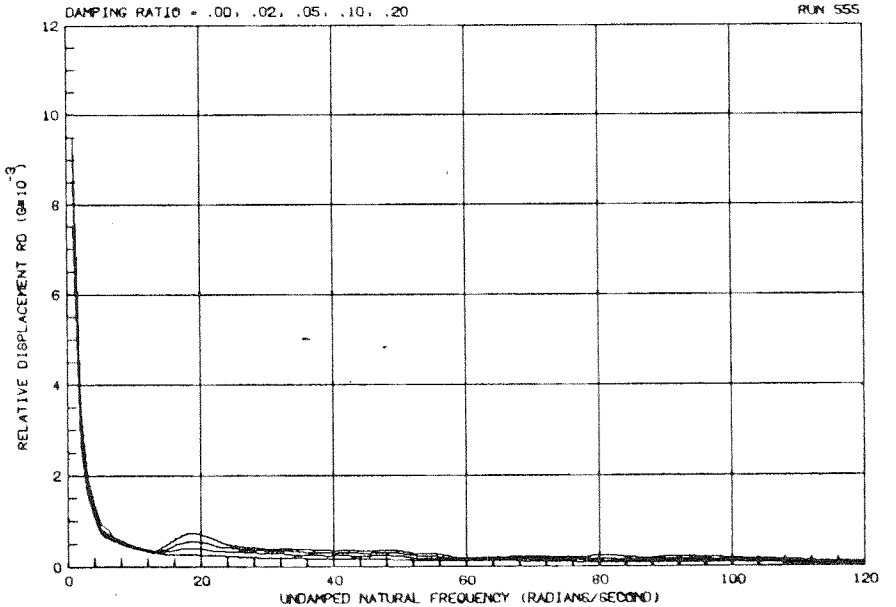

HARDHAT 1091 - TRANSVERSE

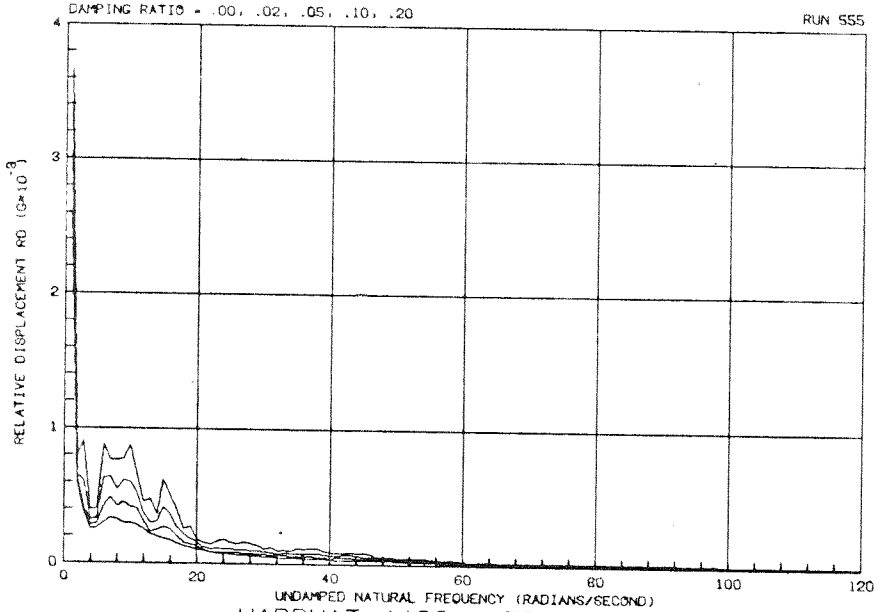

HARDHAT 4496 - TRANSVERSE

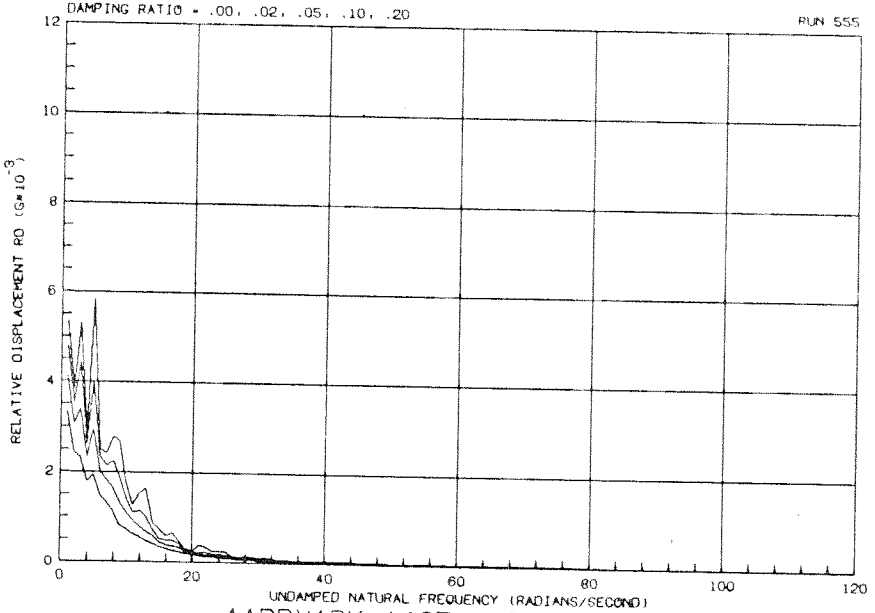

AARDVARK 1437 - TRANSVERSE

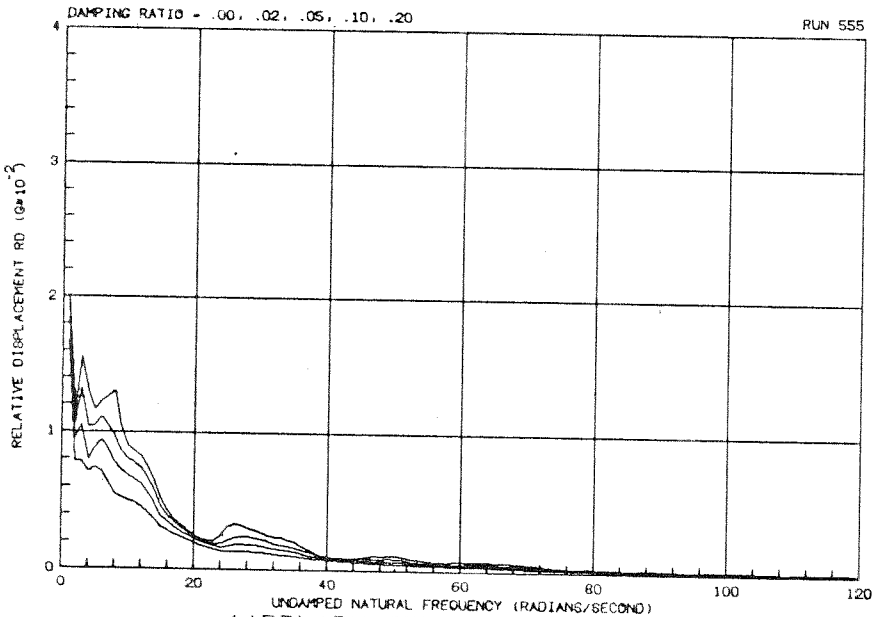

AARDVARK 3773 - TRANSVERSE

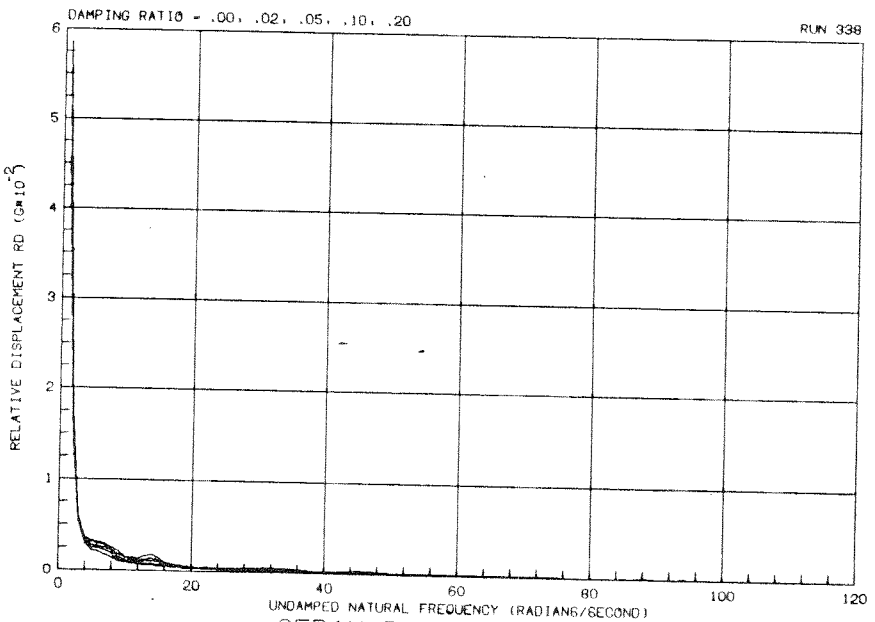

SEDAN RUN 3 - RADIAL

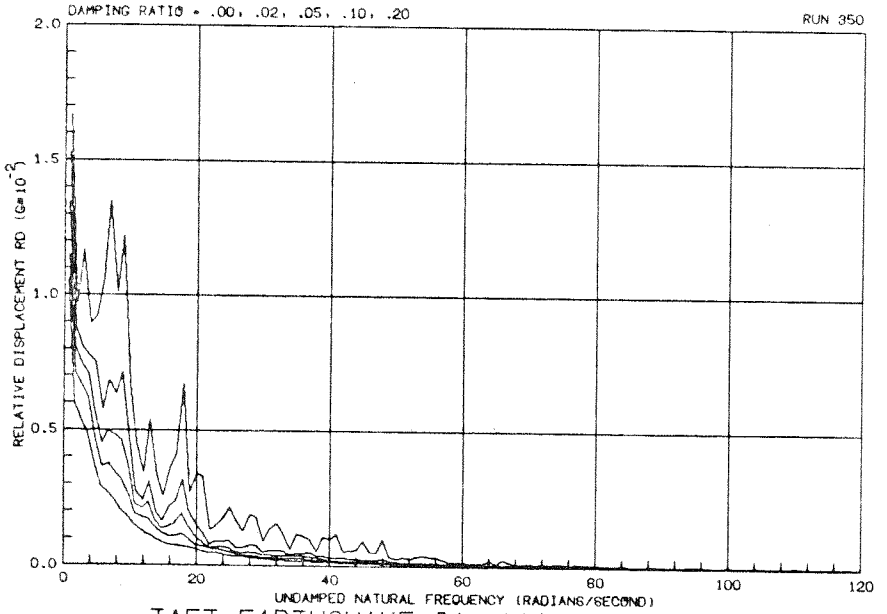

TAFT EARTHQUAKE 21 JULY 1952 - N21E

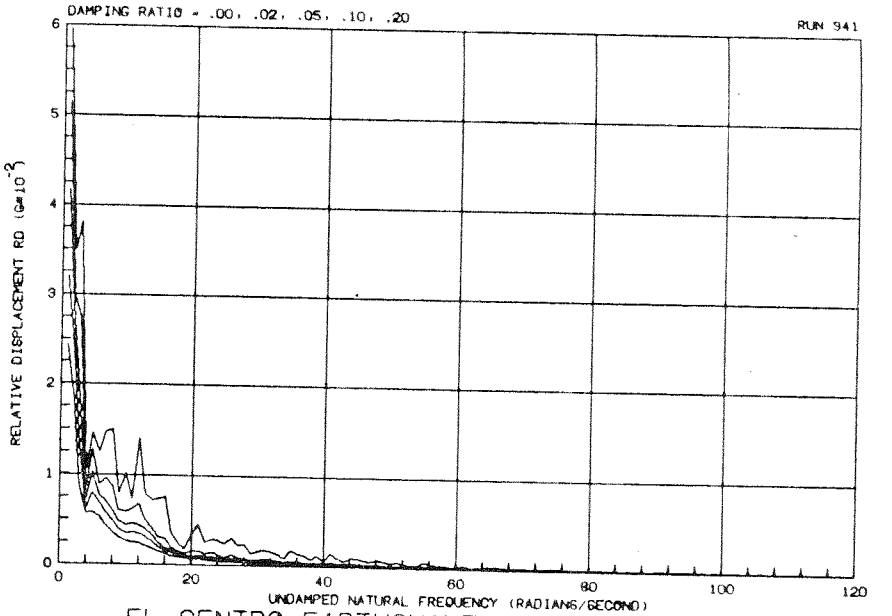

EL CENTRO EARTHQUAKE 18 MAY 1940 - EW

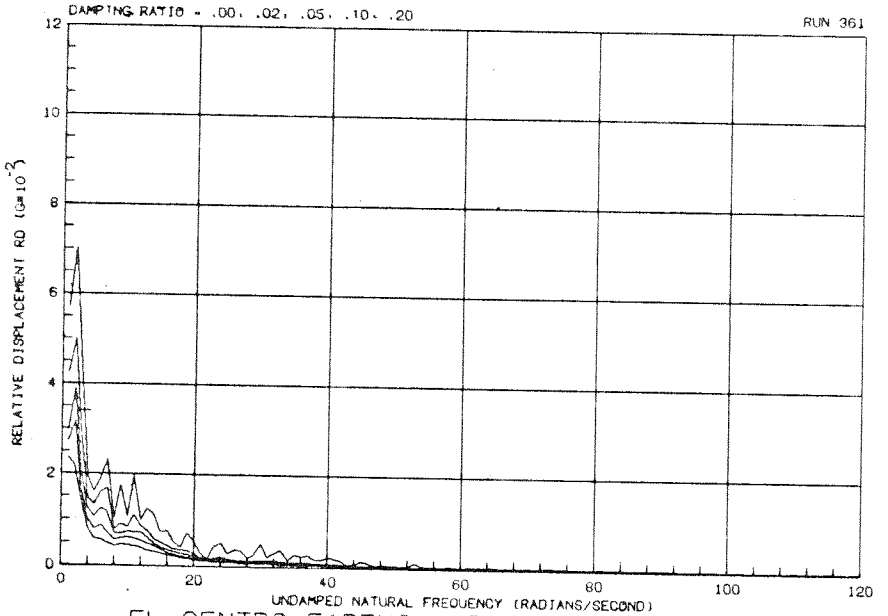

EL CENTRO EARTHQUAKE 18 MAY 1940 - NS

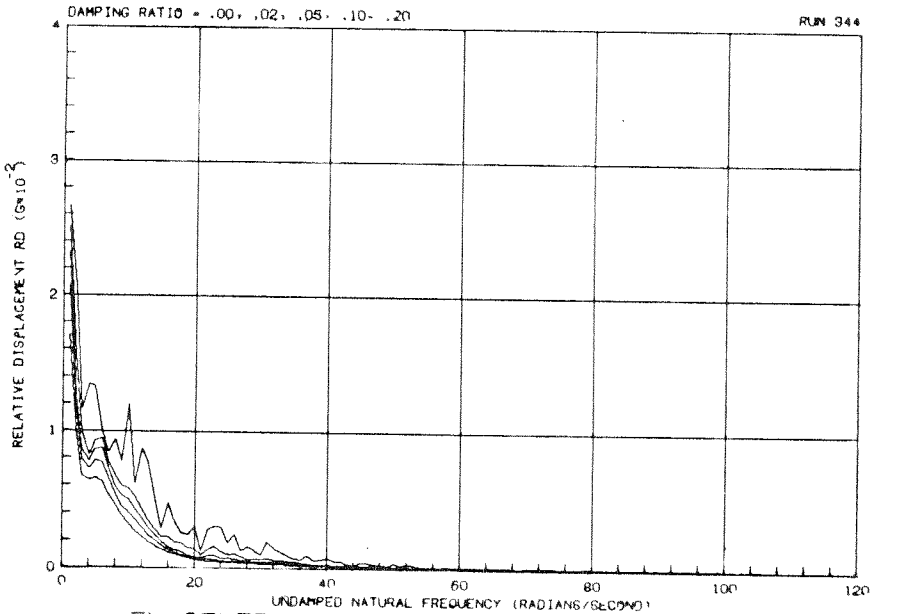

EL CENTRO EARTHQUAKE 30 DEC 1934 - NS

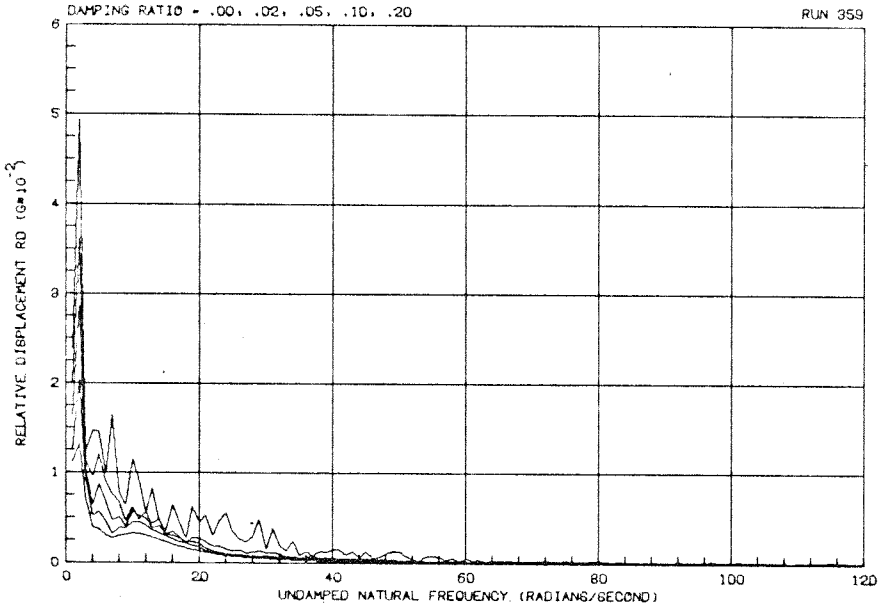

OLYMPIA EARTHQUAKE 13 APRIL 1949 - N80E

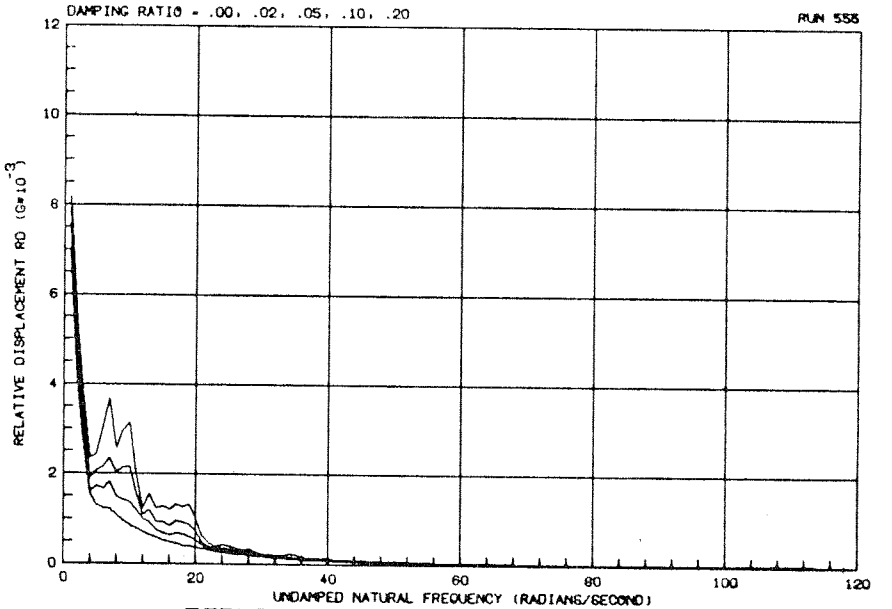

FERNDALE, 3 OCTOBER 1941 - S45E

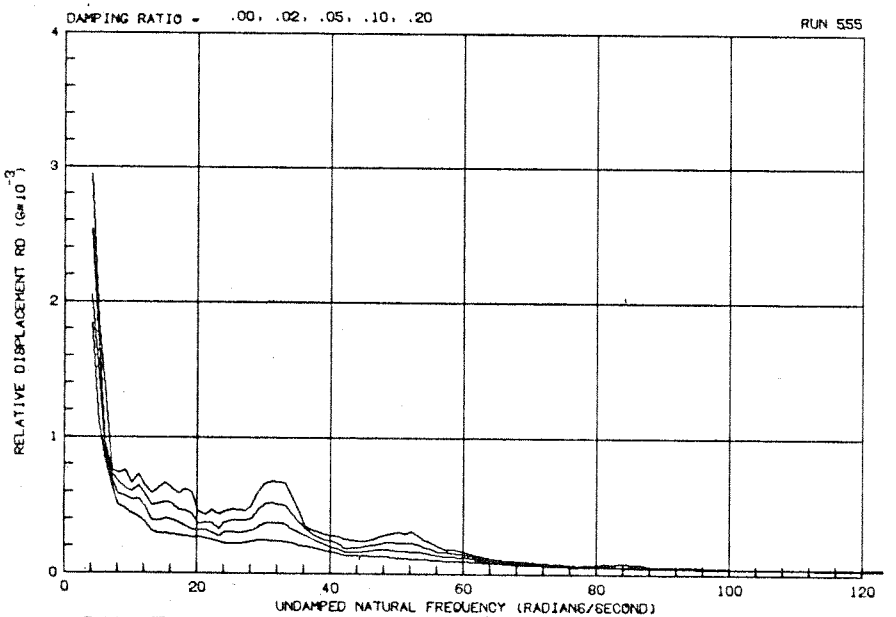

SAN FCO. MARCH 1957 - GOLDEN GATE PARK S80E

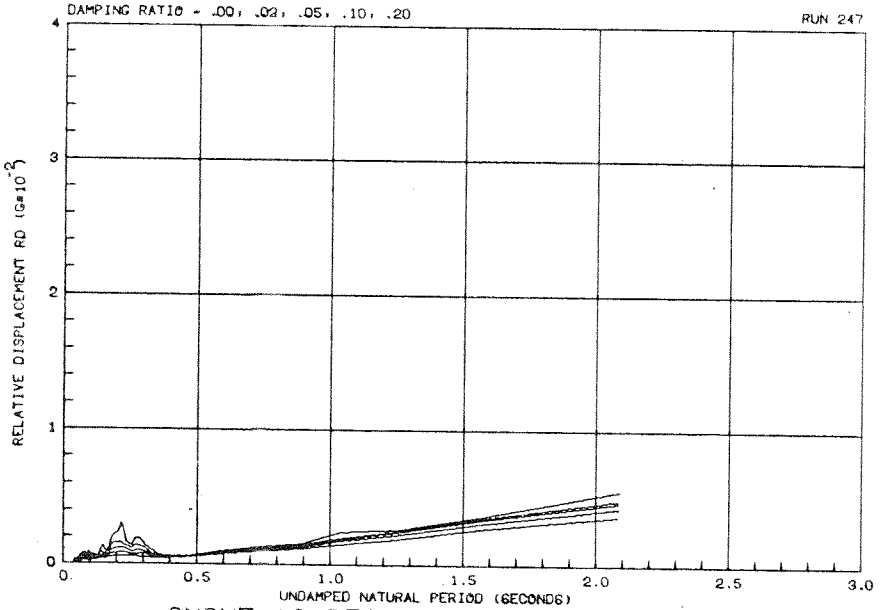

GNOME 10 DEC 1961 - S2 TRANSVERSE

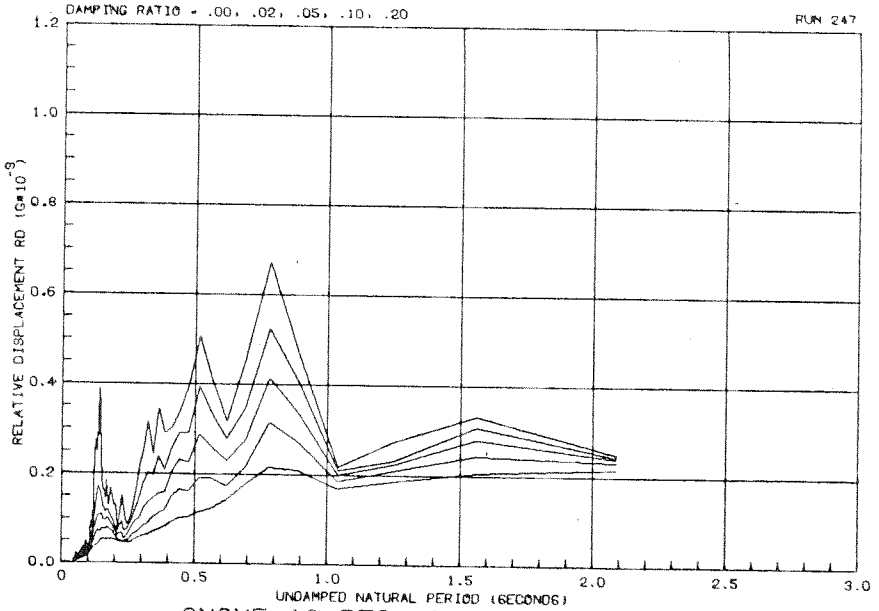

GNOME 10 DEC 1961 - S4 RADIAL

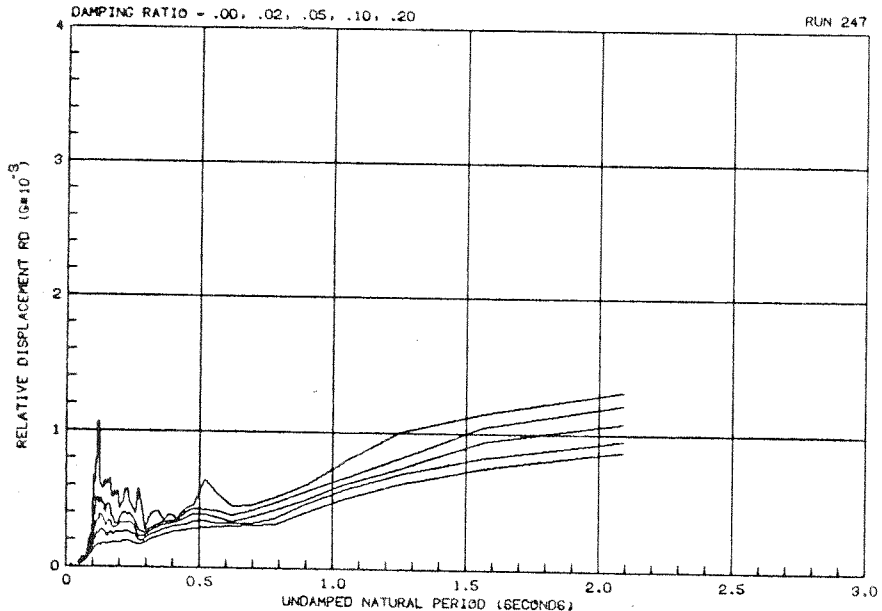

GNOME 10 DEC 1961 - S3 TRANSVERSE

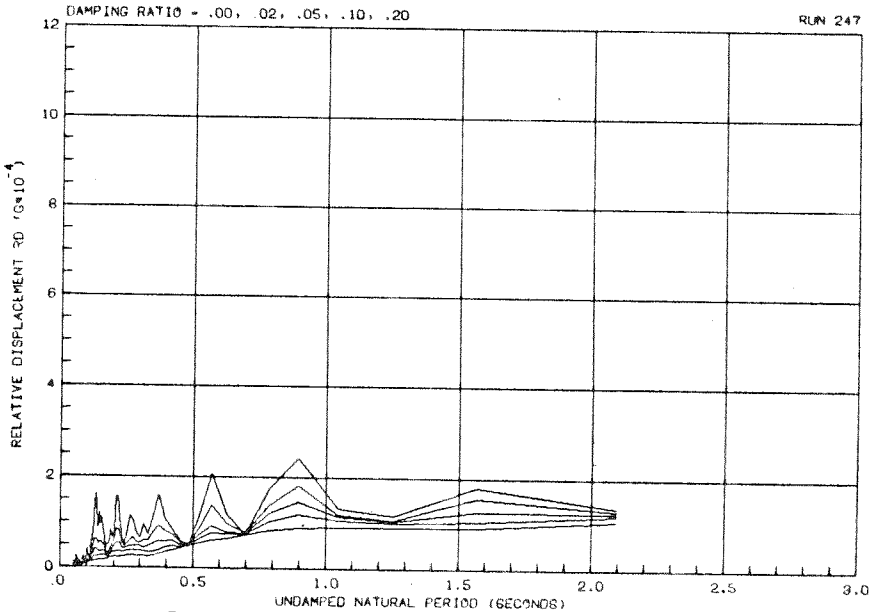

GNOME 10 DEC 1961 - S4 TRANSVERSE

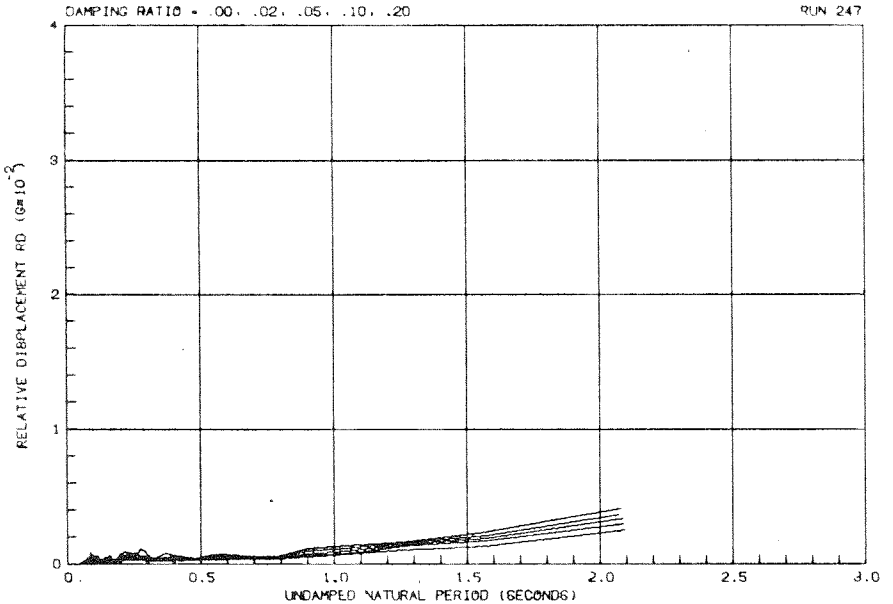

GNOME 10 DEC 1961 - S6 TRANSVERSE

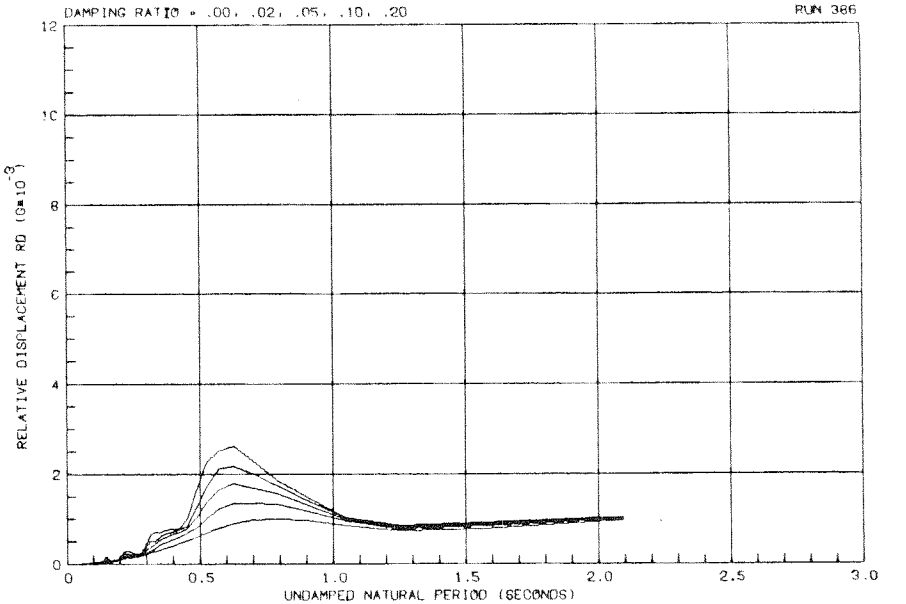

DANNYBOY D5 - RADIAL

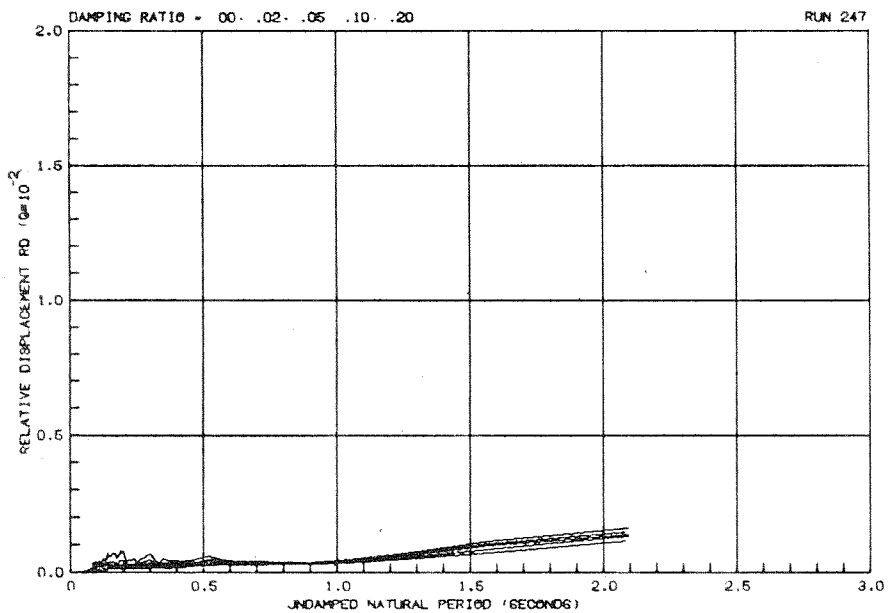

GNOME 10 DEC 1961 - S7 TRANSVERSE

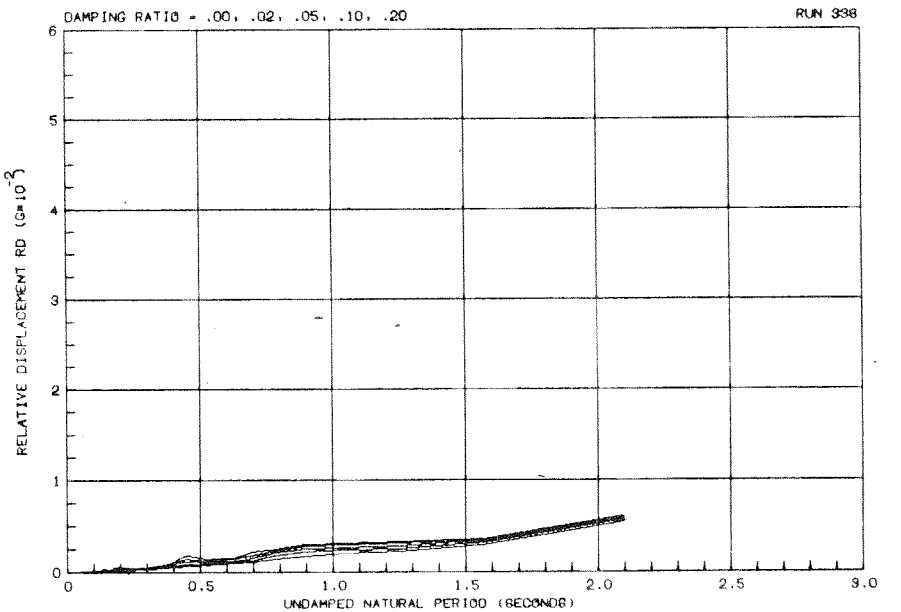

SEDAN RUN 3 - RADIAL

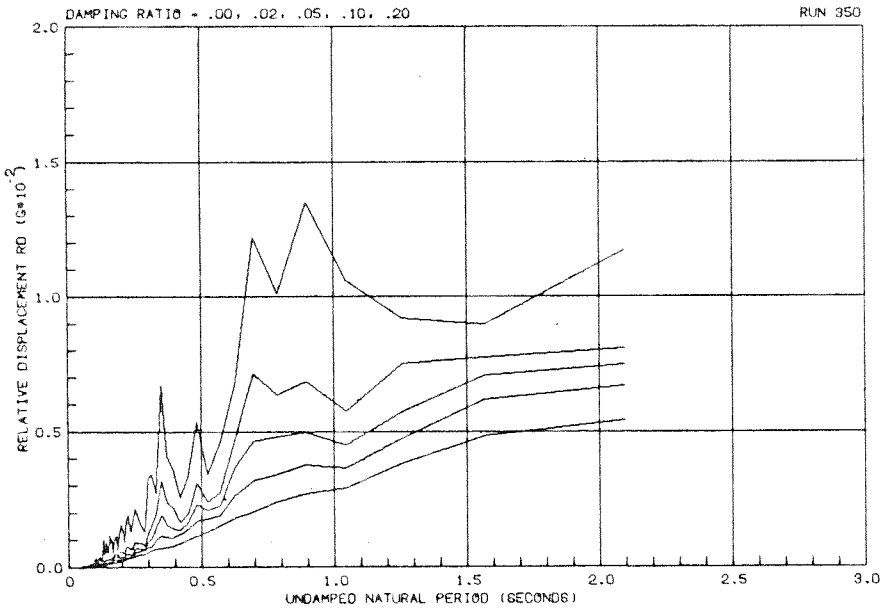

TAFT EARTHQUAKE 21 JULY 1952 - N21E

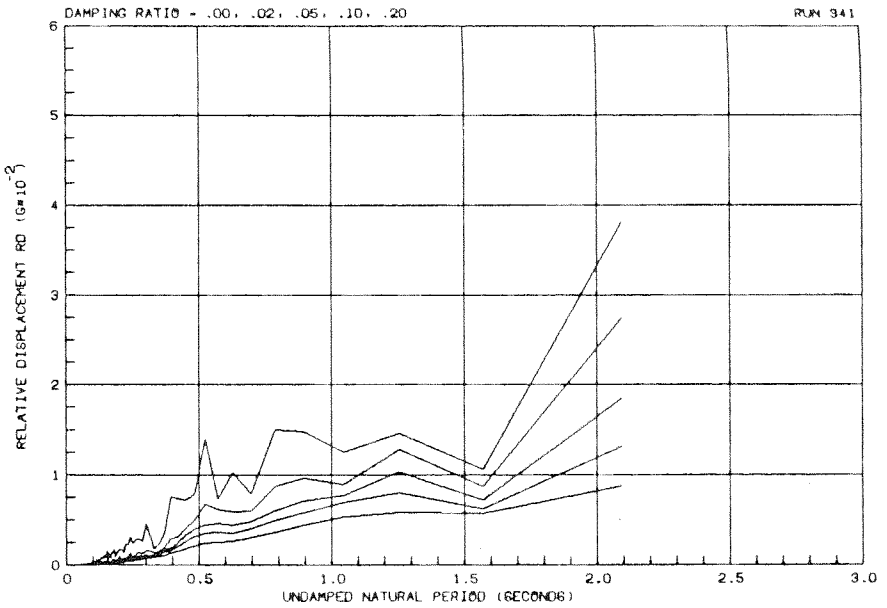

EL CENTRO EARTHQUAKE 18 MAY 1940 - EW

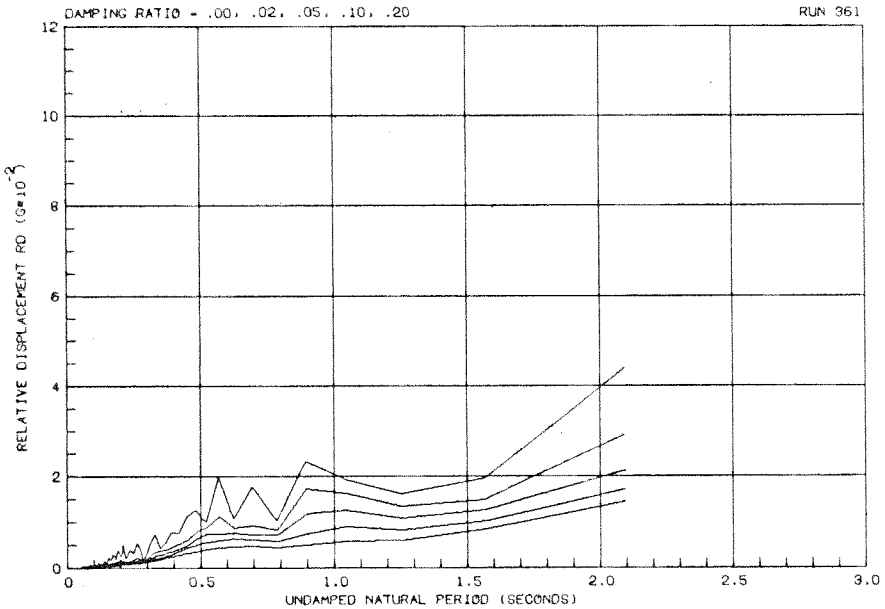

EL CENTRO EARTHQUAKE 18 MAY 1940 - NS

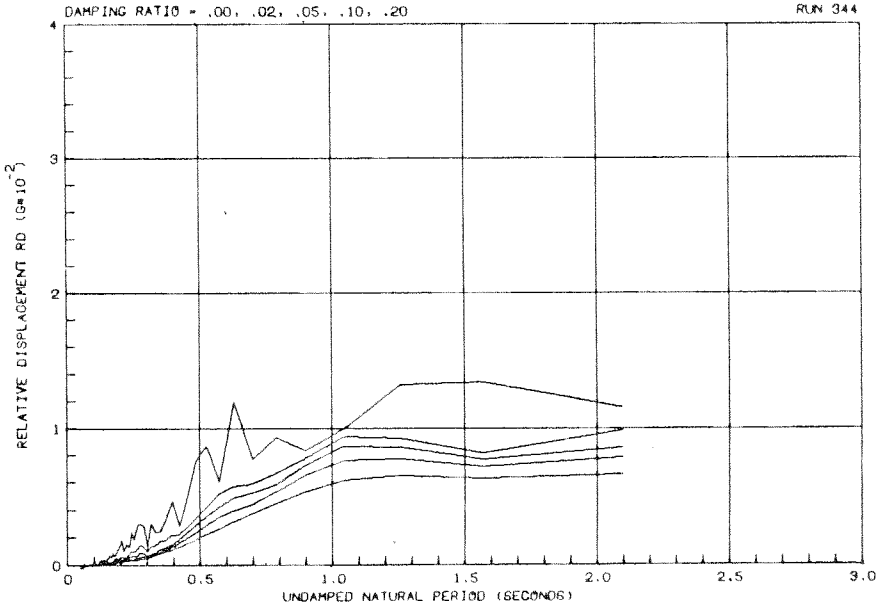

EL CENTRO EARTHQUAKE 30 DEC 1934 - NS

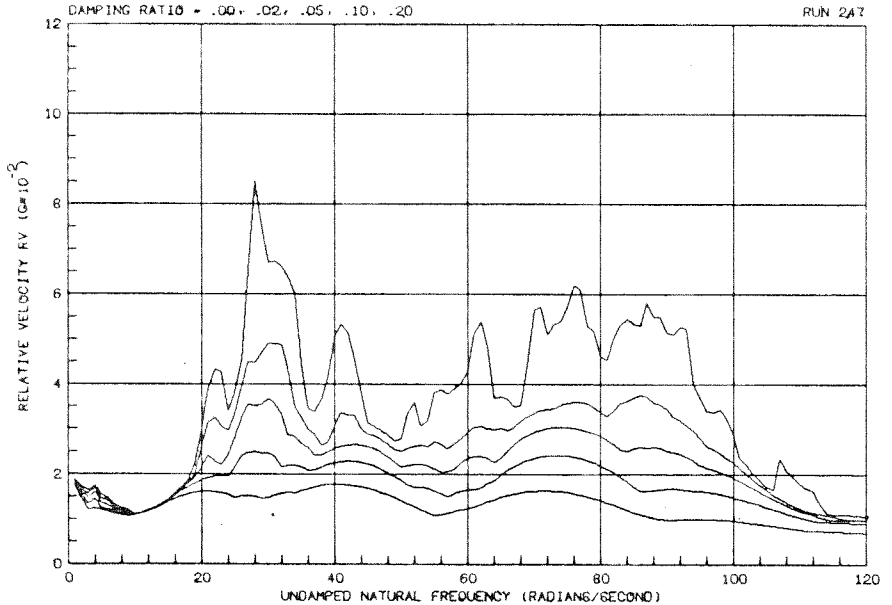

GNOME 10 DEC 1961 - S2 TRANSVERSE

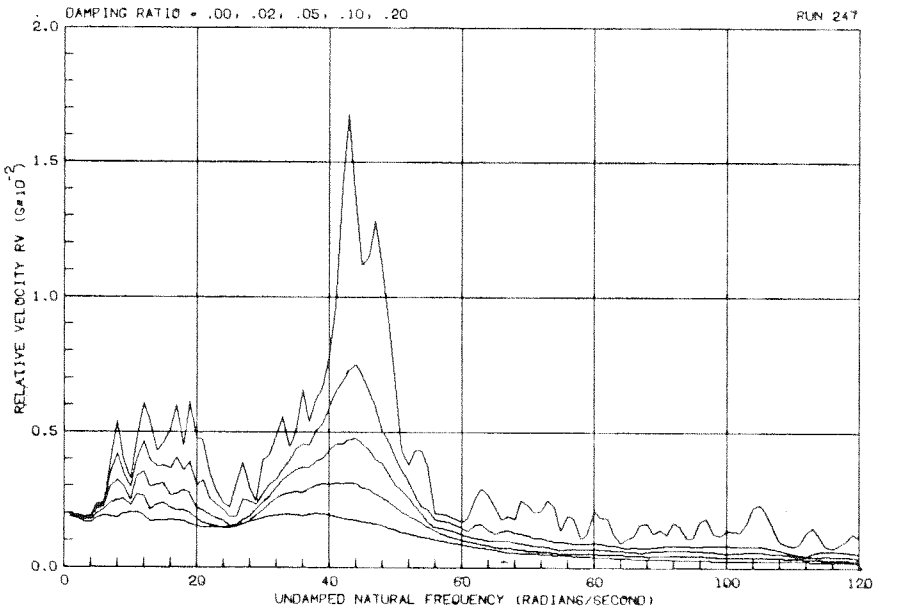

GNOME 10 DEC 1961 - S4 RADIAL

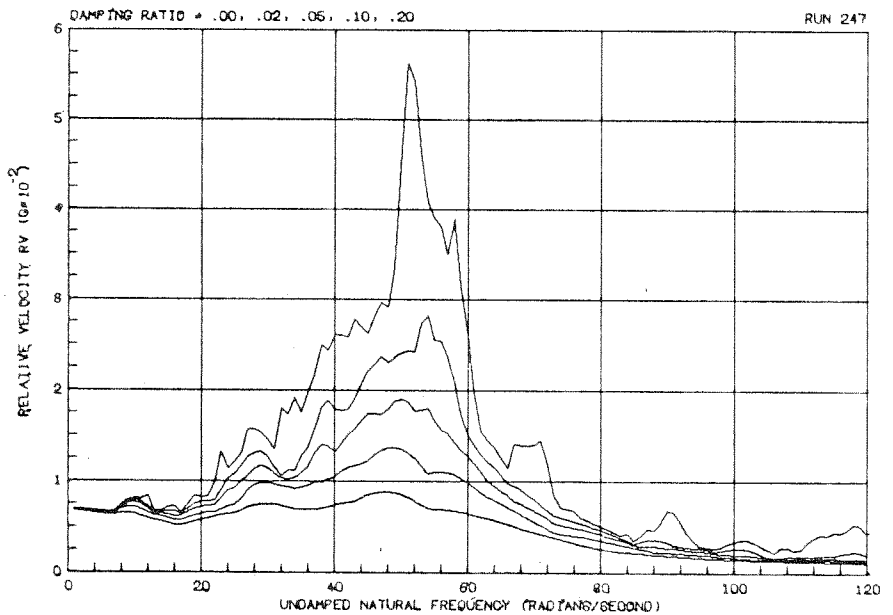

GNOME 10 DEC 1961 - S3 TRANSVERSE

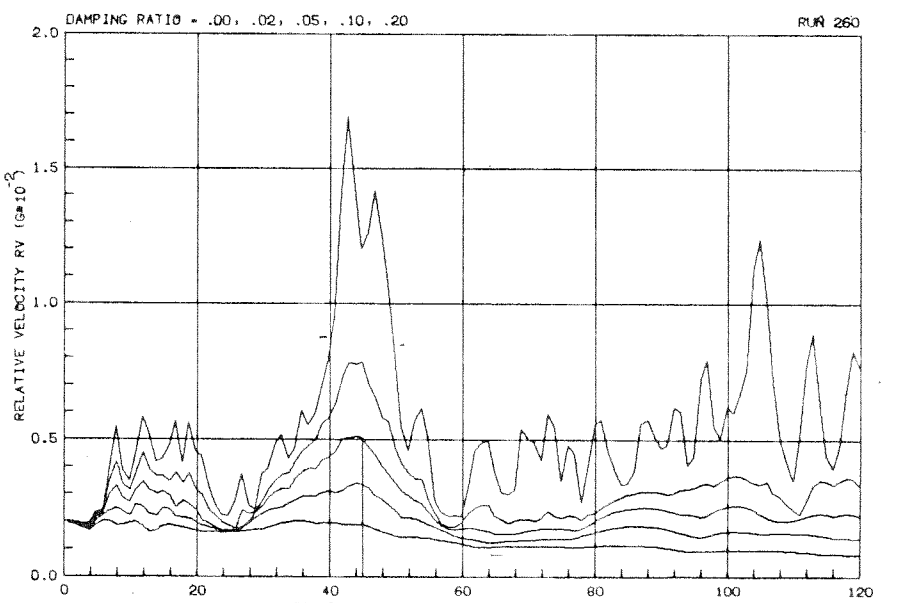

GNOME 10 DEC 1961 - S4 RADIAL

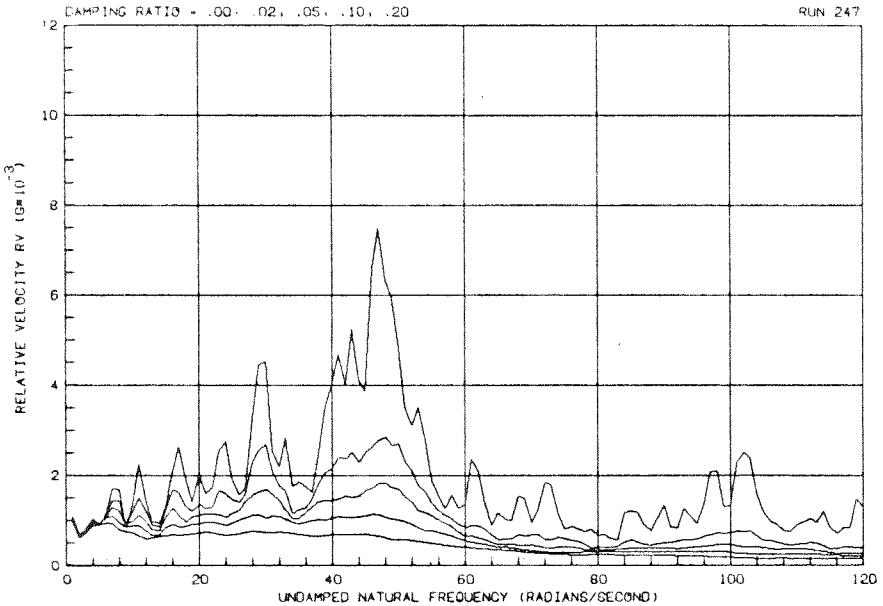

GNOME 10 DEC 1961 - S4 TRANSVERSE

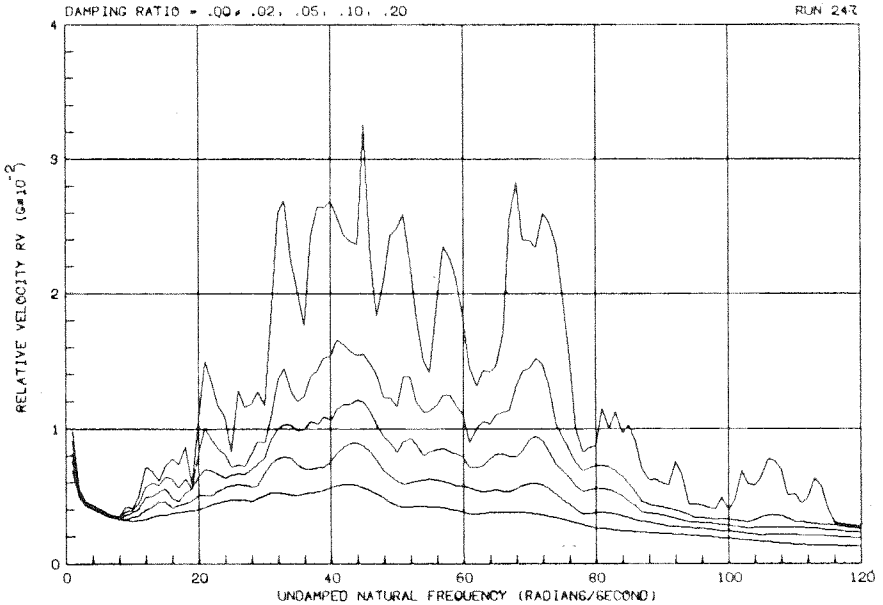

GNOME 10 DEC 1961 - S7 TRANSVERSE

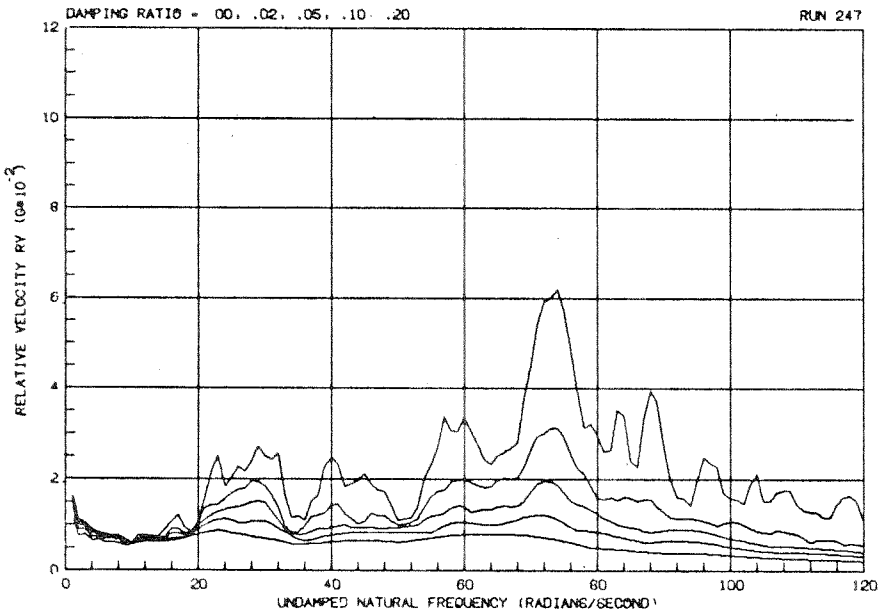

GNOME 10 DEC 1961 - S6 TRANSVERSE

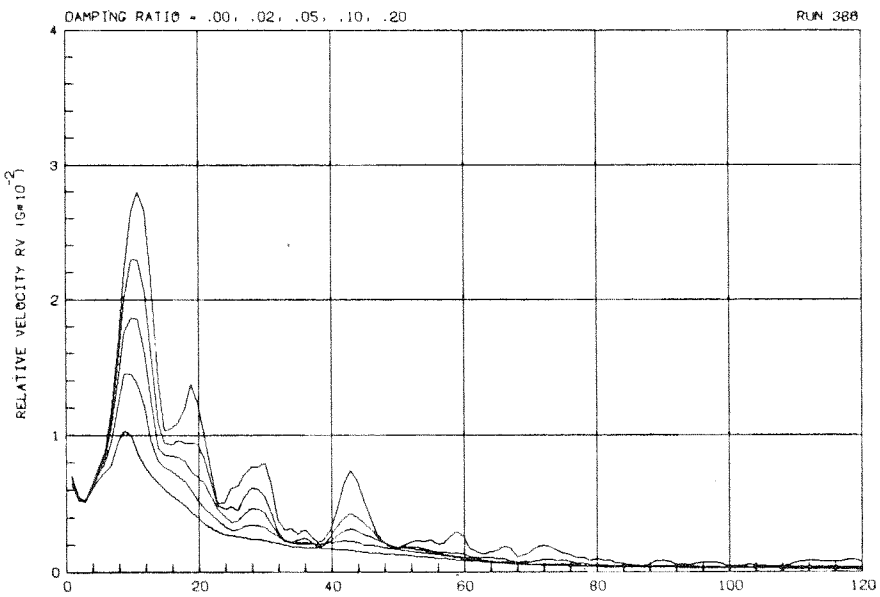

DANNYBOY D5 - RADIAL

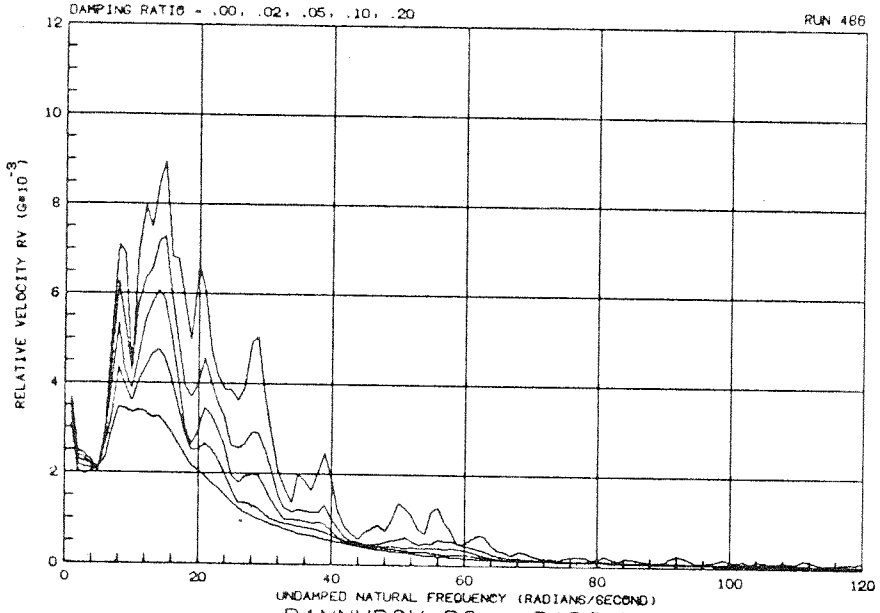

DANNYBOY D8 - RADIAL

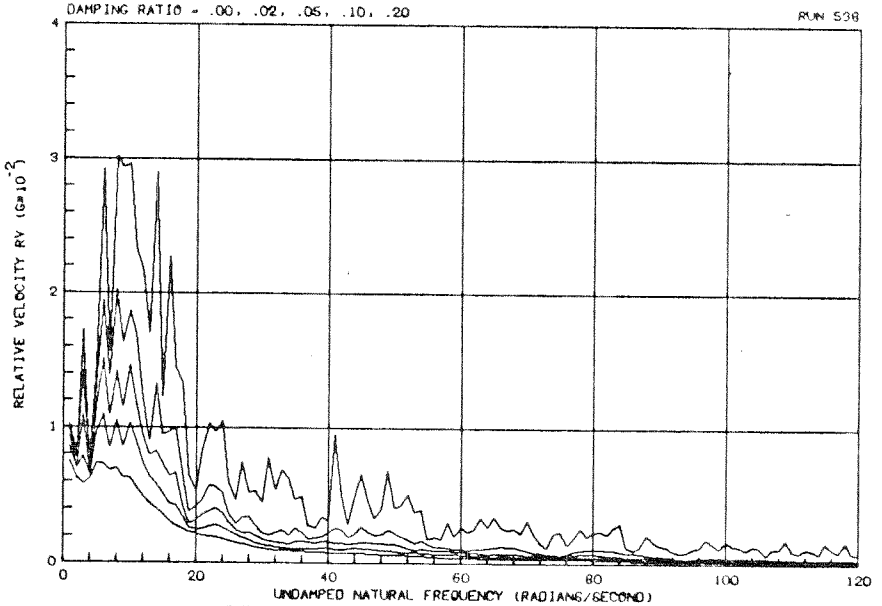

MISSISSIPPI 8228 - TRANSVERSE

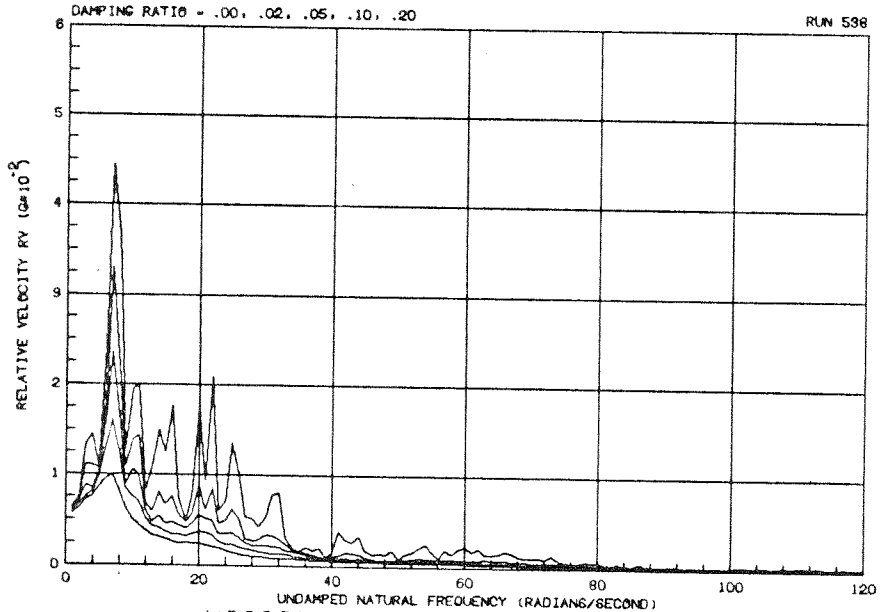

MISSISSIPPI 1777 - TRANSVERSE

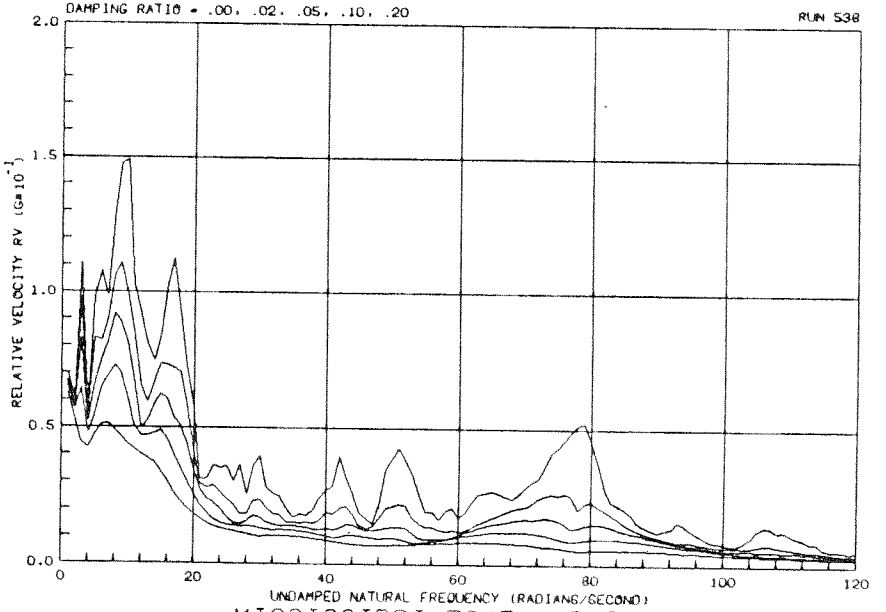

MISSISSIPPI 7245 - RADIAL

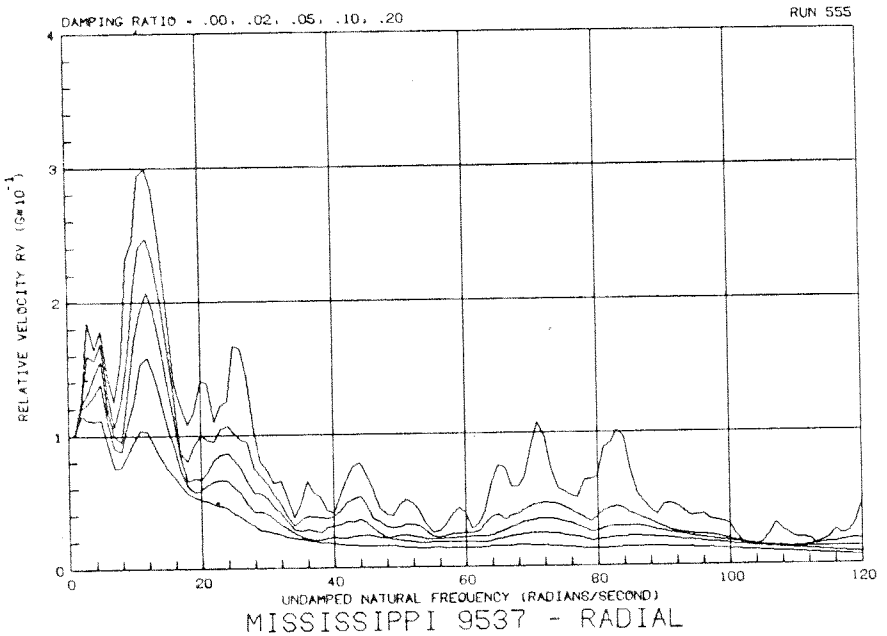

MISSISSIPPI 9537 - RADIAL

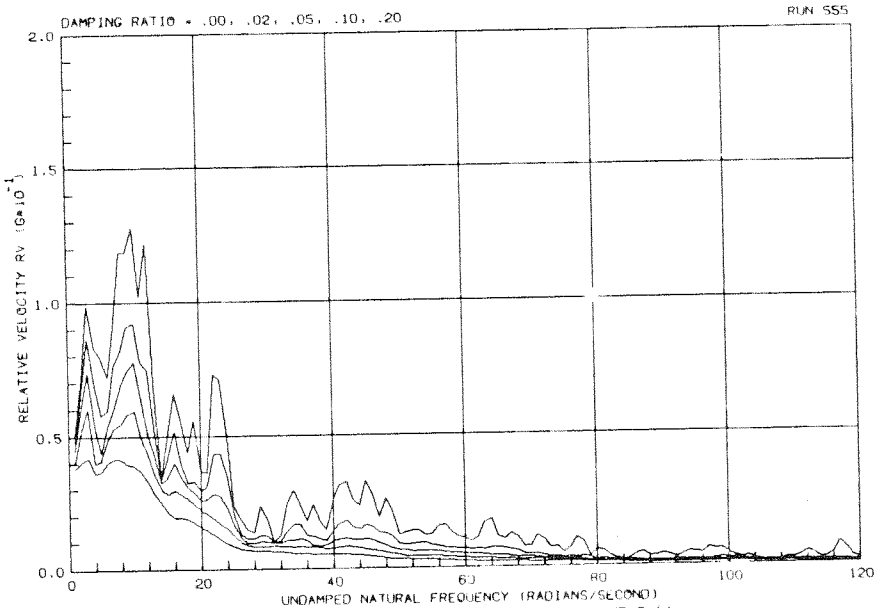

MISSISSIPPI 4074 - RADIAL

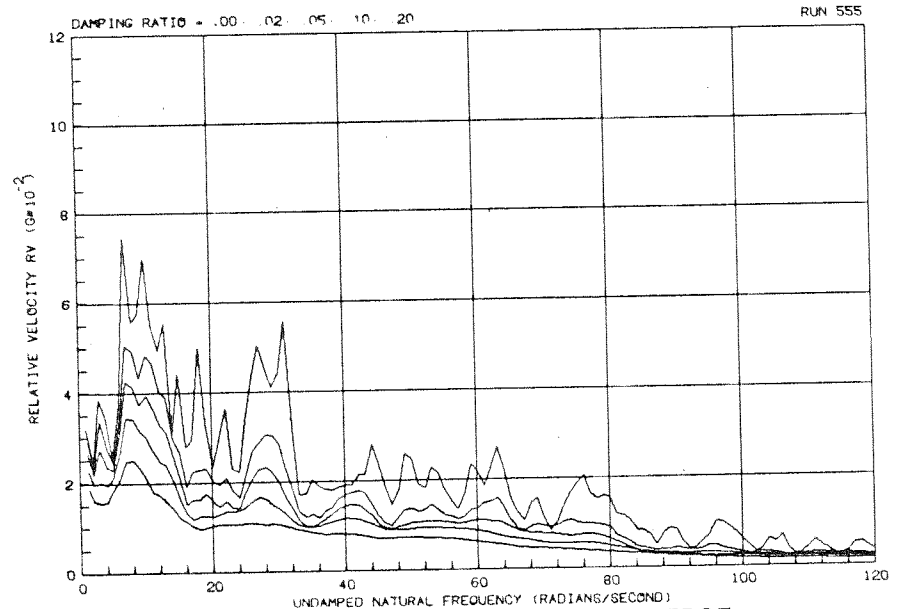

MISSISSIPPI 4074 - TRANSVERSE

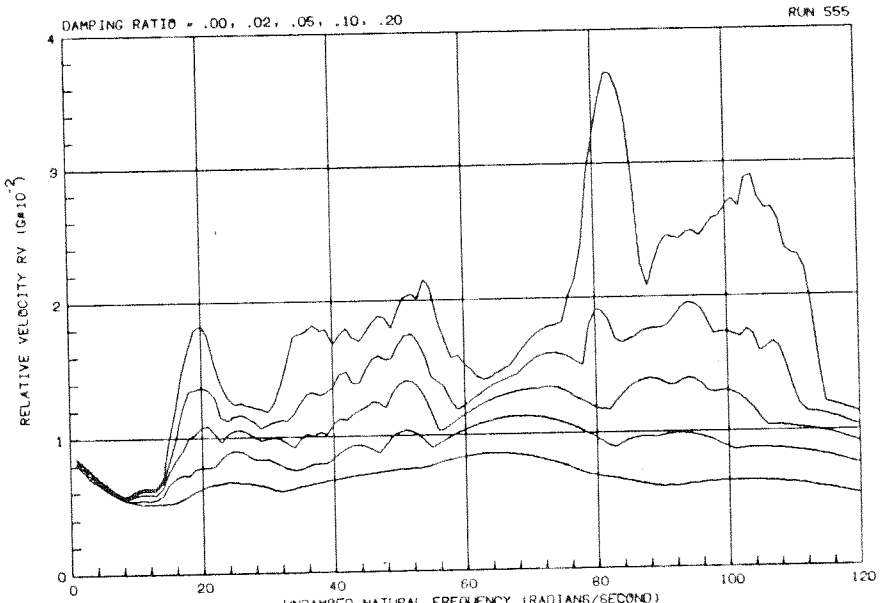

HARDHAT 1091 - TRANSVERSE

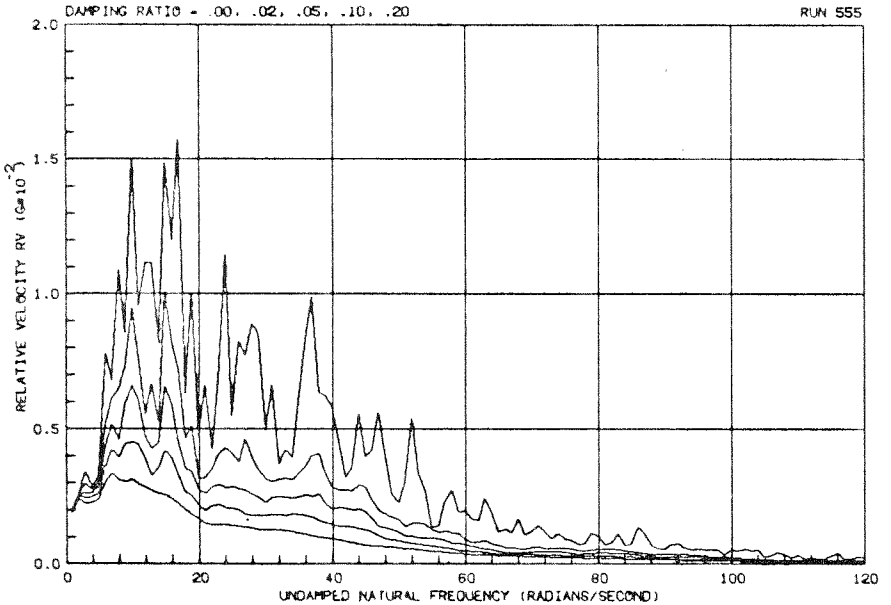

HARDHAT 4496 - TRANSVERSE

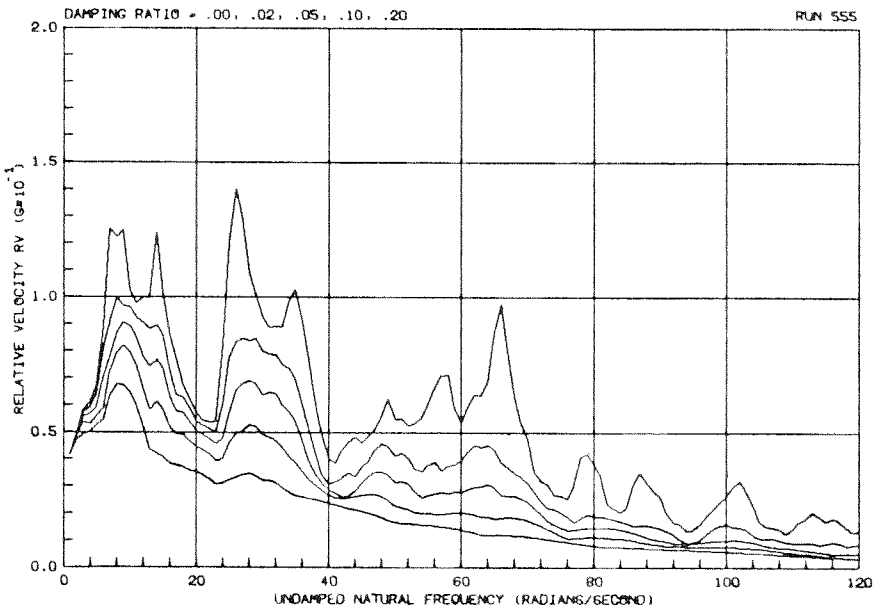

AARDVARK 3773 - TRANSVERSE

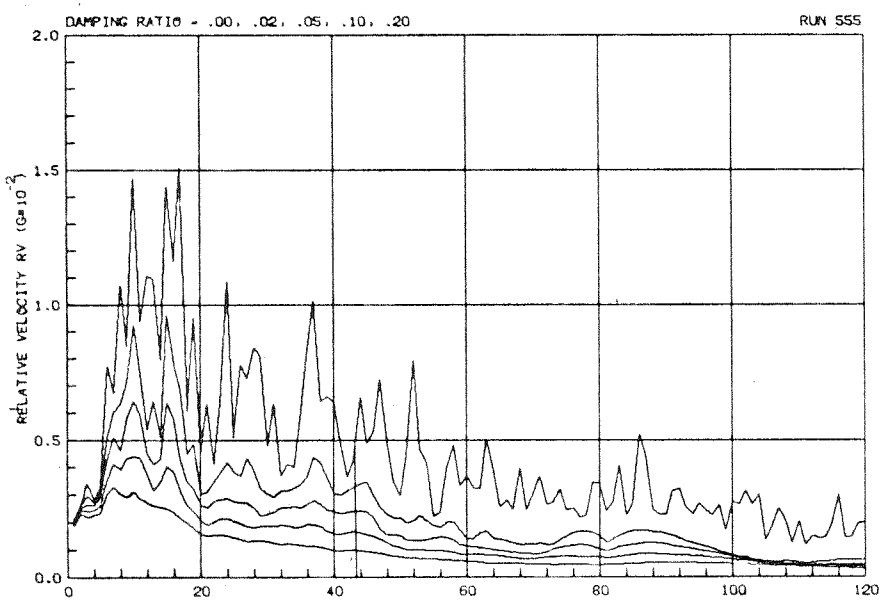

HARDHAT 4496 - TRANSVERSE

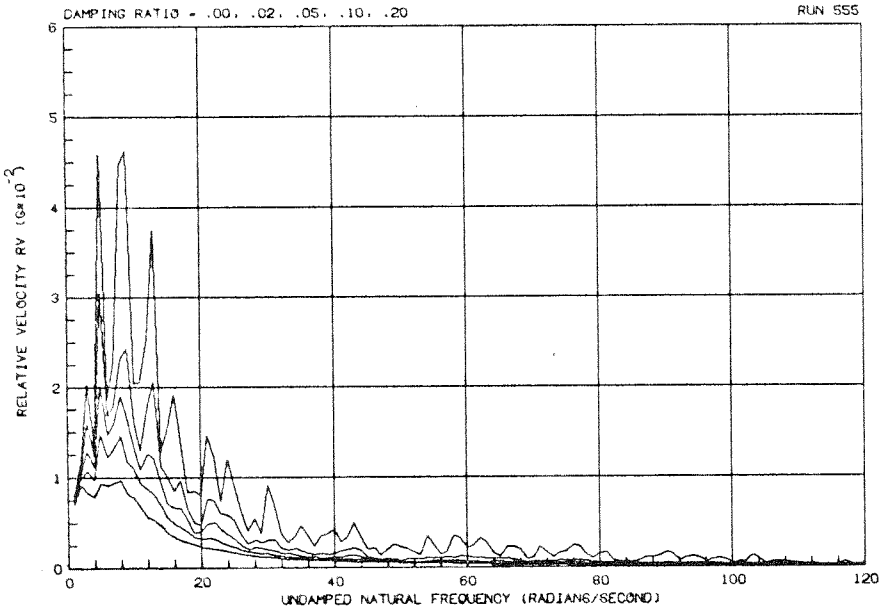

AARDVARK 1437 - TRANSVERSE

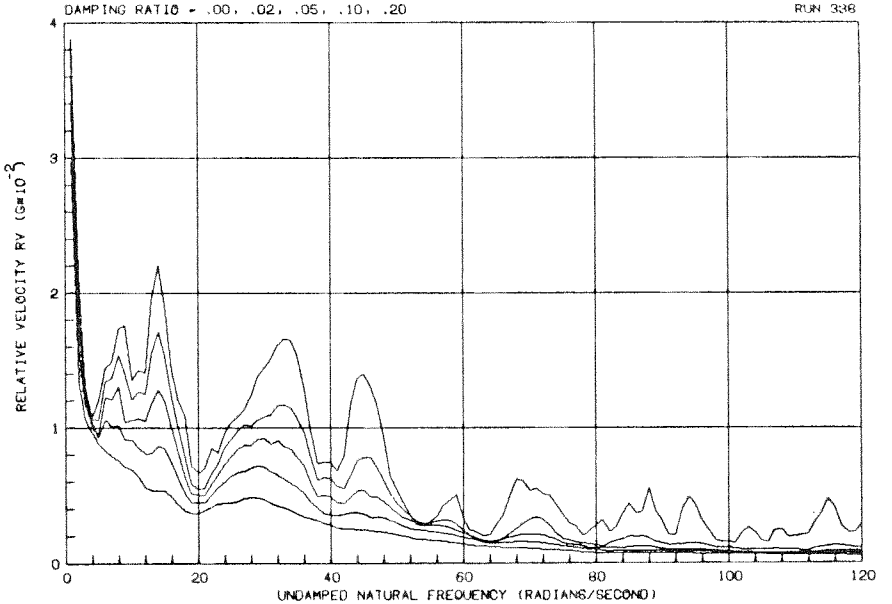

SEDAN RUN 3 - RADIAL

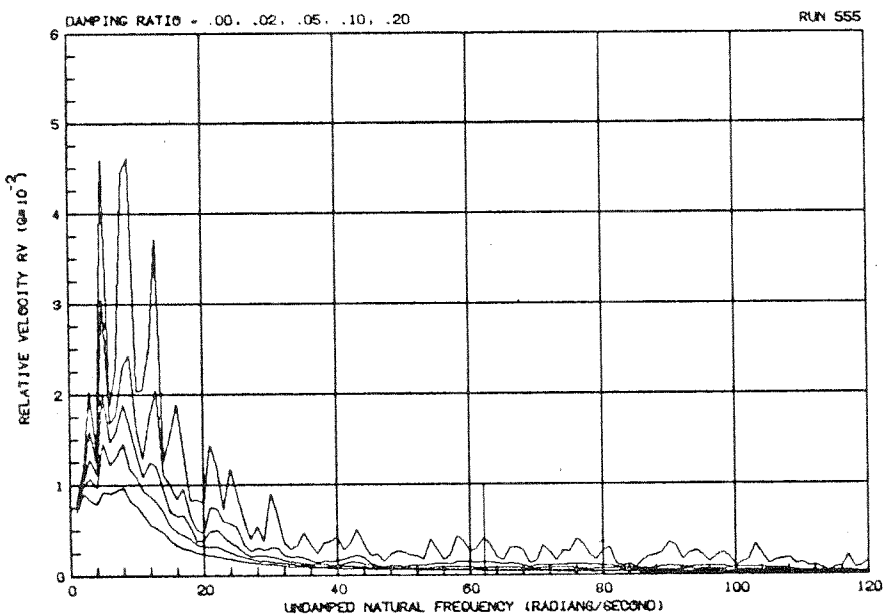

AARDVARK 1437 - TRANSVERSE

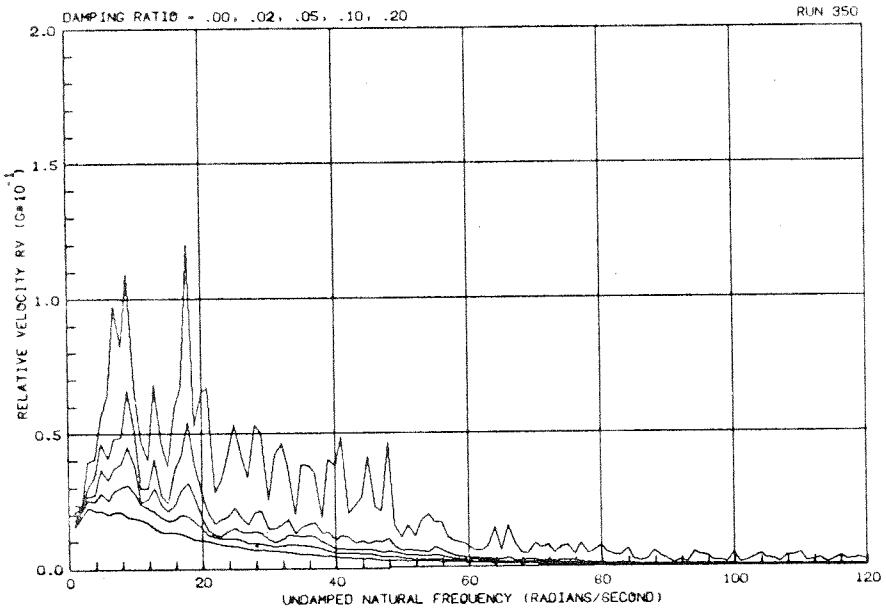

TAFT EARTHQUAKE 21 JULY 1952 - N21E

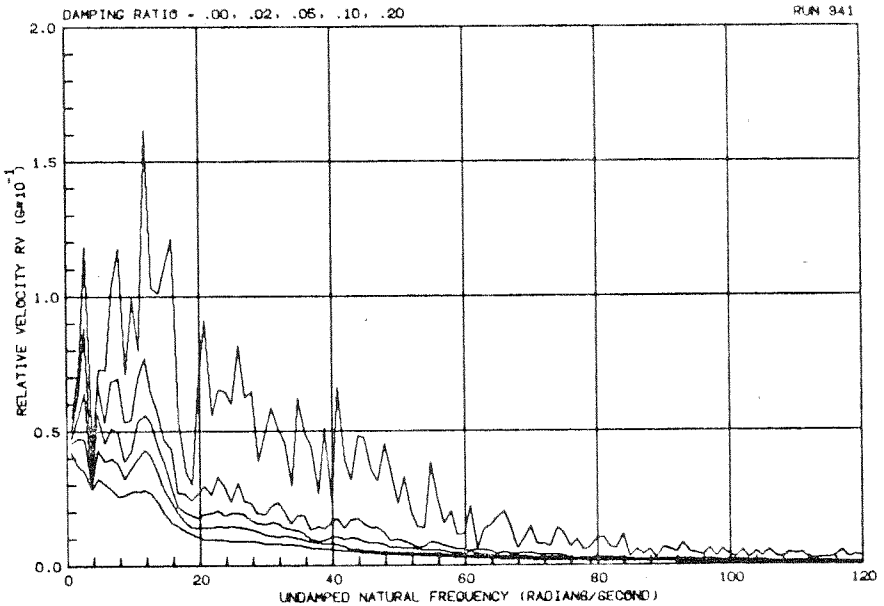

EL CENTRO EARTHQUAKE 18 MAY 1940 - EW

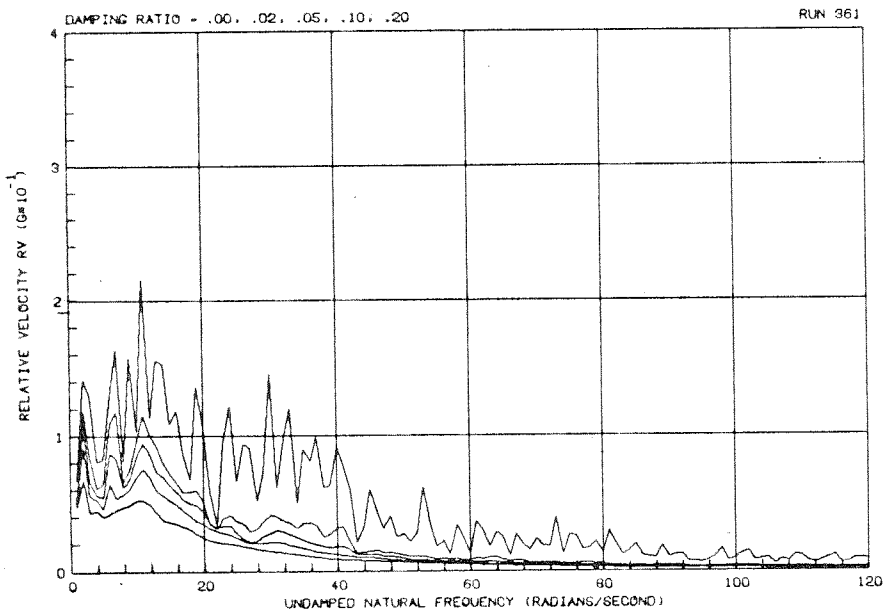

EL CENTRO EARTHQUAKE 18 MAY 1940 - NS

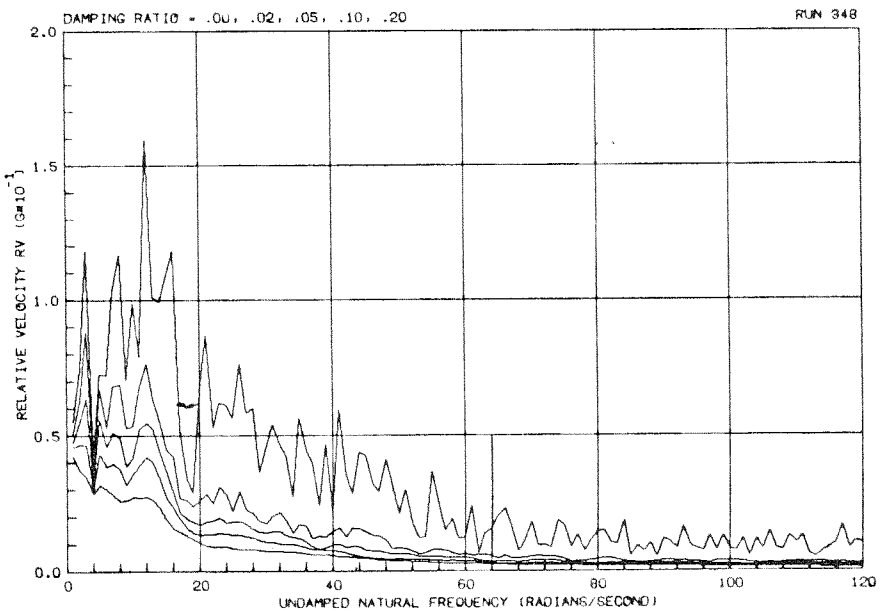

EL CENTRO EARTHQUAKE 18 MAY 1940 - EW

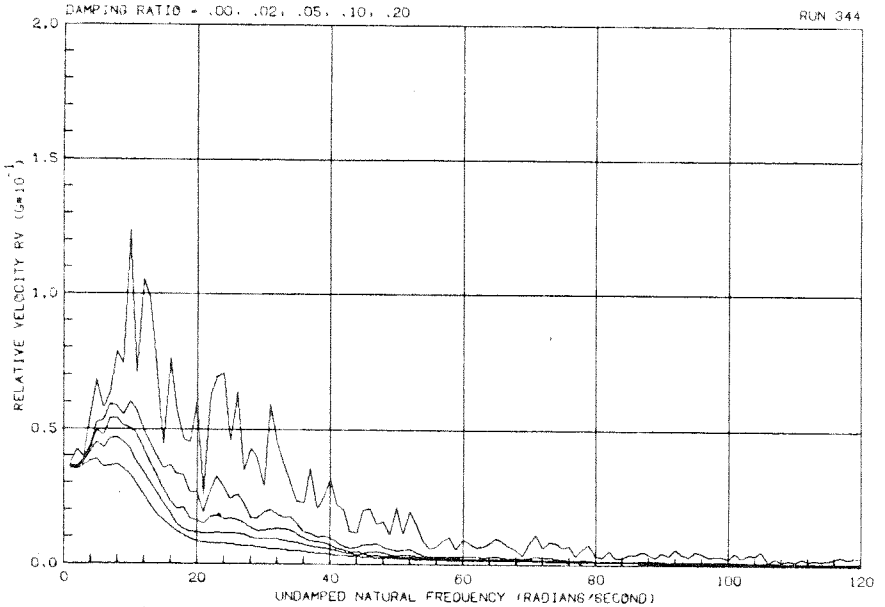

EL CENTRO EARTHQUAKE 30 DEC 1934 - NS

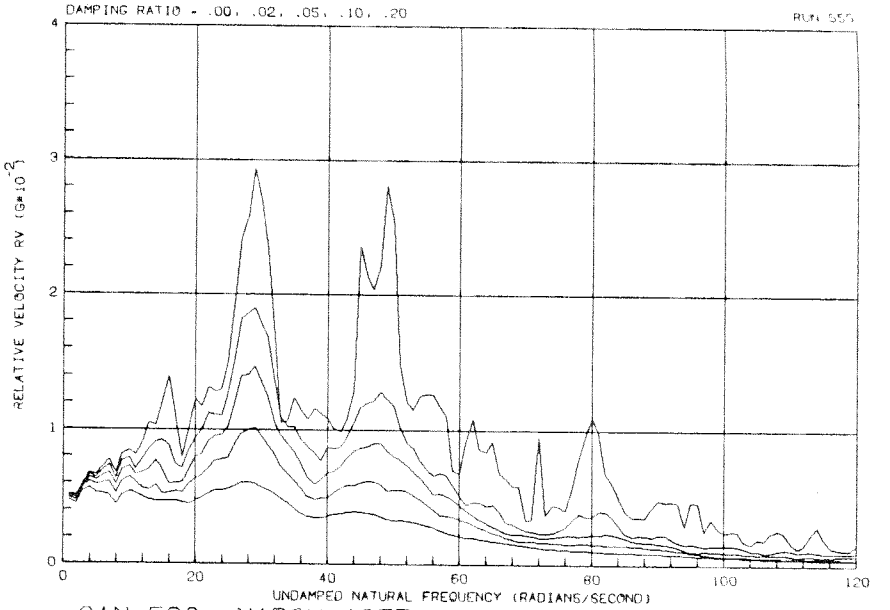

SAN FCO. MARCH 1957 - GOLDEN GATE PARK S80E

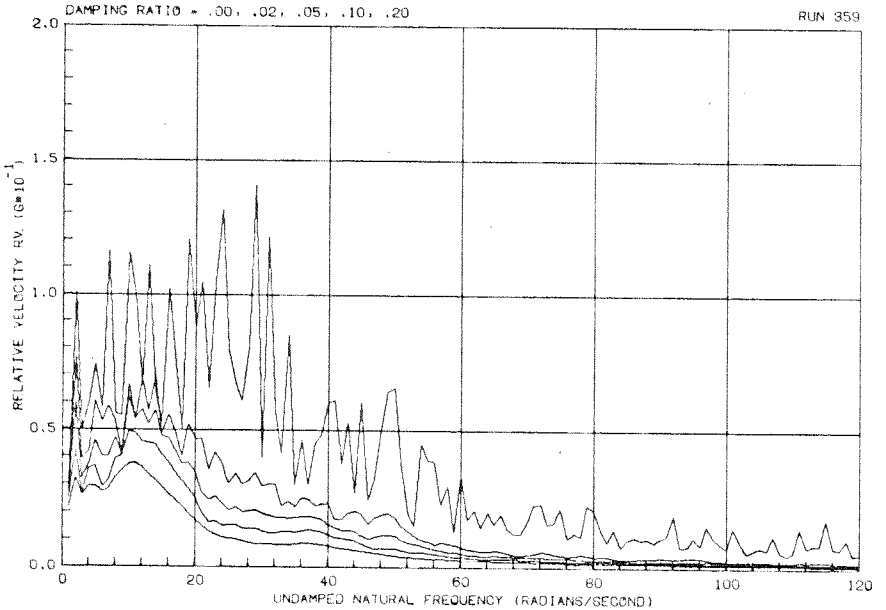

OLYMPIA EARTHQUAKE 13 APRIL 1949 - N80E

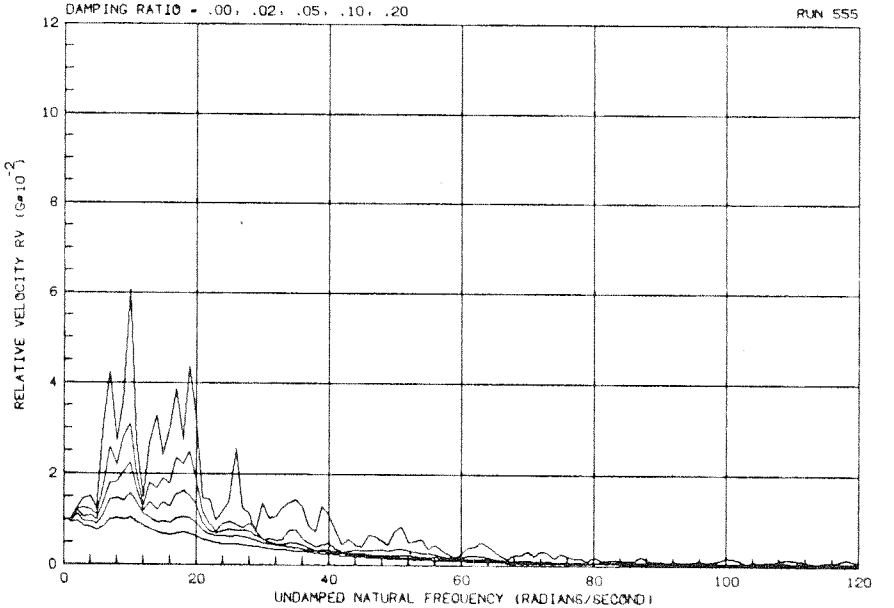

FERNDALE, 3 OCTOBER 1941 - S45E

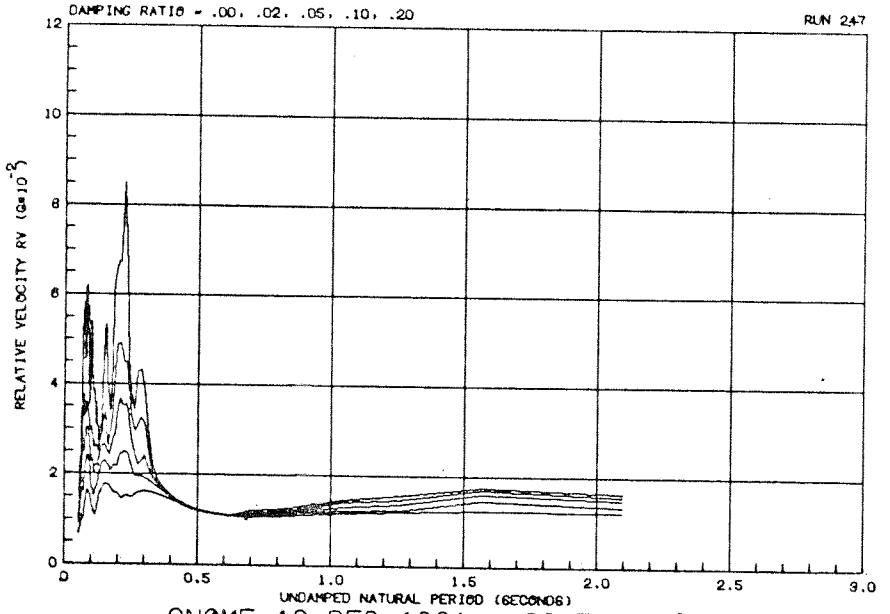

GNOME 10 DEC 1961 - S2 TRANSVERSE

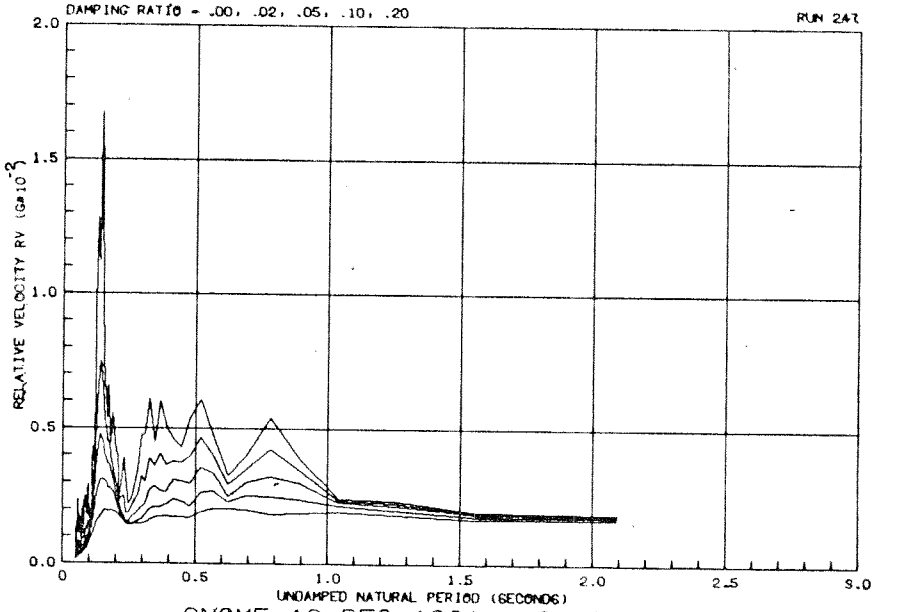

GNOME 10 DEC 1961 - S4 RADIAL

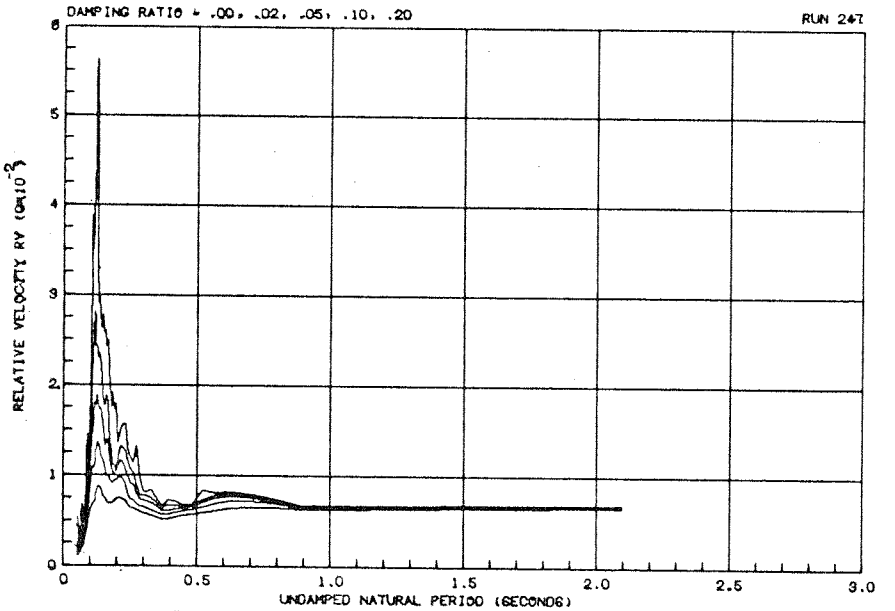

GNOME 10 DEC 1961 - S3 TRANSVERSE

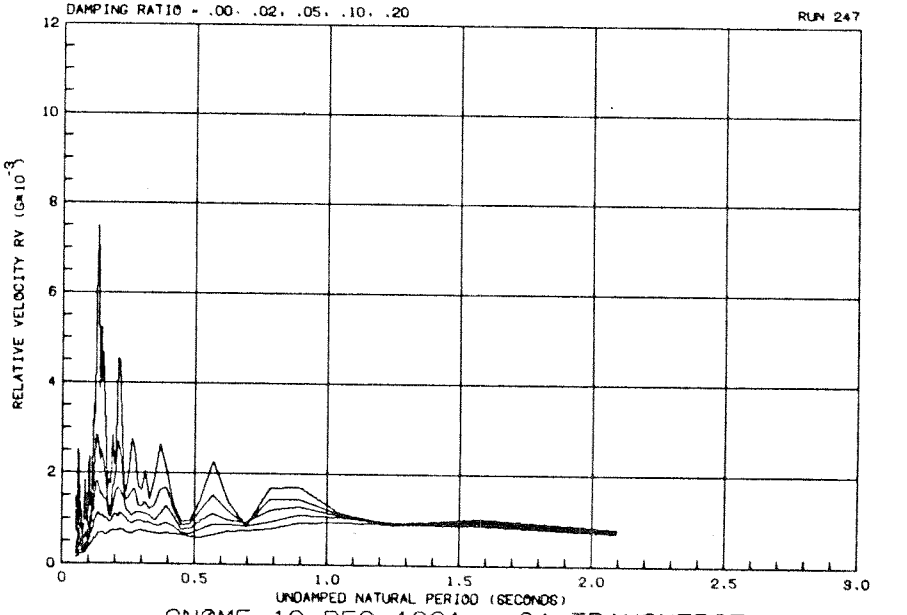

GNOME 10 DEC 1961 - S4 TRANSVERSE

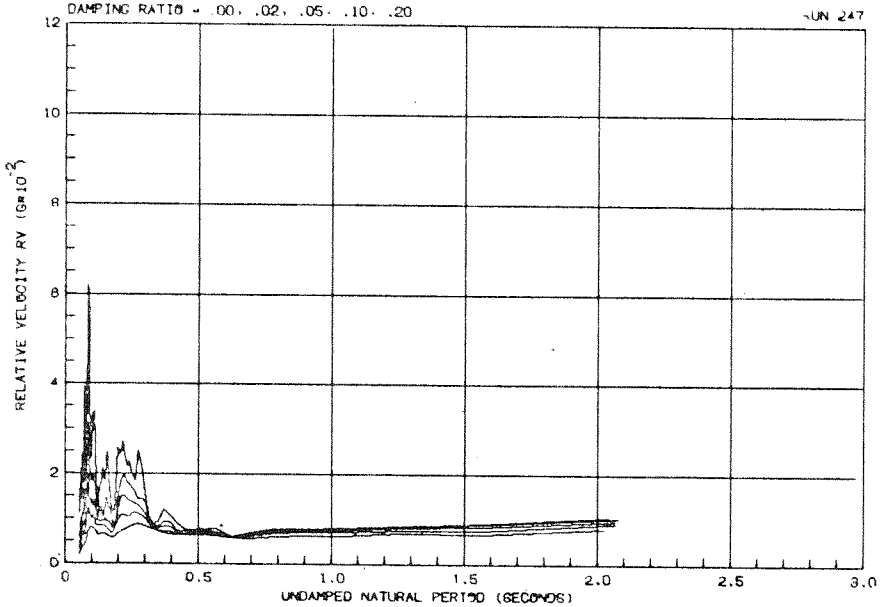

GNOME 10 DEC 1961 - S6 TRANSVERSE

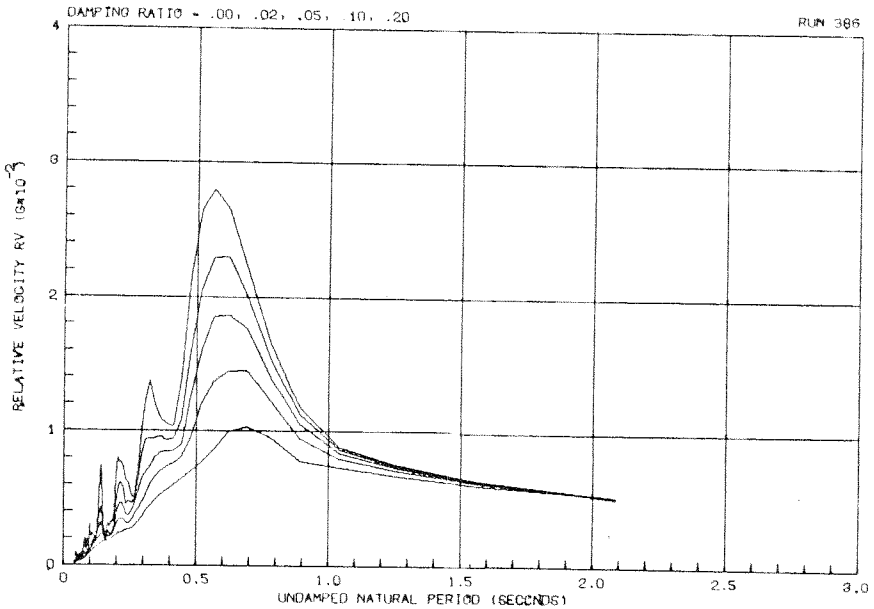

DANNYBOY D5 - RADIAL

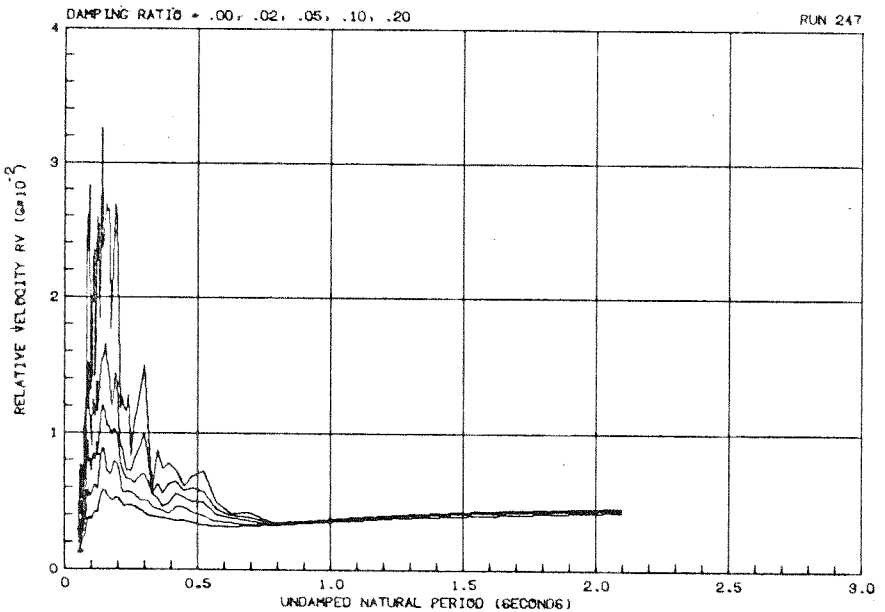

GNOME 10 DEC 1961 - S7 TRANSVERSE

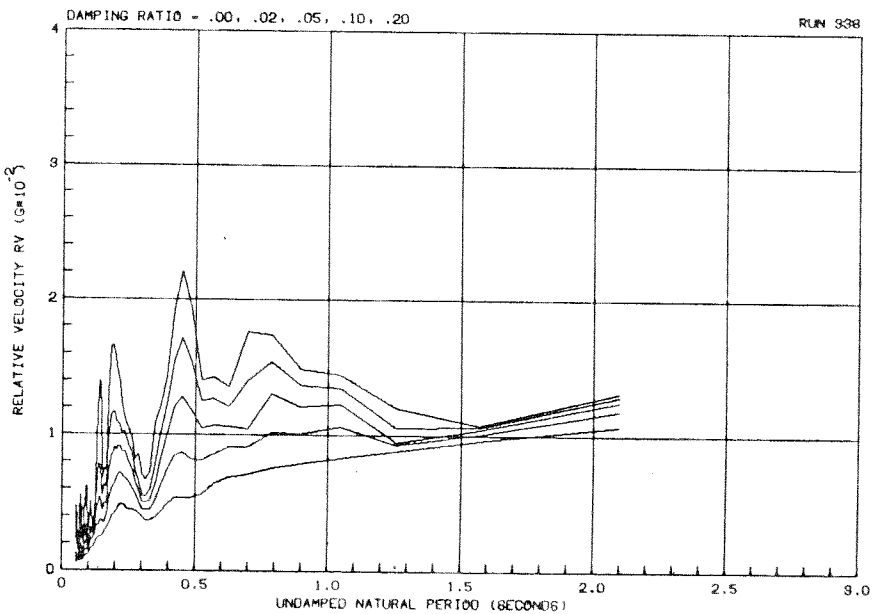

SEDAN RUN 3 - RADIAL

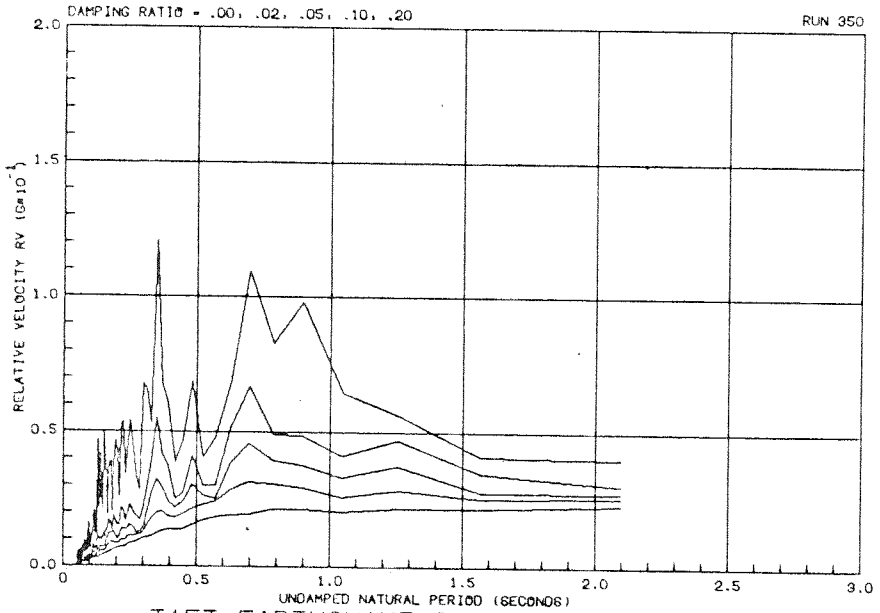

TAFT EARTHQUAKE 21 JULY 1952 - N21E

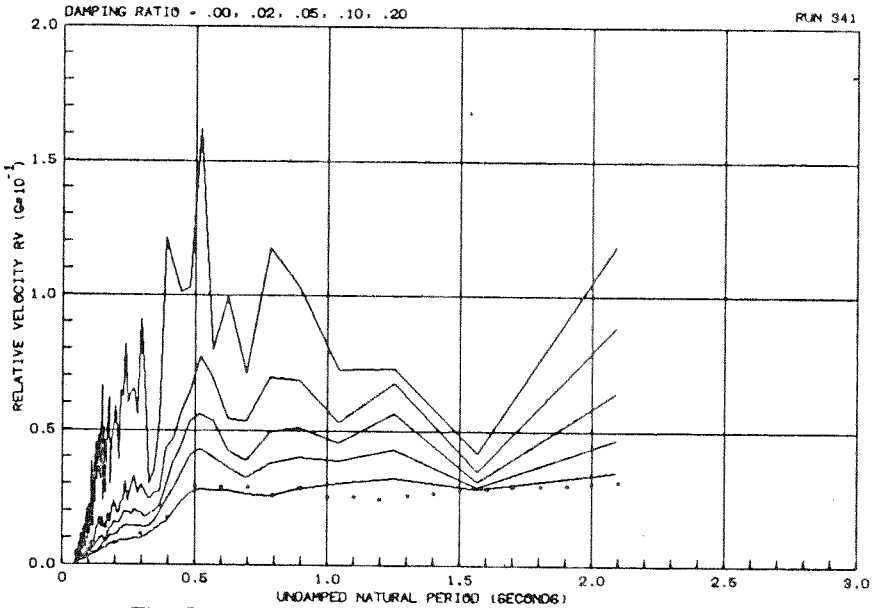

EL CENTRO EARTHQUAKE 18 MAY 1940 - EW

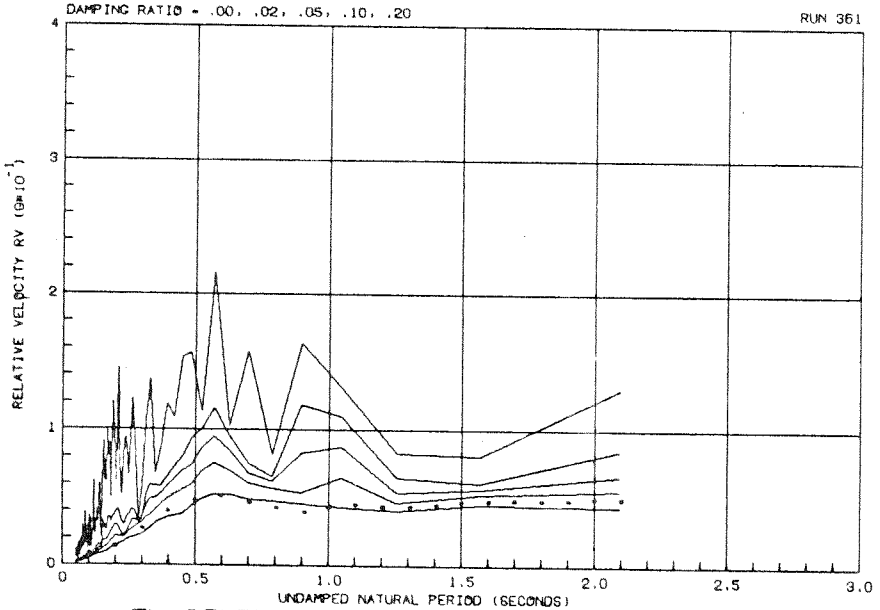

EL CENTRO EARTHQUAKE 18 MAY 1940 - NS

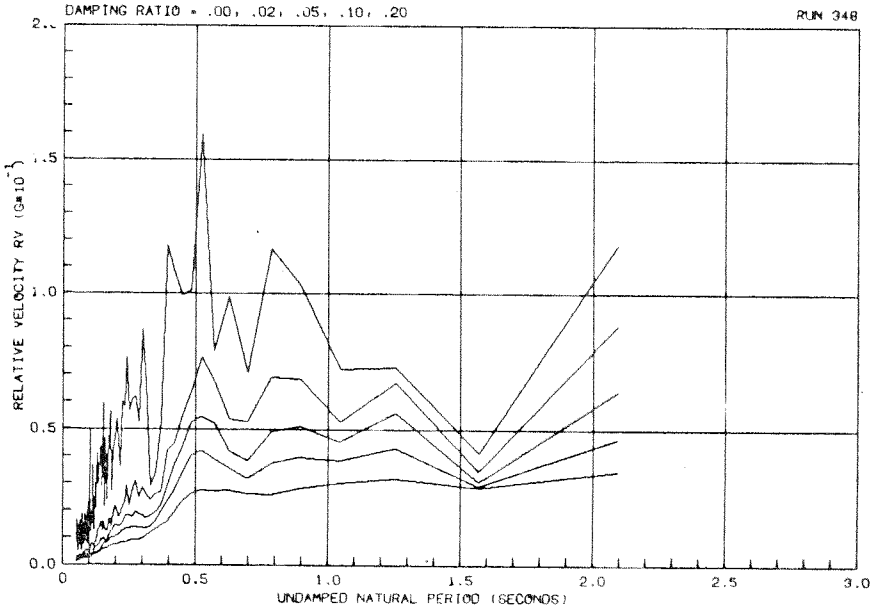

EL CENTRO EARTHQUAKE 18 MAY 1940 - EW

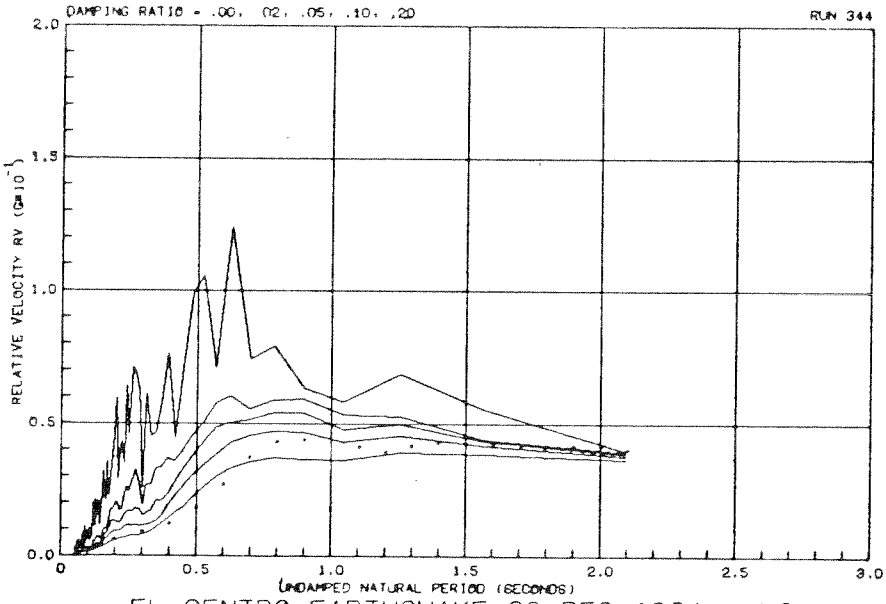

EL CENTRO EARTHQUAKE 30 DEC 1934 - NS

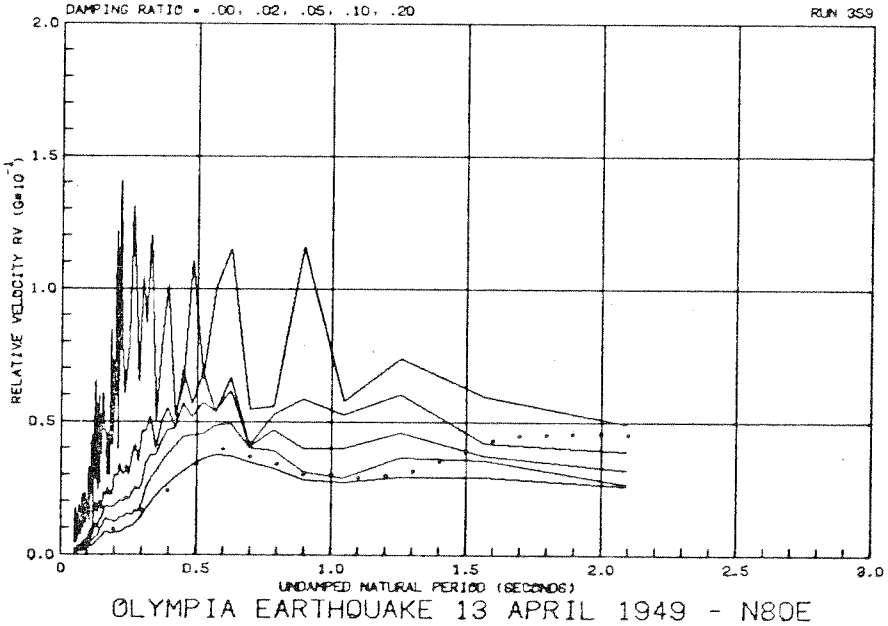

OLYMPIA EARTHQUAKE 13 APRIL 1949 - N80E

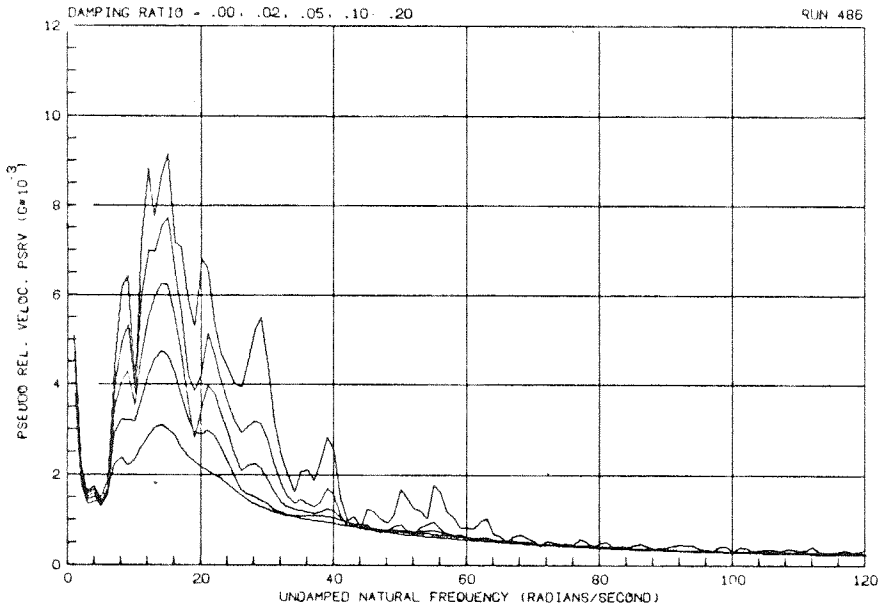

DANNYBOY D8 - RADIAL

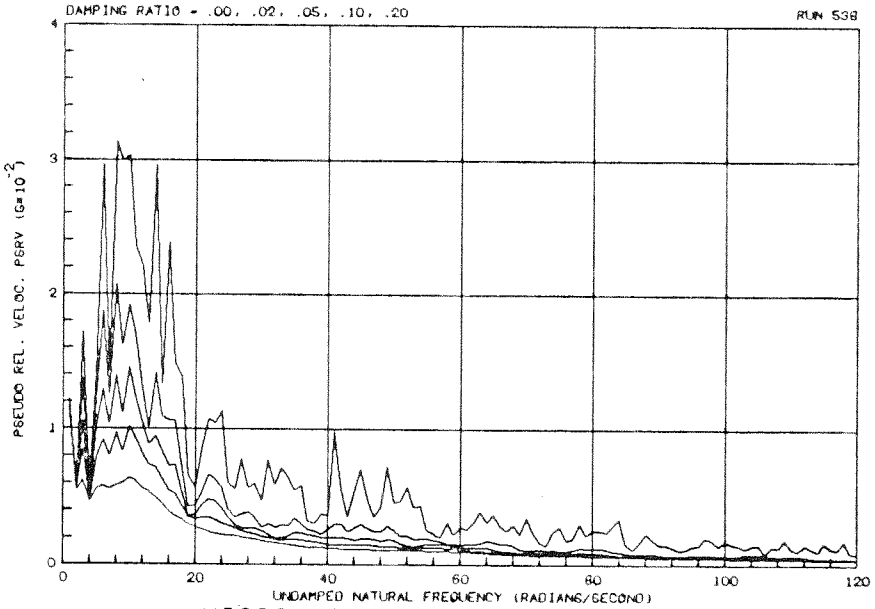

MISSISSIPPI 8228 - TRANSVERSE

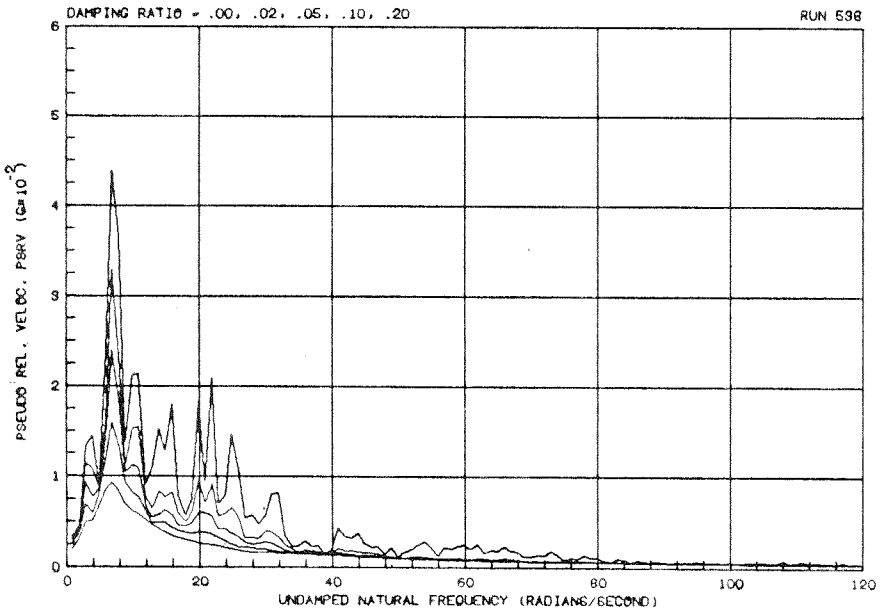

MISSISSIPPI 1777 - TRANSVERSE

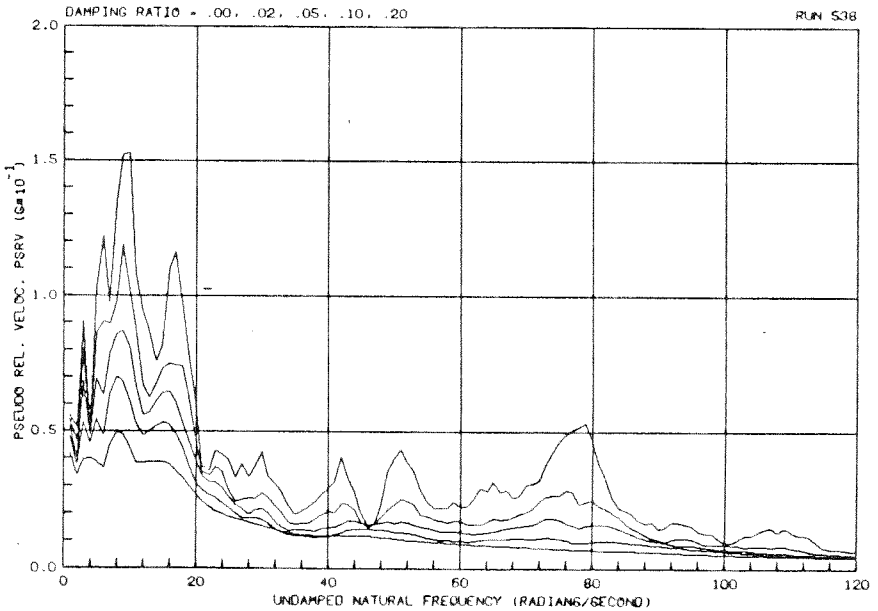

MISSISSIPPI 7245 - RADIAL

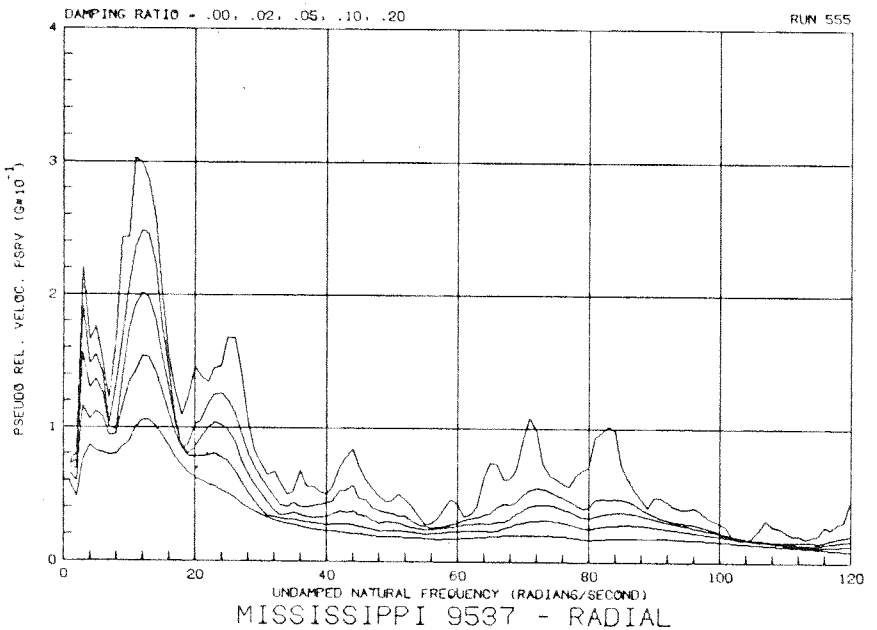

MISSISSIPPI 9537 - RADIAL

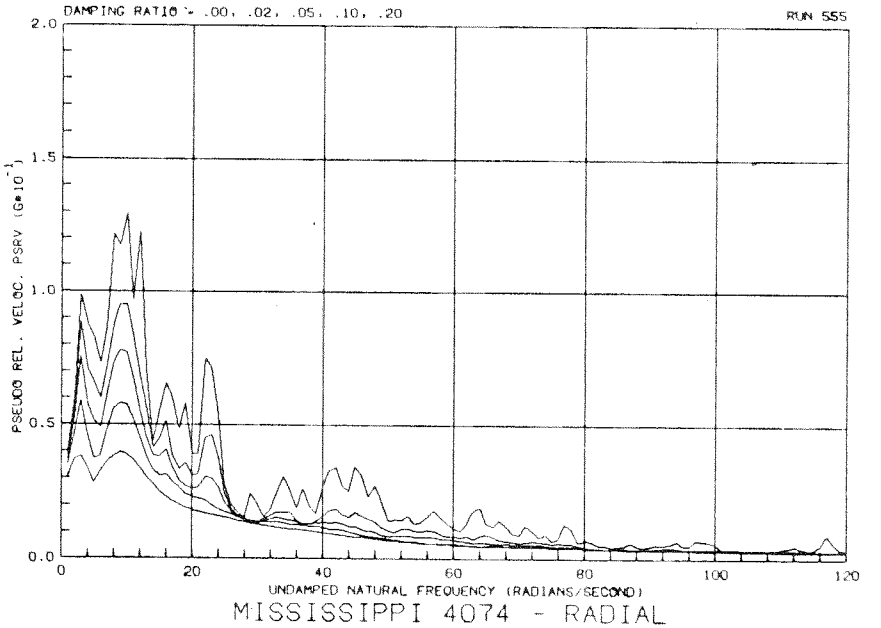

MISSISSIPPI 4074 - RADIAL

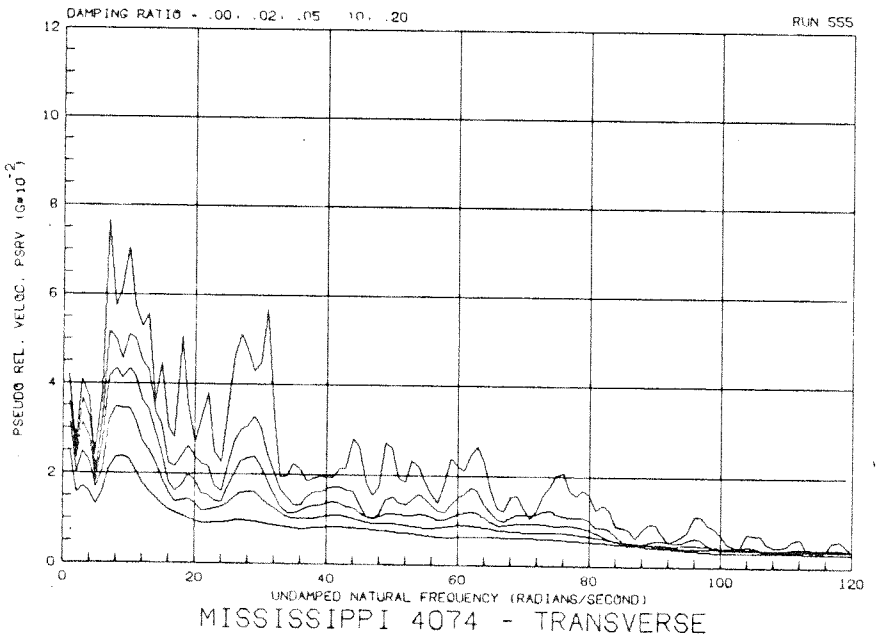

MISSISSIPPI 4074 - TRANSVERSE

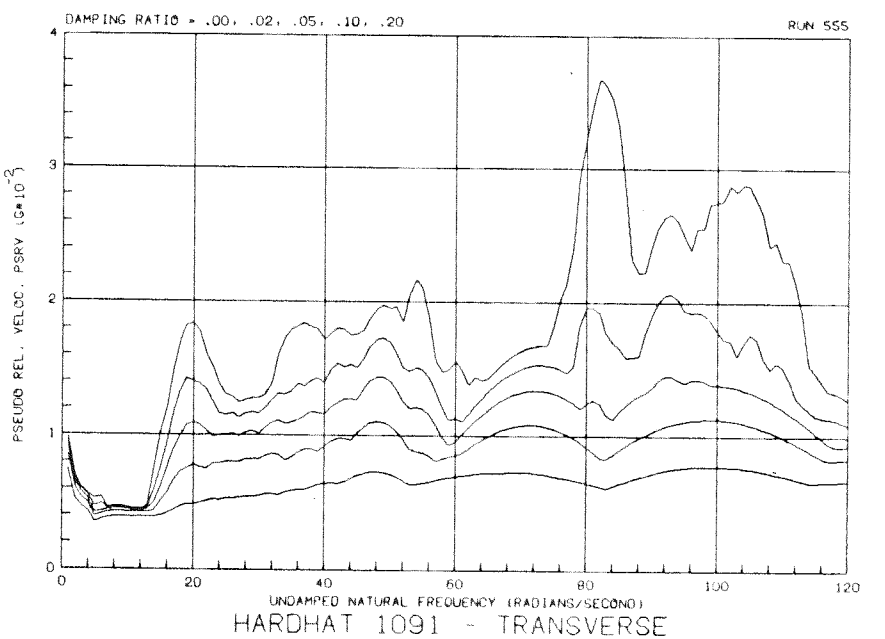

HARDHAT 1091 - TRANSVERSE

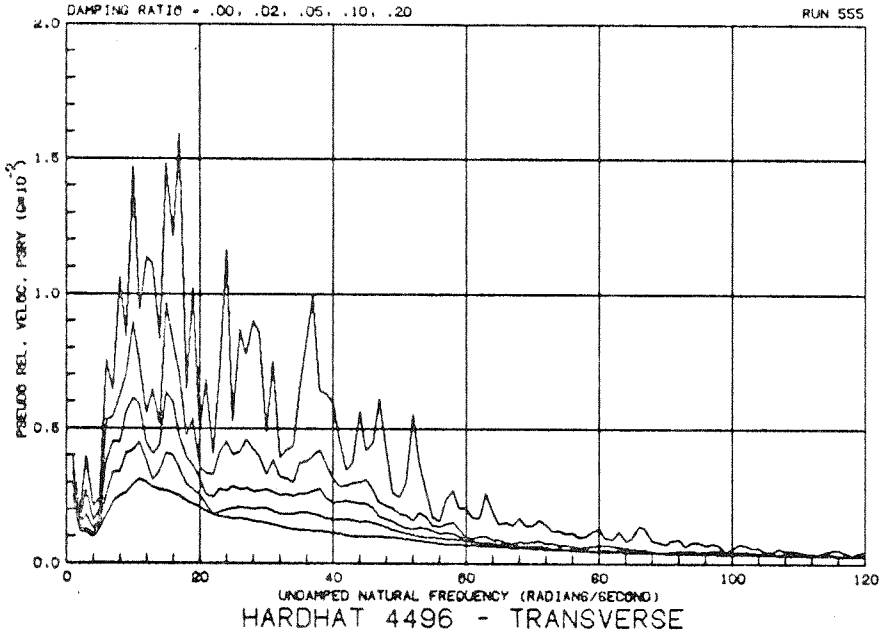

HARDHAT 4496 - TRANSVERSE

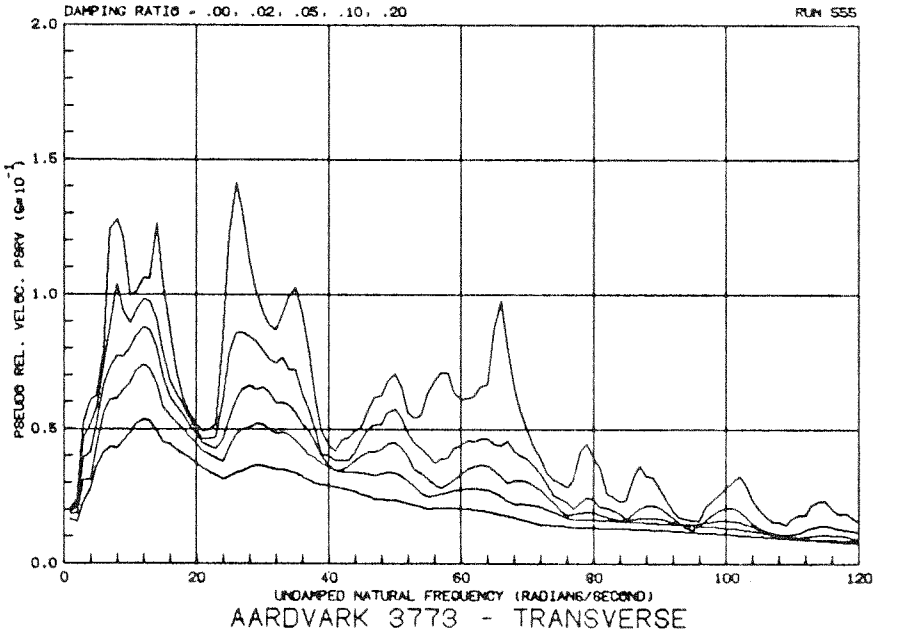

AARDVARK 3773 - TRANSVERSE

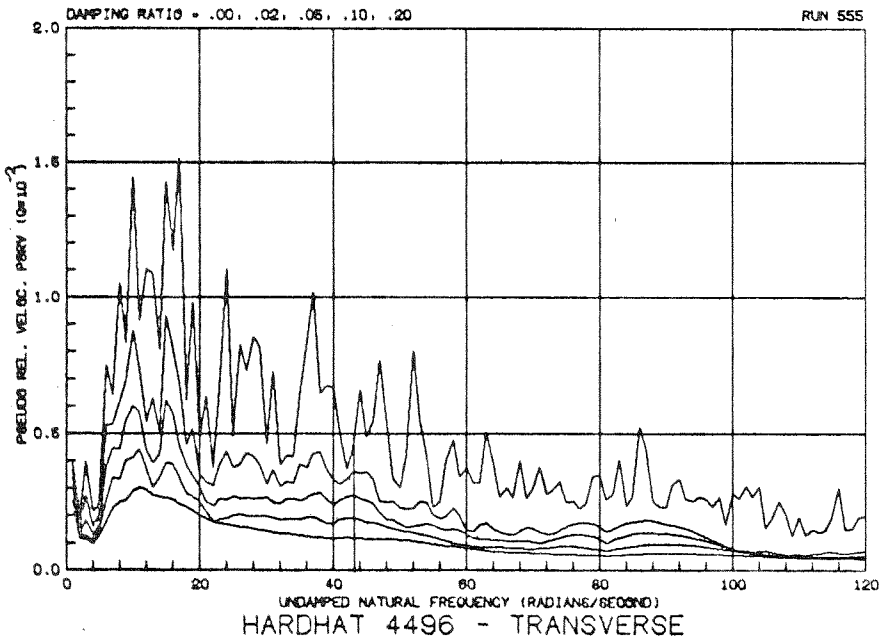

HARDHAT 4496 - TRANSVERSE

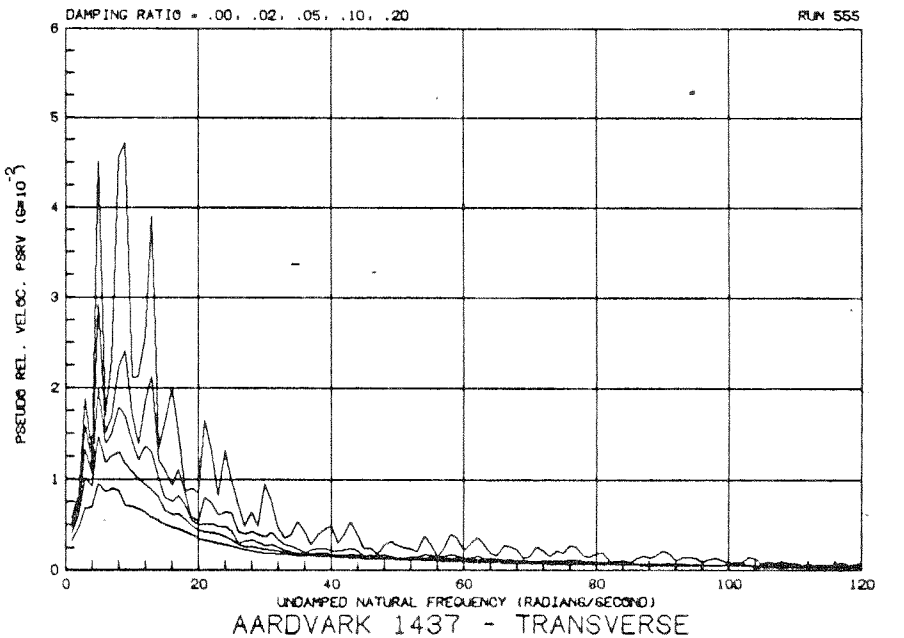

AARDVARK 1437 - TRANSVERSE

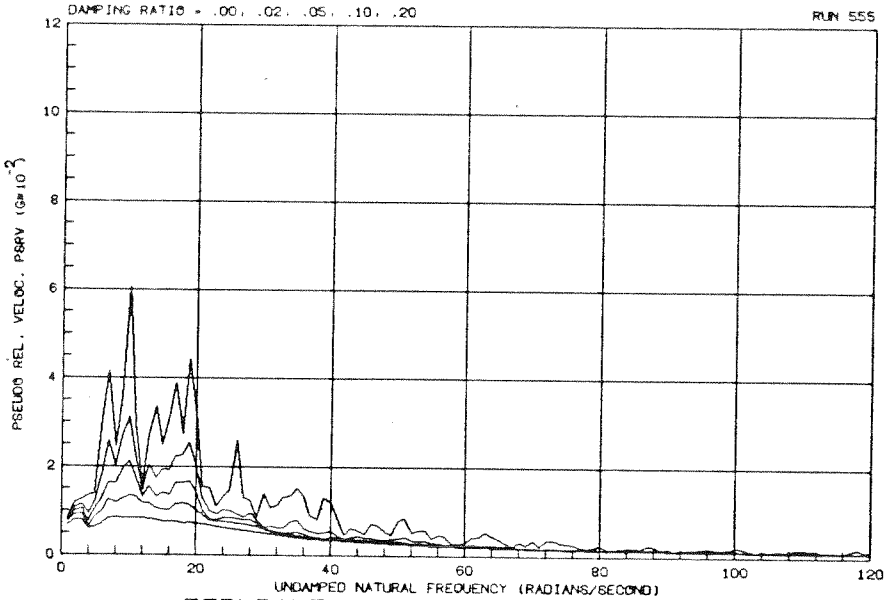

FERNDALE, 3 OCTOBER 1941 - S45E

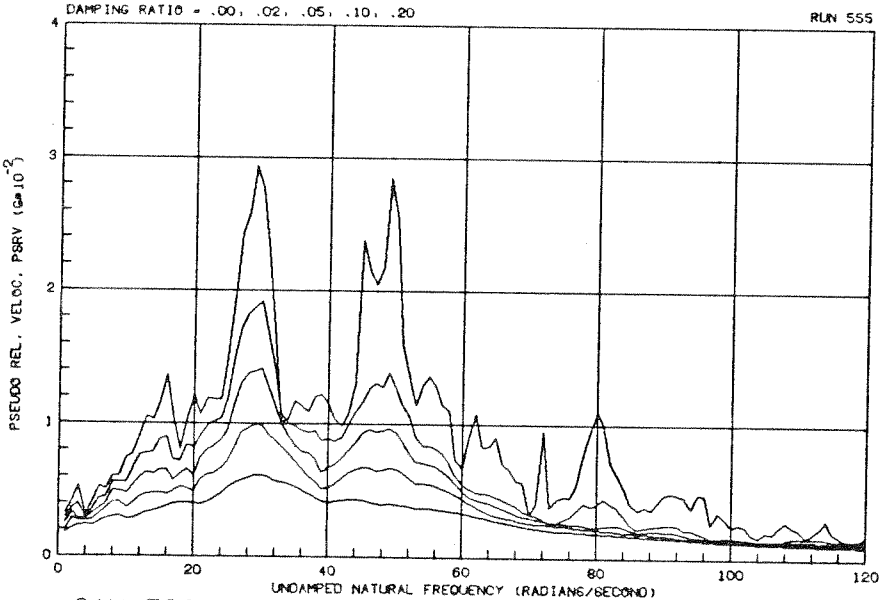

SAN FCO. MARCH 1957 - GOLDEN GATE PARK S80E

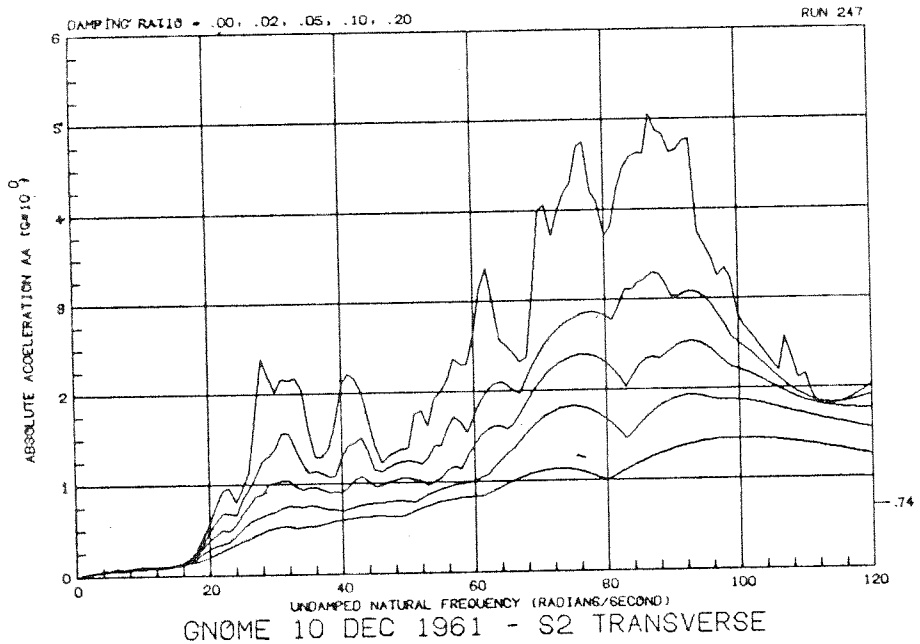

GNOME 10 DEC 1961 - S2 TRANSVERSE

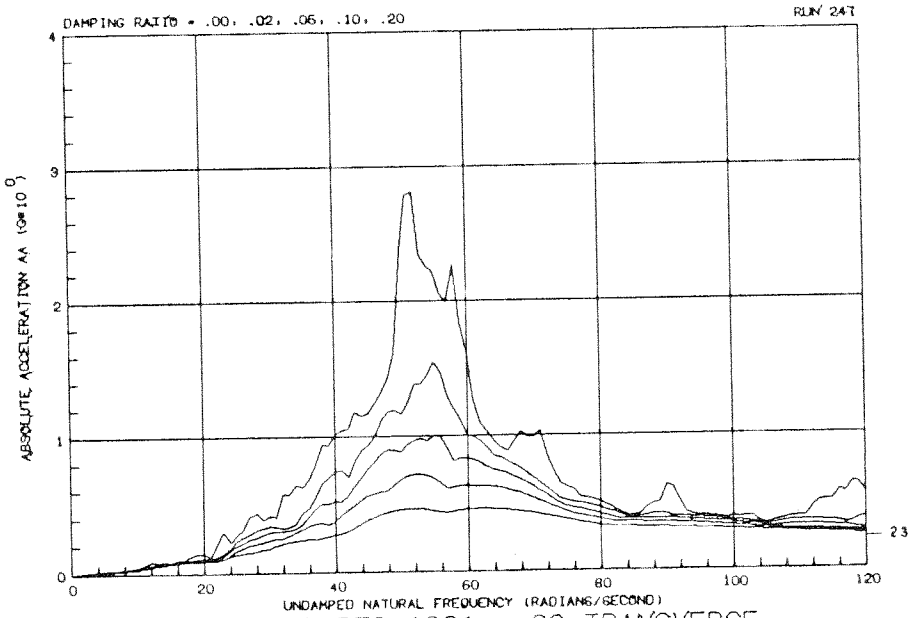

GNOME 10 DEC 1961 - S3 TRANSVERSE

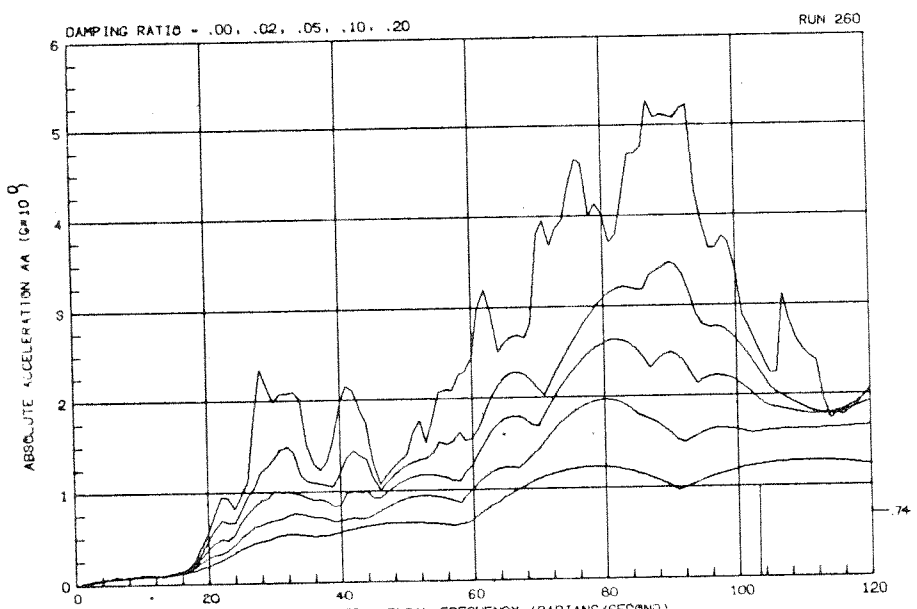

GNOME 10 DEC 1961 - S2 TRANSVERSE

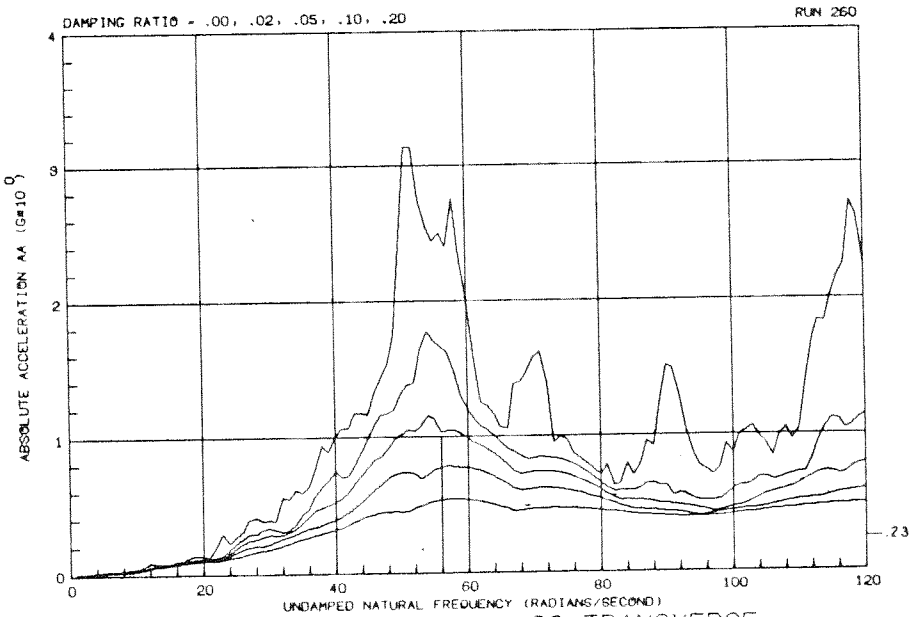

GNOME 10 DEC 1961 - S3 TRANSVERSE

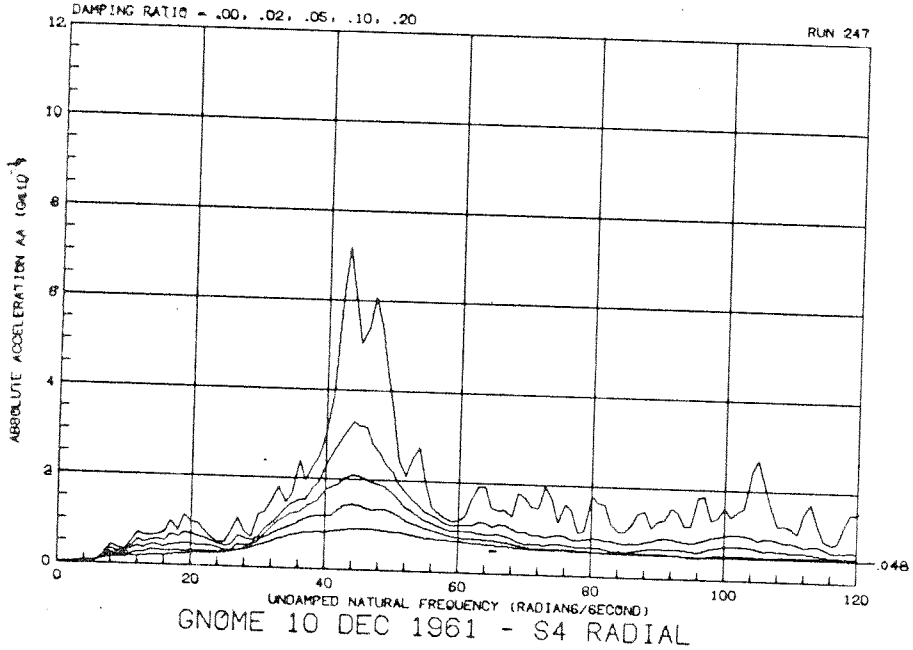

GNOME 10 DEC 1961 - S4 RADIAL

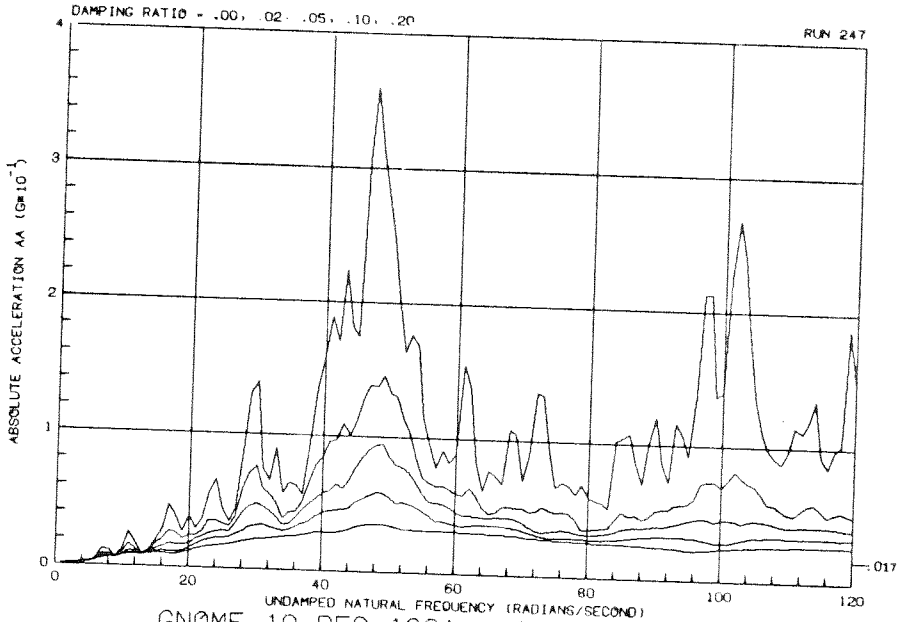

GNOME 10 DEC 1961 - S4 TRANSVERSE

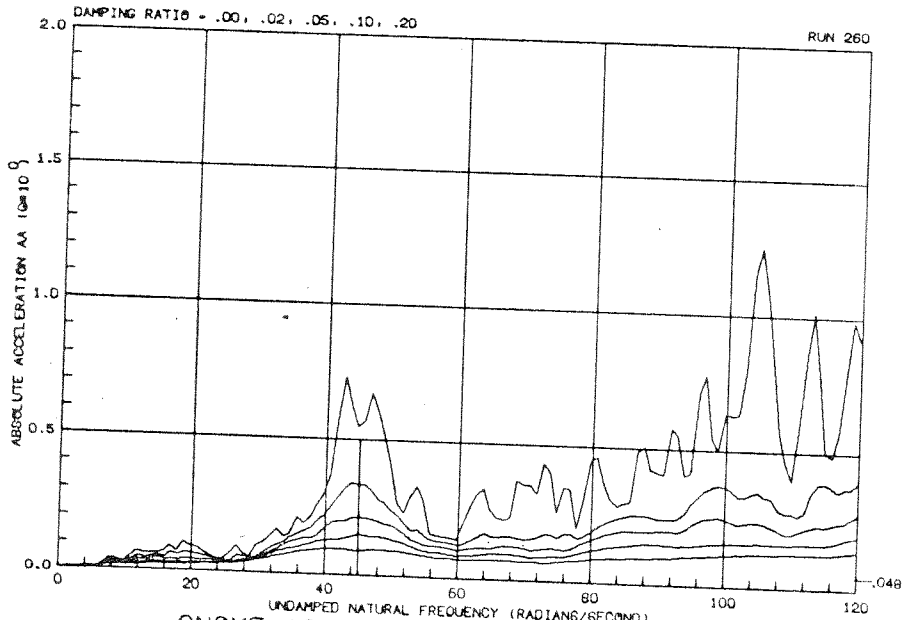

GNOME 10 DEC 1961 - S4 RADIAL

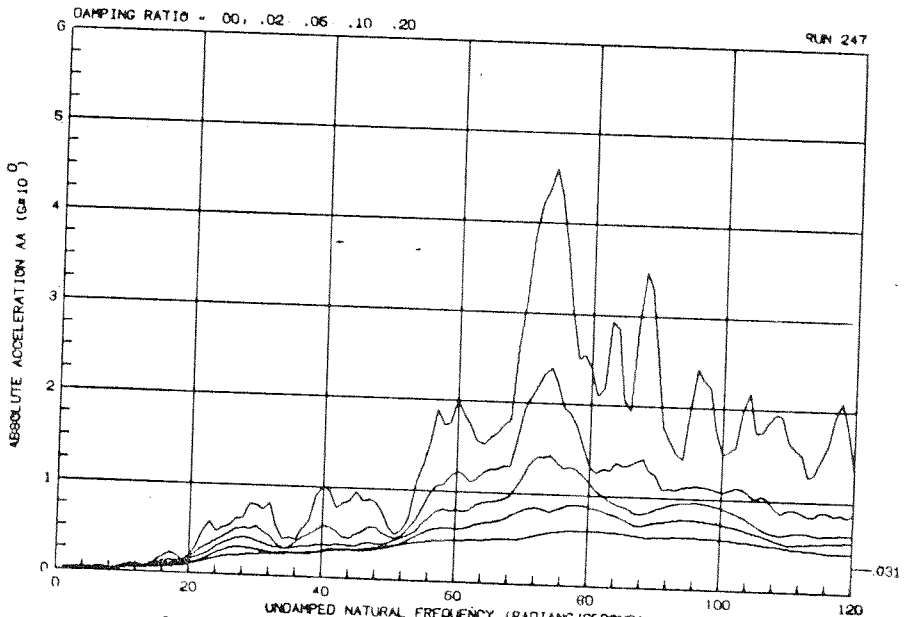

CNOME 10 DEC 1961 - S6 TRANSVERSE

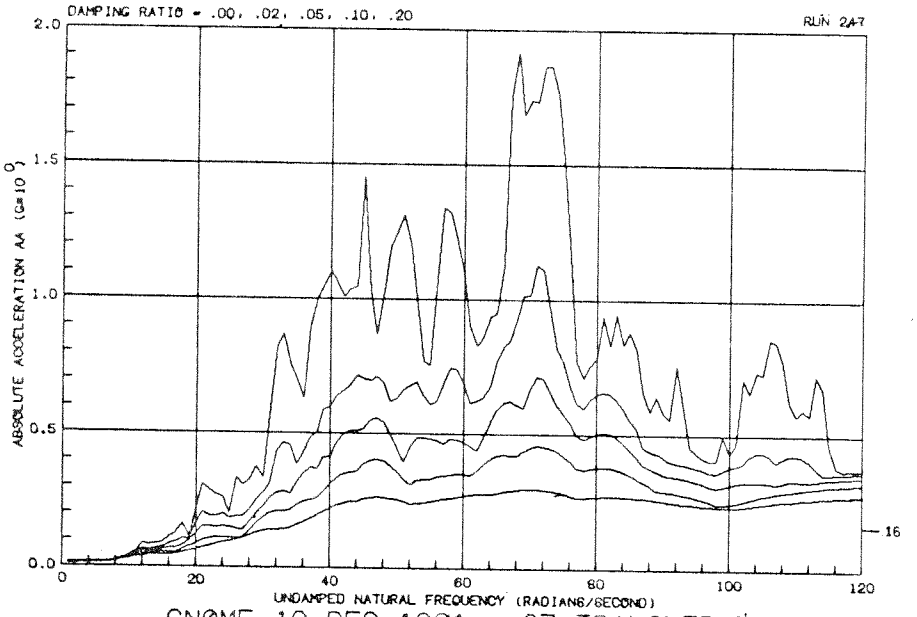

GNOME 10 DEC 1961 - S7 TRANSVERSE

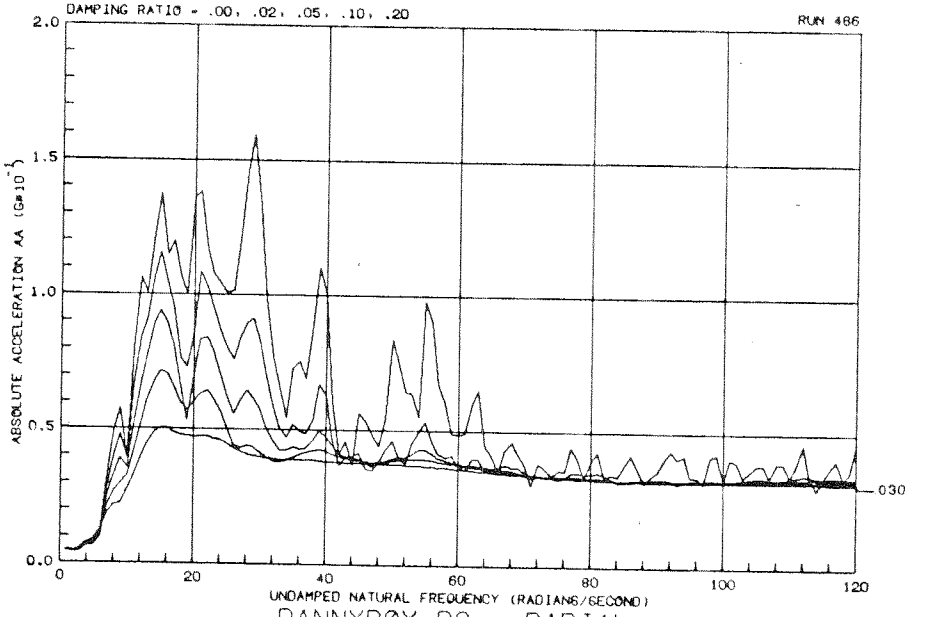

DANNYBOY D8 - RADIAL

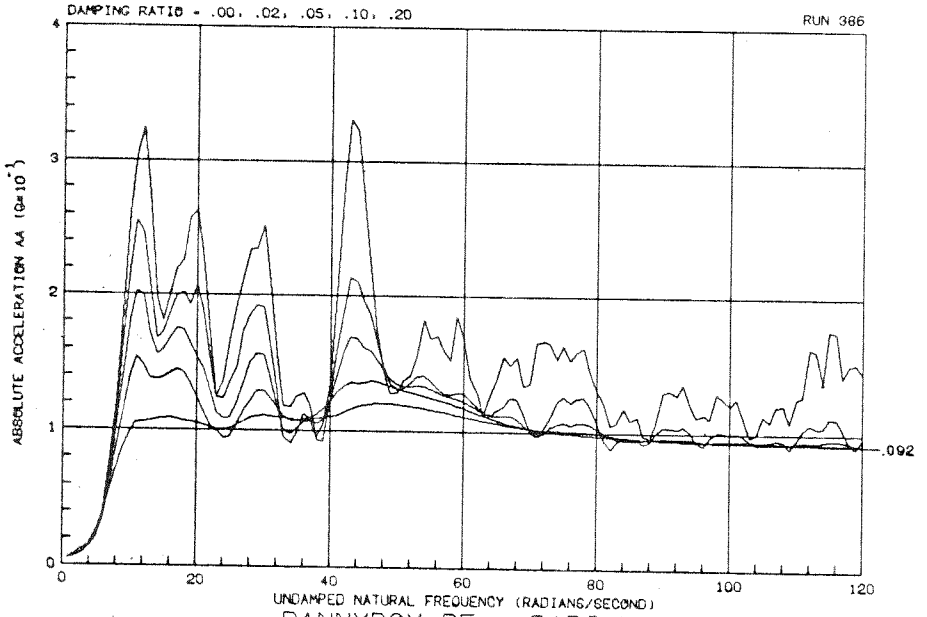

DANNYBOY D5 - RADIAL

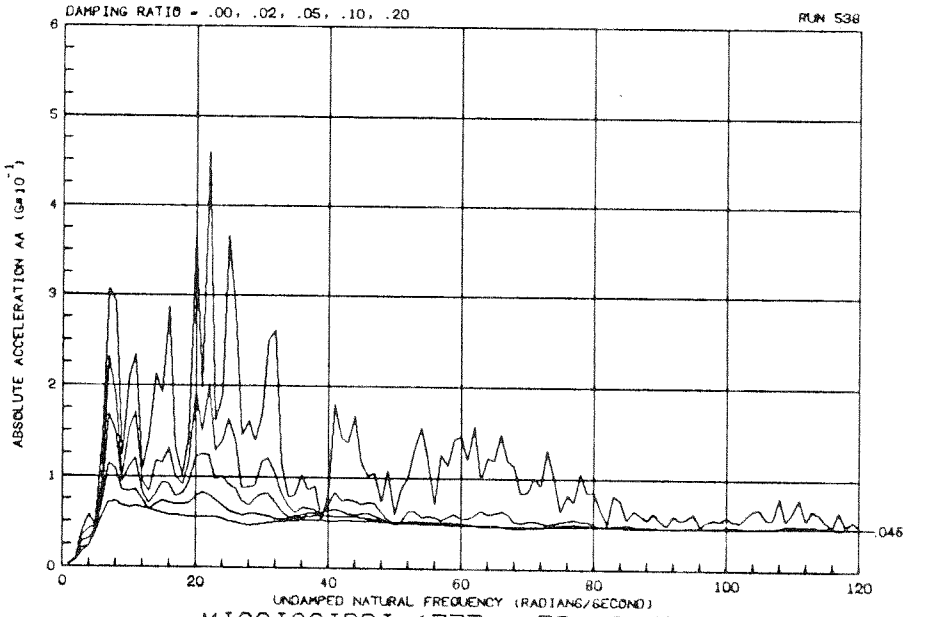

MISSISSIPPI 1777 - TRANSVERSE

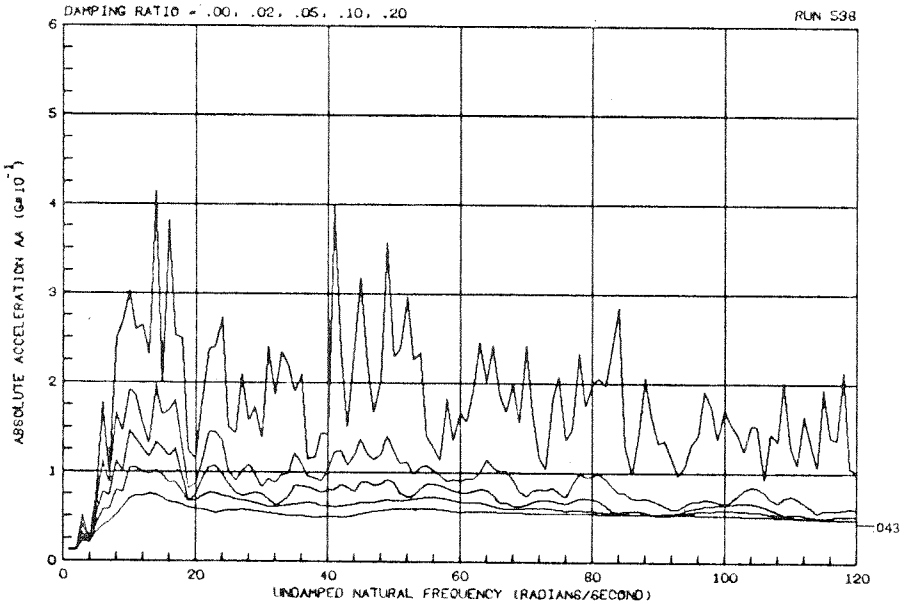

MISSISSIPPI 8228 - TRANSVERSE

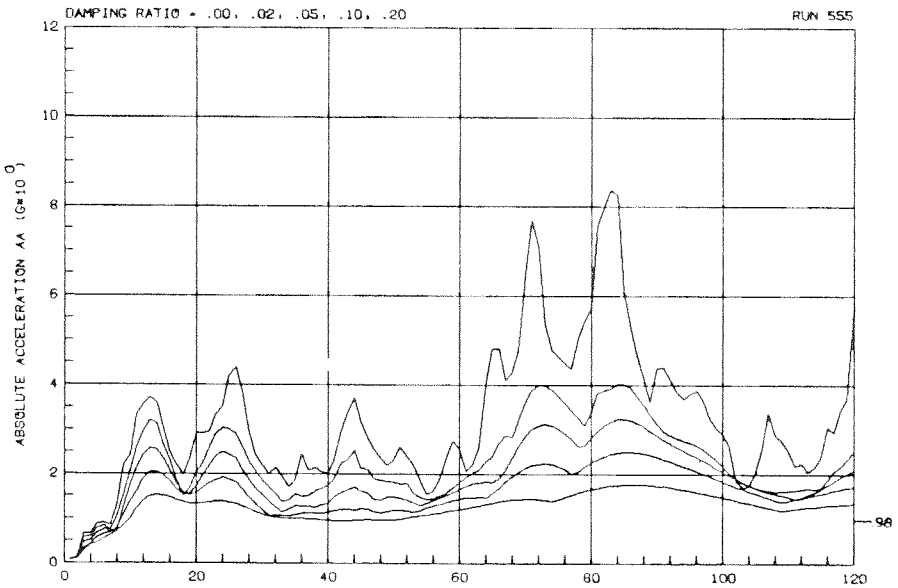

MISSISSIPPI 9537 - RADIAL

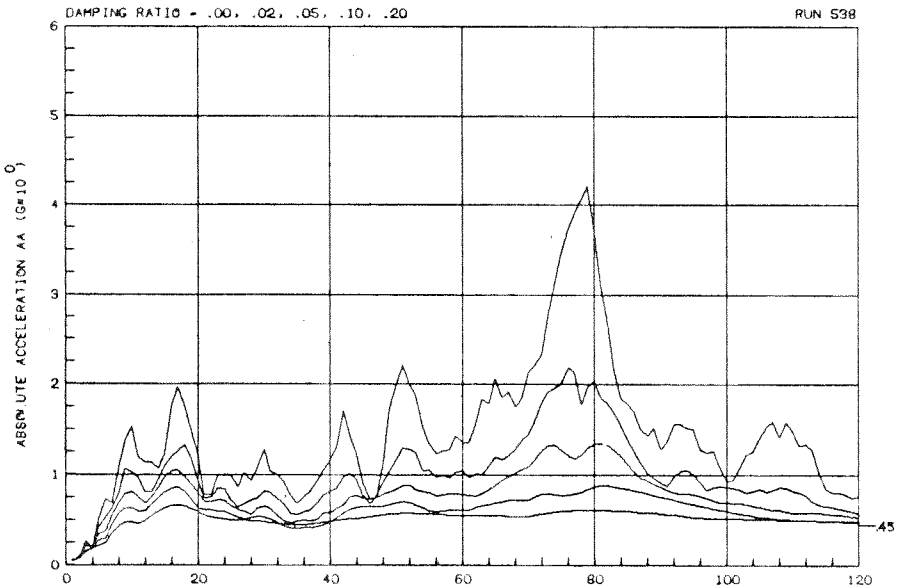

MISSISSIPPI 7245 - RADIAL

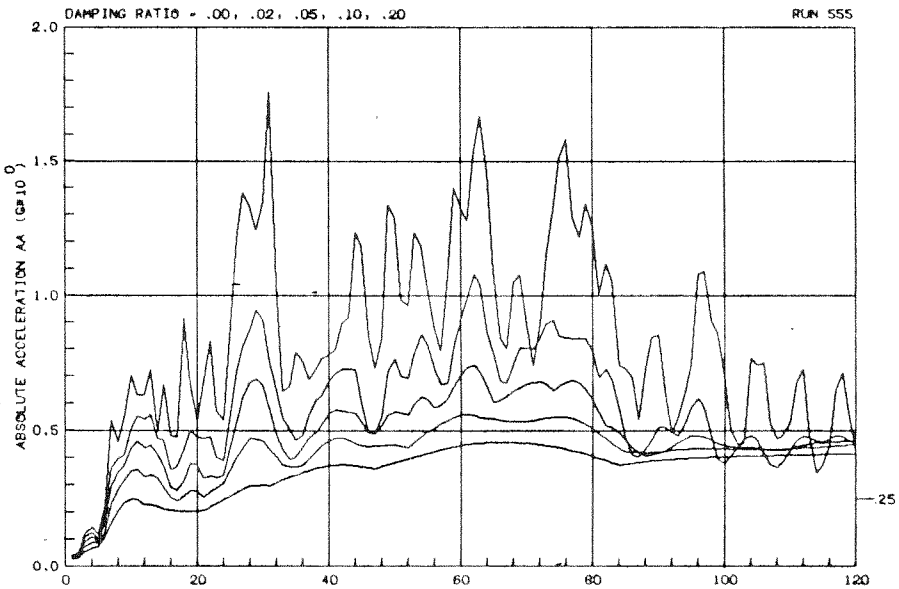

MISSISSIPPI 4074 - TRANSVERSE

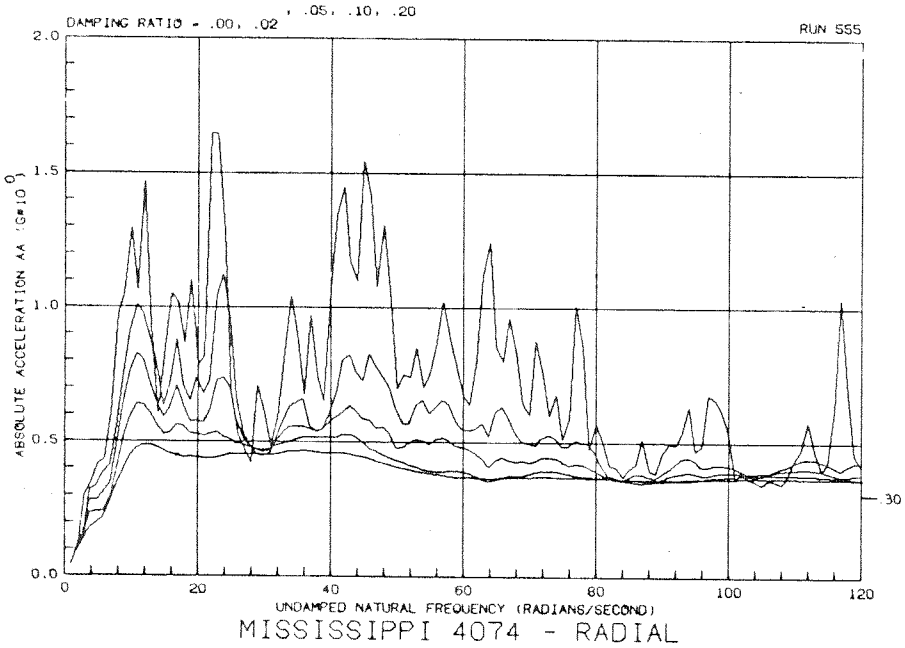

MISSISSIPPI 4074 - RADIAL

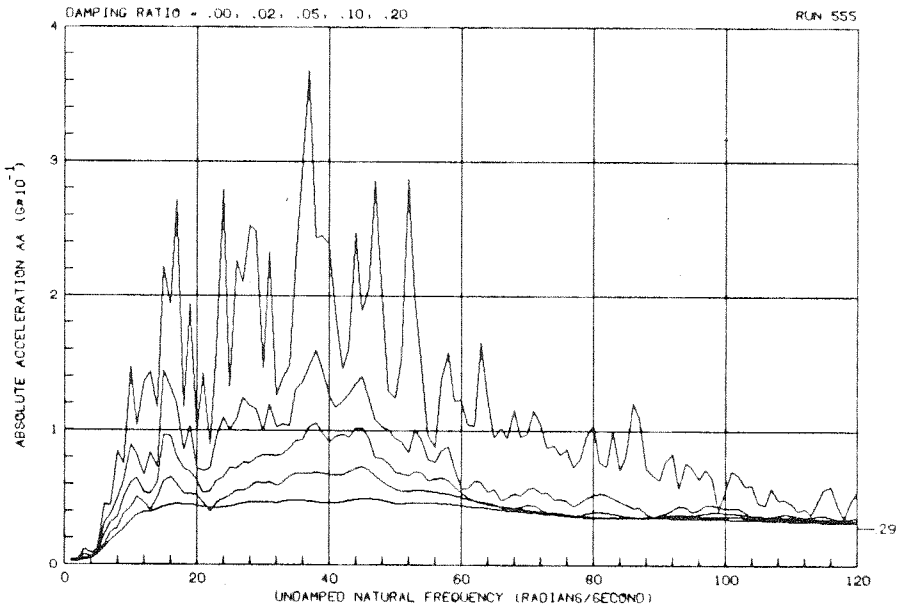

HARDHAT 4496 - TRANSVERSE

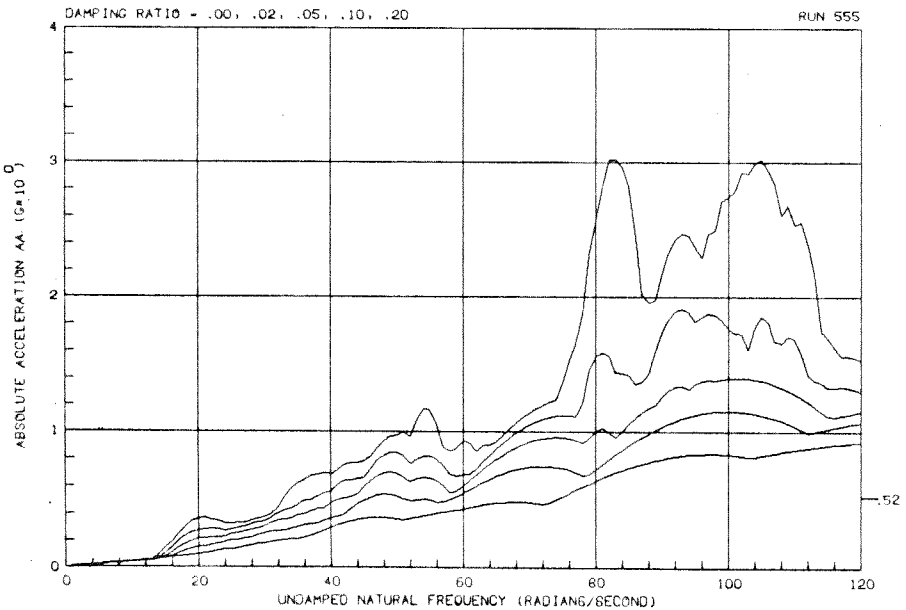

HARDHAT 1091 - TRANSVERSE

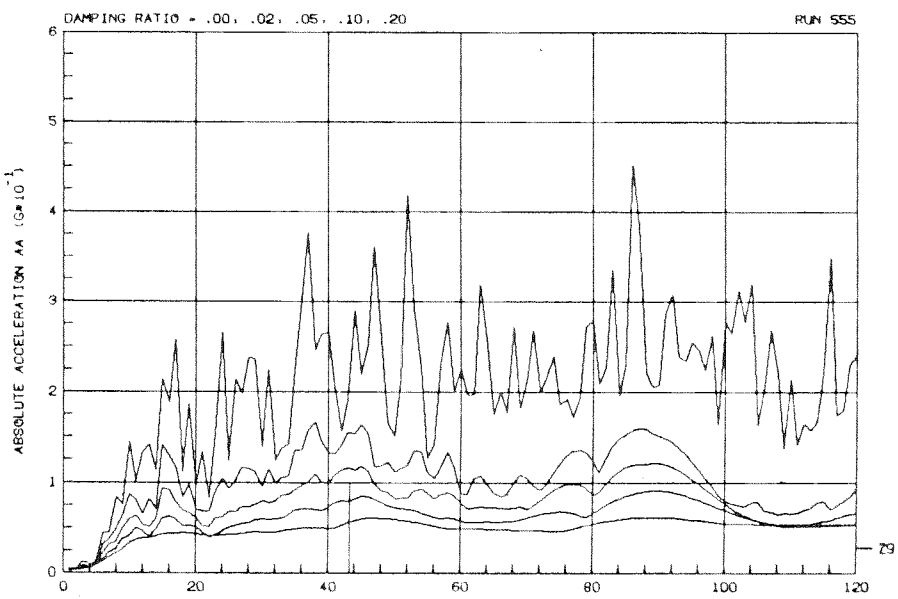

HARDHAT 4496 - TRANSVERSE

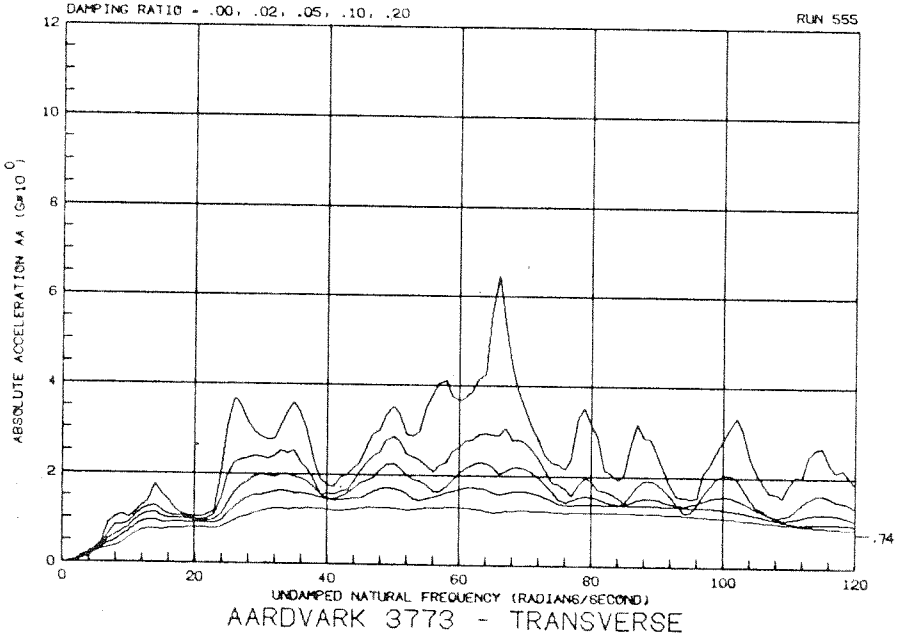

AARDVARK 3773 - TRANSVERSE

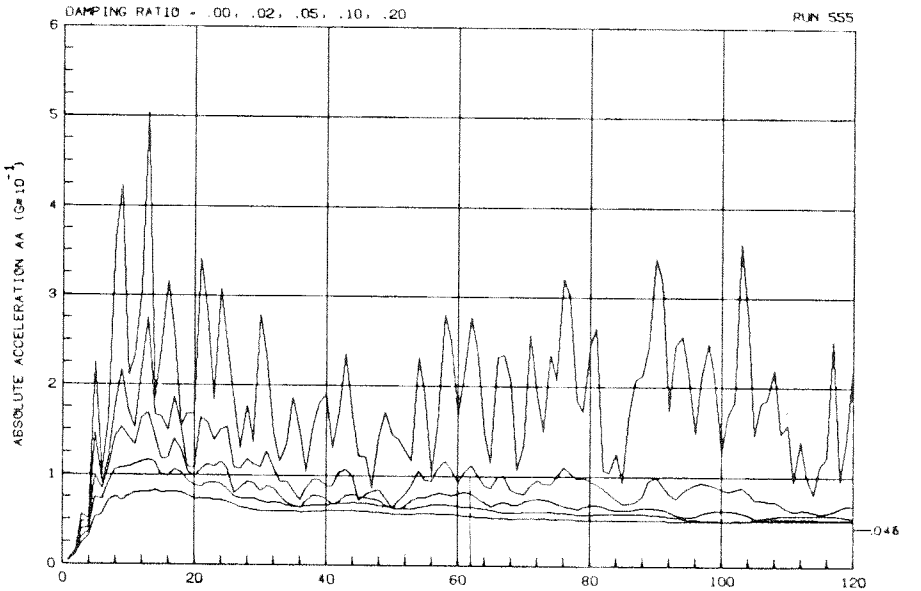

AARDVARK 1437 - TRANSVERSE

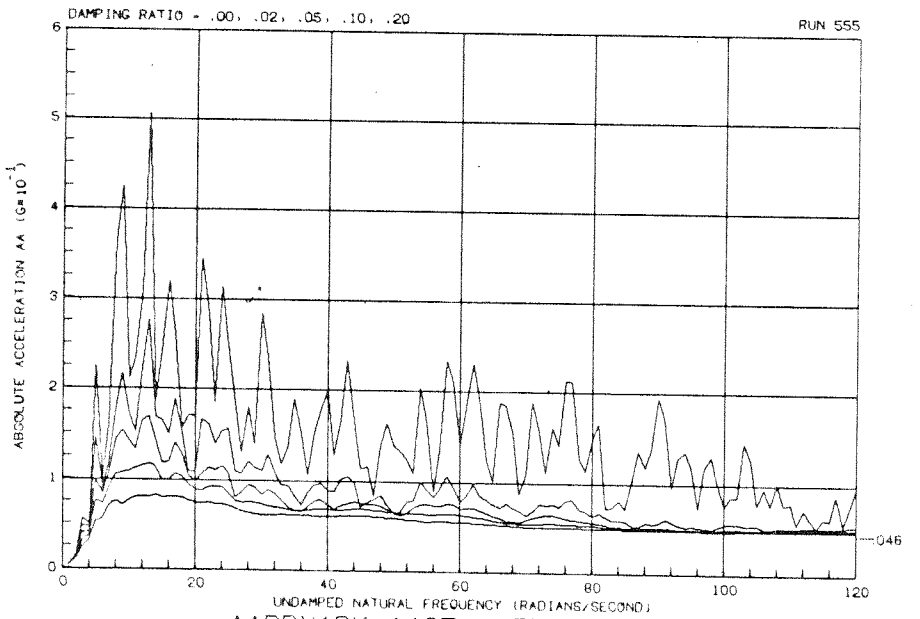

AARDVARK 1437 - TRANSVERSE

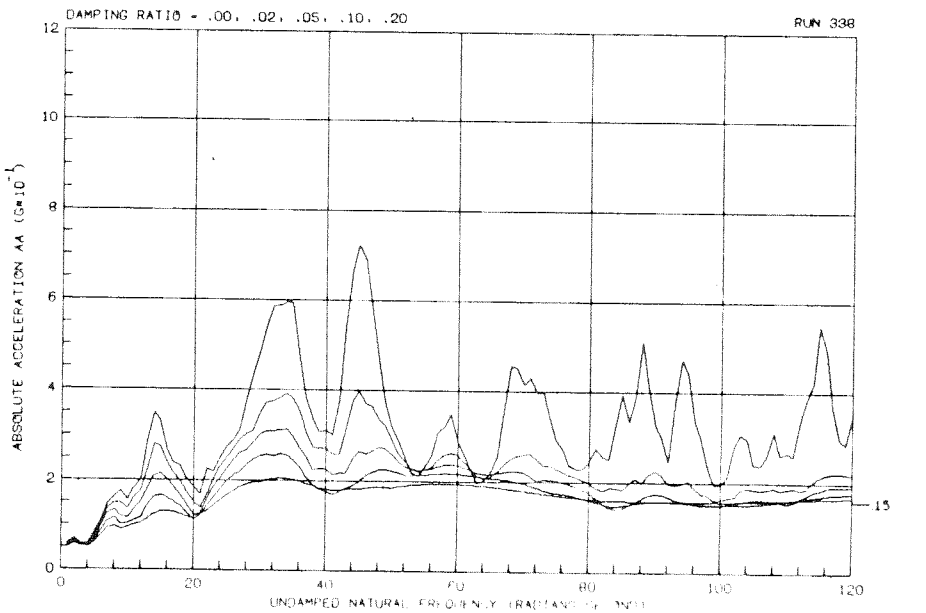

SEDAN RUN 3 - RADIAL

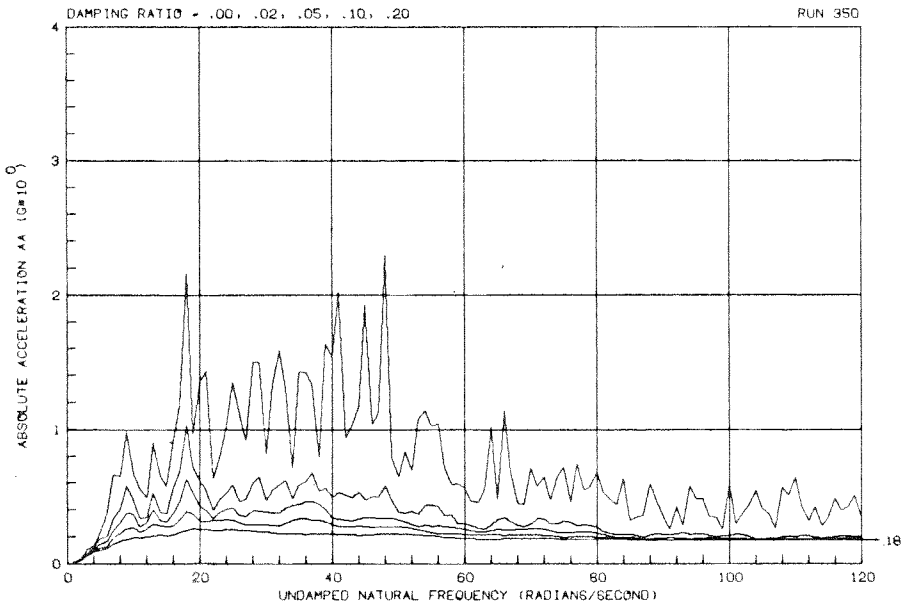

TAFT EARTHQUAKE 21 JULY 1952 - N21E

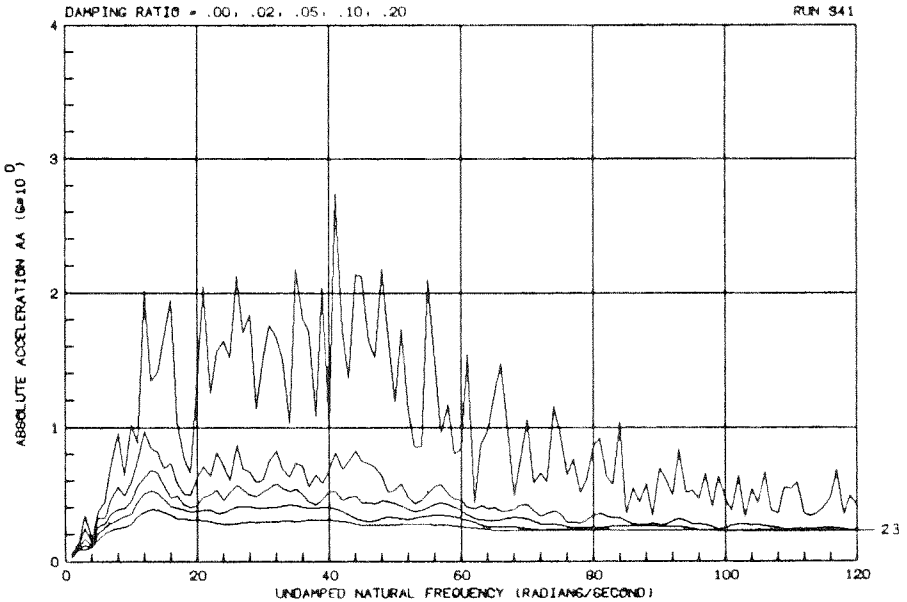

EL CENTRO EARTHQUAKE 18 MAY 1940 - EW

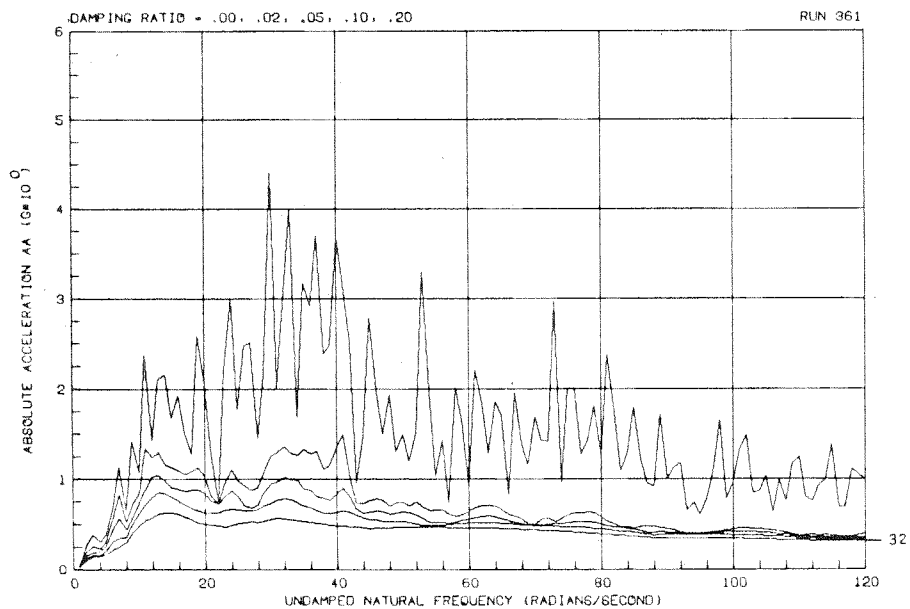

EL CENTRO EARTHQUAKE 18 MAY 1940 - NS

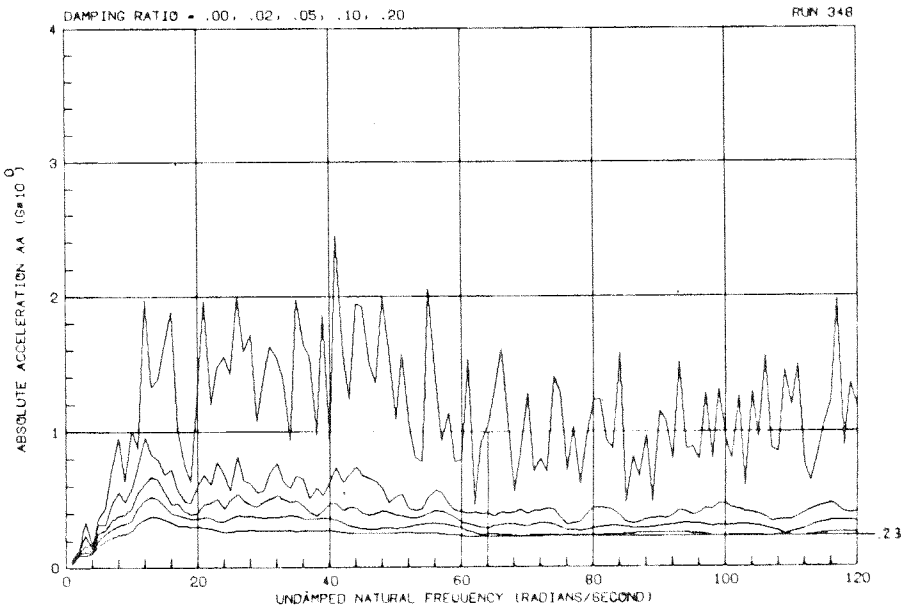

EL CENTRO EARTHQUAKE 18 MAY 1940 - EW

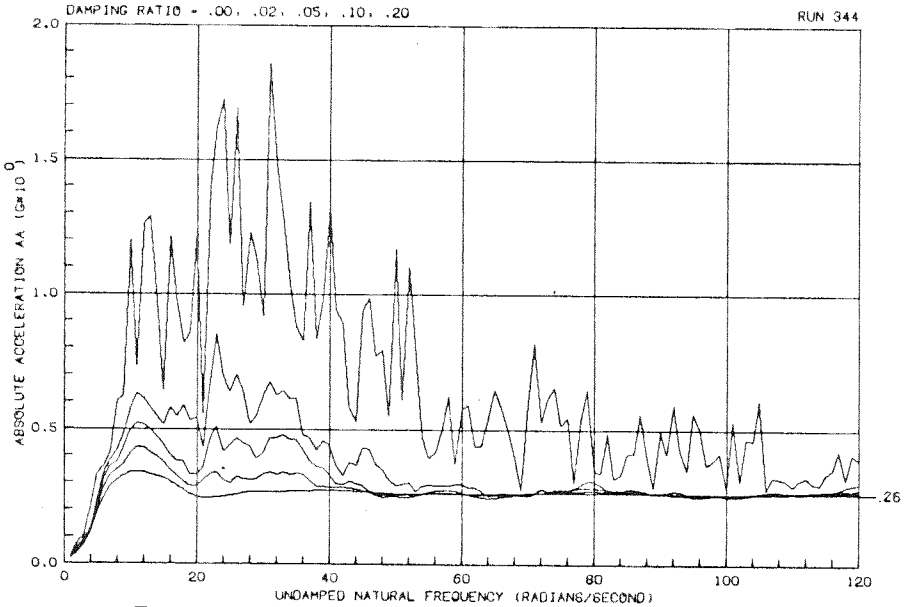

EL CENTRO EARTHQUAKE 30 DEC 1934 - NS

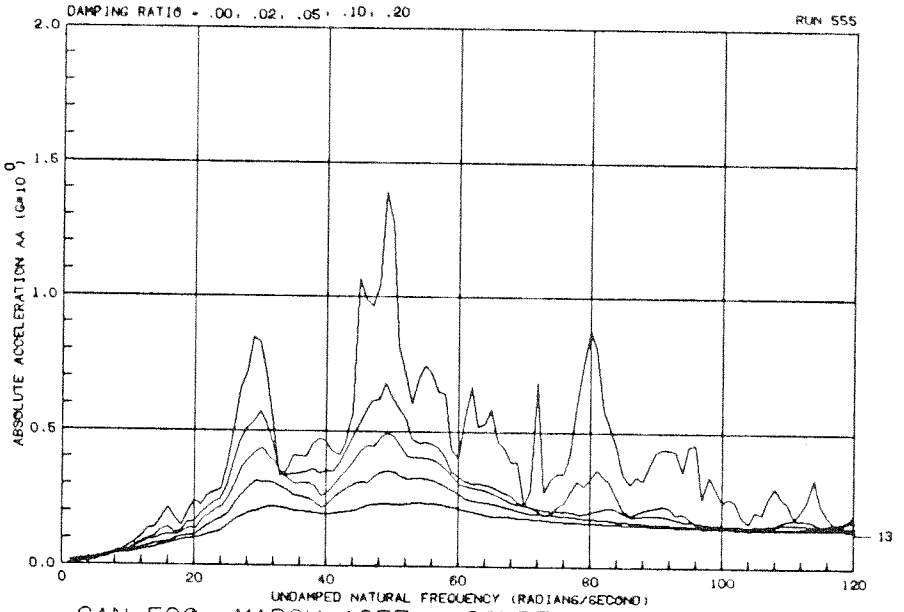

SAN FCO. MARCH 1957 - GOLDEN GATE PARK S80E

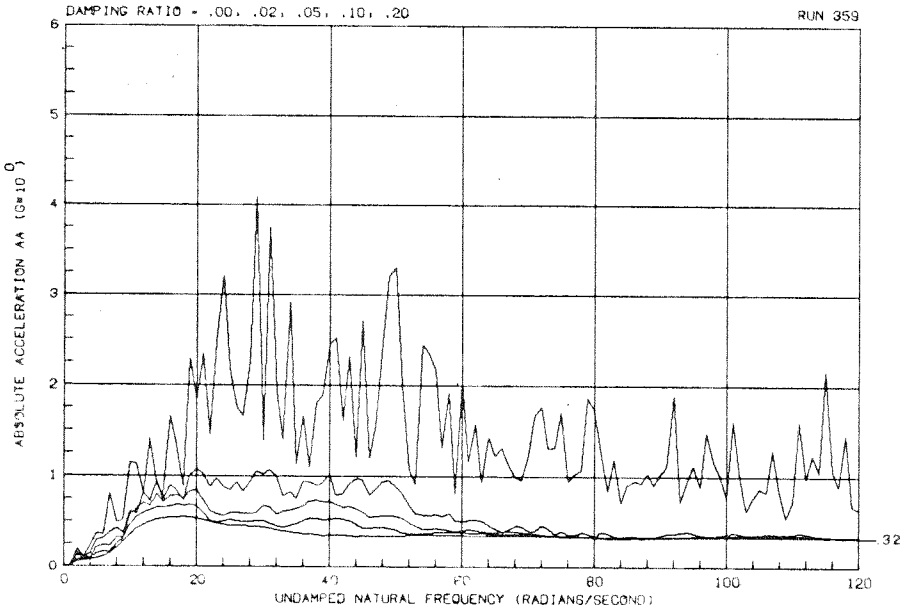

OLYMPIA EARTHQUAKE 13 APRIL 1949 - N80E

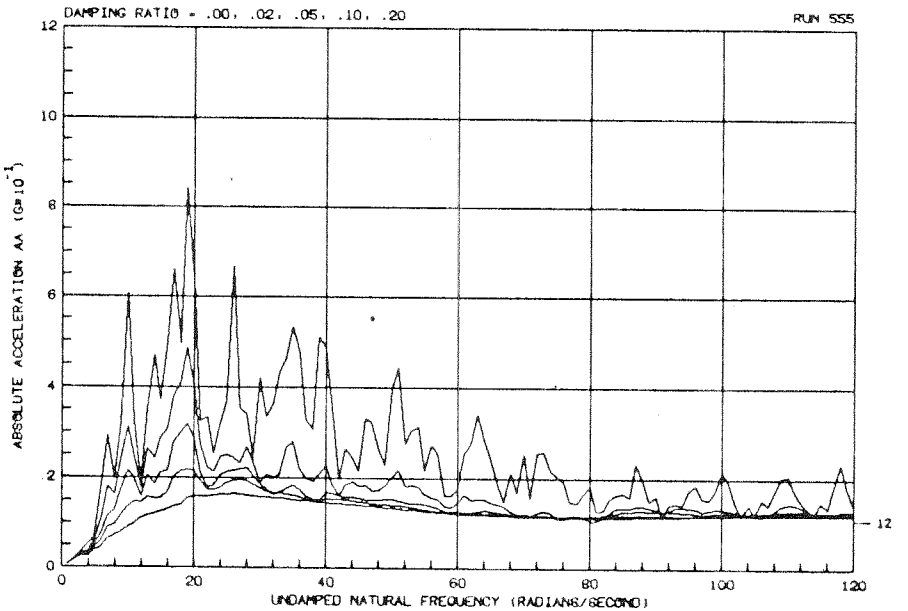

FERNDALE, 3 OCTOBER 1941 - S45E

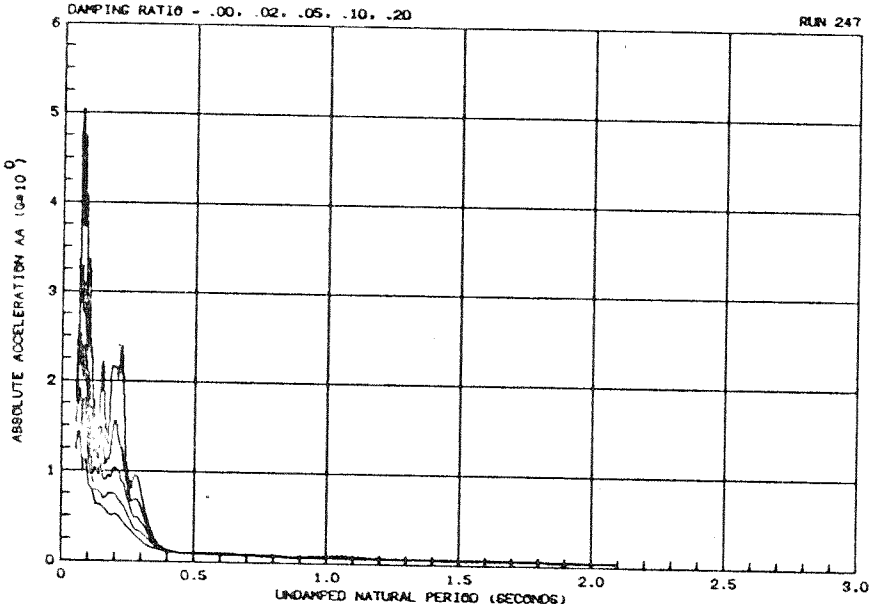

GNOME 10 DEC 1961 - S2 TRANSVERSE

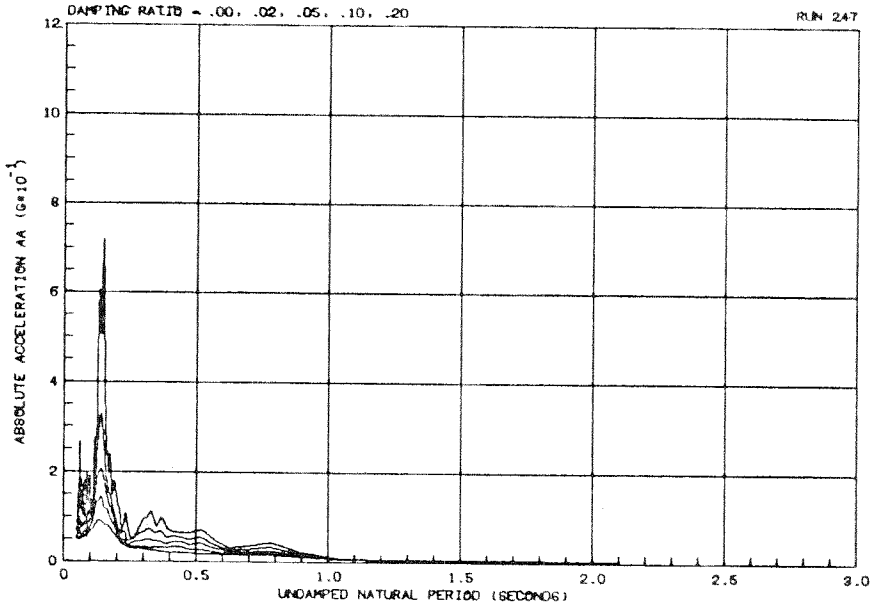

GNOME 10 DEC 1961 - S4 RADIAL

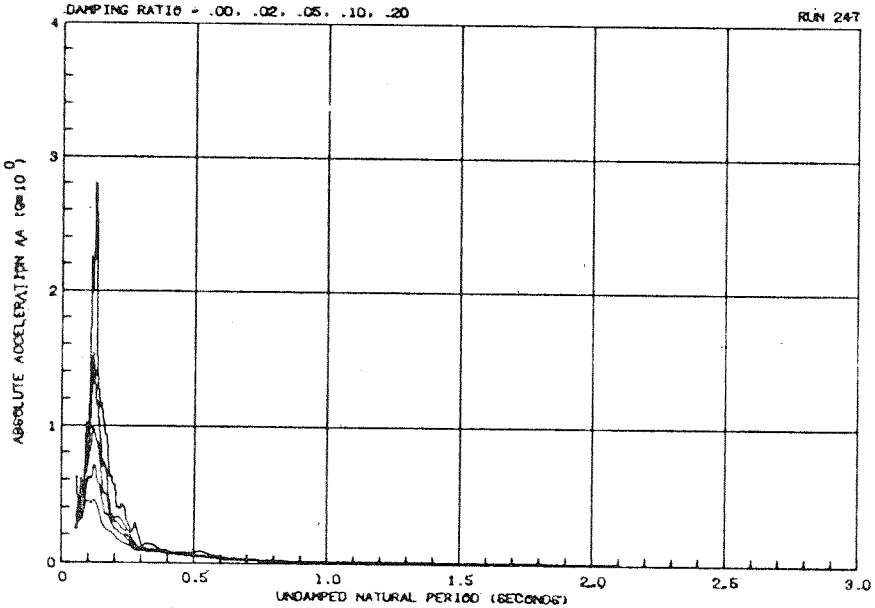

GNOME 10 DEC 1961 - S3 TRANSVERSE

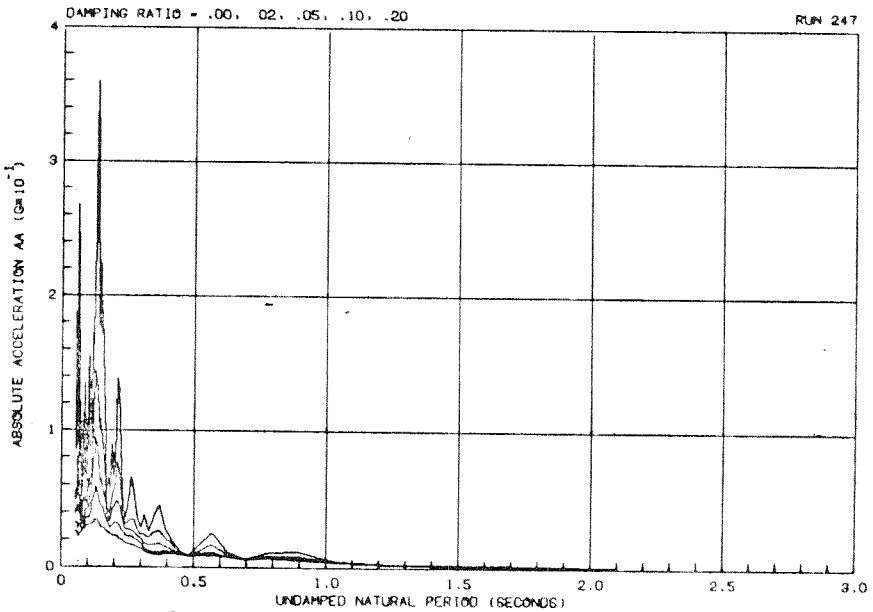

GNOME 10 DEC 1961 - S4 TRANSVERSE

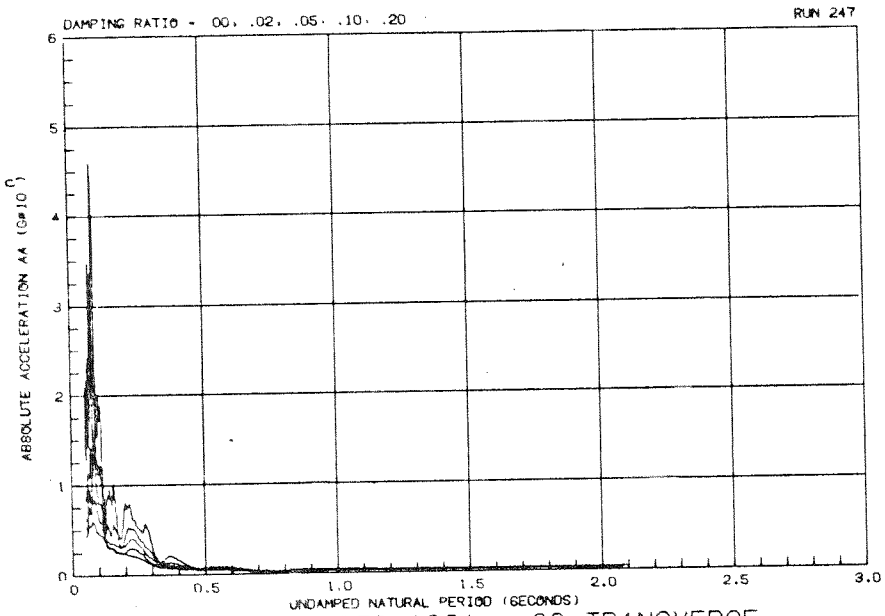

GNOME 10 DEC 1961 - S6 TRANSVERSE

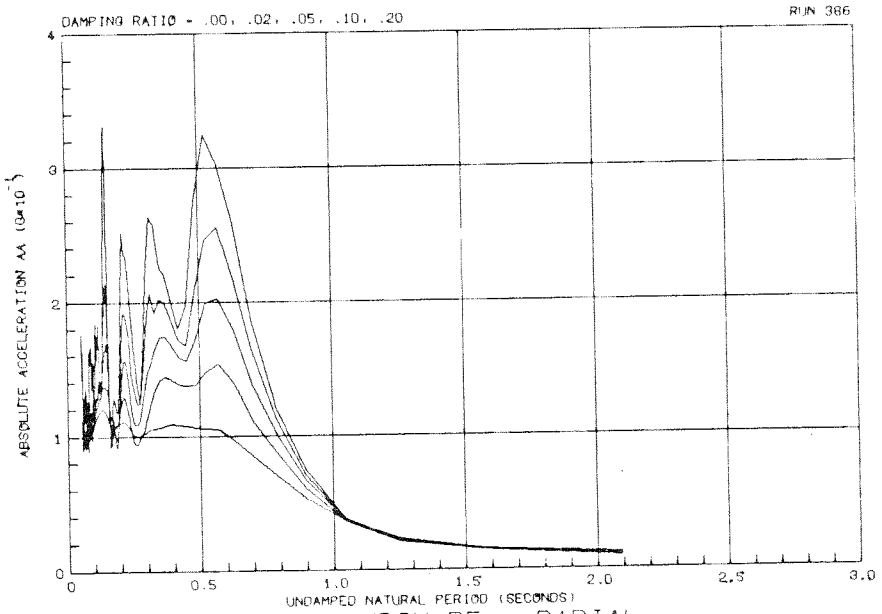

DANNYBØY D5 - RADIAL

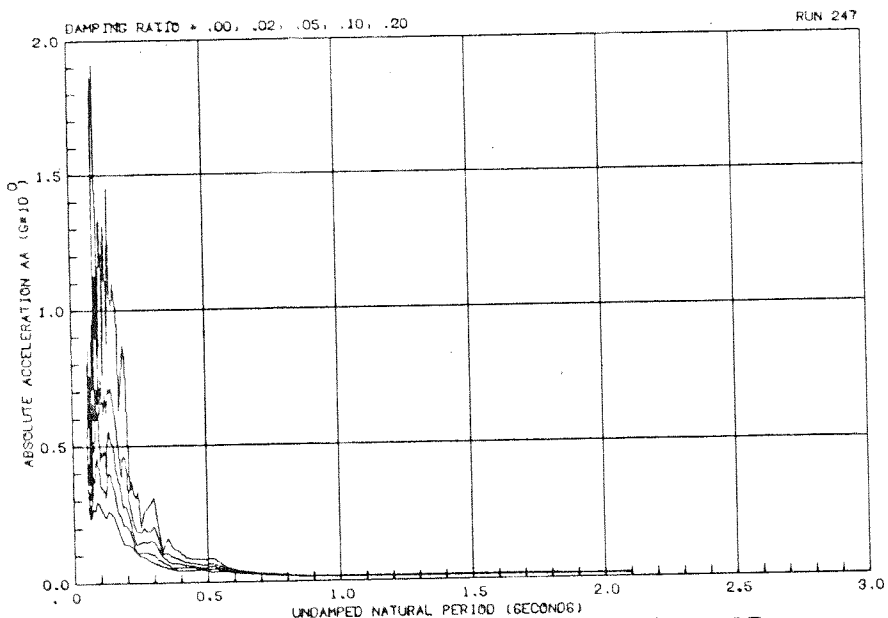

GNOME 10 DEC 1961 - S7 TRANSVERSE

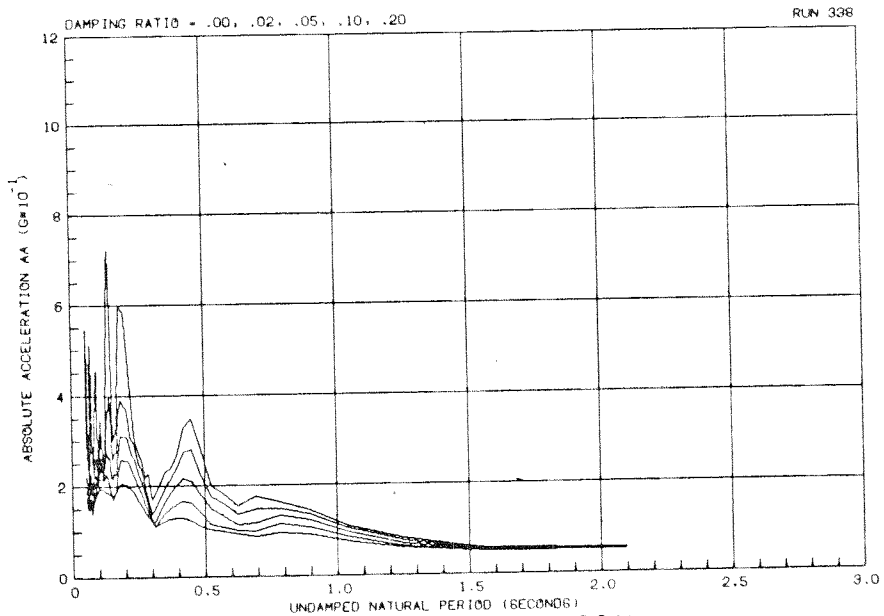

SEDAN RUN 3 - RADIAL

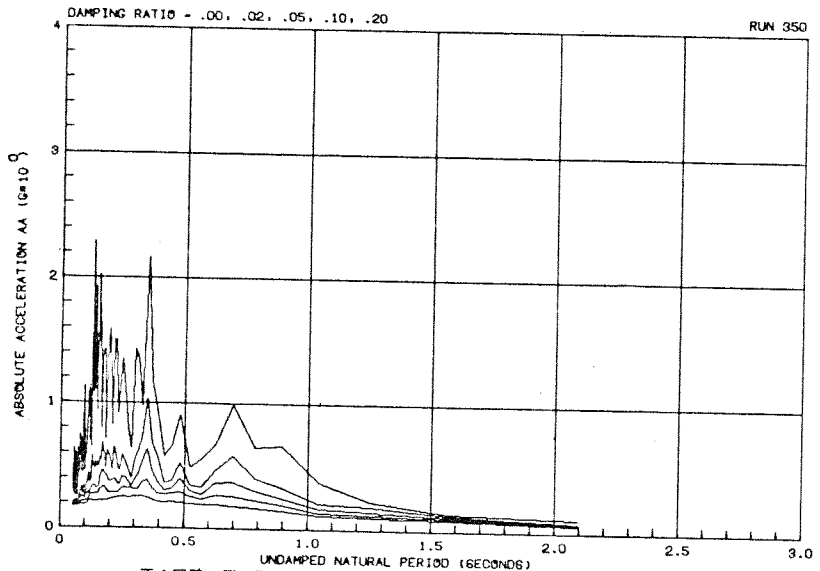

TAFT EARTHQUAKE 21 JULY 1952 - N21E

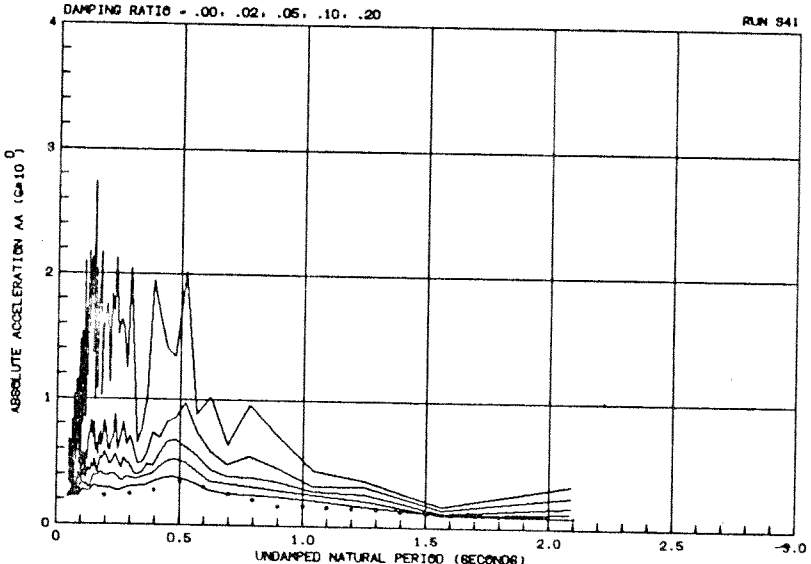

EL CENTRO EARTHQUAKE 18 MAY 1940 - EW

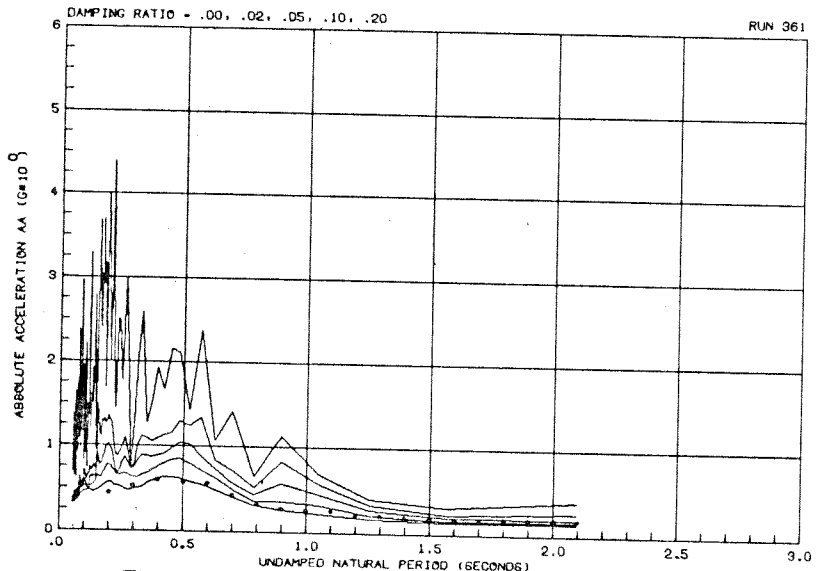

EL CENTRO EARTHQUAKE 18 MAY 1940 - NS

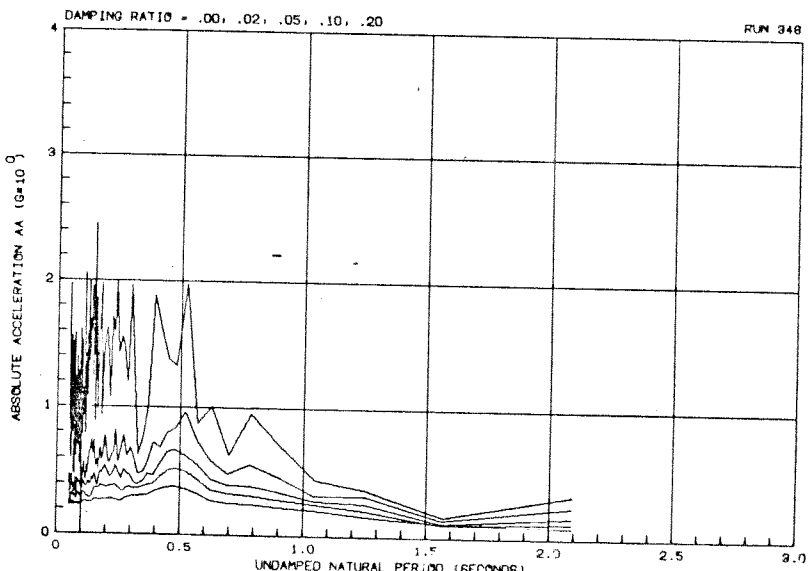

EL CENTRO EARTHQUAKE 18 MAY 1940 - EW

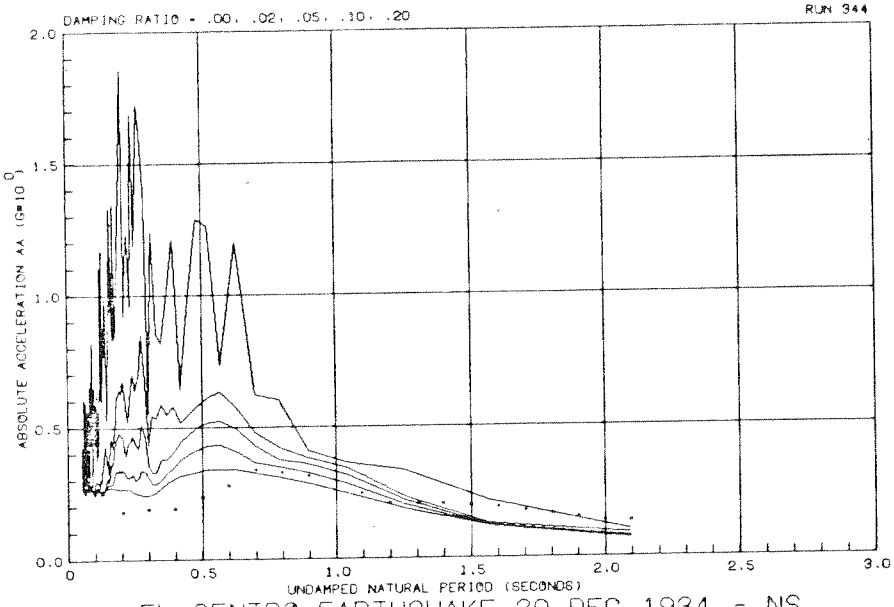

EL CENTRO EARTHQUAKE 30 DEC 1934 - NS

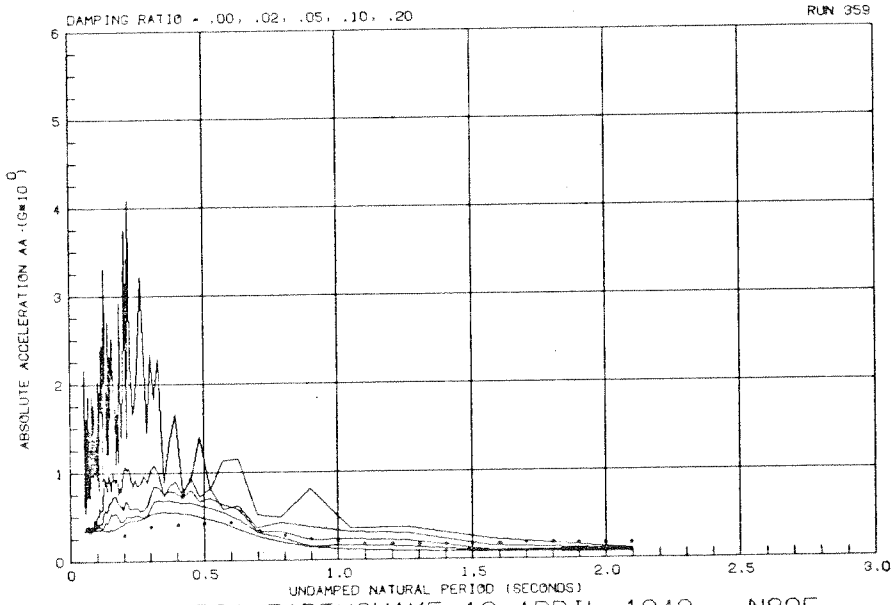

OLYMPIA EARTHQUAKE 13 APRIL 1949 - N80E

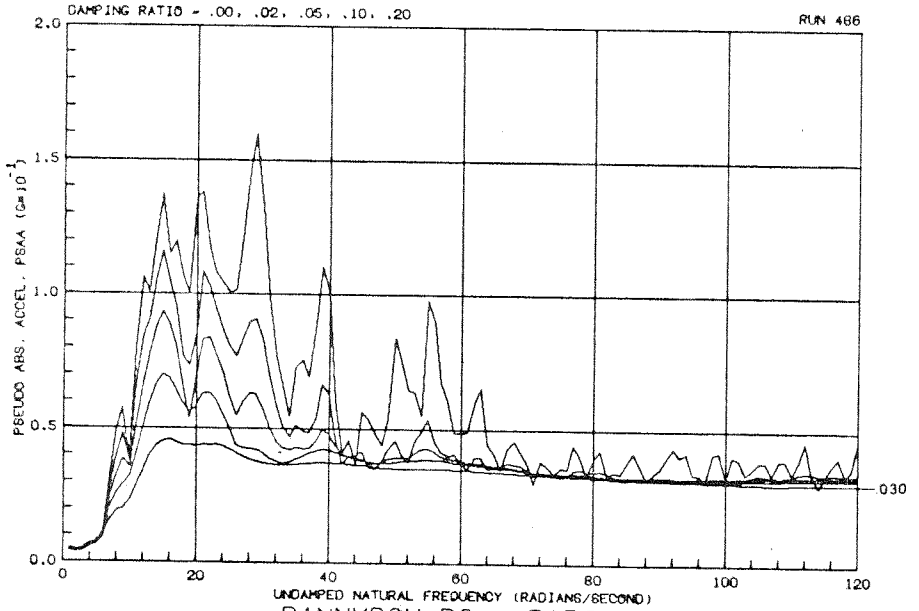

DANNYBOY D8 - RADIAL

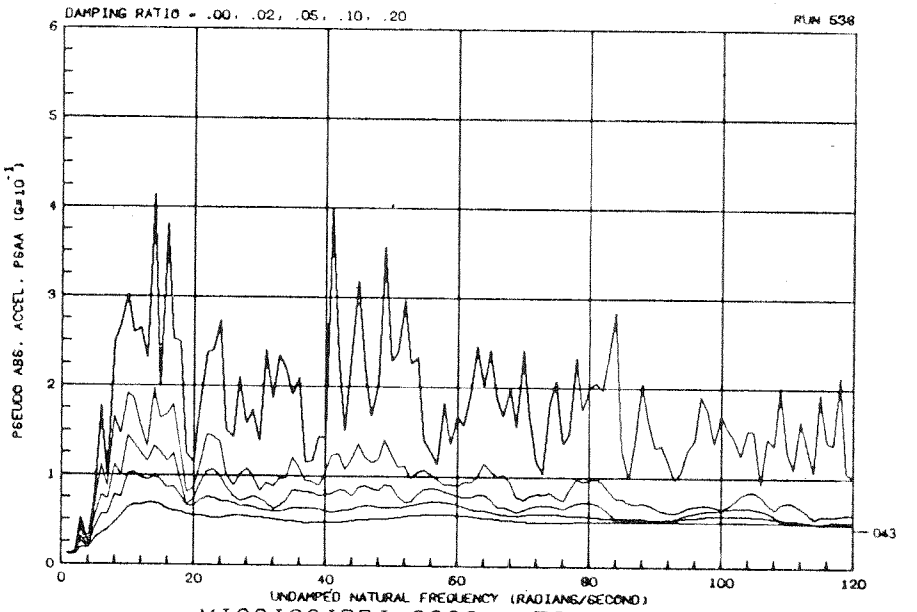

MISSISSIPPI 8228 - TRANSVERSE

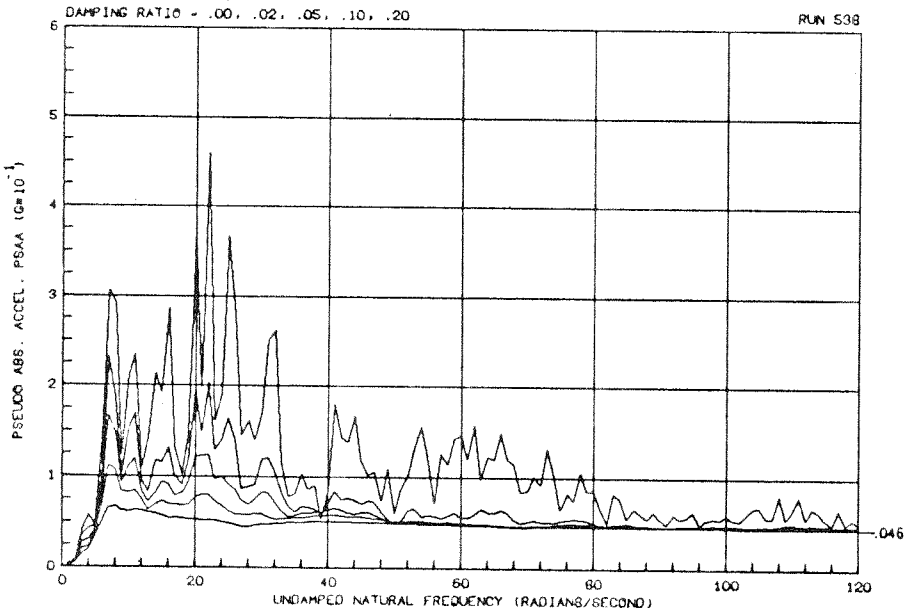

MISSISSIPPI 1777 - TRANSVERSE

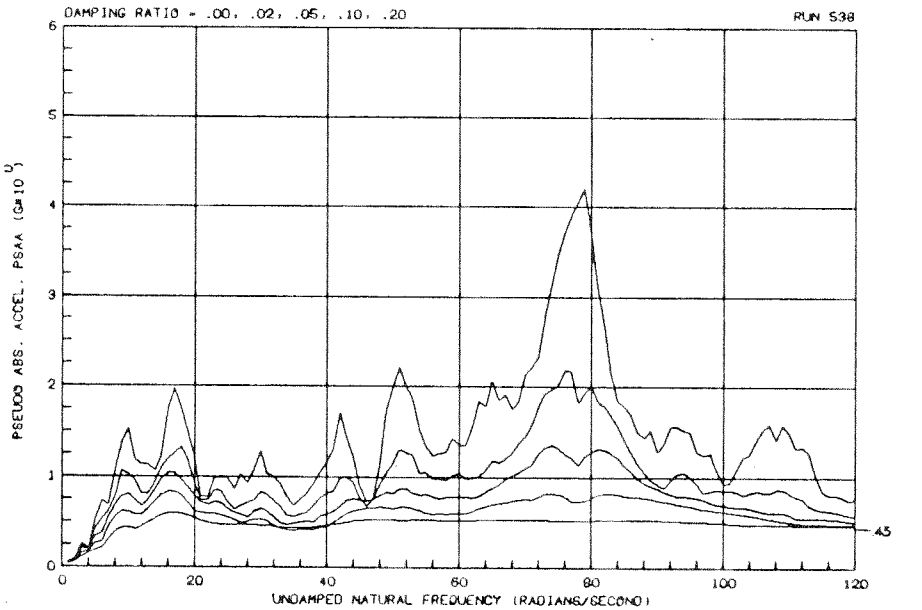

MISSISSIPPI 7245 - RADIAL

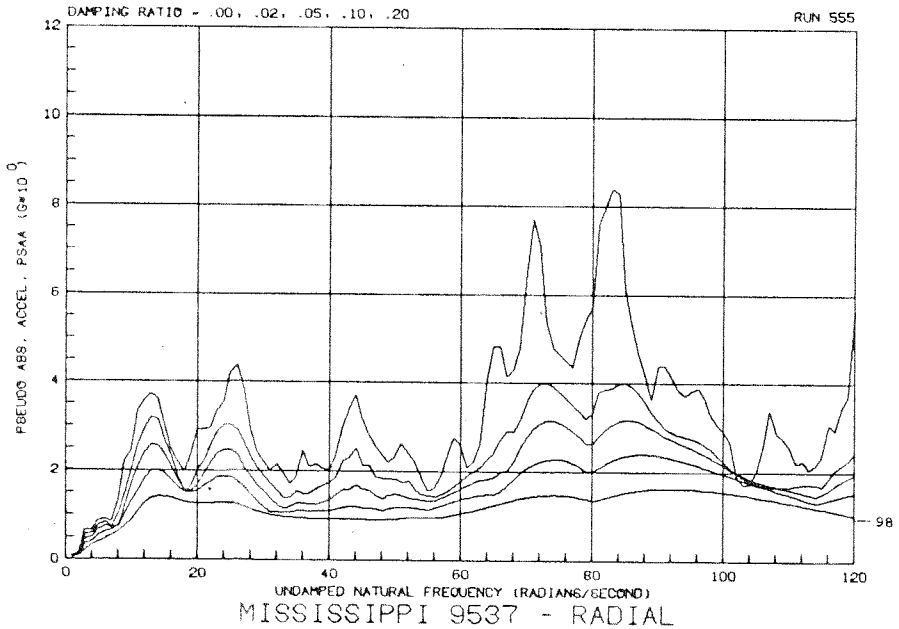

MISSISSIPPI 9537 - RADIAL

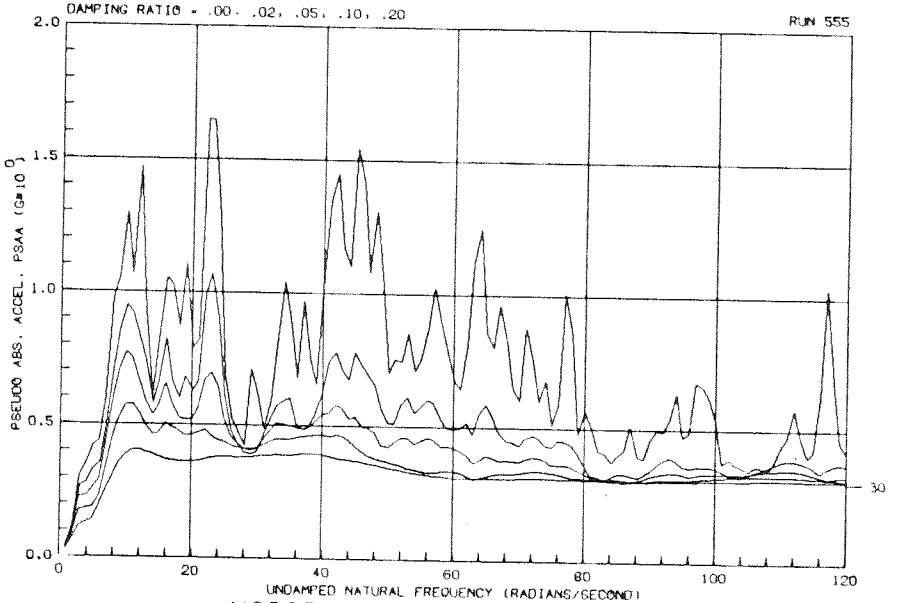

MISSISSIPPI 4074 - RADIAL

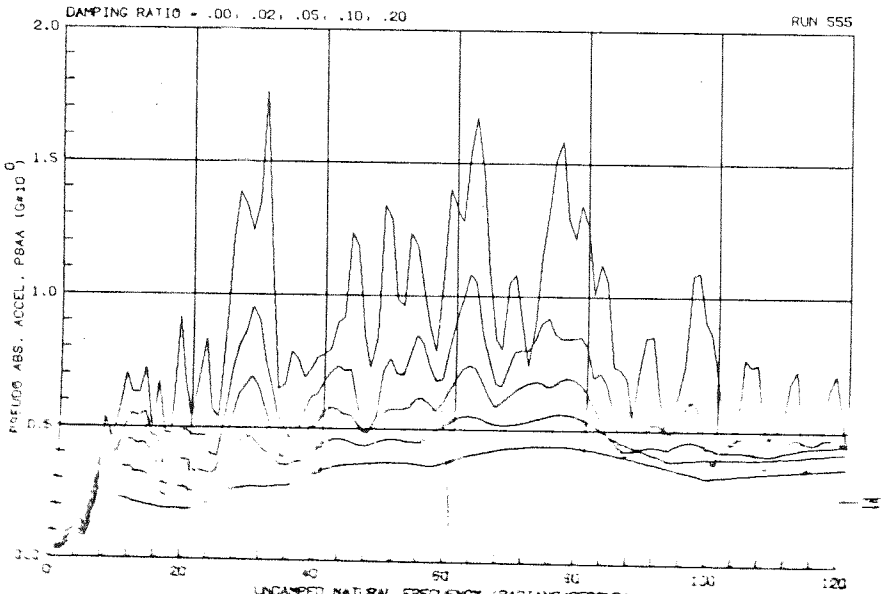

MISSISSIPPI 4074 - TRANSVERSE

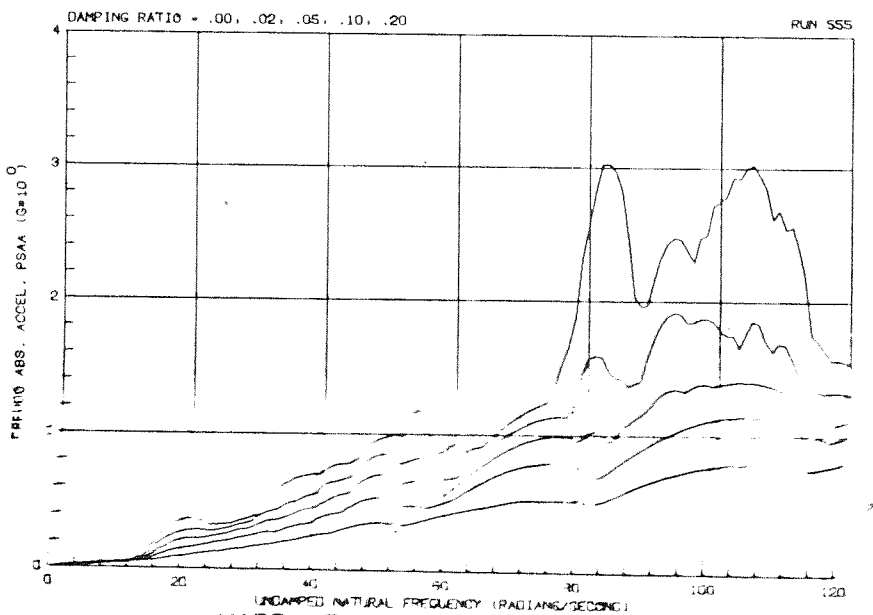

HARDHAT 1091 - TRANSVERSE

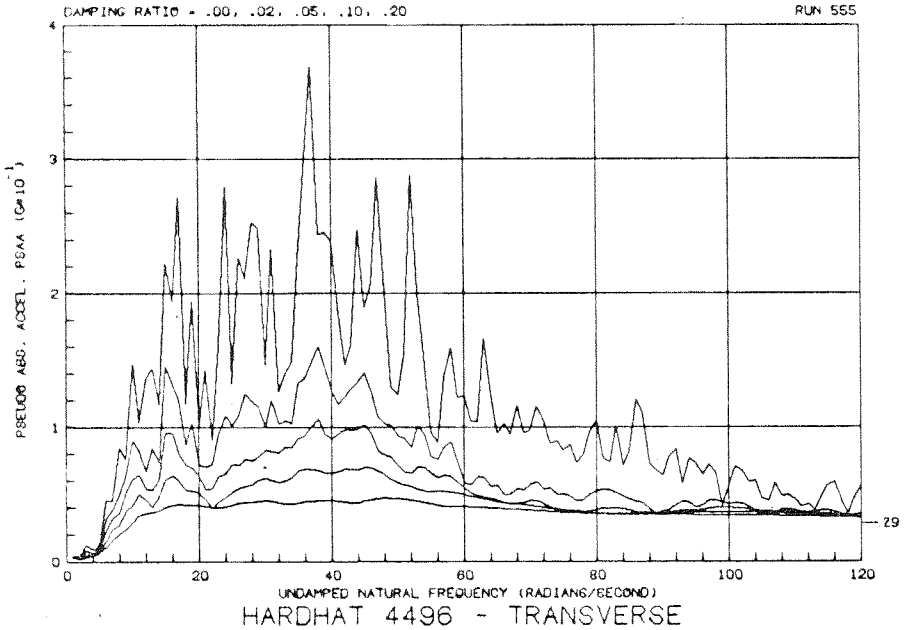

HARDHAT 4496 - TRANSVERSE

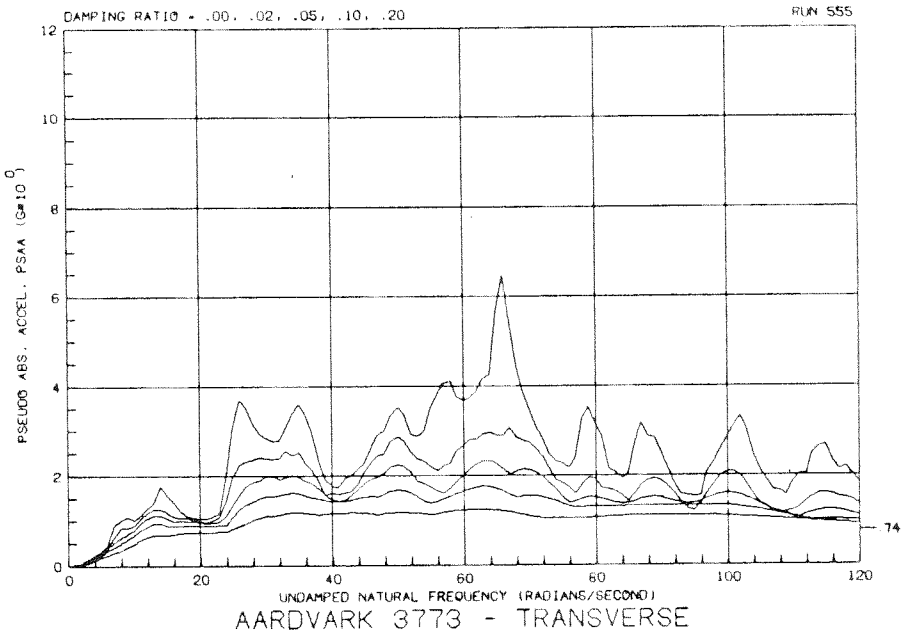

AARDVARK 3773 - TRANSVERSE

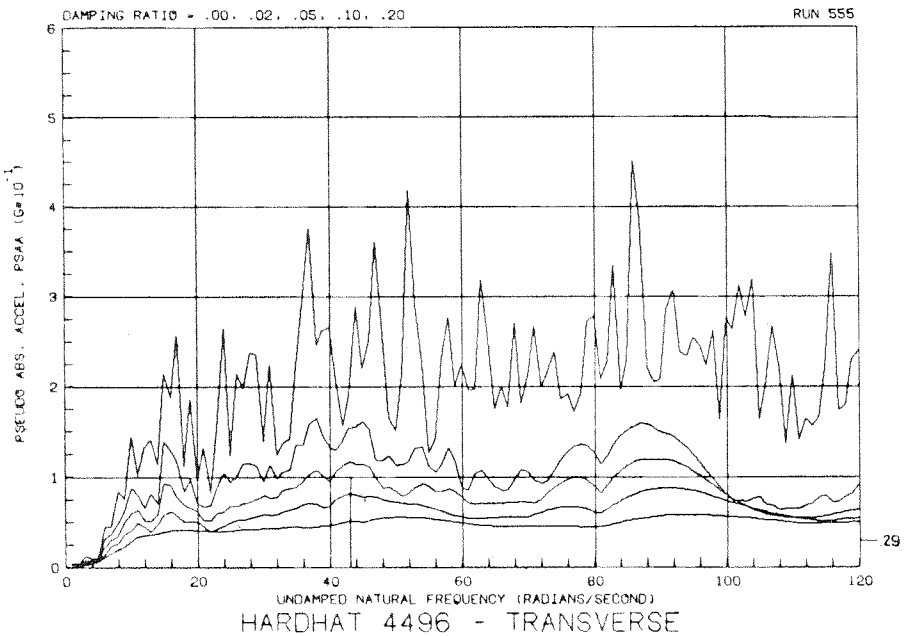

HARDHAT 4496 - TRANSVERSE

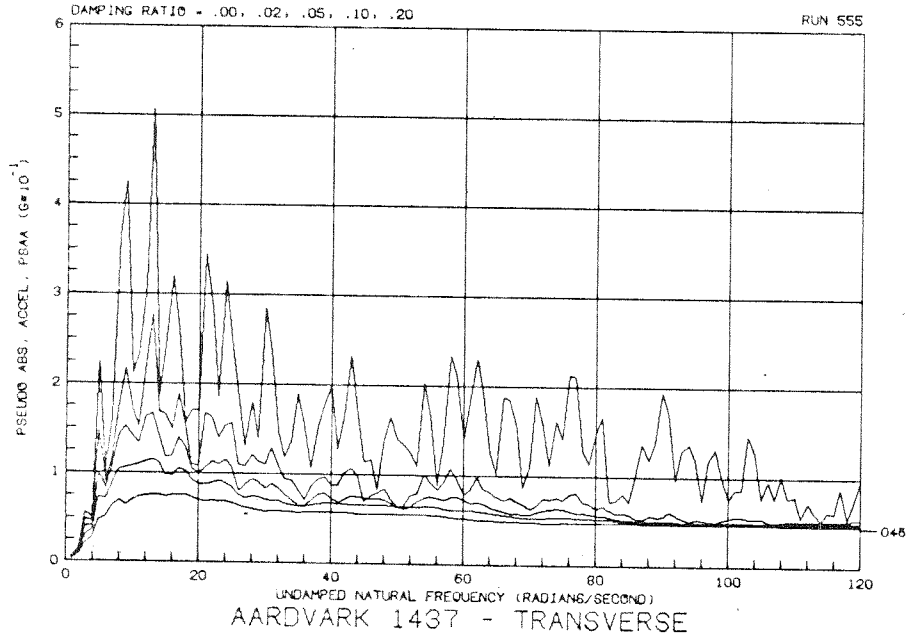

AARDVARK 1437 - TRANSVERSE

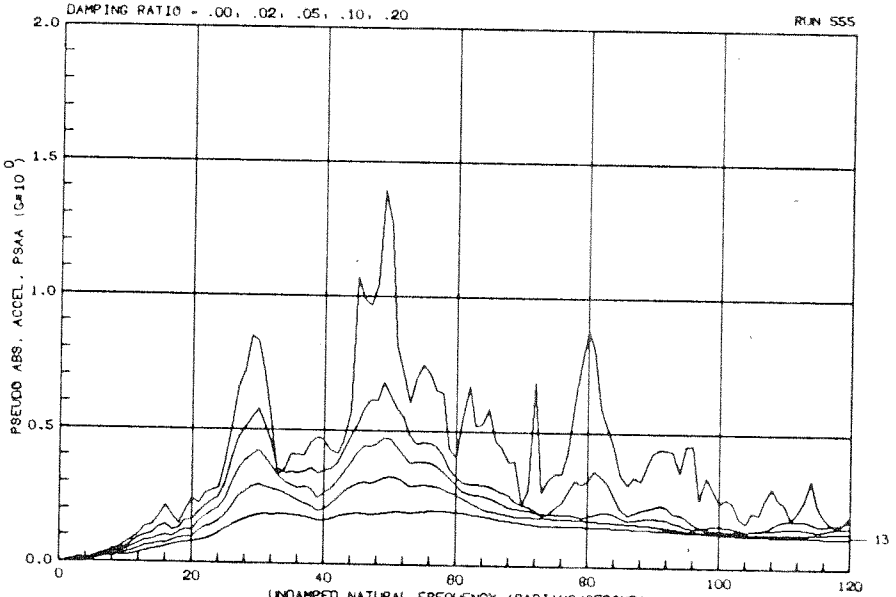

SAN FCO. MARCH 1957 - GOLDEN GATE PARK S80E

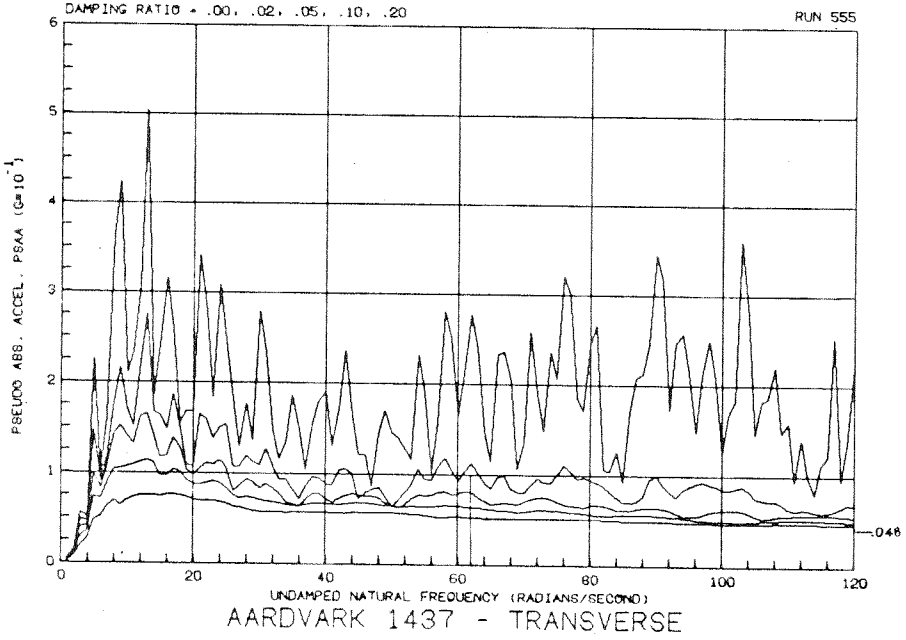

AARDVARK 1437 - TRANSVERSE

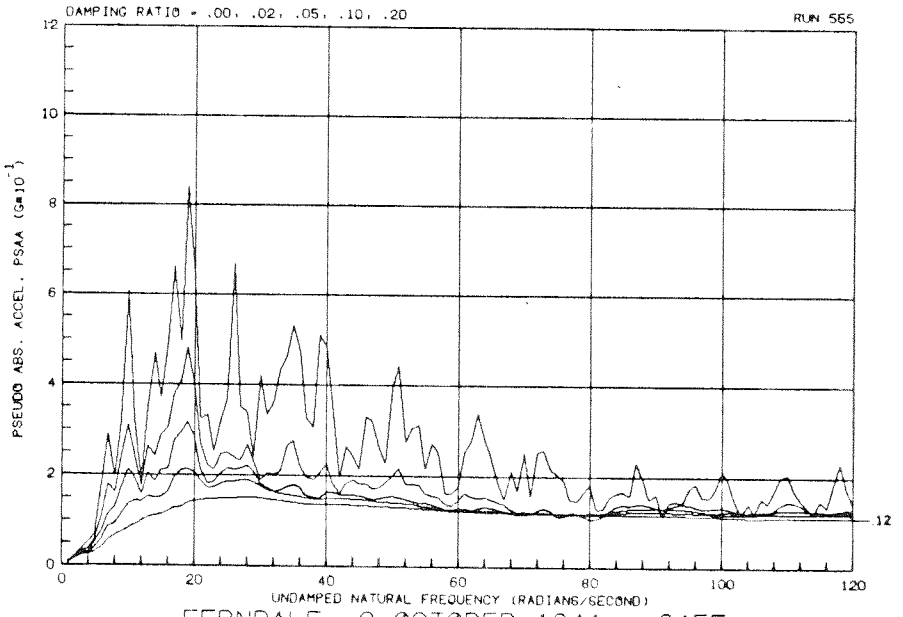

FERNDALE, 3 OCTOBER 1941 - S45E

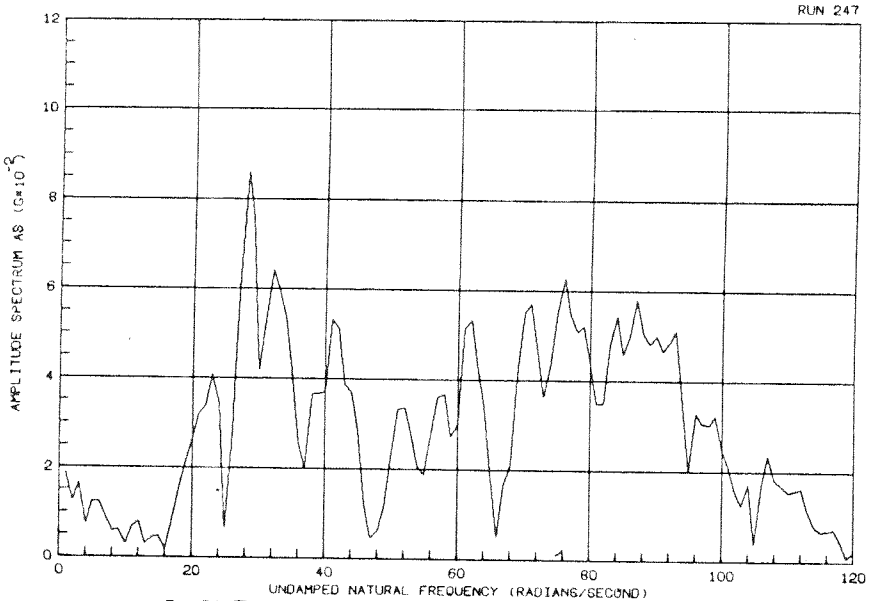

GNOME 10 DEC 1961 - S2. TRANSVERSE

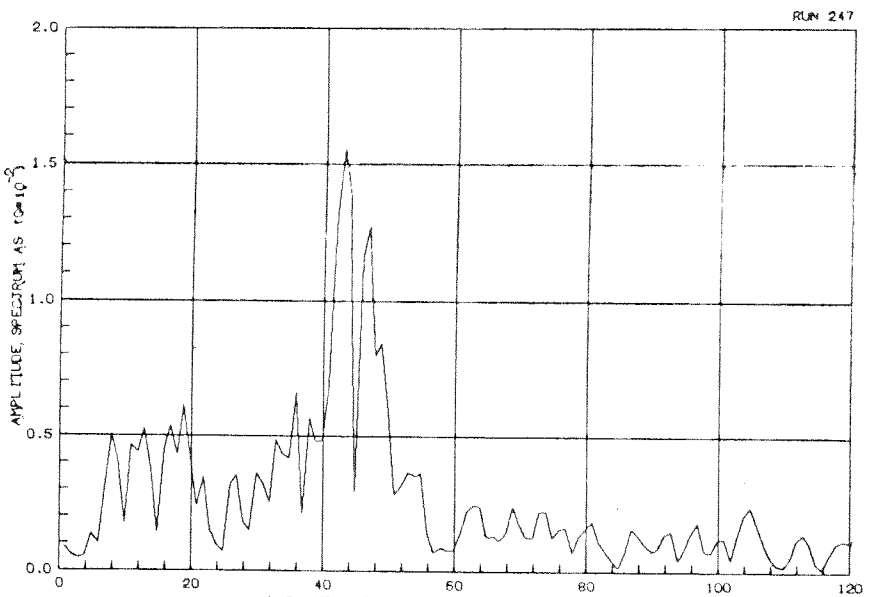

GNOME 10 DEC 1961 - S4 RADIAL

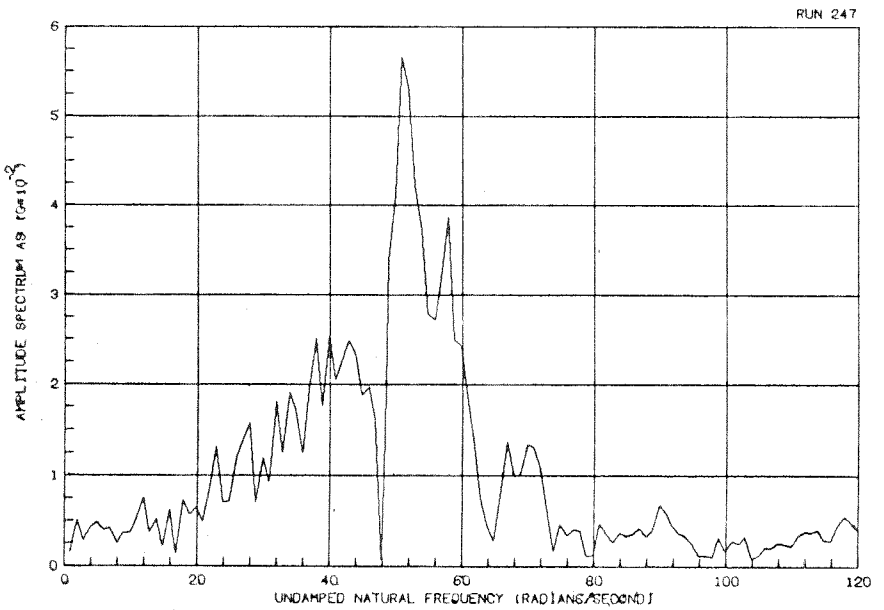

GNOME 10 DEC 1961 - S3 TRANSVERSE

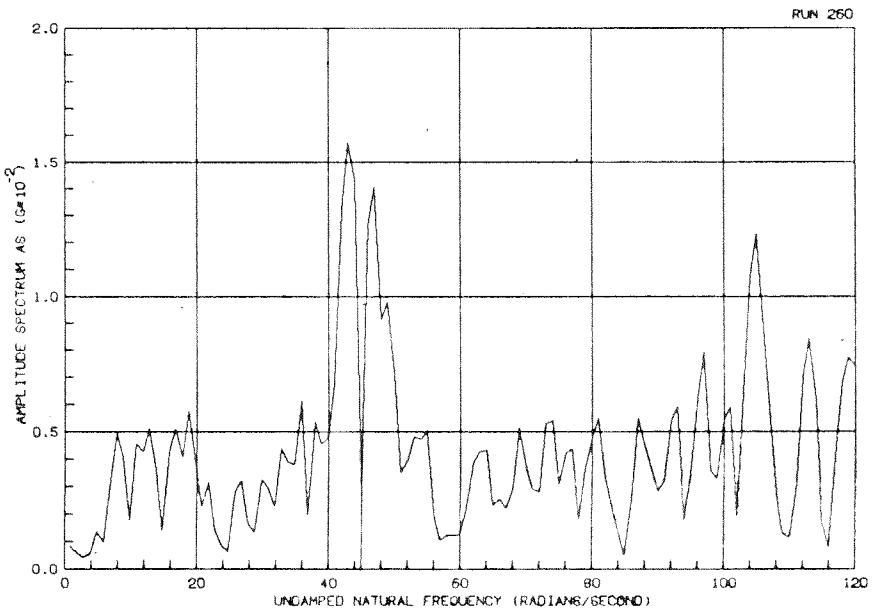

GNOME 10 DEC 1961 - S4 RADIAL

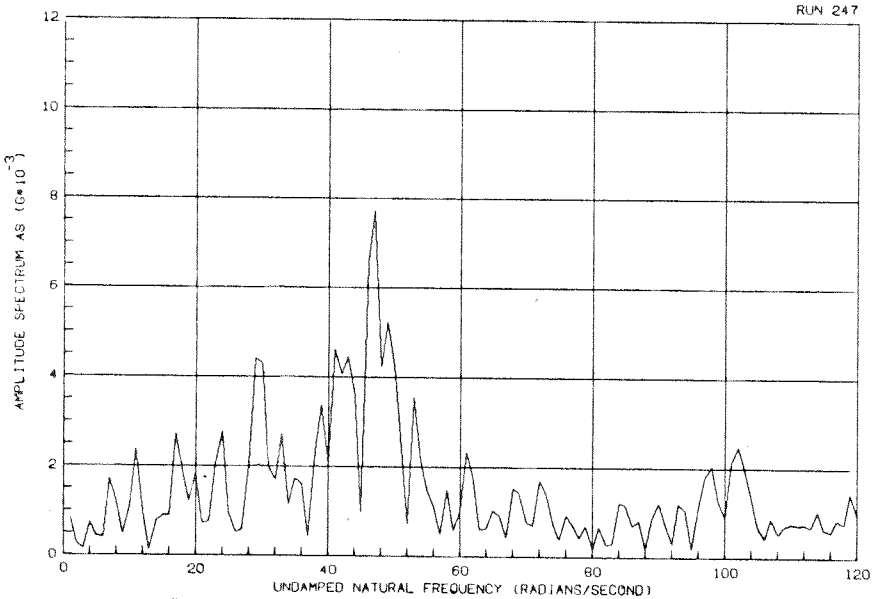

GNOME 10 DEC 1961 - S4 TRANSVERSE

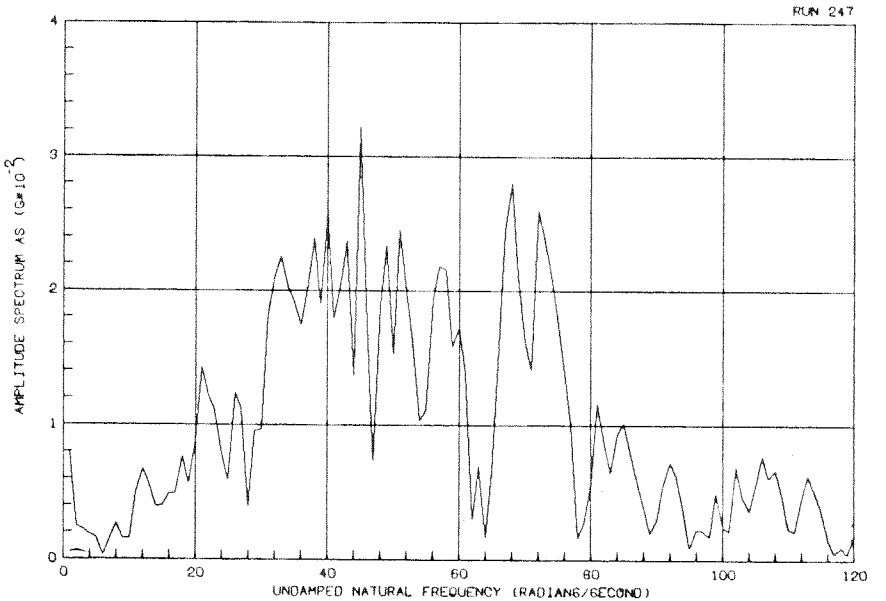

GNOME 10 DEC 1961 - S7 TRANSVERSE

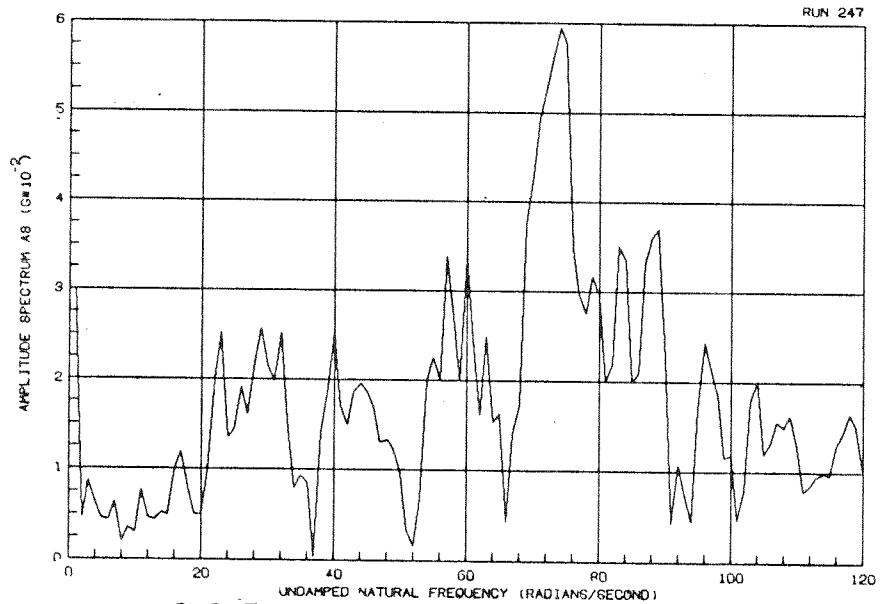

GNOME 10 DEC 1961 - S6 TRANSVERSE

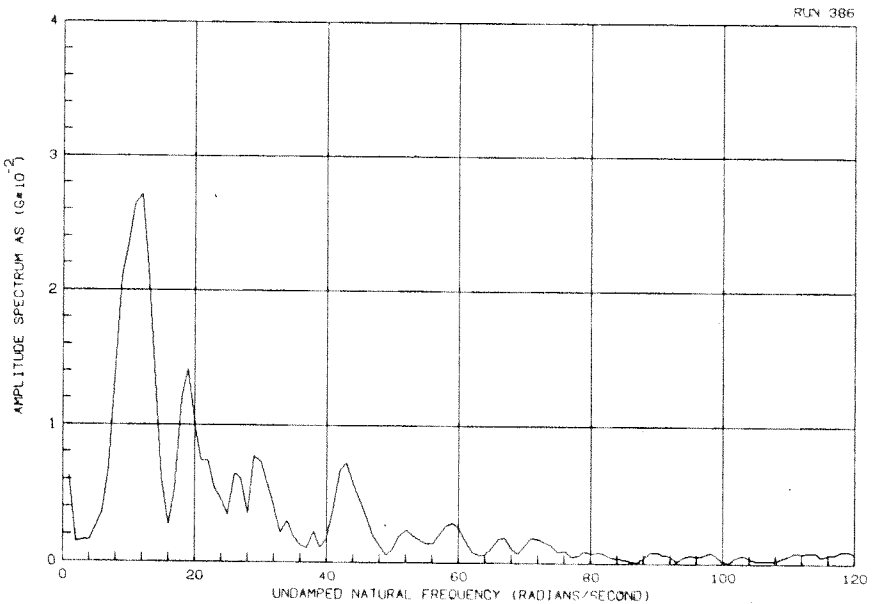

DANNYBOY D5 - RADIAL

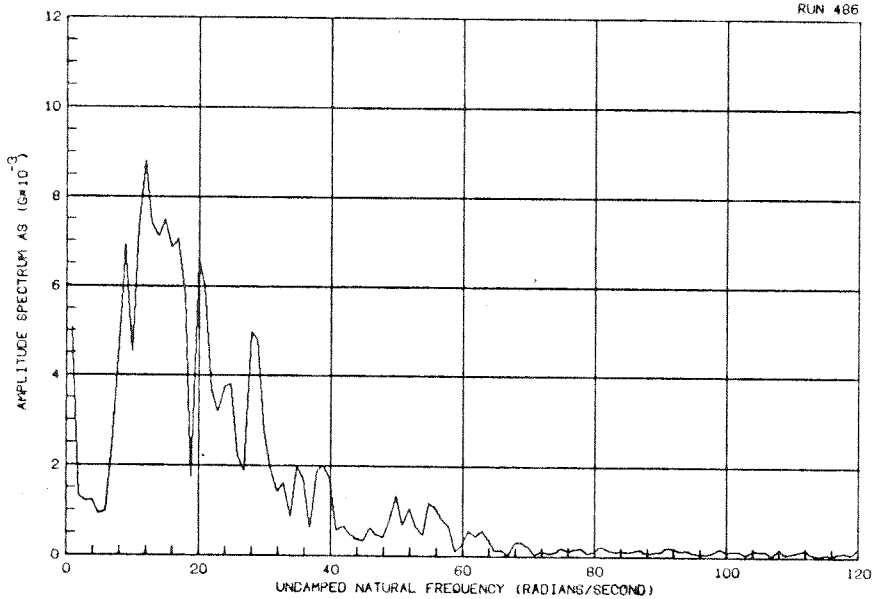

DANNYBØY D8 - RADIAL

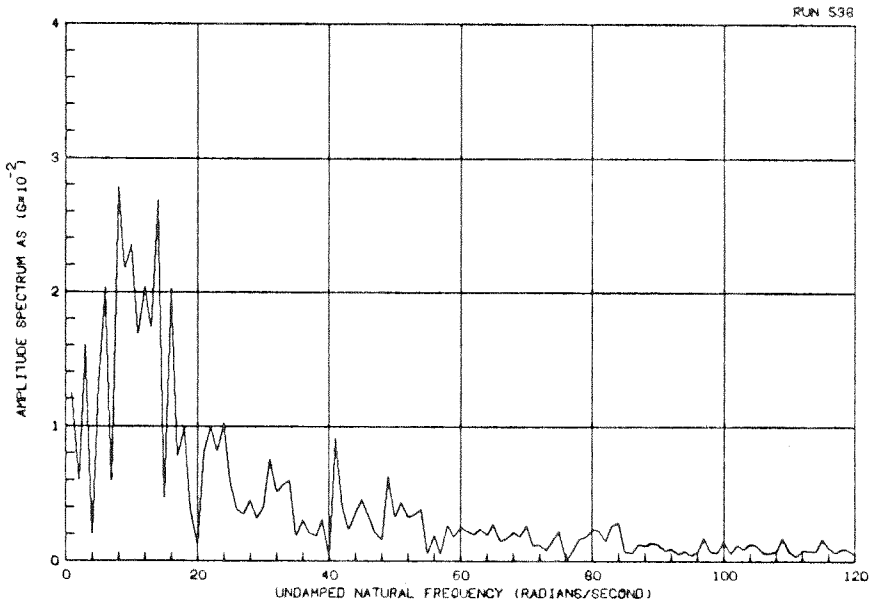

MISSISSIPPI 8228 - TRANSVERSE

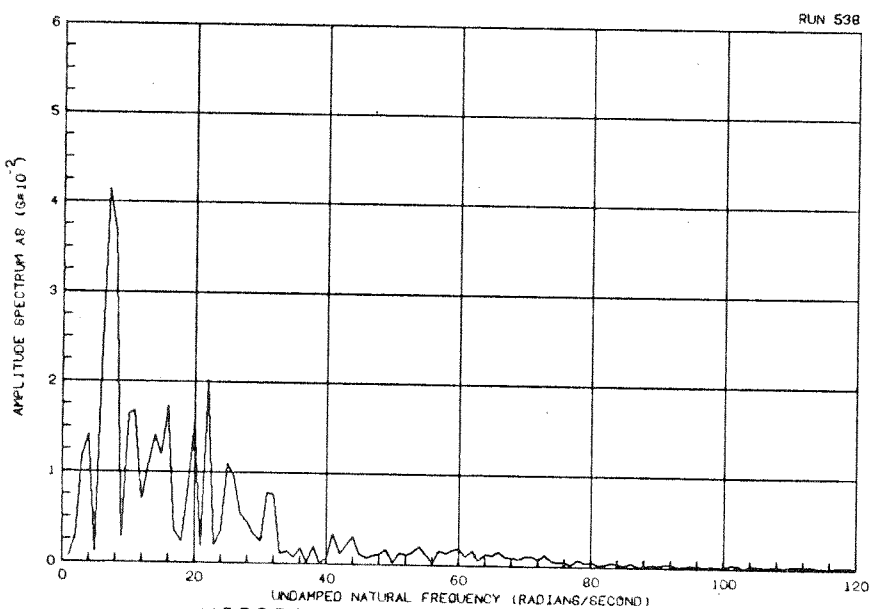

MISSISSIPPI 1777 - TRANSVERSE

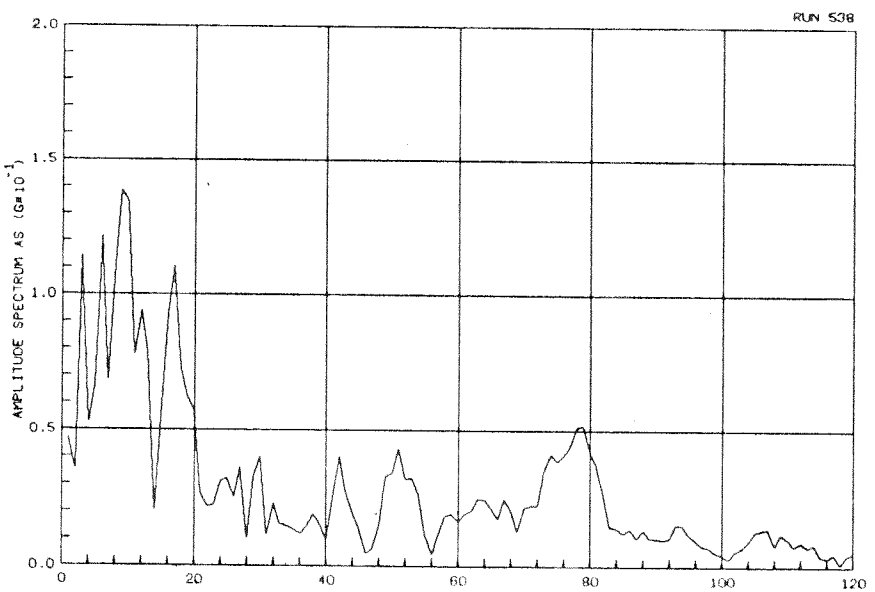

MISSISSIPPI 7245 - RADIAL

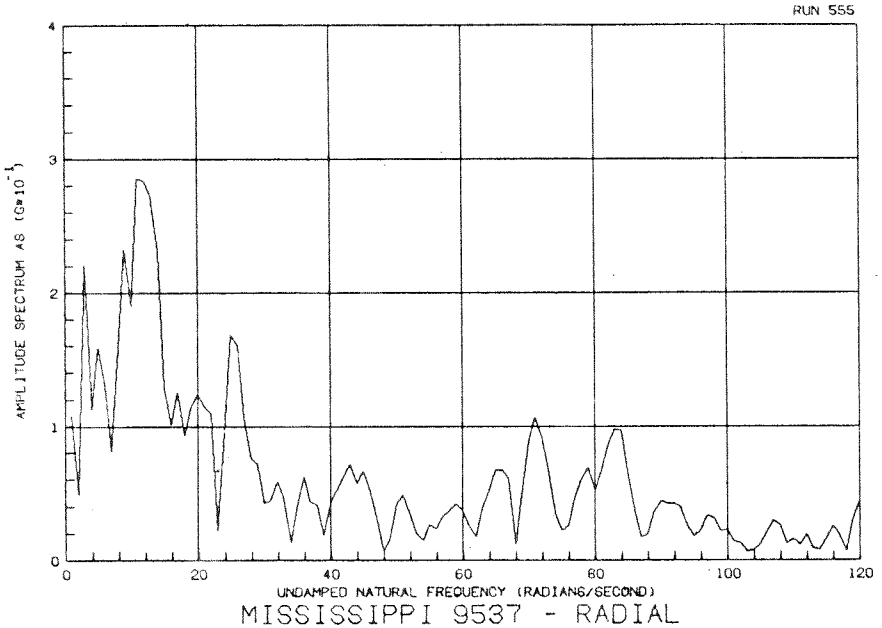

MISSISSIPPI 9537 - RADIAL

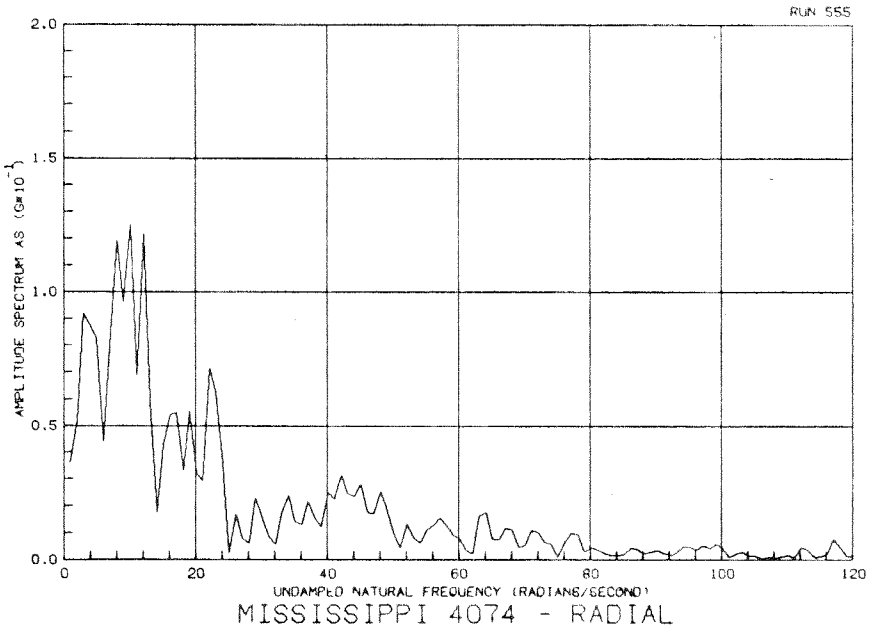

MISSISSIPPI 4074 - RADIAL

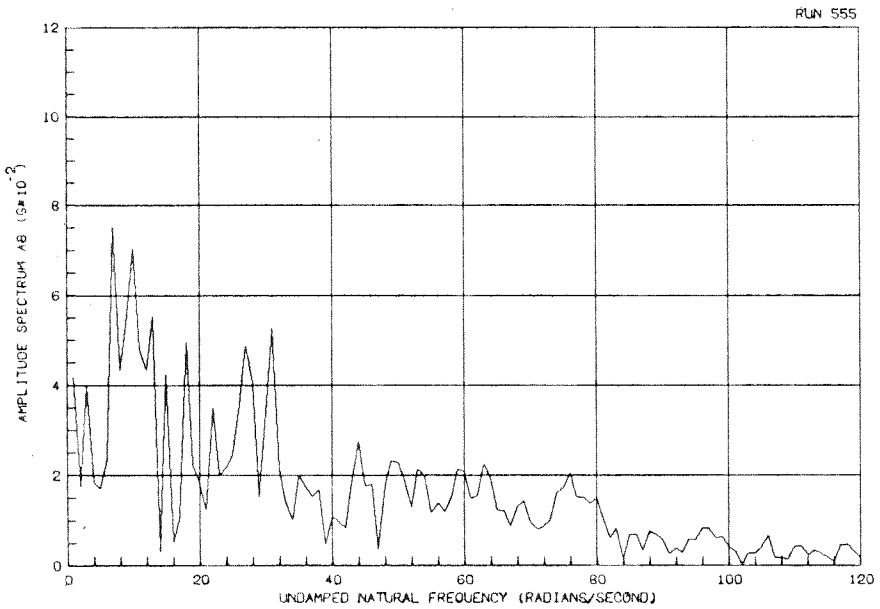

MISSISSIPPI 4074 - TRANSVERSE

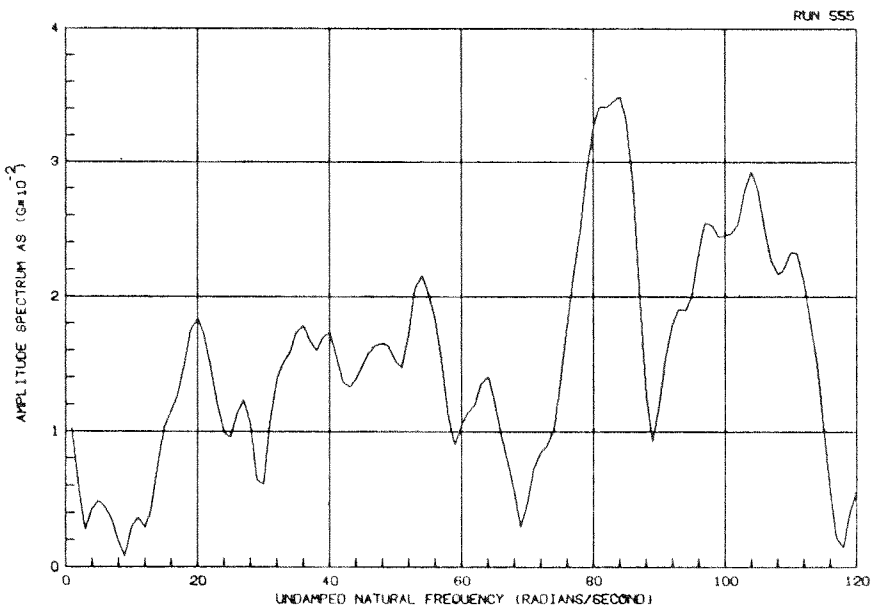

HARDHAT 1091 - TRANSVERSE

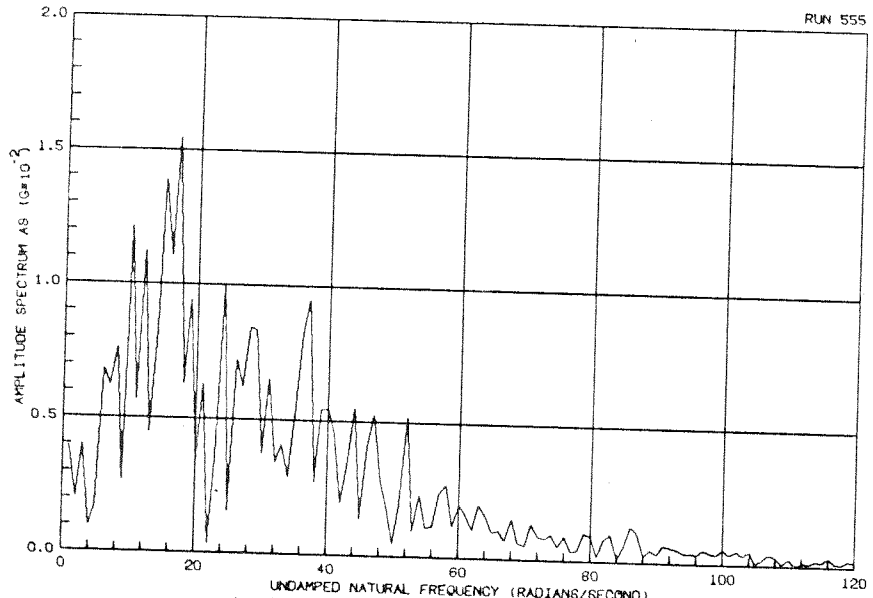

HARDHAT 4496 - TRANSVERSE

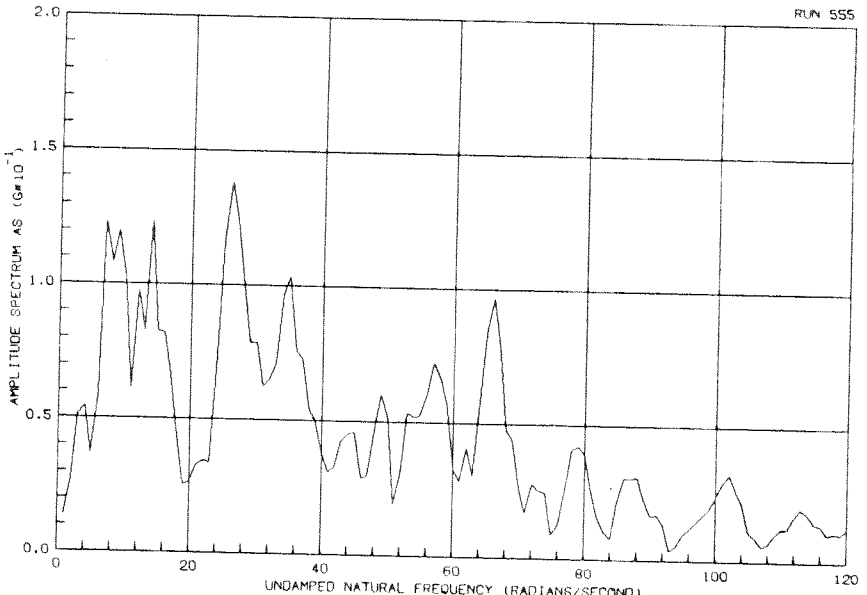

AARDVARK 3773 - TRANSVERSE

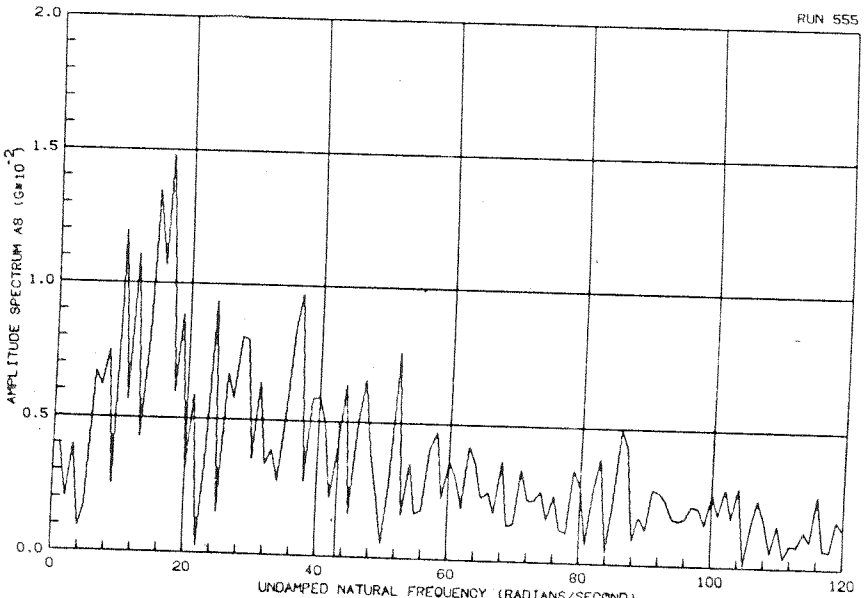

HARDHAT 4496 - TRANSVERSE

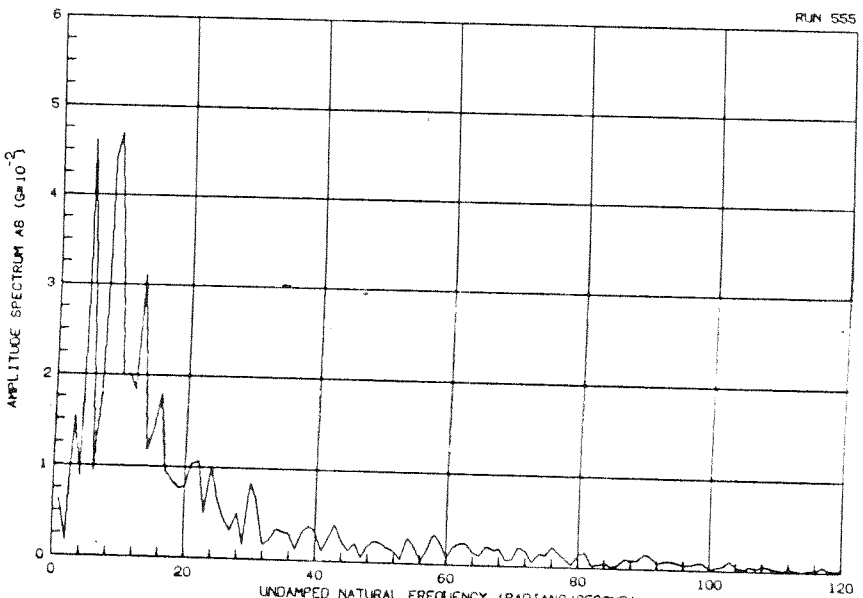

AARDVARK 1437 - TRANSVERSE

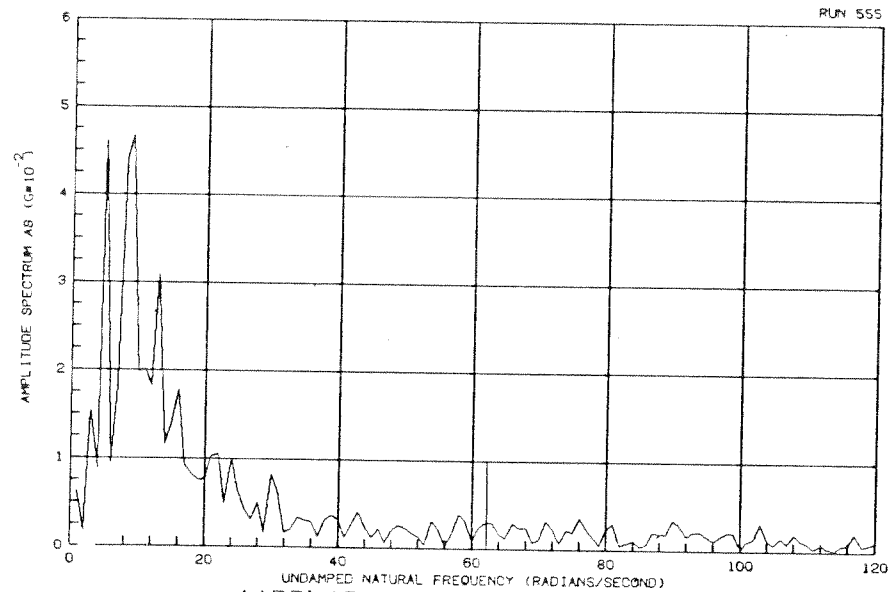

AARDVARK 1437 - TRANSVERSE

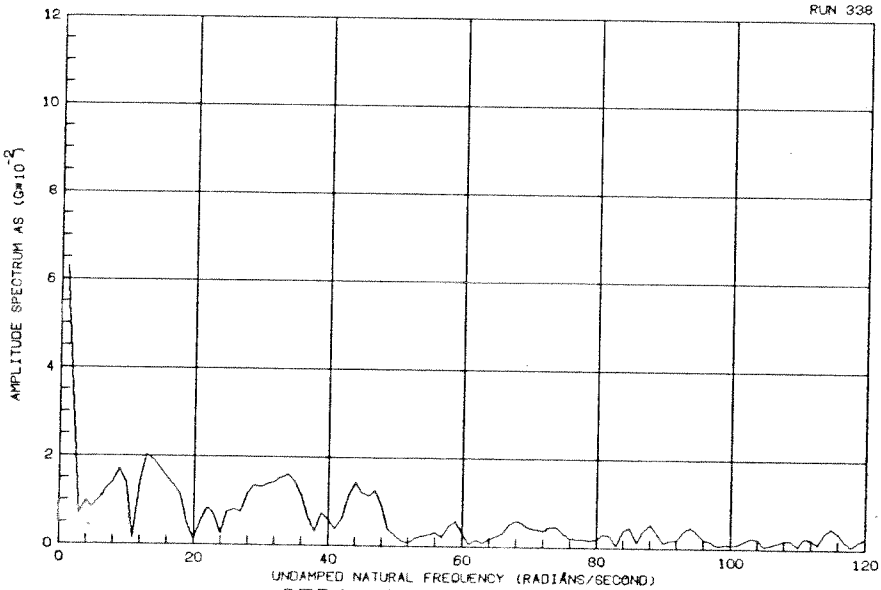

SEDAN RUN 3 - RADIAL

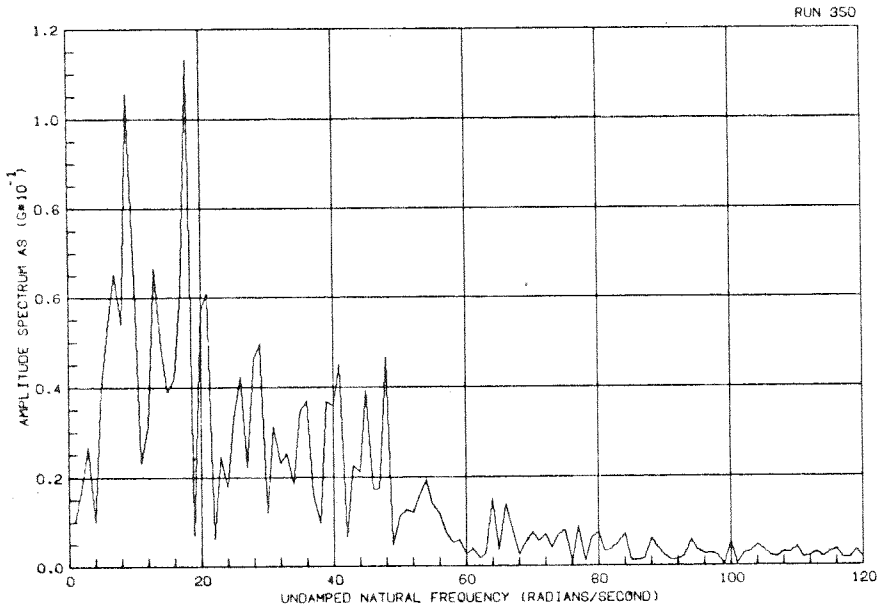

TAFT EARTHQUAKE 21 JULY 1952 - N21E

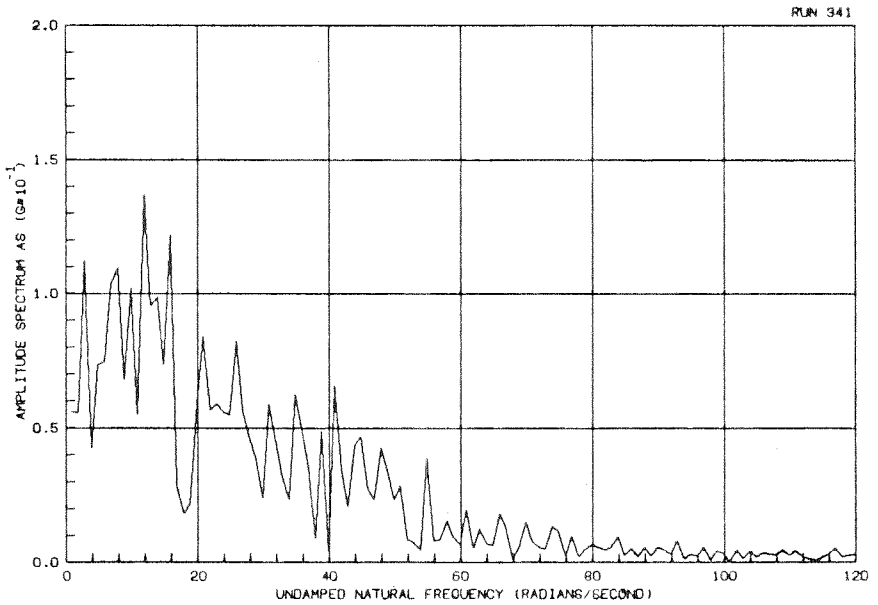

EL CENTRO EARTHQUAKE 18 MAY 1940 - EW

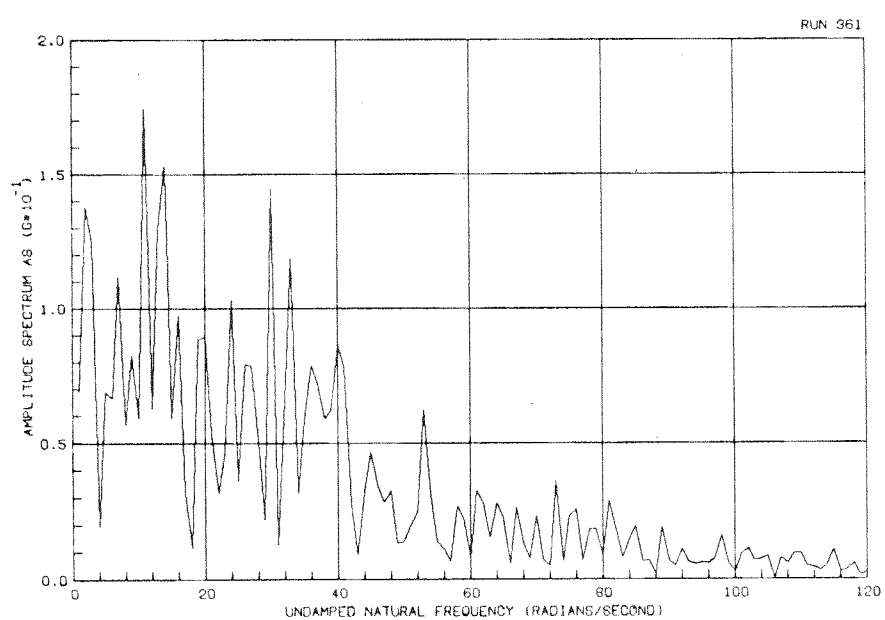

EL CENTRO EARTHQUAKE 18 MAY 1940 - NS

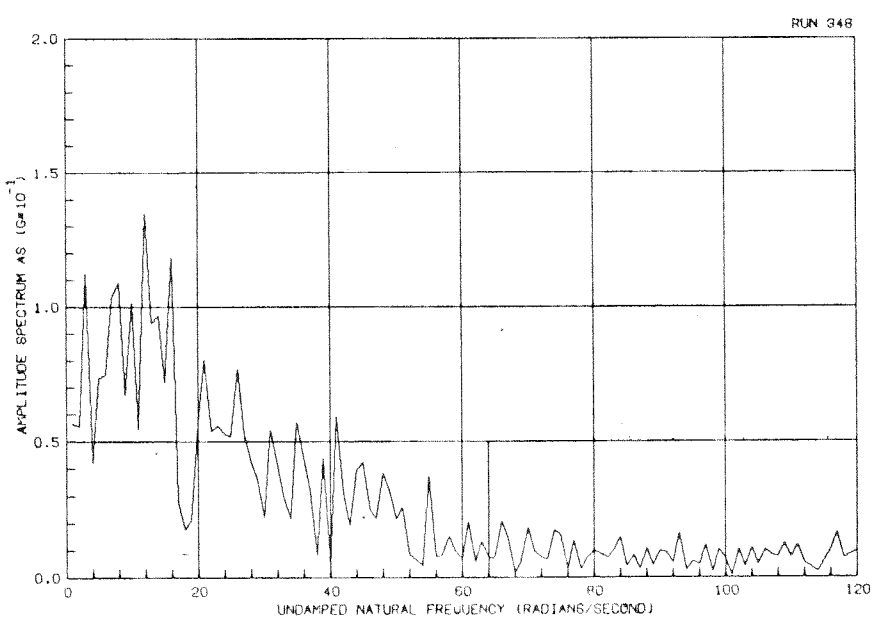

EL CENTRO EARTHQUAKE 18 MAY 1940 - EW

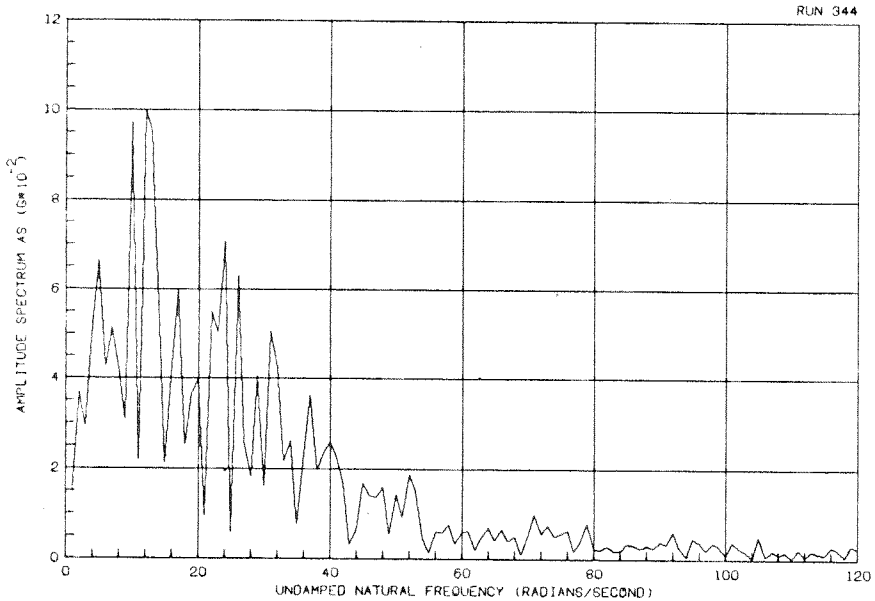

EL CENTRO EARTHQUAKE 30 DEC 1934 - NS

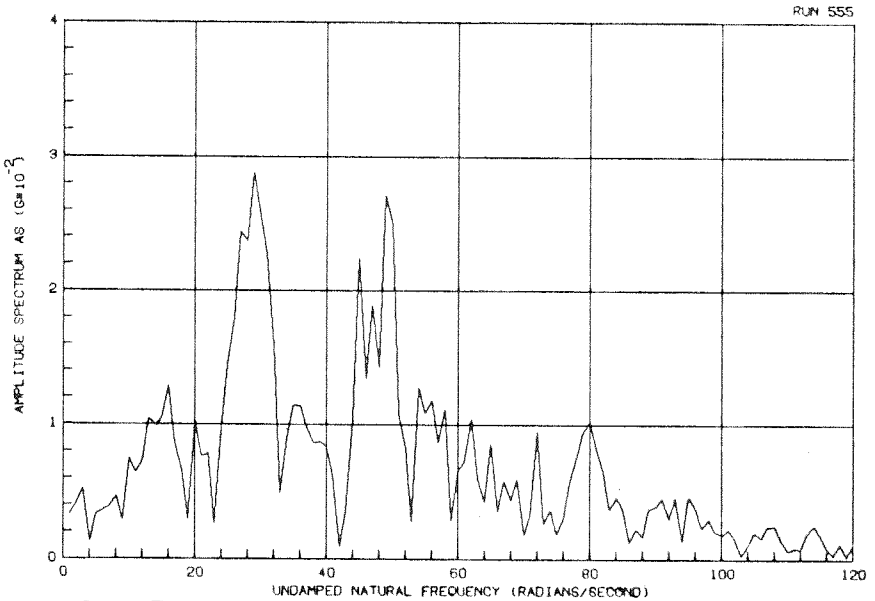

SAN FCO. MARCH 1957 - GOLDEN GATE PARK S80E

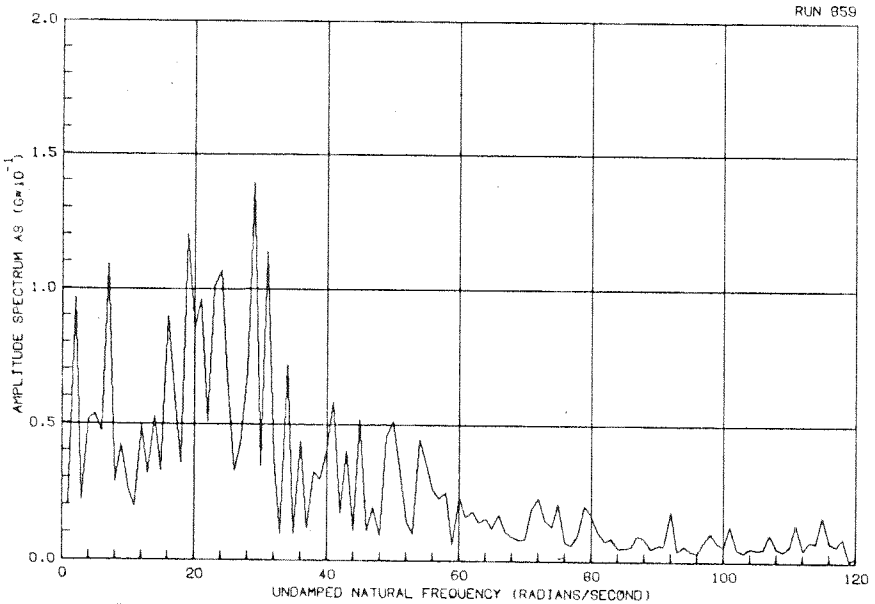

OLYMPIA EARTHQUAKE 13 APRIL 1949 - N80E

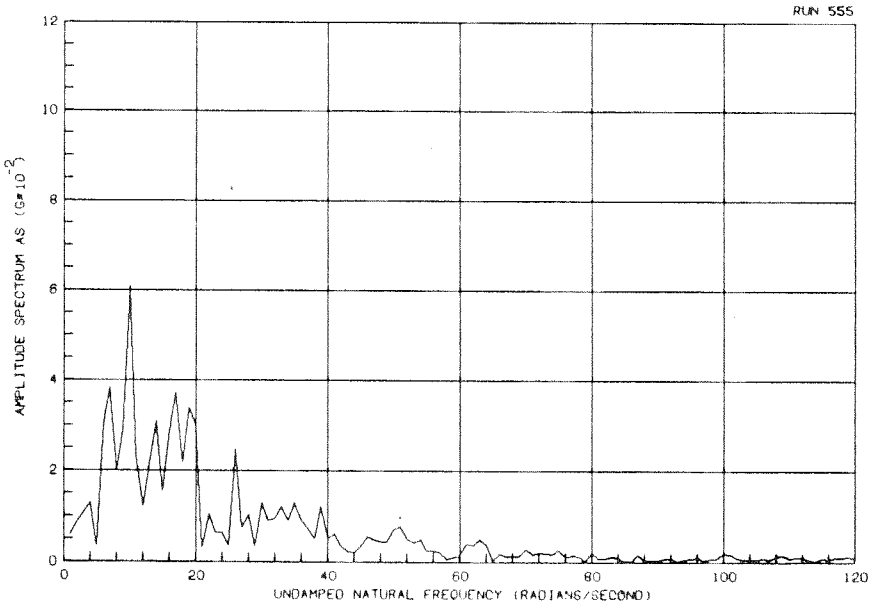

FERNDALE, 3 OCTOBER 1941 - S45E

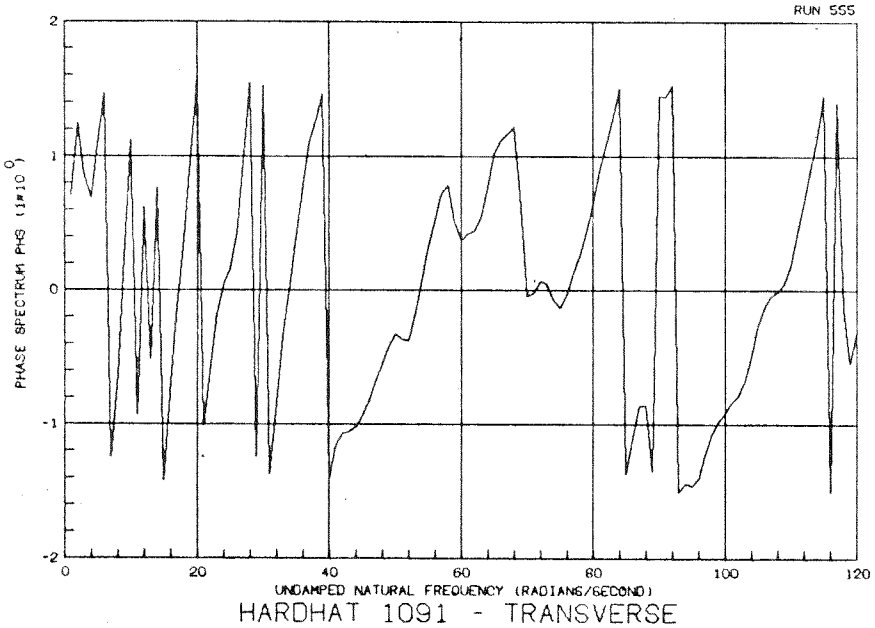

HARDHAT 1091 - TRANSVERSE

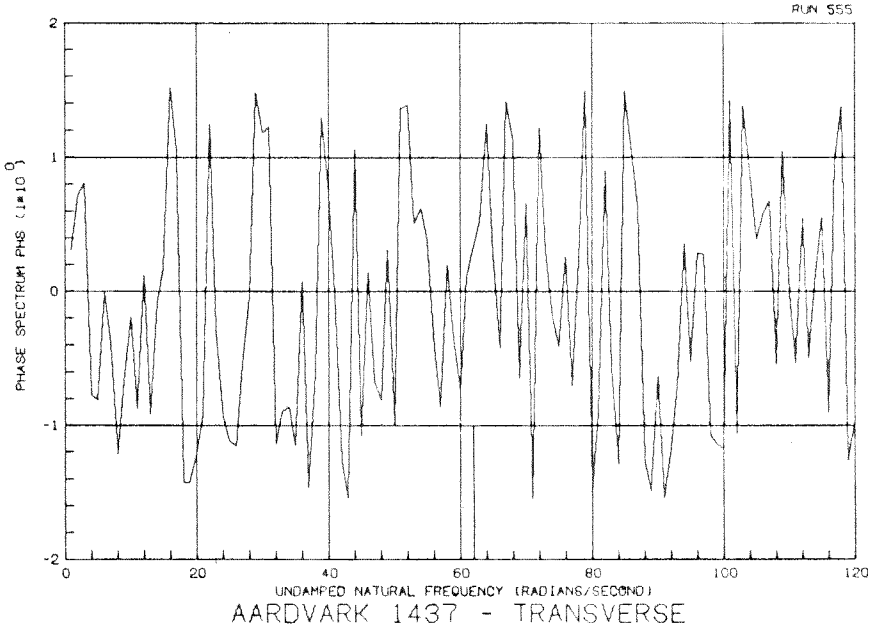

AARDVARK 1437 - TRANSVERSE

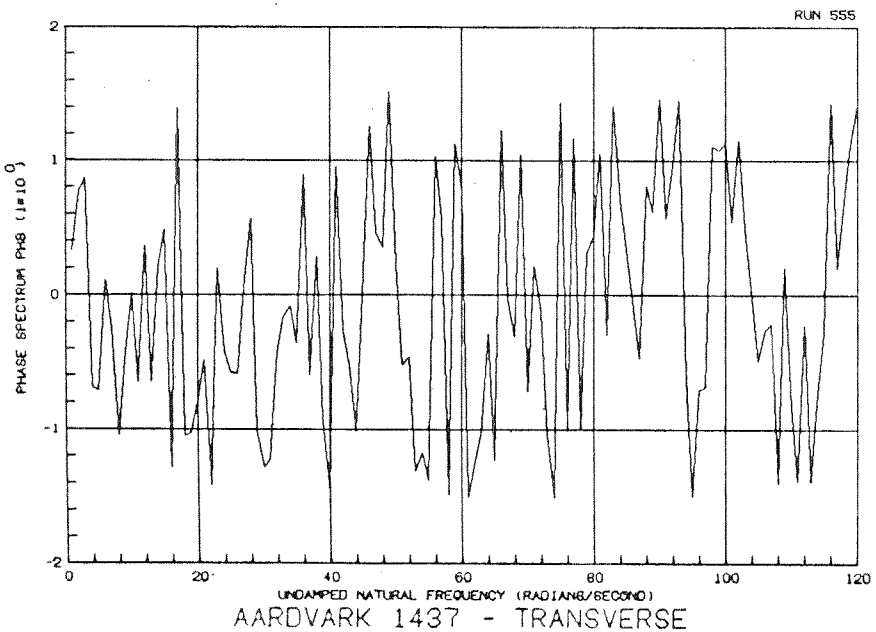

AARDVARK 1437 - TRANSVERSE

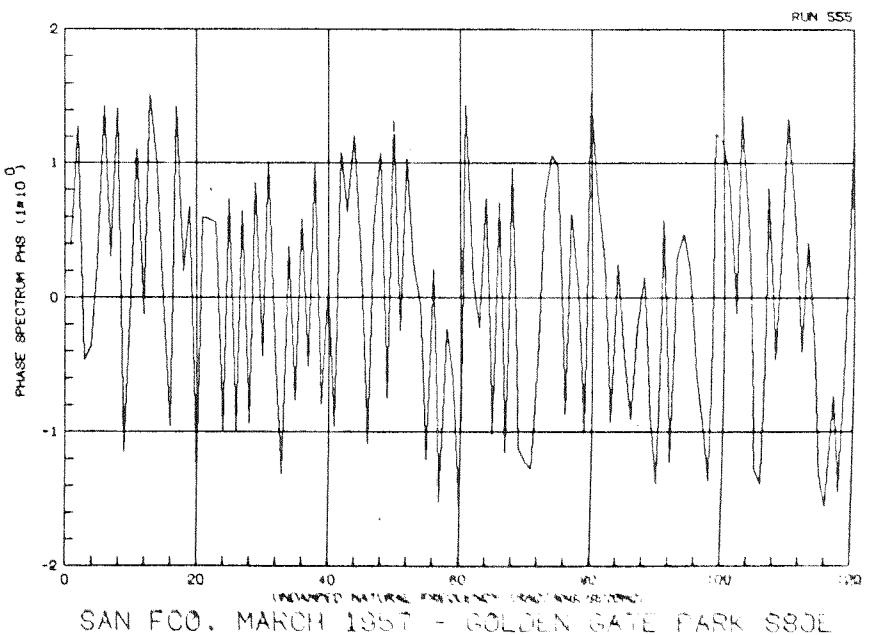

SAN FCO. MARCH 1957 - GOLDEN GATE PARK S80E

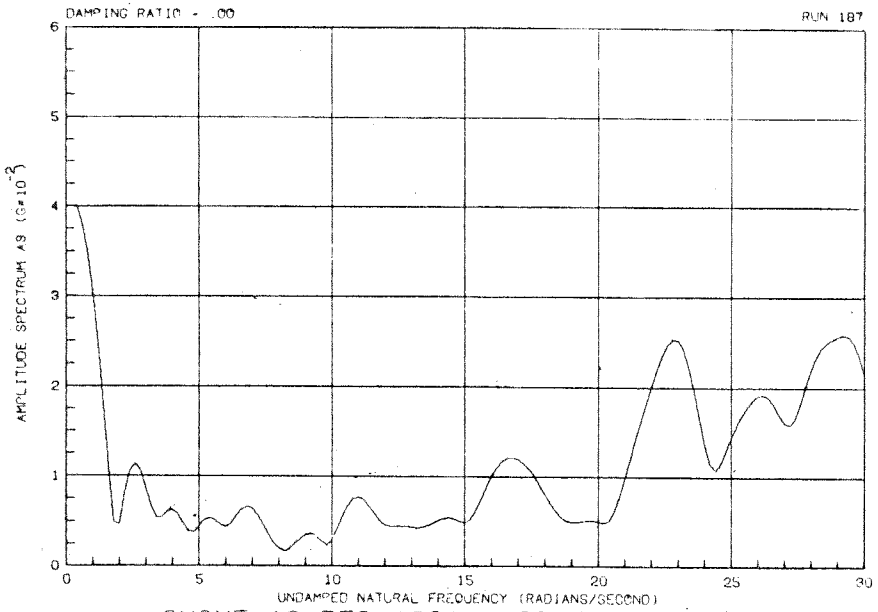

GNOME 10 DEC 1961 - S6 TRANSVERSE

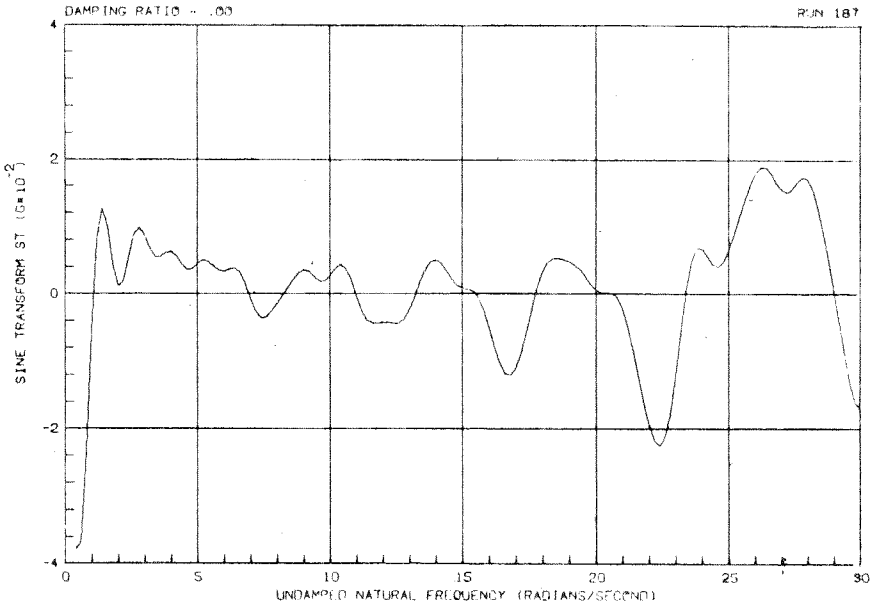

GNOME 10 DEC 1961 - S6 TRANSVERSE

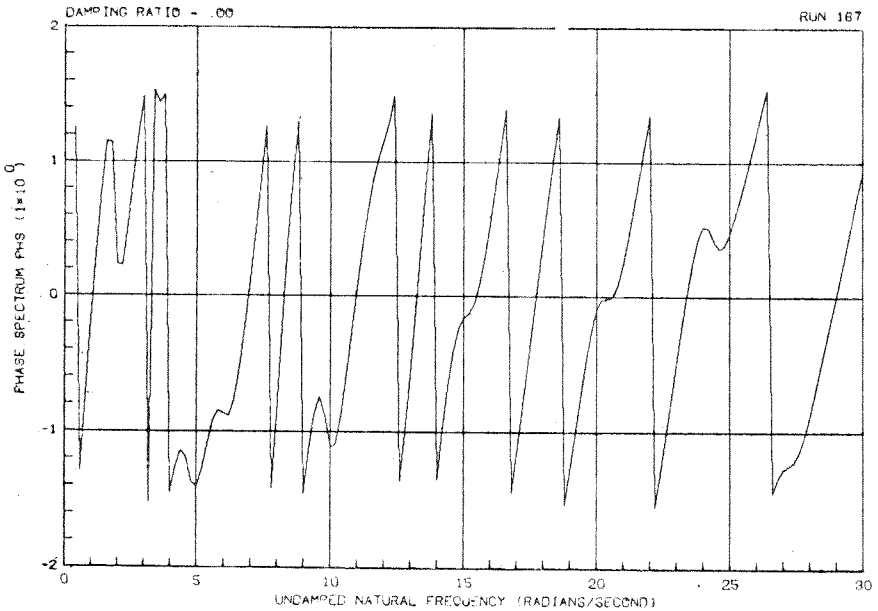

GNOME 10 DEC 1961 - S6 TRANSVERSE

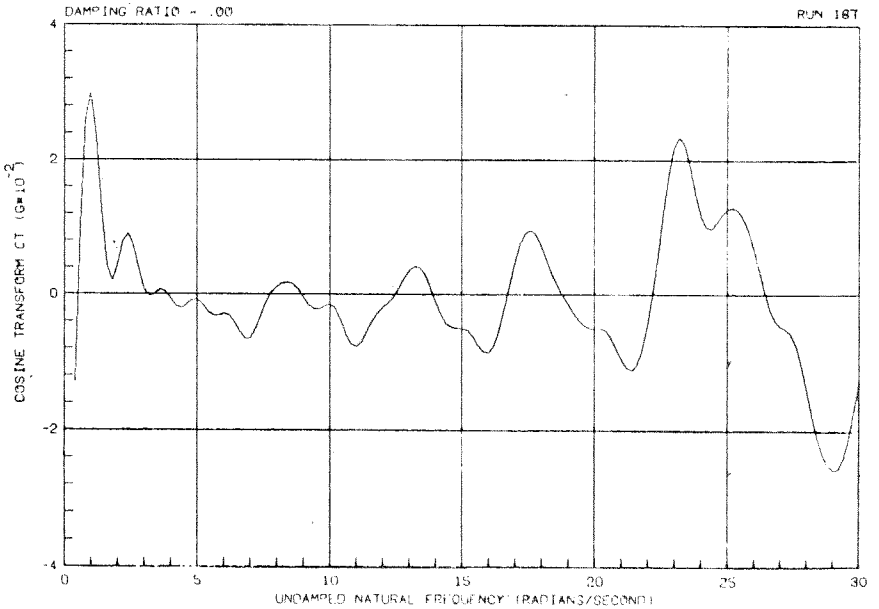

GNOME 10 DEC 1961 - S6 TRANSVERSE

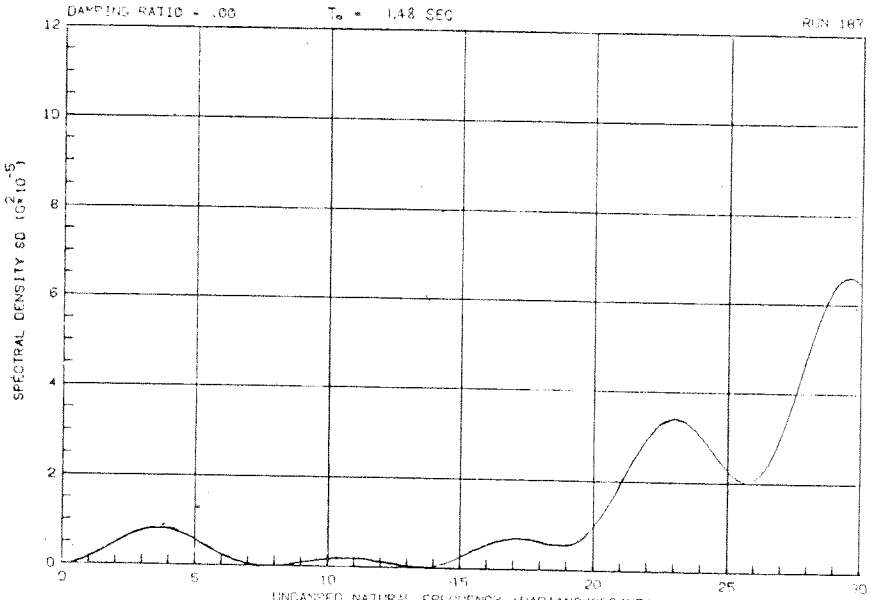

GNOME 10 DEC 1961 - S6 TRANSVERSE

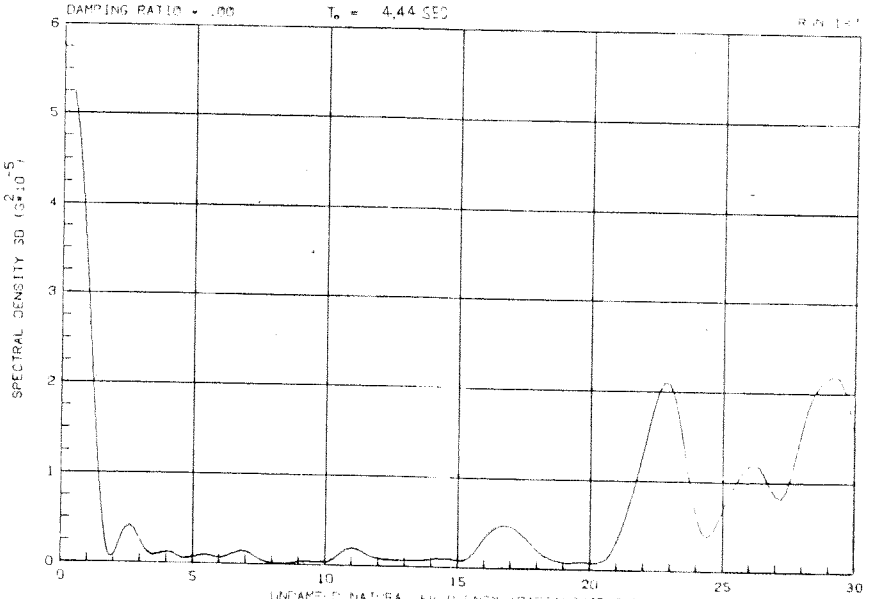

GNOME 10 DEC 1961 - S6 TRANSVERSE

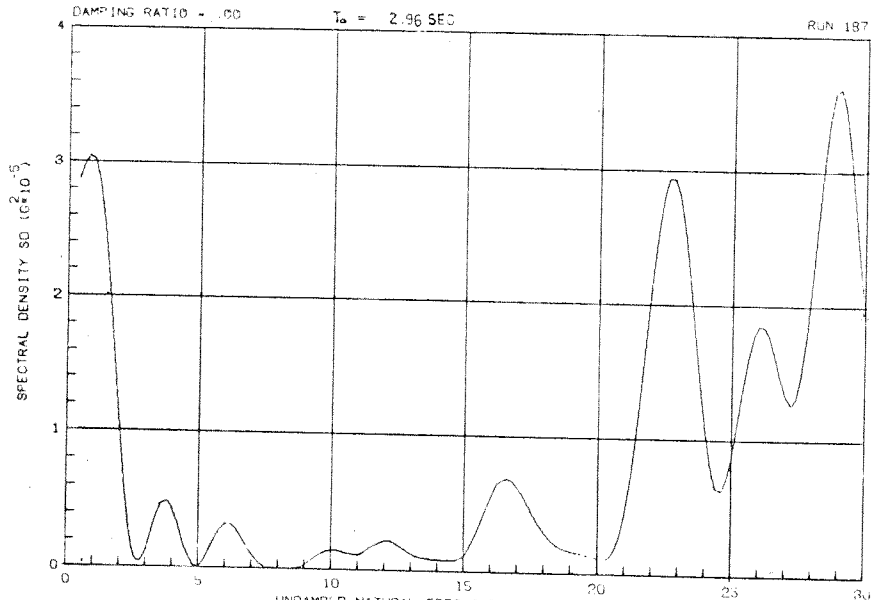

GNOME 10 DEC 1961 - S6 TRANSVERSE

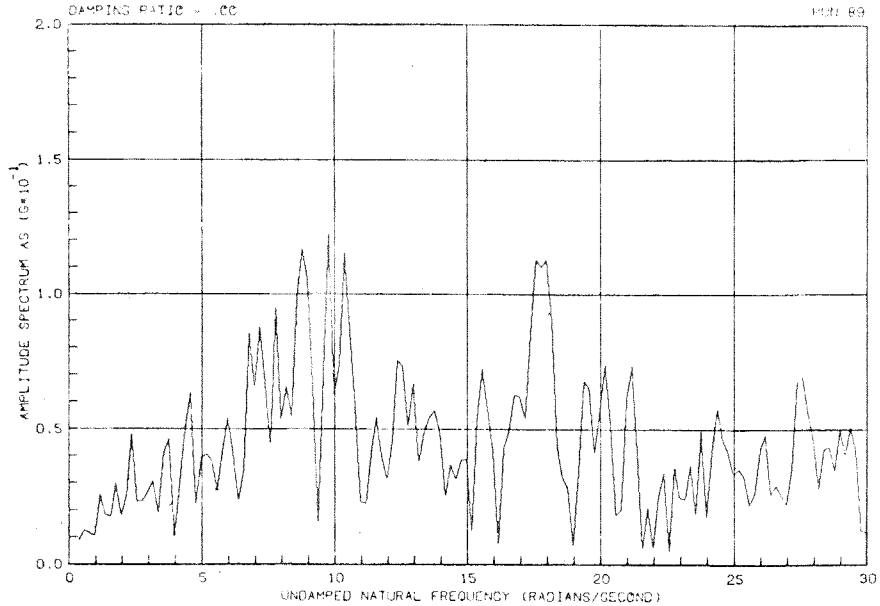

TAFT EARTHQUAKE 21 JULY 1952 - N21E

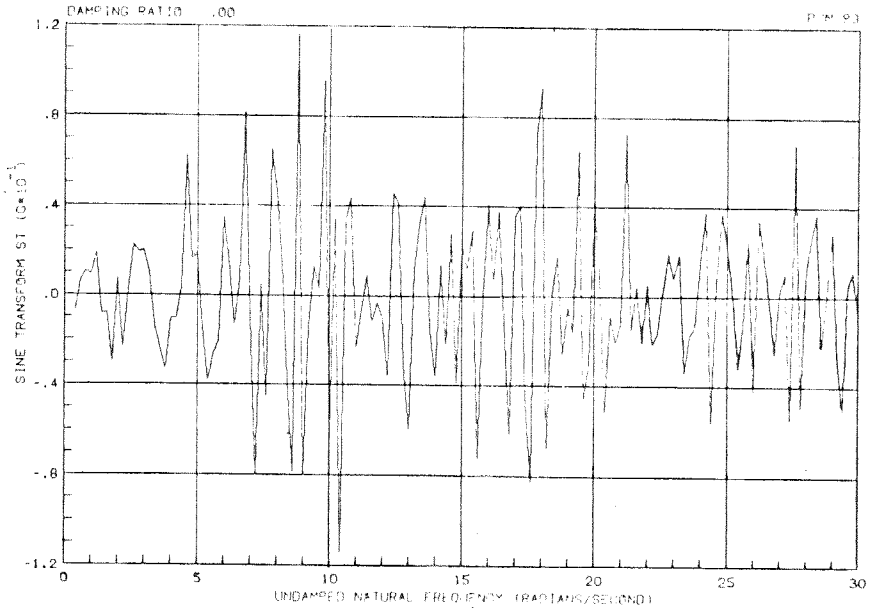

TAFT EARTHQUAKE 21 JULY 1952 - N21E

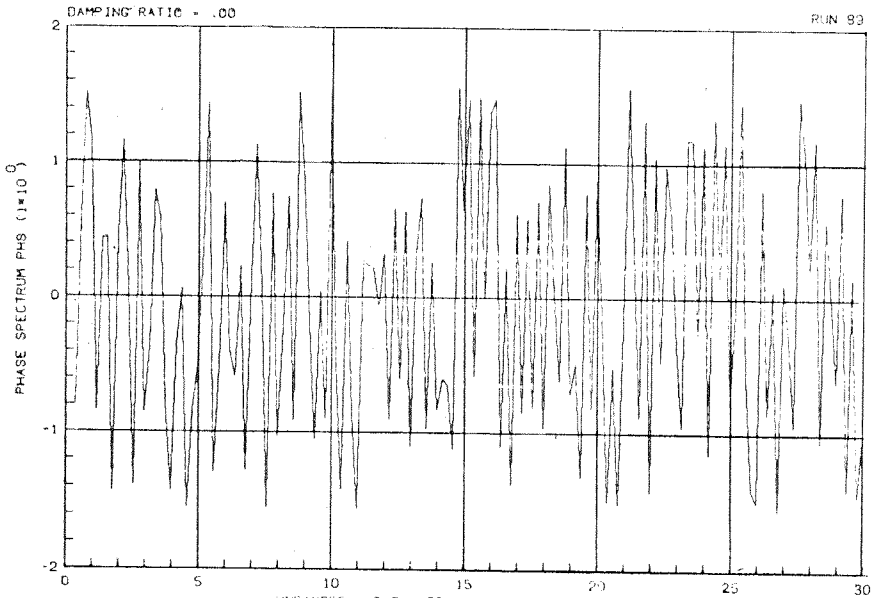

TAFT EARTHQUAKE 21 JULY 1952 - N21E

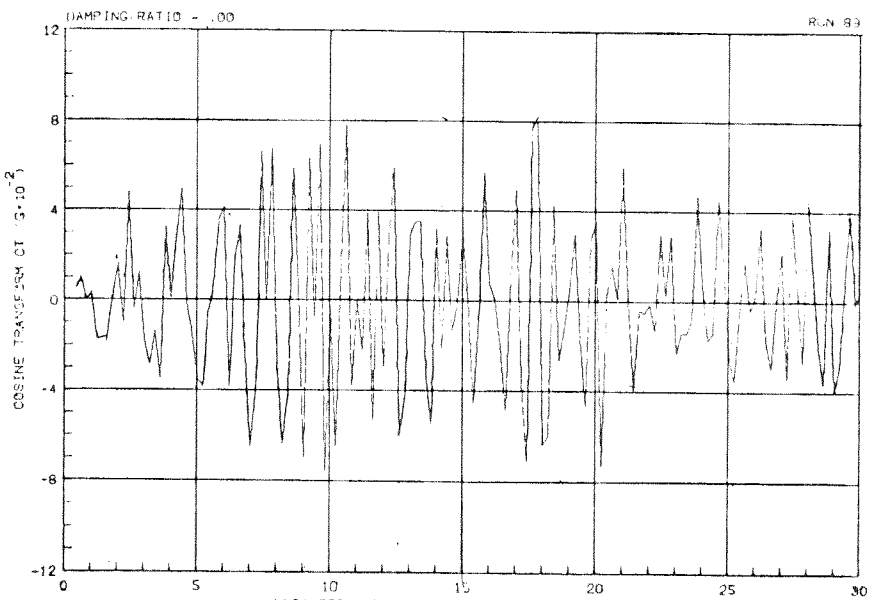

TAFT EARTHQUAKE 21 JULY 1952 - N21E

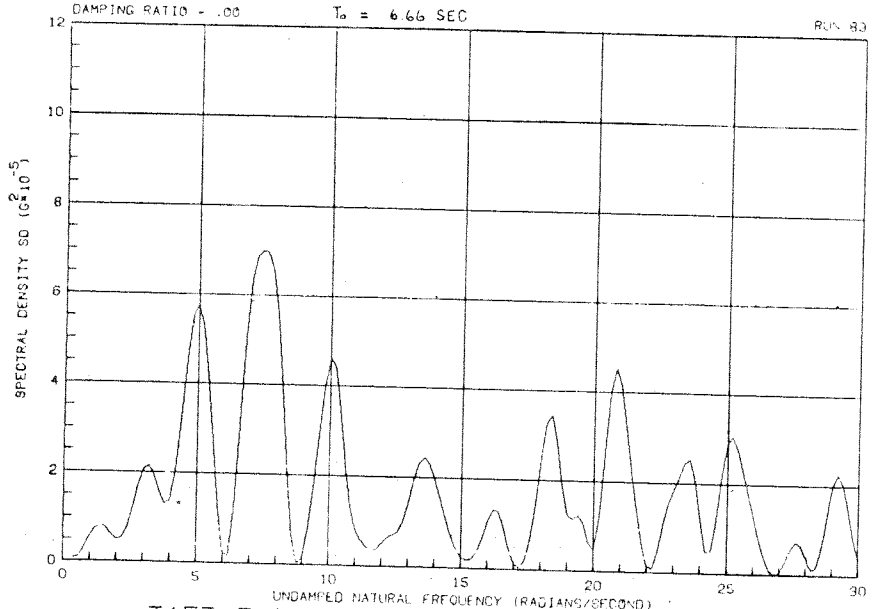

TAFT EARTHQUAKE 21 JULY 1952 - N21E

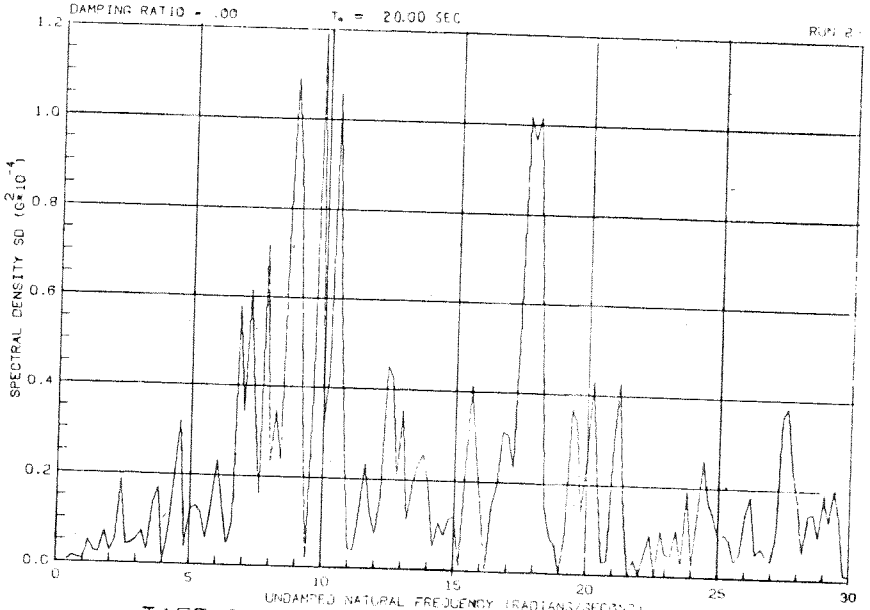

TAFT EARTHQUAKE 21 JULY 1952 - N21E

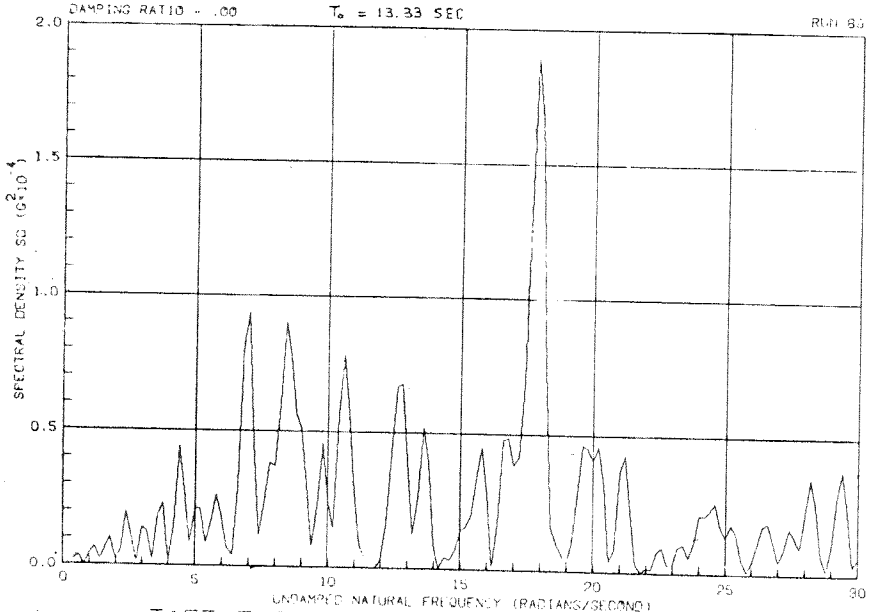

TAFT EARTHQUAKE 21 JULY 1952 - N21E